

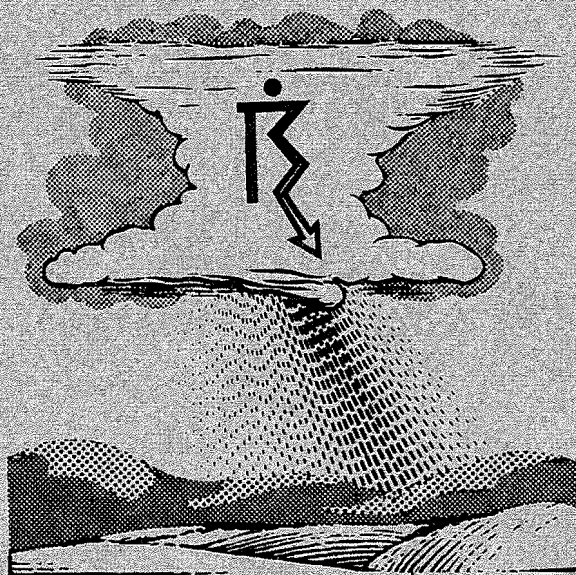
Department of Commerce
Weather Bureau
Office of Hydrologic Director

U. S. Library
Code: 9.446

War Department
Corps of Engineers

HYDROMETEOROLOGICAL REPORT NO. 5

THUNDERSTORM RAINFALL



by Hydrometeorological Section ~ Office of Hydrologic Director

U. S. DEPARTMENT OF COMMERCE
WEATHER BUREAU
OFFICE OF HYDROLOGIC DIRECTOR

U. S. WAR DEPARTMENT
CORPS OF ENGINEERS

HYDROMETEOROLOGICAL REPORT NO. 5

THUNDERSTORM RAINFALL

PART 1
TEXT

BY
THE HYDROMETEOROLOGICAL SECTION
OFFICE OF HYDROLOGIC DIRECTOR

AUGUST 22, 1945

PUBLISHED AT
WATERWAYS EXPERIMENT STATION
VICKSBURG, MISSISSIPPI

1947

Corrections to Hydrometeorological Report No. 5

Part I, Text:

In footnote on page 228, change "page 128" to "page 140".

Part 2, Figures:

Figure 1: Change indicated value for T_d from 0.8°C to -0.8°C .

Figures 38-41, 42-45, 52-55, 56-59, 60-63, 69-72, 80-82: The red overprints on all these figures are the isoceraunics (or lines of equal thunderstorm-day frequency) of figures 28-31. However, the overprints are not accurate reproductions of the original figures and should be considered for only qualitative comparisons. (In some cases, lines are missing or misnumbered.) For greater accuracy, consult the corresponding figure in the original group of figures 28-31.

LETTER OF AUTHORIZATION
(C O P Y)

WAR DEPARTMENT
OFFICE OF THE CHIEF OF ENGINEERS
WASHINGTON

September 4, 1942

Chief of Bureau,
U. S. Weather Bureau,
Department of Commerce,
Washington, D. C.

Dear Sir:

Because of the importance of thunderstorm or cloudburst type of precipitation in the design of many flood control investigations being conducted by this Department, it is considered desirable that the Hydrometeorological Section of your Bureau undertake a study and report on thunderstorms. Such a study is believed to be feasible within the limits of admittedly inadequate data. Papers have been prepared on the subject lately by Professor J. Bjerknes, Consulting Meteorologist, Mr. George N. Brancato of the staff of the Hydrometeorological Section, and Mr. J. A. Browne, Meteorologist for Transcontinental and Western Airways. The Hydrometeorological Section has also prepared a report for the Department of Agriculture on the "Depth-Frequency Relations of Thunderstorm Rainfall on the Sevier Basin, Utah." The above data could be used as the nucleus for the study, subject to such expansion as available material should warrant. It is suggested that the report designate areas in which the frequency of thunderstorms warrants the establishment of networks of sufficient density to adequately sample thunderstorm areas of limited extent.

It is accordingly requested that the Hydrometeorological Section undertake a study and report on thunderstorms as soon as the report on meteorology of storms in the Panama Canal region has been completed. It is desired that the study of maximum possible storms in the Pecos River Basin be undertaken after completion of the report on thunderstorms.

For the Chief of Engineers:

Very truly yours,

JAMES H. STRATTON,
Colonel, Corps of Engineers,
Chief, Engineering Branch,
Construction Division.

PREFACE

The Hydrometeorological Section of the Weather Bureau operates under allotment of funds from the Corps of Engineers, War Department. Late in 1942 the Section was authorized by the Chief of Engineers (see page ii) to undertake a study of thunderstorms as soon as current work permitted. Although the limitations of both theory and observational data were recognized, the importance of thunderstorm rainfall to flood-control design made such an undertaking advisable. Preliminary investigation of the field of data and reconnaissance of the literature on the subject were begun early in 1943.

Other assignments were concurrent with the thunderstorm study. The Section continued and increased its quota of routine hydrometeorological analyses and reviews of storm studies prepared by the Division and District Offices of the U. S. Engineer Department. Other major assignments in progress or completed during the period included estimates of maximum precipitation over the Potomac and Rappahannock Basins, the Pecos River Basin of New Mexico, the Osage River Basin, the Los Angeles area, and the Columbia River Basin. Thus only a small portion of the Section's time and personnel was at any one time devoted to the thunderstorm study.

The report was prepared under the supervision of Merrill Bernard, Hydrologic Director, and A. K. Showalter, Chief of Section. The principal authors, responsible for the basic organization and presentation of the material, are H. K. Gold, P. Light, R. A. McCormick, A. L. Shands, and A. K. Showalter. In the Table of Contents the authors' initials follow the appropriate titles. However, every other member of the Section staff also assisted in the preparation of the report. In lieu of a listing of names in this preface, the Section roster of January 1, 1945, is reproduced at the back of the report. The report was edited by A. L. Shands, with the assistance of Mrs. H. C. Hamilton. The graphic presentation of the material was designed and directed by W. E. Kinnear.

For permission to use data and charts, and for willing cooperation in general, grateful acknowledgment is made to the following: Soil Conservation Service, Department of Agriculture; Department of Public Works, City of Chicago; Divisions of Statistics and Climate and Crop Weather, Weather Bureau; Weather Bureau Offices at San Francisco, Denver, Missoula, Helena, Detroit, and Portland (Maine); The Marley Company, Kansas City, Kansas; L. P. Harrison, Weather Bureau; L. L. Means, University of Chicago; and the University of Chicago Press. The continuing cooperation between the Hydrometeorological Section and the Corps of Engineers, War Department, was, of course, fundamental to the progress of this report, as it has been to all other reports issued under their joint auspices.

CONTENTS

	<u>Page</u>
Letter of Authorization	i
Preface	iii
 CHAPTER I. THUNDERSTORM FACT AND THEORY	
Definition (A.L.S.)	1
Surface-observed characteristics (H.K.G.-A.L.S.)	4
Instability (H.K.G.)	8
The pseudo-adiabatic diagram (H.K.G.)	11
Conditional instability	12
Lifting type (H.K.G.)	12
Icing level (A.L.S.)	14
Insolational type (H.K.G.-A.L.S.)	16
Analysis by slice method (A.L.S.)	19
Convective instability (H.K.G.-A.L.S.)	21
Evaporation effects (H.K.G.-A.L.S.)	25
Comparison of mean soundings (A.L.S.)	28
Oklahoma City	30
Omaha	32
Phoenix	34
Washington, D. C.	37
Thunderstorm updrafts (H.K.G.-A.L.S.)	41
Convergence updrafts (A.L.S.)	47
Thunderstorm downdrafts (H.K.G.)	52
Rain formation (H.K.G.-A.L.S.)	54
Thunderstorm-cell models (H.K.G.-A.L.S.)	63
Lightning (H.K.G.-A.L.S.)	69
The tornado (A.L.S.)	72
References	75
 CHAPTER II. THUNDERSTORM CLIMATOLOGY	
Years of record (A.L.S.)	81
Distribution of thunderstorm days (A.L.S.)	83
Associated wet-bulb temperatures (H.K.G.)	108
Comparison with average precipitation distribution (A.L.S.)	113
Comparison with precipitation-day distribution (A.L.S.)	123
Comparison with daily-intensity distribution (A.L.S.)	129
Comparison with distribution of selected intensities (A.L.S.)	137
Comparison with areal-rainfall frequency (A.L.S.)	141
Comparison with hail distribution (A.L.S.)	144
The hail-thunderstorm ratio (A.L.S.)	158
Comparison with tornado distribution (A.L.S.)	166
The maximum thunderstorm month (A.L.S.)	175
Diurnal variation of thunderstorm frequency (A.L.S.)	178

CONTENTS (contd)

	<u>Page</u>
Diurnal variation of thunderstorm frequency (contd)	
Annual	195
Winter	198
Spring	200
Summer	203
Autumn	205
Numerical relations	206
Maximum hour	211
The nocturnal thunderstorm (A.L.S.)	211
Days with more than one thunderstorm (A.L.S.)	216
Diurnal variation of rainfall (A.L.S.)	221
References	229

CHAPTER III. THE RELIABILITY OF AREAL RAINFALL DETERMINATION

Need for reliability determination (P.L.)	234
Sources of error (P.L.)	235
Statistical theory (P.L.)	236
Analysis of variability (P.L.)	239
Effects of uniform gage spacing (P.L.)	244
The experimental network (P.L.-A.L.S.)	250
References	258

CHAPTER IV. HYDROLOGIC ASPECTS OF THUNDERSTORM RAINFALL

The typical mass curve (R.A.M.-A.L.S.)	260
Area-depth relations (P.L.)	264
Storm profiles (P.L.)	270
Duration-depth relations (P.L.)	273
Maximum thunderstorm rainfall (A.K.S.-A.L.S.)	278
References	287

APPENDIX

Symbols and abbreviations	289
Glossary	292
A selected thunderstorm bibliography (H.K.G.)	304
Roster of the Hydrometeorological Section	331

TABLES

<u>No.</u>		<u>Page</u>
1	Total thunderstorm days, 1904-43	86
2	Maximum and minimum number of days with thunderstorms, 1904-43	89
3	Thunderstorm durations at Peoria, Ill., 1905-31	109
4	Thunderstorm durations at Tampa, Fla., 1890-1904	109
5	Comparison of percentages of normal rainfall with percentages of normal thunderstorm-day frequency during the wettest summers, 1904-43	120
6	Comparison of percentages of normal rainfall with percentages of normal thunderstorm-day frequency during the driest summers, 1904-43	121
7	Comparison of maximum rainfall and maximum thunderstorm-day frequency for July at selected stations, 1904-43	122
8	Total thunderstorm days vs. total days with .01 inch or more at Mobile, Ala., 1914-36	127
9	Total thunderstorm days vs. total days with .01 inch or more at Omaha, Nebr., and Oklahoma City, Okla., 1933-42	127
10	Thunderstorm and non-thunderstorm daily intensities at Mobile, Ala., 1914-36	134
11	Total thunderstorm days without measurable rain at Mobile, Ala., 1914-36	136
12	Percentage of rainfall associated with thunderstorms at Mobile, Ala., 1914-36	137
13	Total days with hail, 1904-43	146
14	Maximum number of days with hail, 1904-43	149
15	Areal thunderstorm-hail-tornado frequencies - Iowa	163
16	Areal thunderstorm-hail-tornado frequencies - Maryland-Delaware- Washington, D.C.	164

TABLES (contd)

<u>No.</u>		<u>Page</u>
17	Total tornado days per state or section, 1880-1942	169
18	Total tornado days per 10,000-square-mile area per state or section, 1880-1942	170
19	Ranking of states or sections in descending order of annual tornado frequency, 1880-1942	171
20	Monthly variation of state or section rank by tornado frequency per 10,000-square-mile area, 1880-1942	172
21	Diurnal variation of thunderstorm frequency, 1906-25	179
22	Average depths and standard deviations of rainfall measure- ments in 6-hour storms (Muskingum Basin)	212
23	Effects of areal size and storm magnitude on 6-hour storm variability (Muskingum Basin)	213
24	Standard and percent standard errors of uniformly spaced network (storms > 0.5 in., Muskingum Basin)	218
25	Means and standard deviations of 24-hour rainfalls	253
26	Correlation coefficients between 24-hour rainfalls	253
27	Average percentage of total thunderstorm rainfall by 10-minute increments	262
28	Highest percentage frequency of each rank for 10-minute increments in thunderstorm rain	262
29	Area-depth values, 6-hour storms (Muskingum Basin)	269
30	Duration-depth values, 275 square miles (Muskingum Basin)	275
31	Duration-depth values, 8000 square miles (Muskingum Basin)	276
32	Maximum observed U. S. rainfall	283

FIGURES

(Figures bound separately, in Part 2 of
"Thunderstorm Rainfall".)

No.

- 1 Evaluations on the pseudo-adiabatic diagram
- 2 Pseudo-adiabatic diagram - conditional instability realized by lifting
- 3 Pseudo-adiabatic diagram - conditional instability realized by insolation
- 4 Normal daily variation of dew-point temperature from June to September, inclusive
- 5 Pseudo-adiabatic diagrams illustrating two ways of realizing convective instability
- 6 Pseudo-adiabatic diagram - comparative mean soundings, July 1942, Oklahoma City, Okla., 2300 EST
- 7 Rossby diagrams - comparative mean soundings, July 1942, Oklahoma City, Okla., 2300 and 1100 EST
- 8 Pseudo-adiabatic diagram - comparative mean soundings, July 1942, Oklahoma City, Okla., 1100 EST
- 9 Pseudo-adiabatic diagram - comparative mean soundings, July 1942, Omaha, Nebr., 2300 EST
- 10 Rossby diagrams - comparative mean soundings, July 1942, Omaha, Nebr., 2300 and 1100 EST
- 11 Pseudo-adiabatic diagram - comparative mean soundings, July 1942, Omaha, Nebr., 1100 EST
- 12 Pseudo-adiabatic diagram - comparative mean soundings, July 1942, Phoenix, Ariz., 2300 EST
- 13 Rossby diagrams - comparative mean soundings, July 1942, Phoenix, Ariz., 2300 and 1100 EST
- 14 Pseudo-adiabatic diagram - comparative mean soundings, July 1942, Phoenix, Ariz., 1100 EST
- 15 Pseudo-adiabatic diagram - comparative mean soundings, July 1942, Washington, D. C., 2300 EST

FIGURES (contd)

No.

- 16 Rossby diagrams - comparative mean soundings, July 1942, Washington, D. C., 2300 and 1100 EST
- 17 Pseudo-adiabatic diagram - comparative mean soundings, July 1942, Washington, D. C., 1100 EST
- 18 Vertical velocities from radial inflow
- 19 Illustrations of convergence
- 20 Vertical velocities from downwind decrease of wind
- 21 Relation of derived to observed minimum surface temperatures produced by thunderstorms.
- 22 Effect of moisture charge on the structure of a convective cell
- 23 Schematic streamlines of air and precipitation in a thunderstorm cell
- 24 Isohyetal patterns drawn for theoretically "ring-shaped" rainfall
- 25 Pseudo-adiabatic diagram - upper-air structure associated with tornadoes
- 26 Thunderstorm-day frequencies at Kansas City, Mo.
- 27 Monthly variation in thunderstorm frequency
- 28 Average number of days with thunderstorms - annual
- 29 Average number of days with thunderstorms - January, February, March, and April
- 30 Average number of days with thunderstorms - May, June, July, and August
- 31 Average number of days with thunderstorms - September, October, November, and December
- 32 Surface wet-bulb temperature exceeded not more than 5% of the time from June to September, inclusive
- 33 Pseudo-adiabatic diagram adapted for dew-point and wet-bulb reductions

FIGURES (contd)

- No.
- 34 Normal daily variation of wet-bulb temperature from June to September, inclusive
 - 35 Critical surface Θ_w associated with thunderstorm days, June to September, inclusive
 - 36 Frequency of surface Θ_w , 1630 EST thunderstorms, July 1942
 - 37 Frequencies of 3-km Θ_E at Omaha, Shreveport, Boston, and Billings - June, July, August, and September, 1936-37
 - 38 Average annual precipitation
 - 39 Average monthly precipitation - January, February, March, and April
 - 40 Average monthly precipitation - May, June, July, and August
 - 41 Average monthly precipitation - September, October, November, and December
 - 42 Average number of days with .01 inch or more of precipitation - annual
 - 43 Average number of days with .01 inch or more of precipitation - January, February, March, and April
 - 44 Average number of days with .01 inch or more of precipitation - May, June, July, and August
 - 45 Average number of days with .01 inch or more of precipitation - September, October, November, and December
 - 46 Ratio of days with thunderstorms to days with .01 inch or more of precipitation - annual
 - 47 Ratio of days with thunderstorms to days with .01 inch or more of precipitation - January, February, March, and April
 - 48 Ratio of days with thunderstorms to days with .01 inch or more of precipitation - May, June, July, and August
 - 49 Ratio of days with thunderstorms to days with .01 inch or more of precipitation - September, October, November, and December
 - 50 Comparative frequencies: days with thunderstorms and days with precipitation of various magnitudes - Kansas City, Mo., 1889-1938

FIGURES (contd)

No.

- 51 Comparative frequencies: hours with thunderstorms and hours with precipitation of various magnitudes - Peoria, Ill., 1905-31
- 52 Average daily precipitation intensity - annual
- 53 Average daily precipitation intensity - January, February, March, and April
- 54 Average daily precipitation intensity - May, June, July, and August
- 55 Average daily precipitation intensity - September, October, November, and December
- 56 Total number of rain occurrences with at least one hourly amount > 0.99 inch - entire period, 1908-37
- 57 Total number of rain occurrences with at least one hourly amount > 0.99 inch - January, February, March, and April, 1908-37
- 58 Total number of rain occurrences with at least one hourly amount > 0.99 inch - May, June, July, and August, 1908-37
- 59 Total number of rain occurrences with at least one hourly amount > 0.99 inch - September, October, November, and December, 1908-37
- 60 Total number of rain occurrences with at least one 24-hour amount > 2.49 inches - entire period, 1908-37
- 61 Total number of rain occurrences with at least one 24-hour amount > 2.49 inches - January, February, March, and April, 1908-37
- 62 Total number of rain occurrences with at least one 24-hour amount > 2.49 inches - May, June, July, and August, 1908-37
- 63 Total number of rain occurrences with at least one 24-hour amount > 2.49 inches - September, October, November, and December, 1908-37
- 64 Depth-frequency curves - thunderstorms in Utah, July and August
- 65 Areal precipitation frequency for 26-week season, April 2 - September 30, Southern Wisconsin

FIGURES (contd)

- No.
- 66 Seven-day areal rainfall equaled or exceeded once in 1, 2, 3, and 5 years, April-September season
- 67 Seven-day areal rainfall equaled or exceeded once in 10, 15, 20, 25, and 30 years, April-September season
- 68 Effect of area on areal precipitation frequency, for 26-week season, April 2 - September 30, Southwest Missouri
- 69 Average number of days with hail - annual
- 70 Average number of days with hail - January, February, March, and April
- 71 Average number of days with hail - May, June, July, and August
- 72 Average number of days with hail - September, October, November, and December
- 73 Ratio of days with hail to days with thunderstorms - annual
- 74 Ratio of days with hail to days with thunderstorms - January, February, March, and April
- 75 Ratio of days with hail to days with thunderstorms - May, June, July, and August
- 76 Ratio of days with hail to days with thunderstorms - September, October, November, and December
- 77 Comparative hail-thunderstorm frequencies - Md.-Del.-D.C. vs. Washington, D.C., and the State of Iowa vs. Kansas City, Mo.
- 78 Monthly variation in tornado days and total number of tornado days per state or section - entire period, 1880-1942
- 79 Monthly variation in tornado days and total number of tornado days per 10,000-square-mile area per state or section - entire period, 1880-1942
- 80 Tornado days per 10,000-square-mile area per state or section - January, February, March, and April, 1880-1942
- 81 Tornado days per 10,000-square-mile area per state or section - May, June, July, and August, 1880-1942

FIGURES (contd)

No.

- 82 Tornado days per 10,000-square-mile area per state or section - September, October, November, and December, 1880-1942
- 83 Months of maximum average: number of thunderstorm days, number of hail days, number of tornado days, and monthly precipitation
- 84 Diurnal variation in thunderstorm frequency - annual
- 85 Percentages of annual thunderstorm occurrences per quarter day
- 86 Diurnal variation in thunderstorm frequency - December, January, and February
- 87 Diurnal variation in thunderstorm frequency - March, April, and May
- 88 Diurnal variation in thunderstorm frequency - June, July, and August
- 89 Percentages of summer thunderstorm occurrences per quarter day
- 90 Diurnal variation in thunderstorm frequency - September, October, and November
- 91 Average number of thunderstorms - June, July, and August
- 92 Average number of thunderstorms during the hours 00-06 local standard time - June, July, and August
- 93 Average number of thunderstorms during the hours 06-12 local standard time - June, July, and August
- 94 Average number of thunderstorms during the hours 12-18 local standard time - June, July, and August
- 95 Average number of thunderstorms during the hours 18-24 local standard time - June, July, and August
- 96 Mean isobars and isotherms at 5,000 and at 10,000 feet, July and August 1941
- 97 Distribution of advective temperature effect in the layer from the first standard level above the surface to 3 km - June, July, and August

FIGURES (contd)

- No.
- 98 Distribution of advective temperature effect in the layer 3-5 km -
June, July, and August
 - 99 Diurnal variation of advective warming effect, surface to 3 km -
August 1938
 - 100 Annual thunderstorm occurrences in excess of thunderstorm days
 - 101 Rainfall-thunderstorm relations - Kansas City, Mo.
 - 102 Rainfall-thunderstorm relations - Lincoln, Nebr.
 - 103 Rainfall-thunderstorm relations - Topeka, Kans.
 - 104 Rainfall-thunderstorm relations - Oklahoma City, Okla.
 - 105 Rainfall-thunderstorm relations - Fort Smith, Ark.
 - 106 Rainfall-thunderstorm relations - Sault Ste. Marie, Mich.
 - 107 Rainfall-thunderstorm relations - Lansing, Mich.
 - 108 Rainfall-thunderstorm relations - Chicago, Ill.
 - 109 Rainfall-thunderstorm relations - Springfield, Ill.
 - 110 Rainfall-thunderstorm relations - New Orleans, La.
 - 111 Rainfall-thunderstorm relations - Tampa, Fla.
 - 112 Rainfall-thunderstorm relations - Memphis, Tenn.
 - 113 Rainfall-thunderstorm relations - Nashville, Tenn.
 - 114 Rainfall-thunderstorm relations - Syracuse, N. Y.
 - 115 Rainfall-thunderstorm relations - Denver, Colo.
 - 116 Rainfall-thunderstorm relations - Portland, Maine
 - 117 Rainfall-thunderstorm relations - Baltimore, Md.
 - 118 Rainfall-thunderstorm relations - San Francisco, Calif.
 - 119 Frequencies of hourly rainfall intensities of selected magni-
tudes at New Orleans, La., 1898-1927

FIGURES (contd)

No.

- 120 Percentage of precipitation occurring at night, April to September, inclusive
- 121 Percentages of excessive-rain occurrences per quarter day - annual and summer
- 122 Isohyetal maps of August 3, 1939 storm, Muskingum Basin, Ohio
- 123 Frequency distribution of recorded rainfall amounts, August 6, 1938 storm, Muskingum Basin, Ohio
- 124 Hyetograph of August 6-7, 1938 storm, Muskingum Basin, Ohio
- 125 Relation between rainfall variability and area for random gage distribution
- 126 Relation between error and number of gages for random gage distribution and storms > 0.5 in.
- 127 Location map of master rain-gage network
- 128 Arrangements of rain gages, 8000-square-mile area
- 129 Arrangements of rain gages, 1500- and 375-square-mile areas
- 130 Errors in uniform rain-gage sampling
- 131 Effect of uniform spacing of gages on accuracy
- 132 Density-area-error graph, uniform network
- 133 Little Mill Creek drainage basin
- 134 One-day storm profiles
- 135 One-day storm profiles
- 136 One-day storm profiles
- 137 Rain-gage combinations used in correlations
- 138 Effect of gage-spacing on degree of rainfall correlation
- 139 Effect of distance from gage on rainfall estimate
- 140 Rainfall-intensity patterns

FIGURES (contd)

No.

- 141 Typical mass curves of one-hour thunderstorm rainfall (point rainfall, fixed station)
- 142 The world's greatest observed rainfalls
- 143 Area-depth curve, August 6, 1938 storm, Muskingum Basin, Ohio
- 144 Area-depth relations below 500 square miles, 6-hour storms
- 145 Percentage area-depth curve, 6-hour storms
- 146 Relations between area-depth curve and storm profile
- 147 Area-depth extrapolation curves, 6-hour storms
- 148 Generalized storm profiles, 6-hour storms
- 149 Typical mass curve of thunderstorm rainfall over a basin
- 150 Duration-depth relations, 375 square miles
- 151 Duration-depth relations, 8000 square miles
- 152 Percentage duration-depth curves for 6-hour summer storms
- 153 Depths of precipitable water in a column of air of given height above 1000 millibars
- 154 Variation with dewpoint of percentage of effective precipitable water at 78°
- 155 Variation with elevation and dewpoint of residual percentage of effective precipitable water

CHAPTER I

THUNDERSTORM FACT AND THEORY

Definition

1. A thunderstorm is defined as the occurrence of thunder. For synoptic purposes or for airways reporting, the definition is further refined to permit reporting a thunderstorm at observation time if thunder, though not current, has been heard within a stipulated period prior to observation time. For the climatological record, the thunderstorm day is defined as the local calendar day on which thunder has been heard, although before 1894 it was Weather Bureau practice to record thunderstorms only if accompanied by rain. Humphreys (1)* has noted that the change in regulations was responsible for a phenomenal increase in annual number of thunderstorms reported in the United States after 1894, but greater attention to thunderstorm activity was also an important factor in the increase. Accepted tabulations of thunderstorm frequencies, such as Alexander's (2), reject the earlier period of record and even the decade of transition prior to 1904.

2. The occurrence of lightning without thunder is not designated as a thunderstorm. The occurrence is reported, of course, but it is not included in the usual summation of thunderstorm days or occurrences. This practice diminishes the area for which a single station can be considered representative of thunderstorm occurrences, the radius of audibility of thunder being much less, ordinarily, than the radius of

* References listed numerically at end of chapter.

visibility of lightning. It is also true, however, that the visibility is much greater at night than in the daylight, so that a diurnal variation of frequencies based on lightning occurrences would not be representative. According to C. E. P. Brooks ⁽³⁾, the radius of audibility is 10 or 12 miles in favorable circumstances:

...but it is unlikely that all thunderstorms occurring within that distance of a station will be recorded, and probably we shall be interpreting the data in a sufficiently generous manner if we consider that the numbers (of occurrences) represent the thunder occurring within a distance of six miles, i.e., in an area of 113 square miles surrounding the station.

3. There is no general agreement on the definition of thunderstorm duration. The beginning is consistently defined as first thunder heard, which is adequate and leads to little confusion since first thunder heard usually precedes first rainfall observed or recorded. Official ending time is the time of last thunder heard, which often follows last precipitation, but not as consistently as first thunder precedes first rain. Only a few statistical studies of duration have been made. Bily ⁽⁴⁾ made such a study for Tampa in 1904, using the elapsed time between first and last thunder. In some cases only one peal was heard, making first and last thunder identical and duration a second or so. Identified in any of these ways, the duration is that which is observed at a point or station. It is not the duration of the thunderstorm as a cell or entity, with origin at one point and end at another. However, the two durations are identical if the storm is stationary. In a study by Brancato ⁽⁵⁾ it was the life of the thunderstorm cell which was considered and the basis of estimate was rainfall duration. In some frequency studies, such as those made in the diurnal-variation section of this report, where time of

occurrence is important, the hour of occurrence is defined as the hour of beginning, and beginning is defined as first thunder heard.

4. For the purpose of this report the duration of prime interest is the duration of measurable rain, although both the duration and direction of the maximum wind are also of importance in flood-control design. The thunderstorm is the subject of the report chiefly because it is often characterized by intense rainfall of short duration and limited extent. The associated phenomena such as lightning, though of interest, are thus only incidental to a study primarily concerned with any rainfall of the "thunderstorm" type. Furthermore, it became clear as the study progressed, that the absence of lightning or thunder should not necessarily exclude from consideration any intense rainfall of limited extent and short duration. However, examination of thunderstorm occurrences yields the greatest number of examples of this rainfall type. Although there are geographical and temporary variations from such a correlation, it is qualitatively true, for instance, as pointed out by Humphreys ⁽¹⁾ that there is a marked similarity between the patterns of the annual variations in number of thunderstorms and in total precipitation. This correlation is shown in figure 106 of "Physics of the Air" ⁽¹⁾, where smoothed averages of annual precipitation for 127 stations widely scattered over the United States are compared with smoothed averages of annual numbers of thunderstorm days at these same stations. Chapter II of this report will present similar data for seasons, months, and diurnal periods. The fact that these more recent statistics do not maintain the correlation throughout does not necessarily destroy the value of using thunderstorm rainfall in a study of this type, but it does suggest that this rainfall class can,

with profit, be made more inclusive.

Surface-observed characteristics

5. The thunderstorm whose characteristics are most often observed in some detail is the "local" type. This is so because such a storm occurs in a setting in which observations of its inception, its growth and, to a more limited extent, its decay are possible. The storms are called local because they are so widely scattered over an area that individual occurrences are not merged into a "general" thunderstorm situation. The time of occurrence is usually the afternoon; the sky is clear or practically so before the storm development begins; and it is usually clearing when the storm is over. Many of the characteristics thus observed are no doubt true also of thunderstorms whose origins and developments are not in such favorable settings, thunderstorms, for instance, occurring above warm-front overcasts or at night. However, some of the characteristics may be restricted to the local type.

6. Before the inception of the storm, cumulus clouds are seen to form. The heights of the bases of these clouds, as will be shown later, can be computed from observations of surface data, a common height being one to two kilometers, or approximately one mile. Both by growth and amalgamation of the cumulus elements, a cloud of greater horizontal and vertical extent then develops, the base height being retained, the whole cloud tapering upward. This is the cumulus congestus, often called the cauliflower cloud because of its bulbous structure. Both its structure and its growth, which is by successive eruptions of small towers, chiefly from the top and center but also from other

portions, are inimical to any notion that the cloud arises from a single impulse or from a uniform ascending current (6). As the vertical growth continues, a thin, cirrus-like veil or scarf cloud may develop immediately above the latest and highest protuberance. It is generally accepted that this results from a lifting of the air above the protuberance by ascending currents below (7), the moisture content of the air above having been increased by turbulent transport from the saturated air below (8). The growing cloud, however, breaks through the veil and penetrates the freezing level. Particularly in the upper levels the bulbous configurations now become less pronounced, the cauliflower appearance disappears, and a tangled, fuzzy, stratiform web of cloud (sometimes called false cirrus) tops the structure, often spreading outward to complete the final anvil shape. At this point the complete cloud structure is called cumulonimbus. Its shape, sometimes also called hourglass, suggests the commonly accepted model of the flow in a convective cell - upflow currents converging toward the waist of the hourglass and diverging at the top (5).

7. It is at this stage of development - the full-grown cumulonimbus - that the rain falls. The first drops are usually few and large; smaller drops apparently cannot fall through the rising currents or are evaporated in descent. Scud clouds and virgae (rain streamers) now beneath the main cloud base are the visible indications of the latter effect. There is a typical or average rain sequence which will be statistically demonstrated in a later chapter but it would be unsafe to consider it invariant. The typical intensity pattern is what Horner has called the "advanced" (9), consisting of a rapidly increasing rate of precipitation, with maximum intensity reached in the first ten minutes of the storm, followed by an

hour or so in which intensities decrease to zero or become inappreciable.

Thunderstorm photographs and motion pictures show the heaviest rain falling from the forward portion of the cloud with diminishing intensities toward the rear. In the paper by Brancato ⁽⁵⁾, the study of several series of half-hourly isohyetal maps indicated that the maximum intensity is achieved within one hour after the beginning of the rain. This is not inconsistent with the pattern of intensity as observed from a point, since the total life of the cell as it moved across an area was being considered. Some series actually showed the maximum intensity on the first map.

8. There are some, but comparatively few, observations indicating that hail also, when it occurs, is usually concentrated near the front or near the edges of the cloud. Most of the lightning and thunder accompanies the rain, and the variations in severity of lightning, thunder, and rain are in general simultaneous. It has often been observed that the rainfall is heaviest after the most violent thunderclap. However, Humphreys ⁽¹⁰⁾ has shown that a simultaneity of occurrence at the level of formation (despite differences in time of observation) can be inferred if one considers the actual velocities of light, sound, and falling bodies - which are in that descending order of magnitude.

9. In considering the average wind sequence it is important to remember that the observations are based on moving storms, since very few storms are entirely stationary. In the local thunderstorm situation the prevailing surface wind is only approximately in the direction of the storm's movement. Before the thunderstorm reaches a particular locality the prevailing wind slackens almost to a calm, changes direction to blow

toward the storm, and freshens as the storm approaches. Just before the rain starts, the wind shifts abruptly to blow in violent gusts outward from the rain area, reaching its maximum velocities during or just before the period of heavy rain, which occurs in the early portion of the storm. Visible indications of the sudden reversal of currents are sometimes the dust whirl at the surface and, more often, the squall cloud at the leading edge of the cumulonimbus base. This squall cloud is a horizontal cylinder of saturated air formed between the rising inflow current and the descending outflow current, with the same direction of rotation and the same general appearance as the squall cloud at a cold front, where the same reversal of current directions is known to occur. As the rain subsides, the wind also diminishes and resumes its prevailing direction. Although the foregoing is the general nature of the wind sequence, many storms are accompanied by winds from all directions in the course of the complete life cycle. The most recurrent characteristic in the sequence is the strong outflow wind during or just before the heavy rain.

10. The temperature at the surface reaches a maximum before the full development of the cumulonimbus, falls slightly as the cloud over-spreads the sky, and then most rapidly during the heavy rain. The minimum temperature reached during the heavy rain may be lower than the wet-bulb temperature of the air before the rain, indicating that evaporation into surface air cannot be the sole cause of the cooling. Within 15 to 30 minutes after the heavy rain abates, the temperature rises a little, and may return to its original value after the rain ends.

11. The barometric pressure falls gradually as the storm approaches or develops but rises abruptly (about one or two millibars) with the

occurrence of the outflow wind and heavy rain, after which it subsides slowly to its former level.

12. The average duration of the rain period is about one hour.

This is, of course, the duration as observed from a station in the path of the storm. In the few instances where it has been possible to trace a single thunderstorm from origin to dissipation across a map, the duration was found to be two or three times as long (5). Its path as a whole can often be identified as parallel to the direction of the wind flow at about 6000 feet above the surface and its rate of movement equal to the speed of the winds at that level (5). However, close examination of the incremental isohyetal patterns for smaller units of time, such as 15 minutes or less, indicates that the correlation can be sustained best for the general or over-all speed and direction of movement. During the smaller intervals, the storm or, more correctly, the isohyetal pattern by which it is hoped to identify its path, moves or spreads up, down and across the wind which apparently controls its total movement.

Instability

13. The upward vertical currents displayed in the growth of the thunderstorm cloud and experienced in airplane and balloon flights are the primary features of the thunderstorm. These currents owe their existence to atmospheric instability, that is, to a thermodynamic condition of the atmosphere such that vertical currents once induced are favored and accelerated. A parcel of air, forced by some initial perturbation to ascend or descend from its original level in an unstable atmosphere, will continue the vertical motion thus begun because it will be less dense than the air through which it ascends or denser than the

air through which it descends. The vertical gradient of density of the environment, in other words, is less than the change of density of the parcel moving through the same height. Neglecting the effect of moisture content on density, this is equivalent to the statement that the atmospheric lapse rate of temperature is greater than the rate of cooling of the parcel.

14. Sir Napier Shaw defines a "Law of Convection" as follows (11):

Convection in the atmosphere is the descent of colder air in contiguity with air relatively warmer.

The law is advisedly stated in this form (although objections may be taken to it for want of strictness) because the driving power of the convective circulation comes from the excess of density of the descending portion, and the excess of density in atmospheric air is due in nearly all cases to low temperature. Differences of density might be caused by differences of pressure or by differences in the amount of moisture contained in equal volumes. But finite differences of pressure cannot persist in contiguous masses of air; the amount of water vapour in air at the ordinary temperatures with which a meteorologist has to deal is only a small fraction of the whole mass, and the colder the air is the less water vapour is required to saturate it. Consequently, although it would be possible in a physical laboratory to display a sample of air which, though warmer, is yet denser than another cooler sample on account of the humidity of the latter, the conditions would not easily occur in nature, and the motive power for convection would be exceedingly small. Such cases may therefore be left out of account, and we may consider that, of two contiguous masses of air, the colder is the denser....

15. During the process in which the instability is realized, potential energy is converted into kinetic energy as the atmosphere attains a more stable state. The vertical currents, as well as increased horizontal wind speeds, are the manifestations of the kinetic energy. The upward currents are responsible for the formation of cloud and precipitation and for the manufacture of hailstones by forcing

repeated excursions of congealed raindrops into regions favorable to their growth. By one theory, to be discussed in paragraph 120, they are also responsible for the generation of electrical charges by rupture of raindrops and therefore, indirectly, for the subsequent lightning discharge and thunder. It will also be indicated later (paragraphs 104-7) that the vertical currents can produce, by concentration of raindrops, a rainfall intensity in excess of any calculable rate of rainfall formation, so that the formation and the fall of rain, in certain instances, should be considered separately.

16. The atmosphere can be described as having absolute instability when its lapse rate exceeds the adiabatic rate of cooling of an unsaturated air parcel. It is then unstable for all vertical perturbations. Similarly, the lapse rate which exceeds the adiabatic rate of cooling of a saturated air parcel is absolutely unstable for saturated air. Such a lapse rate is quite common but usually in an atmosphere which is at the same time unsaturated, at least in the lower layers. For practical purposes, then, two types of atmospheric instability are recognized: conditional instability and convective instability. Both are potential rather than actual; they must be realized. Both are usually found in the atmospheric sounding preceding the occurrence of a thunderstorm.

17. The atmosphere, or a layer within the atmosphere, is conditionally unstable when its lapse rate of temperature exceeds the rate of cooling of a rising, saturated parcel of air at the same pressures and temperatures. Under these conditions, a parcel of air at lower levels, if forced aloft by mechanical or other means, may become saturated and therefore finally warmer and lighter than its environment.

The colder, therefore heavier, environment will then force it to rise at, theoretically, an accelerated rate until the temperatures of parcel and environment are again equalized.

18. A layer of air is convectively unstable, no matter what its lapse rate of temperature, when its vertical distribution of moisture is such that, if the layer is lifted as a whole or cooled by evaporating rainfall into it, its temperature lapse rate will ultimately become absolutely unstable. When such a lapse rate is achieved, the top of the layer is potentially denser than the bottom and any vertical perturbation will thus compel an overturn, i.e., internal free convection. If the layer is also between layers of conditionally unstable air, as it usually is, the convection can penetrate the other layers. More will be said on this point later.

The pseude-adiabatic diagram

19. Atmospheric instability can be evaluated on a pseude-adiabatic diagram. Figure 1 shows a section of this diagram. It is an adaptation of the Clapeyron or p-v diagram in which the pressure in millibars on an exponential scale is the ordinate while temperature is the abscissa. Adiabats appear as straight sloping lines and represent the rate of temperature change of a particle of air raised or lowered without loss or gain of heat as long as condensation does not occur. Pseude-adiabats (also called moist, wet, or saturated adiabats) are curved, dashed lines representing the lesser rate of temperature lapse with height resulting from the difference between the latent heat of condensation released and the adiabatic cooling. There are also w or mixing-ratio lines (solid

and slightly inclined from the vertical) representing the number of grams of water vapor necessary to saturate the space occupied by a kilogram of dry air at the given pressures and temperatures. In figure 1 are also shown, for reference purposes, the graphical methods (with brief textual guide) for the evaluation of the various thermodynamic quantities later to be discussed.

Conditional instability

20. Lifting type. Figure 2 illustrates conditional instability on a chart showing the essential parts of a pseudo-adiabatic diagram. The temperature curve AEFB represents the temperature and pressure of the atmosphere at each elevation and will hereinafter be called the sounding. The pseudo-adiabat representing the change in the moisture and thermal properties of the surface air saturated by lifting is shown as the curved line C'CEFD.

21. If the surface air were lifted dry-adiabatically its temperature changes could be followed on the dry adiabat AC, C being the condensation point (usually called the lifting condensation level, LCL) and determined by the intersection of the dry adiabat and the mixing-ratio line w of the surface air. The mixing-ratio line represents also, as can be seen from figure 1, the change of dew point of the rising particle during the dry-adiabatic lifting process, just as the adiabat represents the change of temperature. Because the decrease of temperature with height in the adiabatic process is about 5.5 F/1000 ft, while the decrease of dew point is about one-fifth as great, or 1 F/1000 ft, at normal air density, the approximate height of the LCL in thousands of feet can be

determined from the difference between the temperature and the dew point at the surface divided by the difference in the rates of decrease, which is 4.5 F. A more accurate method would take into account a wider range of air density because the rate of decrease of vapor pressure in the process is directly proportional to the rate of decrease of the air pressure, and the dew point is a function of the vapor pressure. However, the method outlined yields a close approximation in most thunderstorm situations.

22. From C (figure 2) the surface air follows the pseudo-adiabat until it reaches E, where the pseudo-adiabat and the sounding intersect. As demonstrated in figure 1, the pseudo-adiabat intersects the surface isobar at the original wet-bulb temperature of the rising air, and it therefore represents the rate of decrease of the wet-bulb temperature in the dry-adiabatic process. After saturation, i.e., beyond LCL, the changes of temperature, dew point, and wet-bulb are all represented by the pseudo-adiabat.

23. Until it reaches E the particle of surface air is everywhere colder than its surroundings and tends to return to its former position. At E the particle is in equilibrium with its surroundings, the temperatures being equal. But once sufficient work has been done to lift the surface air above E, the rising particles will find themselves warmer than their surroundings and thus forced to ascend further. The point E is called the level of free convection, LFC. Assuming that the air ascends as a particle passing through an environment continuously possessing thermal properties different from its own, the air will continue to ascend freely to point F, after which it becomes colder than its

environment and is finally halted when it has lost its momentum. The top of its ascent is thus the cloud top which is at H, the level of which is theoretically determined when the area FH (incomplete in figure 2) is equal to the area bounded by pseudo-adiabat and sounding between points E and F.

24. The latter area is called the positive area because it represents work that is realized. FH can be called a negative area because it represents work expended in decelerating the particle. However, the area ACE is the one usually referred to as the negative area since it represents the work necessary to lift the surface air to the level of free convection. A front, an orographic barrier, or convergence may provide the necessary lift.

25. Icing level. Forced lift to LCL, but short of LFC, will produce a cloud whose top is the top of the forced lift. (The realization of convective instability by this lift is not considered at this point because the process being discussed assumes the passage of particles of air through an unchanging environment rather than the mass lift of an entire layer of air.) When lifted beyond LFC, the cloud will tower above the limits of the forced lift. How high it will grow will depend on the height at which the free lift ceases, point F. Clouds are not rain, however, and observational experience has shown that, in general, appreciable rain will not fall nor will a thunderstorm develop unless the saturated particles ascend to a temperature zone where water can coexist in all its three phases - a subfreezing zone. Even in tropical Puerto Rico, where freezing normally occurs at higher levels than in middle latitudes, Choate ⁽¹²⁾ has observed ice-cloud formations

invariably topping the shower clouds prior to rain. There will be further discussion of this item in a later section; at this point two underlying theoretical principles can be stated: first, that before drops large enough to fall as rain can form, the cloud top must be in the ice-crystal stage and, second, before lightning will be discharged the upward vertical velocities must become strong enough to break up the larger raindrops before they become frozen. To achieve the first condition, the freezing level must be low enough; to achieve the second, the distance between LFC and freezing level must be great enough.

26. In so far as the ascension of the particle takes place without environmental mixing, it is the freezing level in the rising air rather than in its environment which must be considered. This is called the lifting or convective ice-crystal level, LICL or CICL, and in conditional instability it is usually higher than the atmospheric freezing level, ICL. The levels are not specifically designated in figure 2, but the first (LICL) is at the intersection of the pseudo-adiabatic path and the freezing isotherm while the second (ICL) is at the intersection of the sounding and the freezing isotherm. The height of LICL is a function of the wet-bulb temperature of the rising air, since that temperature fixes the pseudo-adiabat of ascent. The higher the wet-bulb temperature, then, the higher the LICL, as inspection of the diagram will confirm. And with LICL thus fixed, the height of LFC will vary with the lapse rate: the greater the lapse rate, the lower the LFC. The distance between LFC and LICL will be large, then, when high temperature and high moisture content

combine to produce high wet-bulb temperature and when, in addition, the lapse rate is steep*.

27. Insolational type. In the instability diagram drawn in figure 2, the potential energy of the sounding was realized by lifting. In another type of thunderstorm, variously called the local, air-mass, convective, or heat thunderstorm, insolational heating of the surface layers of air provides the trigger action. It can be designated also as the thermal thunderstorm because it is thermal energy which sets off the conditional instability. Figure 3 shows how instability so realized may be analyzed on the pseudo-adiabatic diagram.

28. Both theory and observation have shown that the atmosphere absorbs comparatively little solar radiation directly ⁽¹³⁾. That which reaches the earth's surface is in part reflected or scattered, and the rest absorbed except for the portion used in evaporation. Over the sea the amounts lost by reflection and by evaporation are greater than over land while the absorbed radiation penetrates to greater depths, so that the resulting temperature changes are less than over the land surface, and may even be negligible. Within the earth's surface the temperature changes will vary with the conductivity, specific heat, and density of the soil. While the sun is down or low, the loss of heat by terrestrial radiation is uncompensated except by atmospheric back radiation, chiefly from water vapor. While the sun is high, the earth's surface is continuously heated by the incoming solar radiation which exceeds

* In meteorological terminology, a lapse rate is "steepened" when the rate of temperature fall with height is increased; thus, on the pseudo-adiabatic diagram, the steeper the lapse-rate curve the smaller the acute angle that it forms with the horizontal.

the outgoing terrestrial radiation if no dense cloud deck intervenes. Although the amount of solar radiation reaches its maximum at noon, the rise in temperature of the earth's surface continues because the loss by terrestrial radiation is not then sufficient to balance the incoming solar radiation. Some hours later, depending on the season and latitude, the balance is reached and after that the earth's temperature falls.

29. The air temperature follows the course of the soil-surface temperature with some lag in the occurrence of the maximum and the minimum. The transfer of the heat upward from earth to air is by a currently unsolved complexity of conductive, radiational, turbulent, and convective processes. The latter two are apparently the most effective in transferring heat to higher levels. The heating from the surface upward forms unstable lapse rates upon which the effect of turbulence and eddy transfer is to produce a dry-adiabatic lapse rate which builds up to moderate levels (varying with ground roughness, initial lapse rate, air mass, season, etc.) by the time the maximum surface temperature of the day is reached. After that, the terrestrial loss of heat, which also begins from the surface, serves to stabilize the lapse rate.

30. The effect of insolation is thus to produce a dry-adiabatic lapse rate in the lower layers, above which the air may be conditionally unstable. The lower air, in this case, has been described as an "isentropic pool" (14). It is all at one potential temperature, that is, all its particles when reduced to a pressure of 1000 mb would have the same temperature. Additional heating at the surface will

create bubbles of air which have higher potential temperatures and must, therefore, rise to the top of the pool. If they become saturated in the process, they can continue upward, warmer than the surrounding, conditionally unstable atmosphere, their own potential temperature continuously increased by the release of the latent heat of condensation of the contained water vapor. Figure 3 illustrates the process.

31. The essential difference between figure 3 for the thermal type and figure 2 for the lifting type of release is that the point C in figure 3, called the convective condensation level, CCL, is determined by the intersection of the sounding and a w line which is an average of the mixing ratios of several lower layers. Ordinarily the average is obtained from the values of the significant points in the first 100 mb, or first kilometer, of the sounding. The assumption is that the convection and turbulence which build up the final adiabatic layer (at constant potential temperature) also result in a constant mixing ratio, in the same way that mixing of salt and fresh water would result in a constant salinity. Because the mixing ratio usually decreases with height, the effect of the vertical mixing is to reduce the dew-point temperature at the surface, an effect borne out by the normal afternoon minimum in the diurnal variations of dew point illustrated in figure 4, from Albright (15). However, other diurnal effects are also suggested in the figure and, in practice, some further adjustment of the moisture values of the sounding may be necessary to include the modifications resulting from advection and evaporation.

32. After point C, or CCL, of figure 3 is determined, a dry adiabat drawn through the point on the diagram intersects the surface isobar at the critical temperature T_c , the temperature which must be reached at the surface before a dry-adiabatic layer is built up to a sufficient height to reach the CCL. Any further heating, even local, will produce the bubbles in the isentropic pool which will rise beyond the CCL and then proceed exactly as above the LFC of figure 2. In the thermal type of diagram the CCL may be, as in figure 3, both LCL and LFC in one. There is no final negative area at the surface except, of course, the area $T_c CA$, representing the amount of thermal energy to be supplied before T_c , and hence CCL, can be reached.

33. Analysis by slice method. The method thus far employed in the analysis of soundings is called the parcel method. However, a theoretical treatment, by J. Bjerknes ⁽¹⁶⁾, of the saturated-adiabatic ascent of air through a dry-adiabatically descending environment has indicated that the atmosphere is always less unstable with respect to a system of real cloud towers than with respect to the infinitesimal saturated particle which is considered in the parcel method. It is likely, therefore, that a method of stability analysis based on the assumption of cloud towers rather than particles would "be better suited for all applications to real nature" ⁽¹⁶⁾. Such a method is called the slice method.

34. The theory of the slice method is also extensively treated in Petterssen's "Contribution to the Theory of Convection" ⁽¹⁷⁾ and a recent practical application of the method is given by Beers ⁽¹⁸⁾. Account is taken of the stability of the sounding, layer by layer

through the atmosphere at least to the 400-mb level, especially beyond the LFC or CCL - the region of cumulus activity. The air column is divided into layers bounded by the critical values reported in the usual radiosonde message and each layer tested separately for instability. The layer is first of all considered dry if a reasonable lift will not saturate it, and wet otherwise. In Beers' application a relative humidity of 70% is regarded as an adequate dividing index. The dry layer contributes to the total instability only if its lapse rate is steeper than the dry-adiabatic - which of course means that its contribution is usually negative. The wet layer contributes to the instability in proportion to the difference between its actual lapse rate and the mean pseudo-adiabatic lapse rate in the layer. Each layer's contribution is weighted by a measure proportional to the layer's depth.

35. The effect of such an analysis is to decrease the number of soundings that can be considered possible thunderstorm-producers. If the sounding shows no conditional instability by the parcel test, the slice method is not even applied. It would only increase the negative character of the sounding. Although the relative-humidity factor, which is considered in the slice method, is neglected in the theoretical consideration of the parcel method, in practice the humidity distribution is always given weight. Willett ⁽¹⁹⁾ states that "about 3-1/2 km seems to be the usual minimum depth of the T_G air mass required in cases of this type of stratification (S air aloft) in order for convective thunderstorms to develop during the day," a commonly accepted criterion being relative humidities over 50% throughout

the 3-1/2-km depth. The slice method, however, brings forward another aspect of the situation which may be of practical interest. Because individual layers are considered in this method, the contribution to instability may be actually negative if the upper layers have a nearly pseudo-adiabatic lapse rate. This may occur even though all layers are moist enough to be called wet, and the sounding, by parcel-method analysis, shows a large positive area. The large positive area may be almost entirely an effect of a very steep, almost dry-adiabatic, lapse rate in the layer immediately above CCL or LFC. It is in such a case that the widest disagreement between forecasts based on the two methods may occur.

36. The slice method may be an improvement on the parcel method. However, by either method more thunderstorm activity than occurs is usually forecast unless other considerations, none of them so diagrammatically neat, are employed. On land and in the afternoon, maritime tropical air almost always has the requisite thermodynamic structure, but the meteorologist will feel little certainty about the thunderstorm prognosis unless a proper dynamic mechanism, such as a front, is also expected. Even then, of course, there is no positive assurance. But the most positive assurance derivable from a thermodynamic analysis is of the non-occurrence of a thunderstorm - and then only if the sounding can be considered representative both in time and in space.

Convective instability

37. Further consideration of the dry-adiabatic layer, the isentropic pool, can serve as an introduction to the diagrammatic analysis of convective instability. The distribution of properties in such a

layer is represented in figure 1 by the triangle with apex at LCL, base on the 930-mb isobar, and sides the 293 A dry adiabat on the right and the 3.8 g/kg mixing-ratio (w) line on the left. The w line intersecting the surface isobar at the dew-point temperature represents the vertical gradient of the dew-point temperature, just as the dry adiabat intersecting the surface isobar at the air temperature represents the vertical gradient, or lapse rate, of the temperature. The pseudo-adiabat finally followed by any air parcels escaping upward from the pool, if extrapolated from the condensation level to the surface wet-bulb temperature as in figure 1, represents the vertical gradient of the wet-bulb temperature. This is the structure of thoroughly stirred, unsaturated air - not always achieved but often approached in nature. All particles within it, if lifted until saturated, will then follow the same pseudo-adiabat; all particles, if cooled to saturation by evaporation of rainfall into the layer, will move to the same pseudo-adiabat. And the layer as a whole, when lifted to saturation or beyond, or cooled to saturation by evaporation, will have a lapse rate identical with the pseudo-adiabatic slope at whatever temperatures and pressures are reached, that slope being part of the pseudo-adiabat extending from the original surface wet-bulb temperature. Saturated air with such a lapse rate is in a state of neutral equilibrium for saturated air. Because its final lapse rate was inherent in the moisture structure of the original layer while it was still unsaturated, the original layer can be identified as convectively neutral. If the original layer were convectively stable, its final lapse rate after saturation would be less than the pseudo-adiabatic, and if

convectively unstable its lapse rate after saturation would be greater than the pseudo-adiabatic. The specific criterion, then, of neutral convective equilibrium is that the vertical gradient of wet-bulb temperature is exactly the pseudo-adiabatic; of convective stability, that it is less than the pseudo-adiabatic; and of convective instability, that the vertical gradient of wet-bulb temperature is greater than the pseudo-adiabatic. After convective instability is realized the lapse rate is conditionally unstable but, since the air is saturated, the final lapse rate is also absolutely unstable. Any vertical perturbation will start an overturn within the layer.

38. Rossby ⁽²⁰⁾ has defined the test for convective instability as a decrease with elevation of Θ_E , the equivalent potential temperature. The equivalent potential temperature is constant along any pseudo-adiabat and, in fact, defines the pseudo-adiabat just as the potential temperature (the air temperature brought adiabatically to a pressure of 1000 mb) defines the dry adiabat. Θ_E is conservative for the condensation or pseudo-adiabatic process, just as the potential temperature is for the dry-adiabatic process, and is defined by Rossby as the temperature of an air particle lifted dry- and pseudo-adiabatically to the top of the atmosphere and then brought back dry-adiabatically to 1000 mb. This involves the realization of all the latent heat of condensation. The values at the top ends of the pseudo-adiabats on the pseudo-adiabatic diagram are equivalent potential temperatures in degrees Absolute. Θ_E can be defined differently ⁽²¹⁾ but the practical difference is negligible. It can be shown that the properties of Θ_E are also the properties of Θ_w , which is the wet-bulb potential temperature, defined

as the wet-bulb temperature brought pseudo-adiabatically to 1000 mb.

As put by Bindon (22):

The wet-bulb potential temperature (Θ_w) appears to have a certain conceptual advantage since it does not require the air to be taken to zero pressure for extraction of its precipitable water. Moreover, the wet-bulb potential temperature is closely related to the wet-bulb temperature, a quantity which can be easily measured.

If the decrease of wet-bulb temperature with height, in other words, is greater than the pseudo-adiabatic, then there is also a decrease with height of both Θ_E and Θ_w . and the layer so characterized is convectively unstable. Thus, by plotting the curve of wet-bulb temperature on the pseudo-adiabatic diagram and comparing its slope with the slopes of the surrounding or adjoining pseudo-adiabats, the fact of convective instability can be determined. In the Rossby diagram, the same kind of comparison is made between the slope of a curve connecting, essentially, successive lifting condensation levels with the slope of a curve of constant Θ_E , which is of course a pseudo-adiabat.

39. In figure 5 the section marked A shows a temperature curve (ABCD) which is conditionally neutral throughout (curve parallel to pseudo-adiabat), convectively unstable between 900 and 700 mb (BCD), and convectively neutral below (AB). This temperature curve is also shown in sections B and C of the figure. The slope of the wet-bulb curve in section A identifies the state of convective equilibrium. The two upper layers (BC and CD), though both convectively unstable, differ in that the upper one is too dry to become saturated in a 100-mb lift. In section B of the figure, the lapse rate resulting

from a 100-mb lift is shown by A'B'C'D' and the changes involved are shown by the arrows. Both lower layers have become saturated, but the lowest one is still in neutral equilibrium while the upper is now unstable for saturated air. Vertical motions, either upward or downward, will be favored, and whether they penetrate beyond the unstable layer depends on the conditions within the adjacent layers. The topmost layer is still unsaturated and shows a slightly steeper lapse rate which is the result of dry-adiabatic lift on any lapse rate originally less than the dry-adiabatic. To isolate the effects of lifting, the process has been carried on without divergence or convergence within the layers, i.e., the pressure difference between top and bottom of each layer has been kept constant. The effects of convergence are the same as the effects of lift, and the effects of divergence the opposite.

Evaporation effects

40. In section C of figure 5 the realization of convective instability by evaporation of rain into the layer is considered. The wet-bulb temperature is, by definition, the temperature to which the air will cool as a result of evaporating water into it at constant pressure. Geometrically, the points on the temperature curve will move along the isobars toward the wet-bulb curve (B'C'). The final lapse rate will be the wet-bulb curve. If for some reason the evaporation is concentrated within a particular layer, as in the illustration, the lesser evaporation above and below may result in an inversion above and a steep lapse rate below, also as illustrated.

41. The amount of moisture necessary to achieve this instability depletes the rainfall and can be computed by the precipitable-water method presented by Solot (23). It is the difference between the amount of precipitable water in the air when saturated at the wet-bulb temperatures and the amount originally present which, at the same pressures, is fixed by the dew-point temperatures.

42. Not only can evaporation set off the convective instability but it also has an important effect on the conditionally unstable medium. If the rainfall evaporates into the environment immediately surrounding the rising air of the conditionally unstable sounding, it will lower the temperature of the environment, i.e., it will increase the temperature span between the pseudo-adiabat of the rising particles and the lapse-rate curve. This increases the positive area, the amount of energy available, and therefore the vertical accelerations.

43. The layers adjoining the convectively unstable layer are usually conditionally unstable. Even when they are only nearly so, conditional instability will probably be achieved by the same lifting which realized the convective instability. This condition will be achieved without the formation of an inversion at the top of the convectively unstable layer, so that further penetrative convection upward is assured. However, no further penetration downward (other than turbulent or inertial) will occur unless the descending air is kept saturated by continual addition of moisture. If it descends dry-adiabatically, its downward penetration will be limited unless the lower layers are superadiabatic, i.e., exhibit an increase of temperature toward the earth's surface greater than the adiabatic

rate of heating of unsaturated air.

44. If the attainment of convective instability by evaporation is considered, other factors become important. Since there is no lifting of the adjoining layers, their lapse rates will remain constant unless evaporation also affects them. Complete evaporation will form a layer stable for saturated air above the convectively unstable layer, while incomplete evaporation will result in greater stability (even an inversion). Immediately below the convectively unstable layer, complete evaporation will also result in stability but incomplete evaporation will cause the formation of a steep (even superadiabatic) lapse rate. If the stability above is slight or the inversion shallow, it may be penetrated and the air proceed upward as in the case of the lifted layer, depending on the conditional instability farther up. But in the special case cited there is no immediate barrier to downward motion - even to dry-adiabatic downward motion at times and for short distances. However, evaporation from heavy rain which saturates the convectively unstable layer may continue below to maintain the saturated condition of the descending air, which will therefore experience pseudo-adiabatic downward motion. Once initiated, as by cooling of air parcels to greater density than their neighbors, a downward current can thus be accelerated by the achievement of convective instability by evaporation. The important downdraft of the thunderstorm is such a current, and intrinsically part of the phenomenon are its accompanying features: the strong, outward gust, the sharp barometer rise, the drop in temperature below the surface wet-bulb temperature. It should also be borne in mind that the necessary

convectively unstable layer is always present in any conditionally unstable sounding which also shows an LFC or CCL (24).

Comparison of mean soundings

45. It is not the intention of this report to present thermodynamic methods of analysis as much more than approaches to the better understanding of the thunderstorm phenomenon. From them a fairly satisfactory but idealized picture of the thunderstorm or cloud development may be obtained, but to forget the simplifications involved is to court the pungently accurate criticism of Boyden (25) who said, concerning a similar analysis, that "the author describes the uses of the tephigram with a certainty that gives the uninitiated the impression that nothing short of carelessness could produce an inaccurate forecast."

46. Others have noted what became apparent during this study: that one reason for the failure to recognize the inadequacy of the thermodynamic analysis of the sounding as a thunderstorm-forecast tool was the textbook practice of analyzing soundings associated with thunderstorm occurrences and assuming that the concurrence of atmospheric instability and the thunderstorm event proved instability to be the sufficient cause. In this study, therefore, soundings on thunderstorm days were compared with soundings on non-thunderstorm days in order to determine what differences, if any, existed.

47. The July 1942 soundings at four stations (Oklahoma City, Omaha, Phoenix, and Washington) were used in the analysis. Each sounding was classified as thunderstorm or non-thunderstorm depending

on whether or not thunderstorm activity (as denoted by reports of thunder or lightning) was reported within the next 12 hours within a radius of about 150 miles of the station. There was no consideration of the causes of the thunderstorm activity other than the generalized causes involved in any analysis of conditional or convective instability.

48. Means at standard elevations for the (approximately) 1100 and 2300 EST soundings, obtained separately for thunderstorm and non-thunderstorm days, are plotted for comparison on both pseudo-adiabatic and Rossby diagrams in figures 6 to 17, inclusive. For Oklahoma City and Omaha the non-thunderstorm soundings were summarized only for days when the surface isobaric pattern showed airflow from the south. In addition to the temperature lapse rates (solid for thunderstorms and dashed for non-thunderstorms), values of mixing ratio and relative humidity at the standard elevations are shown on the pseudo-adiabatic diagrams. The number in parentheses states the number of soundings included in the average. The levels of LFC and CCL are indicated, having been obtained by the methods discussed previously. The top of the positive area is also indicated, as LCC (convective ceiling) when it tops the positive area above LFC and as CCC when it tops the positive area above CCL. In all cases, the values or levels pertinent to the thunderstorm sounding are shown at the left of the curves, the values or levels for the non-thunderstorm sounding at the right of the curves. On the Rossby diagrams elevations in thousands of meters are plotted as closely as possible to the indicated points.

49. Oklahoma City. The 2300 EST soundings at Oklahoma City are shown in figures 6 and 7 (upper half). In figure 6, the pseudo-adiabatic diagram, the thunderstorm sounding is 1 to 3 C colder, the temperature difference gradually decreasing with height to about 330 mb. Above that level there is little temperature difference to 155 mb, after which the thunderstorm sounding is warmer, giving a warmer tropopause with a maximum temperature difference of 4 C in the isothermal layer. The lapse rates in both soundings are about the same, greater than the pseudo-adiabatic to about 500 mb, and after that either conditionally neutral or stable, although the non-thunderstorm sounding continues slightly greater than pseudo-adiabatic to about 350 mb.

50. The relative humidities in the thunderstorm sounding are over 50% to 550 mb, then no lower than 46 to 300 mb, while in the non-thunderstorm sounding they are greater than 50 to only 800 mb, falling to 40 by 700 mb and to 26 around 400 mb. The actual w values are greater in the thunderstorm sounding except from 950 to 850 mb, but relative humidities are greater throughout. The computed values which lend themselves to tabulation are as follows:

	Oklahoma City - 2300 EST						
	Mean w 1st 100 mb	T_c C	T_c F	P at CCL	P at LFC	P at LCC	P at CCC
Thunderstorm	13.4	35.0	95	760	735	200	195
Non-thunderstorm	13.8	39.5	103	715	665	195	180

51. On the Rossby diagram (upper half of figure 7) both soundings are convectively unstable above the surface layer, the thunderstorm sounding to 5000 m and the non-thunderstorm sounding

to 4000 m, but the total decrease of θ_E is greater in the non-thunderstorm case (347-331 A against 345-332 A).

52. Figure 8 and the lower half of figure 7 compare the 1100 EST soundings at Oklahoma City. On the pseudo-adiabatic diagram, figure 8, the thunderstorm sounding is again somewhat cooler in the lower layers, the 2 C to 4 C temperature difference decreasing to about 175 mb, where the temperatures become equal and above which the thunderstorm sounding becomes warmer, with the maximum temperature difference becoming about 3 C in the isothermal layer. There is little to choose between the lapse rates, which are dry-adiabatic in the lowest layer, greater than pseudo-adiabatic to about 500 mb in the thunderstorm sounding and to about 400 mb in the non-thunderstorm sounding, and conditionally neutral or stable above those levels.

53. Relative humidities are above 50% from the surface past 300 mb in the thunderstorm sounding, while the non-thunderstorm relative humidities are over 50 to only 800 mb, falling below 45 at 700 mb and to 30 at 300 mb. Mixing-ratio values are higher in the thunderstorm sounding except in the first 100 mb, as shown in the following tabulation:

Oklahoma City - 1100 EST							
	Mean w	T _c	P at	P at	P at	P at	
	1st 100 mb	C	F	CCL	LFC	LCC	CCC
Thunderstorm	13.3	35.5	96	760	775	195	200
Non-thunderstorm	14.0	40.5	105	715	690	190	180

54. On the Rossby diagram (lower half of figure 7) the 1100 EST thunderstorm sounding is convectively unstable to 5000 m and the non-thunderstorm sounding to 4000 m, but the decrease in θ_E is

345-335 A against 350-333 A, respectively.

55. At Oklahoma City, then, the value of T_c in the non-thunderstorm case should ordinarily be high enough to preclude the forecast of an insolational thunderstorm. This value, it should be noted, results largely from a temperature difference between the soundings, that is, from the comparatively higher temperatures of the non-thunderstorm sounding. The comparative coolness of the thunderstorm sounding is likewise mainly responsible for its lower elevations of CCL and LFC, and such lower values are in agreement with the theoretical prerequisites for thunderstorm activity. The higher relative humidity of the thunderstorm sounding and the greater depth through which the moistness extends are in accord with empirical findings. The greater lapse rate of θ_E (and therefore the greater convective instability) in the non-thunderstorm sounding, however, is somewhat surprising, but it is a natural consequence of the more rapid decrease of moisture with height when the lapse rates of temperature are about the same.

56. Omaha. The average soundings at Omaha show similar characteristics. Figure 9 (for 2300 EST) shows the thunderstorm sounding to be about 2 C cooler than the non-thunderstorm sounding to 550 mb. Between 380 and 310 mb they are at the same temperature, while above that layer the thunderstorm sounding is warmer, with warmer tropopause and stratosphere about 2 C warmer. The lapse rates differ little, being greater than pseudo-adiabatic to about 450 mb, then conditionally neutral or less than pseudo-adiabatic.

57. The thunderstorm sounding exhibits higher relative humidities throughout except around 300 mb. Relative humidity exceeds 50% to 550 mb in the thunderstorm sounding but in the non-thunderstorm sounding it exceeds 50% to only 900 mb and again around 300 mb. Mixing ratios are higher in the thunderstorm sounding except to 950 mb and above 500 mb. The comparative tabulation of computed values follows:

	Mean w 1st 100 mb	Omaha - 2300 EST					
		T_c C	T_c F	P at CCL	P at LFC	P at LCC	P at CCC
Thunderstorm	13.0	37.0	99	740	700	210	200
Non-thunderstorm	11.9	41.5	107	680	620	215	190

58. On the Rossby diagram (upper half of figure 10), both 2300 EST soundings are found to be convectively unstable to 5000 m, except for the first 500 or 1000 m. The decrease of θ_E is only slightly greater in the non-thunderstorm sounding, 343-329 A against 342-329 A.

59. At 1100 EST the thunderstorm sounding at Omaha (figure 11) is about half a degree warmer to 700 mb, then about half a degree colder to 280 mb. At 250 mb the temperatures are the same and above that the thunderstorm sounding is again warmer, with tropopause at 180 mb 2 to 3 C warmer but the stratosphere colder above 100 mb. Except in the surface layers, lapse rates in both soundings are greater than pseudo-adiabatic to about 450 mb, then conditionally neutral or stable.

60. Except at a few levels, the relative humidities of the thunderstorm sounding are greater. They exceed 50% to 850 mb, then average 40 to 300 mb, while the non-thunderstorm humidities exceed 50%

to only 900 mb, averaging 35-40 above that level. The tabulated values follow:

	Mean w 1st 100 mb	Omaha - 1100 EST					
		T_c C	T_c F	P at CCL	P at LFC	P at LCC	P at CCC
Thunderstorm	12.0	38.5	101	710	650	220	200
Non-thunderstorm	11.1	39.5	103	690	595	225	205

61. On the Rossby diagram (lower half of figure 10), the thunderstorm sounding is convectively unstable to 3000 m, the non-thunderstorm sounding to 4000 m. The decrease of θ_E is, in this case, greater in the thunderstorm sounding: 340-327 A against 339-328 A.

62. The differences in the Omaha soundings, although mostly of the same nature as in the Oklahoma City soundings, are of a lesser magnitude, occasionally vanishing. This may be related to a more general phenomenon, dealt with in the following chapter on thunderstorm climatology, namely, the lesser frequency of afternoon or insolation thunderstorms in the area around Omaha. The extremely high values of T_c which appear even in the mean thunderstorm sounding indicate the great amount of surface heating that must be accomplished before the purely insolation thunderstorm can develop. Also noteworthy, as a condition unfavorable to afternoon thunderstorm development, is the low level at which relative humidity falls below 50% even in the 1100 EST thunderstorm sounding.

63. Phoenix. At Phoenix there are important modifications of the differences noted at Oklahoma City and Omaha. At 2300 EST (figure 12) the Phoenix soundings have almost the same temperature at the surface but the thunderstorm sounding is about 1.5 C colder just

above. The temperatures are about equal again from 800 to 300 mb, but at higher levels the thunderstorm sounding is increasingly colder up to its tropopause. The non-thunderstorm tropopause is both higher and colder, however, so that the thunderstorm sounding becomes warmer in the stratosphere. There are only small differences in the lapse rates. Except near the surface, both lapse rates exceed the pseudo-adiabatic to about 500-450 mb.

64. Relative humidities are greater throughout in the thunderstorm sounding but the distribution is peculiar, and relative humidities are comparatively low. In the thunderstorm sounding relative humidities are mostly 30-35% to 700 mb, then from 40 to 60% above that level. In the non-thunderstorm sounding, relative humidities are 25-30% to 700 mb, 30-40% above that. The computed values are compared below:

	Phoenix - 2300 EST						
	Mean w	T		P at	P at	P at	P at
	1st 100 mb	C	F	CCL	LFC	LCC	CCC
Thunderstorm	9.8	46.5	116	665	590	200	195
Non-thunderstorm	9.1	47.0	117	585	575	215	200

65. On the Rossby diagram (upper half of figure 13), the 2300 EST thunderstorm sounding is convectively unstable in the first 1000 m and also between 2000 and 5000 m, with total decrease in Θ_E from 346 to 337 A. The non-thunderstorm sounding is convectively unstable between 500 and 4000 m, the decrease of Θ_E being from 344 to 335 A.

66. The 1100 EST radiosondes at Phoenix (figure 14) show the thunderstorm sounding to be slightly warmer (mostly by less than 1 C) to 700 mb, then at about the same temperature to 250 mb, then colder

to 180 mb, but warmer (as much as 4 C) above. At the tropopause (about 100 mb in each case) the temperatures are equal again, but the thunderstorm sounding is colder in the stratosphere. The lapse rates are similar, greater than pseudo-adiabatic to about 450 mb, stable or conditionally neutral above.

67. There are no important differences in relative humidity although the non-thunderstorm sounding has slightly higher values. In both cases the relative humidities are under 30% to 700 mb, and 30 to 40% above that level. Neither do the computed values show the usual differences:

Phoenix - 1100 EST							
	Mean w	T _c		P at	P at	P at	P at
	1st 100 mb	C	F	CCL	LFC	LCC	CCC
Thunderstorm	8.8	49.0	120	580	540	250	205
Non-thunderstorm	8.8	49.0	120	580	500	290	225

68. On the Rossby diagram (lower half of figure 13), the 1100 EST thunderstorm sounding is shown to be convectively unstable to 6000 m, except in the layers 500-1500 m and 2000-2500 m, with θ_E decreasing from 343 to 334 A. The non-thunderstorm sounding is convectively unstable to 5000 m, except in the layers 500-1500 m and 3000-4000 m, with θ_E decreasing from 341 to 335 A.

69. Although the negligible differences exhibited above indicate that the sounding is a poor guide to thunderstorm forecasting at Phoenix, a closer scrutiny of the data salvages some useful details. Although the T_c values are exceptionally high and too infrequently equaled by observed surface maximum temperatures at Phoenix, they are effectively reached with sufficient frequency at nearby elevated

stations to account for observed thunderstorm frequencies. A consideration of the daily maximum temperatures attained at cooperative stations in Arizona 5000 feet, or more, above the level of Phoenix (1100 feet) shows that they often exceed a T_c of 117 F when reduced dry-adiabatically to the Phoenix level. With elevation a key to its interpretation, even the apparently peculiar distribution of relative humidity in the 2300 EST thunderstorm sounding becomes significant because the distribution provides relative humidities of over 50% above 10,000 feet rather than below. With respect, then, to the elevations of the ground surfaces actually involved in thunderstorm formation in this region, the relative humidities near the surface are about as high as in thunderstorm soundings elsewhere. This is not shown, however, by the 1100 EST sounding at Phoenix - but the number of soundings averaged for that time is only five. At Phoenix the 2300 EST sounding is also closer to the time of occurrence of maximum temperature.

70. Washington, D.C. The last of the stations for which the comparison of soundings was made was Washington, D. C. Appreciable differences between the thunderstorm and non-thunderstorm values can be found. Figure 15 shows the 2300 EST thunderstorm sounding slightly cooler, as has usually been the case. The temperature difference is about 1 C to 300 mb, becoming 2 to 3 C at about 150 mb, which is the pressure at the tropopause of the thunderstorm sounding. This means a colder tropopause in the thunderstorm sounding, which differs from the condition exhibited at the other stations studied. However, the non-thunderstorm sounding has also a second, higher tropopause with a steep lapse rate below it, while the thunderstorm sounding is

practically isothermal or even an inversion at the corresponding levels, so that the thunderstorm sounding is finally warmer above 105 mb and actually 5 to 6 C warmer at the pressure of the higher tropopause in the non-thunderstorm sounding. No explanation of these observations at the higher levels can be offered at this time; they are recorded here to complete the record of the comparisons. It should also be noted that the number of observations included in the average decreases rapidly at the higher levels. The lapse rates, as usual, are in general the same, greater than pseudo-adiabatic between 950 and 710 mb and conditionally neutral or stable elsewhere.

71. At all but a few levels the relative humidities are greater in the thunderstorm than in the non-thunderstorm sounding. In the first case the relative humidities exceed 50% to 500 mb while in the second they fall to 49% by 550 mb. Above these levels, the thunderstorm sounding has humidities varying between 43 and 62% to 300 mb while the non-thunderstorm sounding varies between 45 and 54%. There is not the sharp difference that is exhibited by the Oklahoma City soundings. However, the w values, mostly higher in the thunderstorm sounding, do not differ greatly from the non-thunderstorm values. The computed values compare as follows:

	Mean w 1st 100 mb	Washington - 2300 EST					
		T_c C	T_c F	P at CCL	P at LFC	P at LCC	P at CCC
Thunderstorm	13.4	32.0	90	830	855	205	235
Non-thunderstorm	12.4	35.0	95	790	760	655	315

72. The Rossby diagram (upper half of figure 16) shows convective instability in the thunderstorm sounding to 4000 m, with a θ_E

decrease from 340 to 328 A. The non-thunderstorm sounding is convectively unstable to only 3000 m, with a stable layer between 1000 and 2000 m, and a total Θ_E decrease from 336 to 328 A.

73. The pseudo-adiabatic diagram for 1100 EST (figure 17) shows the thunderstorm sounding to be 1 to 2 C warmer up to 750 mb, then about half a degree cooler to 420 mb, above which the temperatures are equal through an interval of about 70 mb. The thunderstorm sounding is again cooler to 135 mb, with its tropopause at 155 mb, 3 to 4 C cooler than the non-thunderstorm sounding at the same pressure. The non-thunderstorm tropopause is at 135 mb and above that level the thunderstorm sounding is as much as 4 to 5 C warmer. The lapse rates are much the same, greater than pseudo-adiabatic to about 600 mb, about pseudo-adiabatic to 350 mb, and less than pseudo-adiabatic above.

74. Relative humidities in the thunderstorm sounding are higher throughout, greater than 50% to 350 mb, 48% at 300. The non-thunderstorm values fall below 50% at 700 mb and to about 35% at 300 mb. The w values in the thunderstorm sounding are also greater. This fact makes for the most striking differences yet observed in the computed values:

	Washington - 1100 EST						
	Mean w	T_c	F	P at	P at	P at	P at
	1st 100 mb	C		CCL	LFC	LCC	CCC
Thunderstorm	15.1	34.0	93	830	860	190	195
Non-thunderstorm	11.4	39.0	102	730	None	None	315

75. The Rossby diagram (lower half of figure 16), shows the thunderstorm sounding to be convectively unstable to 4000 m, with a Θ_E decrease from 346 to 334 A. The non-thunderstorm sounding shows a stable layer between 1000 and 1500 m but is otherwise convectively

unstable to 3000 m, with a θ_E decrease from 336 to 329 A.

76. Of all the stations considered, it is Washington that exhibits the widest gap between thunderstorm and non-thunderstorm values. However, the comparisons made above are only a sampling of the total field in which comparisons should be made, and they are somewhat weakened, in the cases of Washington and Phoenix, by the fact that non-thunderstorm soundings have not been confined to a synoptic pattern producing flow from the south. The natural expectation would be that the omission of such a synoptic criterion would increase the differences between the two types of sounding. At Phoenix, where the differences are not emphasized, it is probable that other factors, such as orography, are important. However, where the differences are almost negligible despite the use of the synoptic criterion, as at Omaha, the importance of other factors is also indicated. Such other factors are basically dynamic, to be deduced from further synoptic considerations to determine the existence of flow patterns effecting a steepening of the lapse rate or a convergence of air that will result in its mass ascent. It is the latter which results in the sustained lift and the vertical velocity which characterize the widespread thunderstorm situation, rather than the temperature difference between ascending air and environment which is so neatly established by the diagrammatic analysis of the sounding. The assumptions upon which the latter analyses are based are at times remote from reality, although the conclusions reached deserve consideration as qualitative guides.

Thunderstorm updrafts

77. In his experiments with no-lift balloons in England, Dobson ⁽²⁶⁾ found upward currents of one to five meters per second in the first 500 meters. Aviators engaged in gliding or soaring make use of these ascending currents, which they call thermals. Birds soar on these currents. According to Lange ⁽²⁷⁾ they are seldom chimneys or continuous columns but are rather bubbles repeating themselves at intervals. Although practically always in existence, they do not often extend very high except on sunny afternoons or when cold air masses move over a much warmer surface, with unstable lapse rates resulting. If condensation levels are reached, the cumulus formations are begun whose later growth into a thunderstorm depends upon the structure of the air above.

78. When there are upward currents there must also be downward currents, but it is aeronautical experience that the latter are generally spread over larger areas and therefore of lesser magnitude. Accepting the vertical motions as adiabatic and the connecting horizontal motions (of both inflow and outflow) as practically isothermal, the thunderstorm becomes analogous to a heat engine. Its working substance is the atmosphere and its fuel is water vapor. Its heat source is the latent heat of condensation of the water vapor, its cold source, or sink, the atmospheric environment. It requires an impulse to start it - an impulse supplied by insolation, a front, an orographic barrier, or convergence.

79. The maximum efficiency of a heat engine can be expressed in terms of temperature:

$$E = \frac{T_1 - T_2}{T_1}$$

where T_1 is the higher temperature and T_2 the lower. In the thunderstorm engine T_1 is found on the pseudo-adiabat of ascent and T_2 is the dry-bulb temperature of the environment or its wet-bulb temperature when sufficient moisture is evaporated to cool the atmosphere to its wet-bulb temperature. Since temperatures on the thermodynamic scale are in degrees Absolute and T_1 of the order of 300 A, while $T_1 - T_2$ seldom exceeds 10 C, the efficiency of the thunderstorm as a thermodynamic engine can seldom exceed $10/300$, or about 3%.

80. In the ideal condition, where the rising air is considered as a particle surrounded by an atmosphere colder than itself, the upward accelerations are a function of the buoyancy exerted upon the particle because of the difference in density between the particle and its environment. This can be formulated as

$$a = Kg$$

where a is the acceleration of the particle, g the acceleration of gravity, and

$$K = \frac{\rho_1 - \rho_2}{\rho_1}$$

where ρ_1 is the density of the particle and ρ_2 the density of the environment. Since, by the equation of state, the densities can be equated to p_1/RT_1 and p_2/RT_2 , respectively, and since the particle and its environment can be considered to be at the same isobaric level, so that $p_1 = p_2$,

$$K = \frac{\frac{1}{T_1} - \frac{1}{T_2}}{\frac{1}{T_1}} = \frac{T_2 - T_1}{T_2}$$

and a change of sign to give a positive answer for upward acceleration yields

$$K = \frac{T_1 - T_2}{T_2} \quad \text{or} \quad \frac{\Delta T}{T}$$

At any particular level the formula for the acceleration can thus be written $g \Delta T/T$. The factor K , it can be noted, does not differ by much from the maximum efficiency E of a thermodynamic engine.

81. The acceleration thus calculated is greater than actually occurs because the basic theory treats the cloud as an infinitesimal particle rising through an infinite environment at rest. In reality the cloud is not infinitesimal and the upward transport of the cloud air is necessarily connected with the downward transport of the environmental air. The latter is dynamically heated until it reaches the temperature of the cloud. That is, ΔT vanishes. Although the upward accelerations of the air inside the cloud walls may have been ended by this process, J. Bjerknes points out ⁽²⁸⁾, there is still room for internal convection within the cloud itself due to the instability at the cloud top, where the environmental air has not had the opportunity to warm by descent. He notes that, visually, the growth of the storm cloud takes place by repeated eruptions of cloud material from the central core of the cloud. This intermittent growth by successive protuberances continues until the cloud top is at the

temperature of the environment at the top of the positive area.

82. Another qualifying consideration is that there must be interaction between the rising air and its environment. As Shaw ⁽²⁹⁾ points out, the kinematic viscosity of air, weight for weight, is so high as to be suggestive of pitch. The initial moving mass becomes entangled with its environment. Experiments performed by the same author and described in "The Air and Its Ways" ⁽³⁰⁾ showed that air driven by mechanical pressure through an opening carried with it ten times its own volume of air while its initial velocity was correspondingly reduced.

83. Neglecting these effects, which all tend to decrease the vertical velocity, the theoretical velocity can be computed from the formula

$$V^2 = 2Kgh$$

where h is the height to which acceleration is effective. For an approximation a mean ΔT and T can be used. If reasonable values of 5 and 250 A are given to those quantities, h assumed to be 10 km and g 1000 cm/sec², the maximum vertical velocity becomes 63 mps or about 135 mph. The theoretical level at which it occurs is at the intersection of the pseudo-adiabat and the sounding at the top of the positive area (see figures 2 and 3) while the theoretical level of maximum acceleration is where ΔT , the distance between pseudo-adiabat and sounding, is the greatest. The top of the positive area is also the ceiling on the convective acceleration, but the ascent, at the decelerated rate, can theoretically go beyond that ceiling up to the level, as shown on the diagrams, where the negative area becomes equal to the

positive area below. The maximum vertical velocity can also be found by planimetering the positive area on a proper thermodynamic chart such as the tephigram (which the pseudo-adiabatic diagram approximates) and converting to kinetic energy in ergs per gram. By the usual formula kinetic energy is then equal to $\frac{1}{2} V^2$.

84. Vertical velocities of the order computed above, and even greater, have been reported in thunderstorms. That they are not at all steadily maintained is indicated in the XC-35 Gust Research Project of the National Advisory Committee for Aeronautics ⁽³¹⁾. In 134,000 hours of flying time the gust recorders placed on transport planes by the NACA recorded maximum vertical gusts of the order of 82 mph ⁽³²⁾.

85. A commonly accepted proof of the existence of such high velocities is the calculated value of the upward velocity of the air current necessary to support a hailstone of density and diameter known to occur in nature. The meteorological theory basic to the calculation is that the hailstone grows by accretion of liquid water freezing to its surface as the result of the hailstone's repeated upward flights into regions of liquid, and generally supercooled, water. The velocity that will support the hailstone is relative and therefore equal to the terminal velocity of the hailstone when the air is perfectly still. Bilham and Relf ⁽³³⁾ have computed the upper limits of such velocities for hailstones of specific gravity 0.915 and found the following:

Diameter (inches)	Velocity	
	fps	mph
1.0	73	50
2.0	105	72
3.0	130	89

The authors indicate that even higher velocities, though not probable, are possible, particularly in the diameter range above 3 inches, if sufficient and prolonged turbulence is present to decrease the drag coefficient of the stone. Humphreys ⁽³⁴⁾ got similar results and classified the three diameters in the order listed above as "very common," "often reported," and "not extremely rare," adding that diameters of 4 inches and over were doubtful although they have been reported, and even measured and photographed ⁽³⁵⁾. Grimminger ⁽³⁶⁾ and Koch ⁽³⁷⁾ also computed velocities of similar magnitude, the latter obtaining "a maximum ascensional air velocity of 200 feet per second and an optimum hailstone diameter of approximately 3 inches."

86. The obvious question, whether it is valid to assume the necessary existence of an upward current equal to the calculated terminal velocity of the hailstone, has been dealt with by Schumann ⁽³⁸⁾. Assuming that the hailstone grows by collecting all the condensed supercooled water in the volume of air which it sweeps through in its downward path through the cloud, Schumann shows that, with a vertical air velocity of 8 mps, and during a fall from 9 to 4 km, "the concentration of condensed water need not be more than 13 gm/m^3 to produce a hailstone of density 0.6 and a radius of 4 cm" - which means a diameter greater than 3 inches. Measurements of liquid-water content in the upper air are few, but a recent publication of the NACA ⁽³⁹⁾, based on a limited number of observations by the XC-35 airplane, shows a maximum measured value of liquid-water content of 9.25 gm/m^3 below cumulonimbus clouds. Indirect computations of the liquid-water content can be made from the rate of rainfall observed at the ground. The

reported 1-minute rain of one inch at Opid's Camp, California, on April 5, 1926, for instance, indicates a liquid-water concentration of over 50 gm/m^3 , on the assumption of an 8-mps rate of fall of the raindrops. It is obvious that such concentrations of water could not be suspended in the atmosphere without ascending currents to support them, but the velocities necessary to support raindrops are comparatively low, of the order of 8 mps. They will be discussed later in connection with the formation of rain.

Convergence updrafts

87. The possible vertical velocities theoretically deduced in the first part of the last section result from the unstable character of the atmosphere. When they are approached in nature, they appear to be phenomena of small areal extent and short duration, occurring spasmodically. However, large-scale vertical motions are possible which are independent of the stability of the atmosphere, although they cause a steepening of the lapse rate in the lifted air unless the lapse rate is already unstable. The more important vertical motions of this kind arise from the presence of orographic or frontal barriers to horizontal flow or from a dynamic flow pattern producing convergence of air which is compensated by upward motion. In the present state of meteorological knowledge and measuring techniques it is possible to make only approximate estimates of the magnitudes involved.

88. The vertical velocity produced by an orographic barrier is equal to the component of the horizontal wind speed normal to the barrier multiplied by the sine of the angle of the orographic slope.

Neglecting frictional losses, the result is strictly true only of the air in contact with the barrier. In the layers above that, even at the same horizontal wind speed, the vertical component must be reduced, but in a manner which is uncertain because of inadequate knowledge of the streamlines of air crossing mountain barriers. J. Bjerknes (40) considers it a plausible assumption that the vertical component decreases exponentially. For a computation of the effect of Mount Wilson in the Sierra Madre he assumed a halving of the upward component for every 1000-m increase in elevation. A 50-mph wind flowing over a 1:5 slope would thus produce a vertical velocity of about 10 mph* which would decrease to 5 mph at 1000 m, and so forth. The lowest streamlines would follow the slope of the mountain but, higher up, the streamlines would become progressively more horizontal.

89. The frontal surface which is presented by a barrier of colder, denser air acts like the orographic barrier, but even approximate computations are complicated by the fact that the frontal surface or barrier is in motion. The vertical component of the velocity is thus a function of the frontal slope, the wind speed, and the frontal speed, both speeds measured normal to the front. Austin (41) has discussed the practical difficulties of this type of computation. In any case, the known magnitudes of frontal slopes, which are rarely steeper than 1:25, indicate the small vertical velocities possible from frontal effects solely.

* For slopes of 1:5 or less, the tangent of the angle of slope can be used with negligible loss of accuracy.

90. The measurement of convergence, which should be made throughout a substantial vertical depth, is beset with even more difficulties than the measurement of frontal effects. However, it is possible, as Brunt and Douglas ⁽⁴²⁾ have done, to compute the approximate magnitude of the vertical velocities which can result.

91. The ideal convergent-flow model is one of radial inflow toward a center. There is no atmospheric pressure distribution which permits its occurrence as a steady state, but the pattern is approached in a rapidly deepening cyclonic center, at active wave crests on a quasi-stationary front, and possibly in the local or insolational thunderstorm. In the latter case, the convergent pattern may not be readily observed because it is so small, because it is imbedded in a field of translation, and because the Coriolis force acts upon it to make it cyclonic ⁽⁴³⁾. However, if V is the speed of radial inflow at all points on a perimeter $2\pi r$ through a cylindrical depth H , the vertical velocity at height H is equal to $2HV/r$. Figure 18 is a diagram showing the relation of that vertical velocity to the speed of radial inflow for various, comparatively small radii of a cylinder 1 km in depth. Uniform density was assumed in the computation. (To correct for the actual variation of density, the vertical velocity obtained from the figure should be multiplied by the ratio of the mean air density of the column to the air density at height H .) For a constant value of radial inflow, the vertical velocity increases with a decrease in the radius of the cylinder and also with an increase in the cylinder height. For any heights h other than 1 km, the vertical velocities read off the diagram should be multiplied by the ratio h/H . Retaining the 1-km depth

of convergence (which is a common height for the CCL), it can be seen that in the 16-mile diameter (13-km radius) of the local thunderstorm cells examined by Brancato (5), a 10-mps (22-mph) radial inflow velocity would produce only a 1.6-mps vertical velocity at the 1-km level.

92. There are more common types of convergence than that which results, schematically, when the winds from all points on a closed curve blow inward. This is, of course, the most obvious example and it is the case of radial inflow discussed above. It is also the first type illustrated in figure 19, where the schematic patterns are taken from Shaw and Lempfert (14). The extent of the convergence is indicated by the diminution of the area in time from ABCDE to A'B'C'D'E'. A more common type of convergence is illustrated in the second example of figure 19. In this case air from one portion of an area is overtaking the air in front of it while both are moving in the same direction. This type of flow is usually referred to as a downwind decrease of wind and often results from a change of isobaric curvature from anticyclonic to geostrophic, or from either to cyclonic without compensating change of pressure gradient, air density, or Coriolis force. The extent of the convergence is again indicated by the diminution of area from that outlined by the unprimed letters to that outlined by the primed letters. A common variation of the second type of convergence is sketched in the last example of figure 19, where the approach of air toward a cross-current results in the diminution of the area. Warm-sector rains south of a quasi-stationary front often occur in such a condition. The cross-current may act as a barrier to be overrun, or there may be a downwind decrease in the wind approaching the crosscurrent. Both kinds of

activity occurred in the situation used to illustrate this type of convergence. The weather-map examples in figure 19 are selected from periods of heavy rain.

93. For complete accuracy the computation of convergence should include the integration of the inflow around the entire perimeter of the area considered as well as through the effective depth, procedures of no little practical difficulty. Often, however, it is possible to approximate the real condition by assuming a simple downwind decrease of wind over a square or rectangle, since the inflow or outflow across the sides parallel to prevailing direction of wind is comparatively negligible. In such a case, the mean vertical velocity at the height through which the convergence or downwind decrease of wind is effective, is equal to $\Delta V H / Y$, where ΔV is the difference between the mean horizontal inflow and outflow velocities through height H and across distance Y . As in the case of radial inflow, the simplifying assumption of uniform density is retained, so that the result should be multiplied by the ratio of densities, as before. Where H is unity in the units used, the vertical velocity becomes the decrease in wind divided by the distance through which the decrease is accomplished. Figure 20 shows the relationship between vertical velocity and the downwind decrease of wind for a height of 1 mile and various values of the distance Y . For other heights h , the vertical velocity read off the diagram should be multiplied by the ratio h/H . The vertical velocity, for a constant value of ΔV , increases with a decrease in Y or with an increase in H . The maximum depth of convergence (H) and the maximum possible ΔV in the minimum Y are thus manifestly

problems of crucial importance.

94. Figures 18 and 20, although based on certain simplifications, offer another test of the credibility of the vertical velocities deduced from the instability of the sounding or from the terminal velocities of hailstones. The existence of an upward vertical current demands the existence of a field of horizontal convergence to support it, whether the convergence be by radial inflow or downwind decrease of wind. For specific vertical velocities at certain heights and above defined areas, the horizontal velocities that must characterize the convergence pattern are indicated in the figures mentioned. In either flow pattern, it can be seen, the horizontal velocities or velocity differences per unit distance required for the production of great vertical velocities appear to be so large as to be extremely unlikely in nature except for extremely short durations.

Thunderstorm downdrafts

95. Upward currents have been stressed thus far because the primary concern of this report is with rain formation, which results, for all practical purposes, from adiabatic cooling due to upward motion. Before proceeding to the subject of rain formation, however, the most frequently observed thunderstorm wind should also be considered. Often called the thunderstorm squall wind, it is usually experienced as a cold surface current proceeding outward from the storm in violent gusts and often accompanying the heavy rain. It can behave as a minor cold front, acting both to generate further thunderstorm activity in advance of the parent cell and to inhibit further activity in the rear by cutting off the supply of warm air (45).

96. It is originally a downward current that spreads out horizontally, and most actively in the direction of storm movement, when it reaches the ground surface. It is a by-product of the heavy rain rather than a part of the cellular thunderstorm circulation, whose compensatory downward currents are gentle and spread over a wide area. The cooling of the air column by the heavy precipitation is the most important factor in its genesis. This cooling is accomplished by conduction, by melting, and also by evaporation. Brancato ⁽⁵⁾ has demonstrated the importance of the evaporation effect by comparing the wet-bulb potential temperatures aloft with the minimum temperatures finally reached at the surface. Figure 21, adapted from his paper, shows the close agreement obtained. Similar relationships were found in a study of Panama storms ⁽⁴⁶⁾ and in a study of the Pennsylvania storm of July 17-18, 1942 ⁽⁴⁷⁾, both by the Hydrometeorological Section.

97. The accompanying downrush of air is usually attributed to the increased air density due to cooling and to the frictional drag of the falling rain. However, it is of critical importance, though a fact often overlooked, that convective instability achieved by evaporation favors a downward penetration of convection if the pseudo-adiabatic process is maintained in the heavy rain. Neglecting frictional effects and using the vertical-velocity expression $\sqrt{2Kgh}$ for a typical situation where ΔT was 8 A, T 283 A, and h 4000 m, Brancato ⁽⁵⁾ obtained a 37.4-mph mean velocity, to which was added an assumed 15-mph speed of the thunderstorm relative to the earth's surface, giving a squall wind of 52 mph - not an unusual observed velocity.

98. One of the effects of the downdraft is the sharp pressure rise which accompanies it - the "thunderstorm hump" on the barograph. Accepting Levine's (48) suggestion that the pressure rise is less an effect of increased hydrostatic pressure than an effect of the vertical acceleration, Buell (49) has computed the possible vertical velocities based on the magnitude of the pressure rise. He obtained values varying from 29.4 mph for a 1.0-mb rise to 58.8 mph for a 4.0-mb rise. (Part of the pressure rise might also be accounted for by convergence in the lower layers of the atmosphere, temporarily uncompensated by the divergence aloft which accompanies widespread convergence situations.)

Rain formation

99. For the computation of the pseudo-adiabatic curve it is assumed that the water is entirely vapor until 100% relative humidity is reached, at which point it changes to liquid (supercooled, rather than ice, at temperatures below freezing), and that all condensation products fall to earth after formation. Some of these assumptions are contradicted by the results of recent investigations and observations, but the thermodynamic computation is not greatly affected. The latest findings, some still debated, are summarized by Byers (50), Brunt (51), Simpson (52), Houghton (53), and Taylor (54).

100. It has been shown that condensation to the liquid phase is possible only on specific hygroscopic nuclei, the process being a continuous one beginning at relative humidities below 100% but becoming most rapid in the neighborhood of 100% and higher. Specific

sublimation (or crystallization) nuclei are required for condensation directly to the ice phase. As far as is known, more than a sufficient number of condensation and sublimation nuclei are usually present, but sublimation nuclei are less numerous and the existence of liquid droplets at temperatures below freezing is so common in the atmosphere that it is regarded as the rule rather than the exception. The clouds and fogs which form differ from precipitation only in the size and rate of fall of their constituent water droplets. The smallest cloud droplets are apparently in a stable colloidal state, their position in space depending on molecular bombardment rather than gravity. Even when larger, their rate of fall is exceedingly slow and they may evaporate within a short distance. The raindrop can be formed only by further growth and coalescence of the cloud droplets.

101. The growth arises largely from the existence of differences in vapor pressure on adjacent droplets. The droplet containing salt in solution (the dissolved hygroscopic nucleus) has its surface vapor pressure reduced thereby, so that its presence in an environment of saturated vapor results in further condensation upon it - but at a decreasing rate because the concentration of its solute will decrease in the process. The surface vapor pressure of a droplet also varies inversely as its radius of curvature, so that small drops tend to condense on larger. Furthermore, because saturation vapor pressure varies directly with the temperature, warmer drops tend to condense on colder. Most effective of all is the phenomenon of lower surface vapor pressure on an ice surface, so that in the triple-phase state the ice particle can grow at the expense of both the saturated water

vapor and the supercooled water. Findeisen (55) gives the saturation vapor pressure over ice as 91% of that over water at -10 C, and 82% at -20 C. All these processes, especially the last, produce drops large enough to overtake the smaller ones in falling; and the further growth to the size of observed raindrops is probably by collision and coalescence as the larger drops sweep by the smaller ones. Such a probability is increased by Köhler's (56) observation that drop sizes occur in multiples of a unit size and that the chloride concentration of rain water is practically the same as that of cloud water.

102. The cumulonimbus or thunderstorm cloud originates as an iceless water cloud in its cumulus or congestus phases and continues as such to levels considerably above the zero isotherm. According to Findeisen (55), it is only at temperatures below -10 C that ice particles predominate; supercooled drops of water have been observed at temperatures as low as -40 C. At some critical stage, apparently the temperature range between -10 and -20 C, the cloud containing the ice and water particles is saturated relative to water but so supersaturated relative to ice that rapid condensation takes place on the ice particles. These grow rapidly to such a size and weight that they fall through the ascending currents, colliding on their way with both supercooled and other droplets which freeze to them. It is alleged that this process occurs intermittently or repeatedly as indicated by the structure of the hailstone, which is often roughly spherical and composed of successive layers of clear ice and white ice with a core of white ice. The larger hailstones may eventually fall to the ground but the smaller ones melt as they fall below the level of the zero wet-bulb

isotherm ($^{\circ}\text{C}$), usually forming several drops because the liquid drop has a limiting size above which it is broken up by its passage through the resistant air.

103. The terminal velocities of raindrops are much smaller than those of hailstones. As in the case of the hailstone, the frictional resistance offered by the air to the passage of the drop depends upon the relative motion of the two. However, beyond a certain point the terminal relative velocity of the raindrop, unlike that of the hailstone, does not increase with the size of the drop. The drop becomes deformed, spreading out horizontally, so that the air resistance is increased. Drops greater than 5.5 mm in diameter break up before their theoretical terminal velocity is realized. There is no such limit to the size of frozen drops. The latest determinations by Laws (57) show the limiting terminal velocity of the largest raindrop to be 9 mps and, of course, less for the smaller sizes. Prior to his findings 8 mps was considered the limiting velocity. It is higher in the lower density range found in the upper air, the variation being inversely as the square root of the ratio of the air densities. At 3 km above the surface the limiting velocity would thus be about 11.5 mps.

104. It is proper to examine the implications of the terminal velocity of the raindrop. It is a relative velocity and therefore absolutely true only in a vertically still atmosphere. It is less in an atmosphere having an upward vertical velocity of its own, and greater in an atmosphere having a downward velocity. The heavy rain concentrated in the downdraft of the thunderstorm is apparently an instance of the latter type of relative motion. This casts some doubt

on the validity of computations such as the one made in the discussion of vertical velocities (paragraph 86), where the liquid-water concentration aloft was derived from an observed rainfall rate and an assumed rate of raindrop fall of 8 mps. If the rate of fall of the raindrop were greater, the necessary liquid-water concentration would be less. Assuming a 9-mps raindrop velocity with respect to air also moving downward at 9 mps, the Opid's Camp rainfall previously cited (paragraph 86) would indicate a liquid-water concentration of 23.5 gm/m^3 instead of more than 50 gm/m^3 as previously computed. However, the fact that appreciable condensation can occur only in upward currents, i.e., by adiabatic cooling, and the numerous observations and calculations indicating that vertical air currents much in excess of 9 mps do exist, signify that rain already formed will at times remain suspended in space because of its inability to fall through an air current rising faster than the raindrop's limiting terminal velocity. These suspended drops finally reach the earth either by being carried along in the outflow of air above the region of most active convection or as a result of a decrease in the strength of the vertical current. It can be concluded, then, that the so-called terminal velocity of the raindrop is not necessarily equivalent to the velocity involved in rain formation aloft or to the velocity of raindrop fall at the earth's surface in actual situations.

105. If values of moisture content and upward velocity of the air are known, the rate of rain formation can be computed. Its possible magnitude is of interest even though it does not necessarily equal the rate of fall. The total volume of water precipitated in

the formation process, minus the amount left in the clouds and evaporated, will eventually fall to the earth, but at a rate which may differ greatly from the rate of formation. Showalter (58) has proposed the following simple formula for the rate of formation:

$$I = \frac{V_z \rho (w_1 - w_2)}{7}$$

where I is intensity in inches per hour, V_z upward air velocity in mps, ρ density of air at the condensation level in kg/m^3 , w_1 the mixing ratio in g/kg at the condensation level and w_2 the mixing ratio at the top of the lift. The last two values can be read off the pseudo-adiabatic diagram, w_1 at the CCL or LCL, and w_2 at the level of the cloud top (figures 2 and 3). For lift to very high levels w_2 can be considered effectively zero. Since a pseudo-adiabat of ascent with the θ_w value of 26 C is close to the maximum possible, a w_1 of 20 can be assumed for convection originating between sea level and 3000 feet above sea level. Air density in this layer would average about 1.1 in the units above. In a rising current of 1 mps, then, I would equal

$$\frac{1.1 \times 20}{7} = 3.14 \text{ inches.}$$

With a vertical velocity of 9 mps, the rate of formation would be greater than 28 inches per hour.

106. The first is not an uncommonly observed point rate of rainfall and has in fact been approached for an hour's duration in the United States over areas up to 1000 square miles. The higher rate of 28 inches per hour has been exceeded, so far as is known, only over "points," that is, over extremely small areas, and then only for a

duration of seconds or no more than a few minutes. It is obvious that the vertical velocities necessary to produce such high rates of rainfall, if they are considered to be also rates of formation, would, in fact, prevent the fall of any of the rain through the region of the vertical current. The fall would occur elsewhere or when the vertical current subsided.

107. Bentley (59), in the early years of this century, noted the "seemingly inexplicable" descent to earth, simultaneously with vastly larger drops, of numerous minute drops so very light that they descended slowly. This phenomenon, he concluded, furnished reasons for supposing that the air directly beneath such showers does not move violently upward, although such heterogeneity of drop size can also be attributed, in part, to the shattering of drops in fall. It can further be shown that even the existence of a gentle upward current, constant over the area considered and allowing all but the most microscopic drops to fall, does not necessarily imply a uniform distribution of drop sizes in the rain reaching the ground. Drops of different sizes will have different rates of fall; though formed at the same upper level, more large drops will fall to the surface per unit time. A more effective concentration of rainfall at the ground results from the fact that, in the same vertical distance, a horizontal air current transports the slowly falling small drops horizontally farther than the rapidly falling large drops. A shear of the horizontal wind with height would also affect the surface distribution, even if the raindrops were homogeneous in size. In a paper previously mentioned (40), J. Bjerknes found it necessary to make the simplifying assumption of such "homogenized"

rain, since useful measurements of the frequency of various drop sizes in rain are not available.

108. It is possible, under certain circumstances, to neglect the complexity of actual rainfall phenomena, as discussed above, and yet arrive at a method for the computation of rainfall, both maximum possible and actual. Such a method has been described in previous reports of the Hydrometeorological Section on the Ohio River above Pittsburgh ⁽⁶⁰⁾ and on the Sacramento Valley of California ⁽⁶¹⁾. Both on empirical and theoretical grounds, it was assumed that the water vapor entering a region is most efficiently processed in a convective flow model (illustrated in figure 22, taken from the Sacramento report) which is dimensionless except for the height of convection and for the relationship between the height of the convergent layer and the height of convection, a ratio of 1:3. The heights are a function of the dew points in saturated air at 1000 mb. For the computation, then, it is necessary to consider only the horizontal convergence of air (or its contained moisture) into the region. It can be shown that the results of such a computation are not significantly different from the results obtained by use of formulas involving vertical velocities.

109. In the convective-cell model shown in figure 22, the difference between the precipitable-water content of the convergent layer and that of the outflow layer is called the effective precipitable water, W_E . For a surface dew point of 75 F, with the air saturated and in pseudo-adiabatic equilibrium, W_E equals 1.65 inches. The maximum average depth of rainfall over a rectangular area across

which such air was flowing would be $\Delta VW_F/Y$ per unit time, where ΔV is the net inflow velocity or the difference between inflow and outflow velocities in the distance Y . If the area is a 10,000-square-mile square, Y is 100. Using a ΔV of 20 mph, then, the formula yields:

$$\frac{20 \times 1.65}{100} = 0.33 \text{ in/hr}$$

The formula for vertical velocity in such a case is $\Delta VH/Y$. The height of the convergence layer, as assumed in the Hydrometeorological Reports referred to, is about 2 miles. This becomes H in the equation and the vertical velocity at height H then becomes $20 \times 2/100$, or 0.4 mph. However, the total height of the convective cell is 6 miles. Correcting the vertical velocity for density variation and entering it in Showalter's formula for intensity (58), the expression becomes

$$\left(\frac{\Delta VH}{Y} \frac{\bar{p}}{\rho} \right) \frac{\rho (w_1 - w_2)}{7}$$

The density at height H (i.e., ρ) cancels out. Also, since layers instead of particles of air are being considered, mean mixing-ratio values in the inflow and outflow layers of the cell are used. Substituting the appropriate numerical values from a pseudo-adiabatic diagram, and converting from mph to mps, the intensity of rainfall in inches per hour becomes

$$\frac{0.4 \times 1.0 (15.7 - 3.2)}{2.2 \times 7} = 0.32$$

which is in close agreement with the value previously obtained.

110. By either method, then, a valid computation of the average rainfall depth over 10,000 square miles is possible. The distribution

of the rainfall within that area, however, cannot be determined so easily. It is, in fact, the experience of the Hydrometeorological Section, that the W_T method of computation is best adapted to areas of approximately 10,000 square miles (with dimension Y probably not less than 50 miles) and durations not much less than 24 hours, although the shorter durations are not too great a handicap. The complications of raindrop velocities, sizes, and trajectories need not then be considered because for such areas and durations the complications are not reflected in the average depth. The area of the rainfall in a local thunderstorm or the area of locally intense rainfall in a general thunderstorm situation is, however, so small that the complications limit the applicability of any formula based on inflow or vertical velocities. In discussing the margins of safety to be used in excess of computed rainfall values, J. Bjerknes (40) has stated the margin applicable to a "cloudburst of a few minutes" as "incalculable." Because of the inadequate knowledge of the complications, the problem of the maximum possible rainfall for small areas and short durations must at this time be approached statistically, that is, by the collection, envelopment, and reasonable adjustment of known rainfall data. This is discussed in Chapter IV.

Thunderstorm-cell models

111. Many models of the cellular circulation in a thunderstorm have been proposed. Though schematic, they all point to complexities that are unresolved. Besides furnishing the areal rainfall distribution which is the special concern of this report, the model should

also fulfill other requirements. For all ascending air there should be a return flow of descending air. All accelerations upward should be compensated by convergence of mass from the surroundings. The sharp barometric rise in the thunderstorm should be accounted for. Sufficient moisture should be provided to supply the rain. The model should suit the synoptic conditions which release the energy. These are not all the requirements, but no proposed model reconciles all of them.

112. Perhaps the best-known model is the so-called Benard cell, observed experimentally in the laboratory by Benard and brought to the attention of meteorologists by Brunt ⁽⁶²⁾. Benard showed that when a shallow layer of volatile fluid is cooled at the upper surface by evaporation, the liquid forms a number of separate cells in each of which there is upward motion at the center, divergence at the top, and descending motion in the outer portions. The convective cell of figure 22 approximates the central portion of the Benard cell. The diameter of the latter is about 3.5 times the depth of fluid but the cell is non-existent below a critical depth of fluid. It is hexagonal in shape in very steady conditions and becomes drawn out into long strips when a motion of translation is imposed. Brancato ⁽⁵⁾ suggested that in the atmosphere the equivalent of the liquid depth is the height of the instability layer, that is, the height of the positive area. In the maximum case this would also be the height of the tropopause, about 9 miles. The cell diameter would then be about 32 miles and the diameter of the cumulonimbus cloud, coinciding with the region of upward currents, about 16 miles. Assuming that the rain falls

from about two-thirds the width of the cloud, the instantaneous rain pattern would then have a diameter of about 12 miles. The latter dimension was borne out approximately by the half-hourly 0.1-in. isohyets of summer thunderstorms in the Muskingum Basin.

113. It would be wrong, however, to conclude that this is either the average or the limiting size of the individual thunderstorm cell or of its rain pattern. It is merely a commonly observed size in a frequently occurring type of thunderstorm cell. In the paper referred to ⁽⁵⁾ it was pointed out that the tendency for thunderstorms to develop into groups or families complicated the investigation of the areal extent of individual thunderstorms. As a matter of fact, the investigation is complicated to the extent that the very existence of individual cells in the widespread thunderstorm situation cannot be proved. Furthermore, the local storm, which produces an isohyetal pattern that can be reasonably delineated as a unit, not only does not equal the widespread storm as an areal-rainfall producer (which was naturally to be expected) but it also does not equal it as a point-rainfall producer. Examination of all the published half-hourly isohyetal maps of the Muskingum area for the summer months indicated that the highest average and extreme half-hourly amounts at individual stations occurred in situations where the rain was so general that the delineation of individual cell patterns was impossible, whether the assignable meteorological cause was frontal or otherwise. The short rainfall period used seems to rule out the possibility that the higher amounts are largely due to the chance succession of individual cells over the same point. Unfortunately, the Muskingum data

do not include many examples of excessive rates of rainfall, but the observation that the highest point rainfall occurs in the widespread rather than the local storm is also confirmed by the analyses of major storms throughout the United States. While it is perhaps true, then, that the "most conclusive results," as the Brancato paper puts it, "could be obtained by considering only non-frontal thunderstorms and using situations when only a few thunderstorms occurred within the area," it is also true that any conclusions so reached are applicable only to a minor rainfall phenomenon.

114. The synoptic pattern most often characterizing the group-thunderstorm situation is one of convergent flow. The occurrence of higher point rainfall in such situations may be taken as additional evidence of the probability that the lesser, but more sustained, vertical velocities resulting from convergence are actually more important in the production of rainfall than the greater velocities deduced from the instability of the sounding or the terminal velocities of hailstones. It is true, as has been indicated previously, that a convergence pattern is difficult both to locate and to evaluate but it is nevertheless usually found in widespread-thunderstorm situations. Of late it has become customary to belittle the use of convergence as a meteorological cause because it is too often employed merely as a disguise for inadequate comprehension; and an Army Air Forces summary of thunderstorms findings ⁽⁶³⁾ says, ironically, "A good explanation for any unknown weather phenomenon is 'convergence' or 'instability'." However, the possible abuse of the concept does not warrant its exclusion from synoptic analysis or exposition. It is a fundamental

dynamic phenomenon, basic even to the frontal causes which have become more easily accepted.

115. Of particular interest to this report are the models, constructed by J. Bjerknes ⁽²⁸⁾, of the streamlines of air and precipitation in a thunderstorm cell. They are reproduced in figure 23. A central core of upward velocities exceeding 8 mps (i.e., exceeding the limiting terminal velocity of raindrops) is assumed. Thus the central portion of the storm area is deprived of the precipitation formed in and above the zone of maximum upward velocity, and in the stationary storm the precipitation would finally come to earth in a ring-shaped zone surrounding the central core of rapidly rising air. The central region would not necessarily be completely devoid of rainfall, but it would have smaller amounts than its surroundings. From the edges of the anvil top, precipitation in the form of frozen particles would fall into the clear air, probably to be evaporated. Transport pilots have at times observed hail in the clear air in advance of the thunderstorm cloud ⁽⁶³⁾.

116. The rainfall records of the Muskingum and other dense networks were carefully searched for an example of the ring-shaped rain pattern, but without success because of the difficulties involved. In the first place, a stationary storm is unlikely unless it is orographic in origin and, secondly, the synchronization of weighing-gage clock mechanisms was so far from perfect that an instantaneous rainfall pattern could never be surely delineated. Another fact of equal importance is that there seems to be a natural tendency to avoid the ring-shaped pattern in drawing isohyetal maps. A test was made in the

Hydrometeorological Section by plotting a reasonable distribution of rainfall amounts in such a way that they could have fallen as part of a true ring-shaped pattern. Members of the Section were then asked to draw isohyets, their only other information being that the rain fell from a local thunderstorm during a short period. There were several differing results but none was ring-shaped. The differing patterns are compared in figure 24. Although the test described is not conclusive, it is doubtful that anyone who is not told to look for the ring shape will draw it unless the data force it as a unique solution.

117. Even in the stationary storm, illustrated in the first half of figure 23, it can be seen that the concentration of rainfall at the ground will differ from its concentration as it is formed aloft. In general, however, the storm is imbedded in a horizontal air stream which carries it along and whose velocity increases with height so that the storm cloud becomes tilted in the direction of movement, as illustrated in the right half of figure 23. With a central core of upward velocities exceeding the raindrop terminal velocities, the streamlines of precipitation are further distorted to produce a concentration at the forward edge of the storm area, a type of concentration often observed in photographs of active cumulonimbus precipitation. Because the intense rainfall at the leading edge of the cloud results from a concentration of drops formed in a large volume of cloud, any "cloudburst" intensity can be accounted for by constructing a theoretical flow model capable of producing the entire volume of precipitation and allowing the wind to concentrate it over a limited area.

Such a model would not require extreme upward air velocities to produce extreme rates of rainfall. The difficulty is that the possible magnitude of the concentration is unknown except as indicated by known rainfall rates. It should be noted, too, that the effect of a variation in the sizes of the raindrops is ignored in these models.

118. The small arrow representing air descending from the moving storm and blowing outward is the cold downdraft, which runs ahead of the storm beneath the warm air ascending into the cloud from the surface and the storm is apparently regenerated by this activity. In the prolonged thunderstorm, then, the convection seems to be of the open type, the rainfall itself, perpetuating the storm by causing the outward-flowing downdrafts, the air in the storm being continually replaced as the storm advances. In the local storms selected by Brancato ⁽⁵⁾ two hours was found to be the average duration from origin to dissipation, but the conclusion must be limited to the data used. The duration of station rainfall would, of course, be a fraction of that time. Assuming that the rain area is constant in length in the direction of movement, the duration of station rainfall would be that length divided by the velocity of the storm's movement. There is an equally simple relation between the total area of rainfall, the "rain-cell area", and the velocity of propagation ⁽⁵⁾, the limiting assumptions being the same.

Lightning

119. It has been suggested that the thunderstorm might more accurately be called the lightning storm ⁽⁶⁴⁾ because the thunder is

an effect of air compression caused by the tremendous and rapid heating (hence explosive expansion) of the air by the lightning stroke (65).

Mechanisms for the generation of the electrical charges inducing the lightning stroke are still debated and two of the most prominent theories are presented briefly in this section. The reader should be reminded, however, that such electrical manifestations are usual but not invariable accompaniments of intense rainfall. Cameron (66) has noted their complete absence, for instance, in the storm of August 31 - September 1, 1942, which produced many record 24-hour rainfall amounts at stations in New Mexico.

120. The Simpson "rupture theory" of the origin of thunderstorm electricity (67) cites as the essential cause of lightning the breakup of the raindrop by the force of convection, the water becoming positively and the air negatively charged in the process. An electrical separation then takes place, the positively charged drops being concentrated in a region near the cloud base where ascending currents can hold the raindrops in suspension while the negative charge becomes attached to the minute cloud particles which become distributed in the middle and upper portions of the cloud. The lightning discharges are thus from the positively charged lower region of large raindrops in the cloud to the negatively charged upper cloud and to the ground.

121. Wilson's "capture theory" (68) takes into account the previously existing atmospheric gradient, which is positive toward earth. In such a field the lower surface of the drop becomes positively polarized, the upper surface negatively polarized. When the velocity of the drop exceeds the velocity of the ions driven by

the field, the descending positive ions will not overtake the drop, while the ions overtaken by the drop will be repelled by the positive charge on the lower surface. The upward-moving negative ions, however, will be attracted to the lower surface, the drop finally becoming negatively charged. The final distribution of charges within the cloud will thus differ from Simpson's, being negative in the lower portions, positive at the top, and neutral between.

122. Weaknesses have been pointed out in both theories. The discharge from cloud to ground is inadequately explained by Simpson. Wilson does not explain the absence of lightning when drops large enough to fall rapidly are formed in other than thunderstorm situations. Further observations (69) have indicated, however, that Wilson's distribution of charges within the cloud is probably the correct one. Byers (70) emphasizes that the later findings also show that the region of the strongest positive gradient (midway between the centers of positive and negative charge) occurs at about the level of the -10°C isotherm. This is the region also characterized by the coexistence of the liquid, solid, and vapor phases of water, a region already considered of critical importance in the formation of rain. Any causal relation between the triple-phase state and the electrical distribution, however, is unknown.

123. It is a possibility, though, that the position of the icing level (LICL) with respect to the positive area of the unstable sounding bears some relation to the occurrence of hail, lightning, and thunder. In both Simpson's and Wilson's theories, a shattering of the raindrop is a factor in the distribution of electrical charges.

If the LICL is near the top of the positive area, that is, at about the height of the maximum vertical velocities, there will be plenty of opportunity for the shattering of raindrops below the freezing level but little opportunity for further freezing since the velocities will rapidly diminish above that level. The result will be lightning (and thunder) but no hail. If the LICL is near the base of the positive area, there will be little shattering of raindrops because they will freeze early and be borne aloft as frozen drops. The result might then be hail without thunder. However, if the vertical velocity at the LICL is sufficient to suspend and rupture drops and the LICL is at the middle of the positive area, then there is opportunity for both thunder and hail.

The tornado

124. Except in rare cases the tornado is associated with thunderstorm activity. The indications are that it is not in itself an event of hydrologic importance although it may be closely associated with thunderstorm conditions producing heavy rainfall. It seems that in a tornado the lift of moist air does not extend far enough above the condensation level to produce heavy rain. A simple rain-producing thunderstorm must carry the moist air to heights above the ice-crystal level in order to produce appreciable rain.

125. The tornado occurs in a variety of synoptic situations but widespread tornado situations are found almost exclusively in the vicinity of a front, that is, near a junction of air masses either at the surface or aloft. There seems to be no "local" tornado

comparable to or associated with a local thermal thunderstorm. One theory assumes that its peculiar, funnel-like cloud formation is the bending to earth of the squall cloud - the rolling, cylindrical cloud formation often seen at the leading edge of the active cumulonimbus or at the cold front (71). The horizontally elongated structure of the cloud in many photographs seems to bear out this theory. With the rising motion in the forward portion of the squall cloud, it can be seen that the rotation will be anticyclonic when the squall cloud dips to earth on the right of the advancing current and cyclonic when on the left. Very few instances of an anticyclonic whirl have been observed, however, and those observations are considered doubtful. The important fact may be that the tornado also occurs invariably in a field of motion inducing cyclonic vorticity.

126. Thermodynamically the tornado has usually been assumed to result from very great atmospheric instability, and, in fact, obviously resulted from such a condition at San Luis Obispo, California, in 1926, when tornadoes were generated above an oil fire (72), and at Tokyo at the time of the earthquake and fire of September 1923 (73). Brunt (73) has computed the rotational velocities that might have resulted from the oil-fire instability and has found them to be of the same magnitude as those estimated from evidence of destruction by tornadoes, i.e., velocities of about 300 mph.

127. Using data collected by the Hydrometeorological Section, Showalter (74) has recently advanced a theory of tornado genesis which seeks to reconcile the three striking meteorological features which have usually been noted in connection with, or in the vicinity of, a

tornado situation. These are the presence of a dry inversion or stable layer above a layer of moist air at the surface, the presence of dry air above the inversion, and the occurrence of hail in the vicinity of the tornado.

128. A schematic version of the typical sounding in a tornado situation, showing the temperature and wet-bulb lapse rates, is given in figure 25, reproduced from Showalter's paper. In the figure, layer AB has a high moisture content and is convectively unstable. It must, however, be lifted above point D (LFC for point B) before free convection of all parcels within the layer can take place. BC is the stable layer or inversion. It is also convectively unstable, and markedly so, because of the rapid decrease of moisture with height. CD has low moisture content and is conditionally unstable, its lapse rate approaching the dry-adiabatic.

129. Comparison with the section of figure 5 illustrating convective instability attained by evaporation shows that evaporation concentrated in the layer BC will result in a cooling of C to C' and a superadiabatic lapse rate immediately below C'. A new inversion, as shown in figure 5, may develop immediately above point C'. Violent convection or overturning will result but only its penetration downward will be favored. Above, there will be the inversion lid preventing penetration. It is argued that this condition forces the potential energy to be released over a small vertical extent and therefore in a short time and over an area of small diameter; the vertical constraint on the overturning results in the tornadoic whirl.

130. The evaporation must be from precipitation falling through the layer BC. The precipitation can result only from a forced convection, that is, from the mechanical lift of air within layer AB past point D by convergence or a front. It is not likely that insolation could wipe out the inversion. But, at a front or in the convergence zone associated with a front, there can occur the forced convection past point D, already at a temperature below freezing, producing the thunderstorm and the hail. The hail is of importance because its melting results in a sharp discontinuity of terminal velocities, since raindrops fall at a much slower rate than hail. If this discontinuity occurs in the region of layer BC, the evaporation may be concentrated in that layer, with the consequent release of convective instability already mentioned.

131. The theory thus requires that the thunderstorm occur before the tornado, that the thunderstorm be the frontal or convergent rather than the insolational type, and that hail accompany the thunderstorm. With few exceptions, these are the conditions reported in tornado descriptions.

References

132. Abbreviations used in the list of references are explained in the Bibliography. See Appendix.

1. W. J. Humphreys, Physics of the air, 3d ed., 1940, chap. XVII.
2. W. H. Alexander, The distribution of thunderstorms in the United States, MWR, v. 43, 52, and 63, Jul. 1915, Jul. 1924, and May 1935 respectively. (The author made three such studies: for the years 1904-13, 1904-23, 1904-33, published respectively in the volumes listed above.)

3. C. E. P. Brooks, The distribution of thunderstorms over the globe, GBMO, Geoph. Mem., v. 3, no. 24, 1925, p. 153.
4. Joseph Bily, Jr., Thunderstorms at Tampa, Fla., MWR, v. 32, Oct. 1904, p. 457-60.
5. G. N. Brancato, The meteorological behavior and characteristics of thunderstorms, HMS, Off. of Hyd. Dir., USWB, Apr. 1942. (Also published in Aviation, Oct.-Nov. 1942.)
6. S. Petterssen, Weather analysis and forecasting, 1940, p. 73.
7. W. J. Humphreys, Physics of the air, 1940, p. 304-5.
8. Ref. 6, p. 82.
9. W. W. Horner and S. W. Jens, Surface runoff determination from rainfall without using coefficients, Proc. ASCE, v. 67, Apr. 1941, p. 533.
10. Ref. 7, p. 358-9.
11. W. N. Shaw, Principia atmospherica, Proc. Roy. Soc. Edinburgh, v. 34, no. 9, 1914.
12. H. L. Choate, Some observations of showers at San Juan, P.R., BAMS, v. 22, Nov. 1941, p. 371-3.
13. D. Brunt, Physical and dynamical meteorology, 1939, chap. VI.
14. W. N. Shaw, Manual of meteorology, v. 3, 1930, p. 303-5.
15. J. C. Albright, Summer weather data, The Marley Co., Kansas City, Kansas, 1939.
16. J. Bjerknes, Saturated-adiabatic ascent of air through dry-adiabatically descending environment, QJRM, v. 64, 1938, p. 325 ff.
17. S. Petterssen, Contributions to the theory of convection, Geofys. Publ., v. 12, no. 9, 1939.
18. N. R. Beers, Atmospheric stability by slice method, USNA, 1944.
19. H. C. Willett, Discussion and illustration of problems suggested by the analysis of atmospheric cross-sections, MIT Papers, v. 4, no. 3, 1935.
20. C.-G. Rossby, Thermodynamics applied to air mass analysis, MIT Papers, v. 1, no. 3, 1932.

21. Ref. 6, p. 23-6.
22. H. H. Bindon, Relation between equivalent potential temperature and wet-bulb potential temperature, MWR, v. 68, Sept. 1940, p. 243-5.
23. S. B. Solot, Computation of depth of precipitable water in a column of air, MWR, v. 67, Apr. 1939, p. 100-103.
24. E. W. Hewson and R. W. Longley, Meteorology theoretical and applied, 1944, p. 244.
25. C. J. Boyden, Discussion of R. M. Poulter's Cloud forecasting: the daily use of the tephigram, QJRMS, v. 64, 1938, p. 290.
26. G.M.B. Dobson, Observations of wind structure made at Upavon in 1914, Brit. Adv. Comm. for Aeronautics, Rpts. and Mem., no. 325, London, 1917.
27. K. O. Lange, Soaring meteorology, in Flight without power, ed. by L. B. Barringer, 1940, chap. VI.
28. J. Bjerknes, Memorandum on local summer storms, U. S. Eng. Off., Corps of Eng., War Dept., San Francisco, 1940.
29. Ref. 14, p. 307.
30. W. N. Shaw, The air and its ways, 1923, p. 103 ff.
31. NACA, XC-35 Gust Research Project, bull. 1-6, 1941-3.
32. H. K. Gold, Maximum downdraft velocities, unpubl. ms., HMS, Off. of Hyd. Dir., USWB. (In part an interpretation of data in W. G. Walker's Gust loads on transport airplanes, NACA Bull., Jul. 1942.)
33. E. G. Bilham and E. F. Relf, The dynamics of large hailstones, QJRMS, v. 63, 1937, p. 149 ff.
34. W. J. Humphreys, The uprush of air necessary to sustain the hailstone, MWR, v. 56, Aug. 1928, p. 314.
35. T. A. Blair, Hailstones of great size at Potter, Nebr., MWR, v. 56, Aug. 1928, p. 313.
36. G. Grimminger, The upward speed of an air current necessary to sustain a hailstone, MWR, v. 61, Jul. 1933, p. 198-200.
37. A. A. Koch, The dynamics of raindrops and hailstones, Proc. Eng. Conf., S. Pacif. and N. Pacif. Div., Corps of Eng., War Dept., San Francisco, Feb. 1940, p. 241-68.

38. T.E.W. Schumann, The theory of hailstone formation, QJRMS, v. 64, 1938, p. 16.
39. H. B. Tolefson, Flight measurement of liquid-water content of clouds and precipitation regions, NACA, XC-35 Gust Research Project, bull. 9, May 1944.
40. J. Bjerknes, A method of approximate computation of orographical precipitation, S. Pacif. Div., U. S. Eng. Off., Corps of Eng., War Dept., San Francisco, Aug. 1940. (Mimeo).
41. J. M. Austin, Cloudiness and precipitation in relation to frontal lifting and horizontal convergence, MIT Papers, v. 9, no. 3, Aug. 1943.
42. D. Brunt and C.K.M. Douglas, The modification of the strophic balance for changing pressure distribution, and its effect on rainfall, Mem. RMS, v. 3, no. 22, Sept. 1928.
43. H. R. Byers, Nonfrontal thunderstorms, Inst. of Met. (Dept. of Met.), Univ. of Chicago, Misc. Rpt. no. 3, June 1942.
44. W. N. Shaw and R.G.K. Lempfert, The life history of surface air currents, 1906, p. 18-19.
45. G. A. Suckstorff, The formation of cold air masses by precipitation, MZ, v. 55, Aug. 1938, p. 287-92. (In German; translation available in USWB Lib., Washington, D. C.).
46. HMS, Off. of Hyd. Dir., USWB, Maximum possible precipitation over the Panama Canal Basin, Rpt. no. 4, in coop. with Eng. Dept., Corps of Eng., War Dept., Nov. 1942.
47. WBO, Hyd. Unit, USWB, Meteorological analysis of the storm of July 17-18, 1942, over Pennsylvania and New York, Hyd. Supp., Albany, N. Y.
48. J. Levine, The effect of vertical accelerations on pressure during thunderstorms, BAMS, v. 23, Feb. 1942, p. 52-61.
49. C. E. Buell, the determination of vertical velocities in thunderstorms, BAMS, v. 24, Mar. 1943, p. 94-5.
50. H. R. Byers, Synoptic and aeronautical meteorology, 1937, chap. X.
51. Ref. 13, chap. III, p. 49-56.
52. G. C. Simpson, On the formation of cloud and rain, QJRMS, v. 67, Apr. 1941, p. 99-133.

53. H. G. Houghton, Problems connected with the condensation and precipitation processes in the atmosphere, BAMS, v. 19, Apr. 1938.
54. G. F. Taylor, Aeronautical meteorology, 1942, chap. 13.
55. W. Findeisen, Die kolloidmeteorologischen Vorgänge bei der Niederschlagsbildung, MZ, v. 55, Apr. 1938, p. 121-33.
56. H. Köhler, On water in clouds, Geofys. Publ., v. 5, no. 1, 1927.
57. J. O. Laws, Measurements of the fall-velocities of water-drops and raindrops, SCS, USDA, 1941.
58. A. K. Showalter, Rates of precipitation from pseudo-adiabatically ascending air, MWR, v. 72, Jan. 1944, p. 1.
59. W. A. Bentley, Studies of raindrops and raindrop phenomena, MWR, v. 32, Oct. 1904, p. 450-56.
60. HMS, Off. of Hyd. Dir., USWB, Maximum possible precipitation over the Ohio River Basin above Pittsburgh, Pennsylvania, Rpt. no. 2, in coop. with Eng. Dept., Corps of Eng., War Dept., June 1941.
61. HMS, Off. of Hyd. Dir., USWB, Maximum possible precipitation over the Sacramento Basin of California, Rpt. no. 3, in coop. with Eng. Dept., Corps of Eng., War Dept., May 1942.
62. Ref. 13, p. 219 ff.
63. AAF, Off. of Dir. of Weather, Weather Central Div., Thunderstorms, a review of several airline reports, Washington D. C., 1941 (?).
64. J. F. Shipley, Discussion of his article, The air currents in a lightning storm, in Discussion on thunderstorm problems (by various writers), QJRMS, v. 67, Oct. 1941, p. 360.
65. Ref. 1, p. 379.
66. D. C. Cameron, Tropical storm of August 31-September 1, 1942, in eastern New Mexico, WBO Albuquerque, Oct. 1942.
67. G. C. Simpson, The mechanism of a thunderstorm, Proc. Roy. Soc. of London, ser. A, no. 144, 1927.
68. C.T.R. Wilson, Some thundercloud problems, Jour. Franklin Inst., v. 208, July 1929, p. 1-12.

69. G. C. Simpson and F. J. Scrase, The distribution of electricity in thunderclouds, Proc. Roy. Soc. of London, ser. A, no. 906, v. 161, Aug. 1937, p. 309-52.
70. H. R. Byers, General meteorological aspects of thunderstorm electricity, BAMS, v. 20, May 1939, p. 181-6.
71. E. van Everdingen, The cyclone-like whirlwinds of August 10, 1925, Proc. Kon. Akad. Wetensch., v. 28, no. 10, Amsterdam, 1925, p. 871-89.
72. J. E. Hissong, Whirlwinds at oil-tank fire, San Luis Obispo, Calif., MWR, v. 54, Apr. 1926, p. 161 ff.
73. D. Brunt, Tornadoes started by an oil fire, Met. Mag., v. 62, Jan. 1927, p. 292-4.
74. A. K. Showalter, The tornado, an analysis of antecedent meteorological conditions, in Preliminary report on tornadoes, HMS, Off. of Hyd. Dir., in coop. with WACM, USWB, 1943.

CHAPTER II

THUNDERSTORM CLIMATOLOGY

Years of record

133. Before proceeding to a description of thunderstorm distribution in the United States, it is profitable to examine the type of frequency value used and the period of record which may provide an acceptable normal. The record most available is that of the average number of days with thunderstorms per month and per year. The lengths of record vary and suspicion has been cast on the record prior to 1904 by Humphreys ^{(1)*}. The comparative-data summaries issued periodically by the first-order stations of the Weather Bureau are based on total records sometimes beginning as early as about 1870. The annual-distribution map on page 729 of "Climate and Man" ⁽²⁾ is ostensibly based on the period of record 1899-1938 but examination of the basic data submitted by the stations contributing to this summary indicated that many stations used their total record rather than their 1899-1938 record. However, unless the record terminated many years before 1938, this did not make too much practical difference. Consideration was given to the weakness of the early record by Alexander, whose three decennial papers ⁽³⁾ on thunderstorm distribution in the United States included no data prior to 1904. His last paper brought the summarization up to 1933. For this report his tabulations are brought up to 1943, making a 40-year record.

* References listed numerically at end of chapter.

134. Because many stations had been opened and closed during this period, some criterion was needed to determine how short a record should be included in the final summary. In some sections of the country, however, the distribution of thunderstorms may be so erratic that any length of record would be more useful than none at all - at least as a guide where otherwise there would be no data. Because of the limitations of time, the test of the reliability of the mean was limited to the compactly summarized data for Kansas City ⁽⁴⁾. Figure 26 is a graphical analysis of the variation of thunderstorm-day occurrences at Kansas City, the annual record and the maximum-month (June) record being illustrated. The annual occurrences during the 50 years deviate on the average 6.9 days from the final mean of 56.1, the extreme deviation being 24.1. The 1904-43 mean is 56.2. The average June deviation is 2.5 from a mean of 9.9, the extreme deviation being 10.1. The graph of progressive annual averages shows a comparative steadiness of the mean after about 10 years, while the moving 10-year averages give some assurance that with such a length of record, particularly in the 20th-century era of more accurate observations, there is at least an even chance of an acceptable mean. The 10-year annual mean deviation from the final mean is only 2.9, the extreme 7.5. The deviations are equal to or less than the mean deviation in 56% of the cases. The mean deviation of the 10-year June averages is only 0.6, the extreme being 1.5. In 54% of the cases the actual deviations are less than the mean deviation. A 10-year record was thus considered acceptable for this study.

Distribution of thunderstorm days

135. Figure 27 shows, by histograms, the monthly variation of the frequency of thunderstorm days at some 200 stations in the United States. Most of the data for the chart were obtained from the periodical station summaries ("comparative data"), discussed in the previous section, the first year of record varying widely and the final year of record varying in most cases from 1938 to 1942. Some additional data were obtained from the 1930 Section Summaries of Climatological Data, and some by mail, for stations no longer operating. A few California stations were added from an unpublished compilation by L. G. Gray, on file at the San Francisco Weather Bureau Office.

136. The chart shows a gradual confinement of thunderstorm activity toward the midsummer maximum westward and northward from the Gulf of Mexico. There are exceptions to the trend, however. Pacific Coastal stations have their maximum thunderstorm activity in the winter although the actual numbers of occurrences per month are too small to appear on the chart. Texas stations and some island or extreme coastal stations on the Atlantic are characterized by rather flat histograms, although close inspection of the data reveals May as the peak month characteristic of most of Texas. Another variation of the trend is that in the region directly north of the Gulf there is greater winter thunderstorm activity on the west side of the Appalachians than on the east at the same latitude. From the Rockies westward there is almost no winter activity except along the extreme Coast. In general, however, the monthly variation in thunderstorm days corresponds to the monthly variation in the altitude of the sun.

137. C.E.P. Brooks ⁽⁵⁾ has shown that the latitudinal decrease northward of thunderstorm activity is characteristic of the global distribution. In the United States such a decrease is maintained in general, but several distorting influences are imposed on the annual pattern, and especially on some of the monthly patterns. In the Far Western States the annual pattern shows a distinct decrease of frequency toward the Coast. Such a gradient arises from the fact that the thunderstorm activity in that region, with the exception of the immediate Coast, hinges on the extent of westward displacement of the Atlantic High or the summer midcontinental high-level anticyclone ⁽⁶⁾. Even though the current displaced is from the south, and therefore a diminishing source of moisture as it goes northward, its east-west displacement is the more important factor. The south-north gradient of thunderstorm activity is also varied by a sharp secondary maximum in annual frequency over the southern Rockies, an effect of the orographic barrier intercepting a northwestward trajectory of air from the Gulf of Mexico. There is also a longitudinal decrease westward across the Plains States and, associated with it, what might be called a sustained activity northward through the Mississippi and Missouri Valleys. It will be shown later in the analysis of the diurnal variation of thunderstorm activity, that the Plains States and the Upper Missouri and Mississippi Valleys are also the region of the maximum occurrence of nocturnal thunderstorms. Means ⁽⁷⁾, in an analysis discussed in the diurnal-variation section, has shown that a regional summer flow pattern, not operative on the same scale elsewhere in the United States, is largely responsible for the

nocturnal maximum and, hence, also for the apparently excessive or "sustained" activity. The distortions mentioned are more easily visible, both annually and monthly, in figures 28 through 31. These charts also make obvious what only a close scrutiny of figure 27 can elicit; the month of mean maximum thunderstorm activity is not the same at all stations. It will be demonstrated later that this variation has a consistent geographical pattern.

138. For the charts in figures 28 to 31 the most acceptable averages were those obtained from the record since 1904, i.e., from a tabulation, brought up to date, of the data collected by Alexander (3). Although Alexander's maps were available through 1933, his totals for each station were available only through 1923, published with the second of his papers on the subject. These totals were accepted as published, except in the few cases where other uses of the data revealed discrepancies great enough to require checking. The next 20 years of record were obtained from the Meteorological Yearbooks (formerly Reports of the Chief of the Weather Bureau) through 1940 and from the manuscript pages of the unpublished Yearbooks for 1941-43. One of the purposes of table 1 is to make available the final totals for future use. All the 217 stations used in figures 28-31, inclusive, are listed in the table and the total length of record in whole years indicated for each station. Table 2 lists the maximum and minimum numbers of days with thunderstorms, for each month and for the year, at each of the 217 stations for the period of record indicated.

139. From the tabulation of total occurrences, annual and monthly means were computed and plotted. The isoceraunics, i.e.,

Table 1
TOTAL THUNDERSTORM DAYS, 1904-43

Station	Yrs.	J	F	M	A	M	J	J	A	S	O	N	D	Ann.
Abilene, Tex.	40	27	41	91	186	302	250	211	227	124	94	44	26	1623
Albany, N. Y.	40	5	3	25	61	140	242	292	198	105	30	10	5	1116
Albuquerque, N. Mex.	12	2	4	11	27	56	78	168	169	74	35	5	5	634
Alpena, Mich.	40	1	2	37	70	156	208	248	199	142	43	15	4	1125
Amarillo, Tex.	40	7	9	34	111	260	273	291	283	158	98	17	2	1541
Anniston, Ala.	25	23	57	104	129	192	313	369	305	165	41	25	29	1752
Apalachicola, Fla.	18	32	40	67	62	86	220	323	291	190	32	21	23	1387
Asheville, N. C.	40	12	22	82	128	287	459	550	419	187	30	9	7	2172
Atlanta, Ga.	40	32	64	150	169	260	435	534	426	186	36	26	30	2348
Atlantic City, N. J.	40	7	23	45	95	144	229	252	209	95	41	18	10	1168
Augusta, Ga.	40	28	47	103	141	204	387	489	371	167	44	23	19	2023
Austin, Tex.	17	19	21	56	90	109	92	90	72	61	35	22	19	686
Baker, Oreg.	39	0	0	4	36	85	165	151	122	67	15	1	0	646
Baltimore, Md.	40	4	17	52	90	206	269	353	254	115	35	6	7	1408
Bentonville, Ark.	17	25	31	79	113	167	195	144	142	99	61	38	20	1114
Binghamton, N. Y.	40	4	12	42	60	179	240	322	216	113	40	7	3	1238
Birmingham, Ala.	40	49	83	162	206	296	491	591	497	266	66	46	47	2810
Bismark, N. Dak.	40	0	0	1	35	149	281	333	262	116	26	1	0	1204
Block Island, R. I.	40	4	16	41	68	103	140	167	167	71	36	24	4	841
Boise, Idaho	40	4	7	30	51	121	145	129	103	69	23	9	4	695
Boston, Mass.	40	4	4	31	42	112	153	200	165	79	19	5	7	821
Broken Arrow, Okla.	12	11	13	53	102	112	123	99	105	70	50	23	13	774
Brownsville, Tex.	21	6	10	27	48	95	61	97	86	101	38	9	17	595
Buffalo, N. Y.	40	7	16	52	68	174	226	265	220	140	66	30	5	1269
Burlington, Vt.	38	2	1	17	38	139	225	301	223	113	39	3	2	1103
Cairo, Ill.	40	55	64	167	240	331	417	390	334	217	86	69	35	2405
Canton, N. Y.	37	5	7	29	47	109	181	252	193	112	52	11	1	999
Cape Henry, Va.	36	11	29	78	130	217	327	342	296	136	44	18	11	1679
Cape May, N. J.	22	4	13	25	61	64	121	144	112	51	12	8	1	616
Charles City, Iowa	39	3	5	43	117	247	317	321	282	197	83	23	2	1640
Charleston, S. C.	40	25	68	89	135	234	377	493	466	220	48	29	20	2204
Charlotte, N. C.	40	16	40	99	133	235	387	478	357	154	37	20	12	1968
Chattanooga, Tenn.	40	30	61	165	187	283	457	493	431	202	43	32	22	2406
Cheyenne, Wyo.	40	0	0	6	100	208	457	548	468	188	38	0	0	2093
Chicago, Ill.	40	14	21	89	133	223	306	288	273	184	75	37	3	1646
Cincinnati, Ohio	40	24	31	128	161	284	368	451	313	200	72	27	18	2057
Cleveland, Ohio	40	9	22	73	114	201	263	314	225	163	81	27	7	1499
Columbia, Mo.	40	33	40	126	206	337	391	336	359	234	111	66	22	2258
Columbia, S. C.	40	22	37	86	149	239	388	485	393	175	34	15	15	2025
Columbus, Ohio	40	17	28	112	146	250	378	389	276	164	57	32	10	1859
Concord, N. H.	35	2	1	15	29	100	143	208	168	76	19	5	4	780
Concordia, Kans.	40	2	11	55	149	263	383	332	351	213	85	29	7	1880
Corpus Christi, Tex.	40	31	44	94	138	234	163	201	169	235	101	44	47	1501
Dallas, Tex.	30	52	65	25	200	247	214	162	169	118	96	52	51	1551
Davenport, Iowa	40	8	19	76	143	272	345	322	296	211	84	40	11	1827
Dayton, Ohio	29	14	29	81	119	188	273	271	224	133	51	23	9	1435
Del Rio, Tex.	38	13	21	56	130	182	123	123	108	81	61	26	16	940
Denver, Colo.	40	1	1	21	81	212	407	501	462	181	41	2	1	1941
Des Moines, Iowa	40	7	10	80	155	275	369	347	320	242	118	35	5	1963
Detroit, Mich.	40	7	23	71	111	201	280	287	242	153	74	23	4	1476
Devils Lake, N. Dak.	39	0	0	2	36	126	277	304	260	110	23	2	0	1140
Dodge City, Kans.	40	3	8	41	124	252	379	355	336	172	85	19	4	1778
Drexel, Nebr.	10	0	4	17	50	79	133	124	117	76	19	6	1	626
Dubuque, Iowa	40	3	15	64	135	241	325	317	268	193	80	34	3	1678
Due West, S. C.	11	4	27	48	57	100	148	178	122	88	23	7	14	816
Duluth, Minn.	40	2	3	13	50	146	260	274	232	133	45	11	0	1169
Eastport, Maine	40	4	3	13	15	61	117	172	112	55	32	10	2	596
Elkins, W. Va.	40	6	29	71	126	256	373	429	287	166	52	9	8	1812
Ellendale, N. Dak.	15	0	0	5	23	58	110	116	114	52	13	4	1	496
El Paso, Tex.	40	9	14	27	48	112	197	370	375	151	88	18	11	1420
Erie, Pa.	40	10	23	62	109	188	250	261	213	160	91	28	7	1402
Escanaba, Mich.	40	0	5	37	63	150	242	317	236	159	66	18	1	1294
Eureka, Calif.	40	28	23	18	5	10	2	6	4	14	14	20	26	170
Evansville, Ind.	40	36	46	142	200	290	366	348	305	198	82	56	31	2100
Flagstaff, Ariz.	9	1	4	3	17	21	29	148	177	74	18	5	0	497
Ft. Smith, Ark.	40	62	70	165	253	336	369	301	313	187	136	65	40	2297
Ft. Wayne, Ind.	32	10	20	73	107	180	235	257	196	128	59	19	9	1293
Ft. Worth, Tex.	40	61	78	148	260	338	275	237	243	166	130	60	42	2038
Fresno, Calif.	40	5	18	25	37	27	15	14	5	17	18	9	10	200
Galveston, Tex.	40	65	78	101	163	191	186	317	307	244	100	67	82	1901
Grand Haven, Mich.	29	4	13	42	80	136	159	166	157	115	50	26	5	953
Grand Junction, Colo.	40	1	7	33	76	161	207	446	407	203	69	9	3	1622
Grand Rapids, Mich.	40	7	24	65	115	204	261	274	247	189	83	40	8	1517

Table 1 (contd)

Station	Yrs.	J	F	M	A	M	J	J	A	S	O	N	D	Ann.
Green Bay, Wis.	40	0	13	37	90	179	245	283	232	168	62	19	2	1330
Greensboro, N. C.	14	7	17	35	39	97	152	180	133	58	14	5	5	742
Greenville, S. C.	21	10	23	62	77	147	208	279	201	98	27	8	13	1153
Groesbeck, Tex.	12	20	33	58	73	98	97	75	67	68	55	26	22	692
Hannibal, Mo.	29	15	21	90	125	196	239	214	224	160	62	31	10	1393
Harrisburg, Pa.	40	5	15	38	92	206	287	357	266	113	48	6	4	1437
Hartford, Conn.	38	6	9	36	66	137	198	277	214	96	40	13	6	1098
Hatteras, N. C.	40	32	48	96	125	188	250	316	264	147	49	40	31	1586
Havre, Mont.	40	0	0	5	24	111	295	282	213	73	6	0	0	1009
Helena, Mont.	40	4	0	8	47	206	349	409	313	118	20	2	1	1477
Houghton, Mich.	29	0	3	19	35	88	139	153	130	100	36	9	0	712
Houston, Tex.	34	56	72	107	143	192	240	353	328	213	111	56	78	1949
Huron, S. Dak.	40	0	3	23	80	216	356	353	320	186	54	7	0	1585
Independence, Calif.	20	0	0	1	8	19	24	84	69	19	12	1	0	237
Indianapolis, Ind.	40	18	31	120	172	269	366	362	302	207	72	50	19	1988
Iola, Kans.	26	14	22	64	132	203	219	189	189	156	77	28	6	1299
Ithaca, N. Y.	35	3	7	29	53	156	210	267	182	119	45	8	2	1091
Jacksonville, Fla.	40	41	75	122	164	315	556	752	637	336	86	21	33	3138
Jupiter, Fla.	10	3	13	29	35	77	118	150	112	81	40	8	8	704
Kalispell, Mont.	40	1	0	6	21	121	205	239	162	66	13	1	0	835
Kansas City, Mo.	40	20	43	121	222	309	402	344	342	255	129	50	14	2251
Keokuk, Iowa	40	14	33	104	167	293	362	335	323	213	108	45	10	2027
Key West, Fla.	40	45	59	77	121	204	376	510	540	478	178	40	49	2677
Knoxville, Tenn.	40	16	50	125	182	282	397	449	362	180	28	27	17	2115
La Crosse, Wis.	40	2	6	48	119	264	343	293	224	81	23	1	1	1738
Lander, Wyo.	40	0	0	2	39	106	202	246	231	75	11	1	0	913
Lansing, Mich.	33	1	19	58	94	182	255	235	217	165	60	25	4	1315
Lewiston, Idaho	29	1	3	9	28	61	102	105	87	45	15	1	1	458
Lexington, Ky.	29	20	35	72	118	190	278	306	227	140	38	20	17	1461
Lincoln, Nebr.	40	3	9	48	141	253	379	350	330	225	86	22	4	1850
Little Rock, Ark.	40	68	87	192	278	285	372	368	324	184	99	83	60	2400
Los Angeles, Calif.	40	22	26	43	29	16	10	6	16	19	21	8	20	236
Louisville, Ky.	40	40	39	137	176	245	347	349	234	177	60	44	19	1917
Ludington, Mich.	20	2	10	28	55	85	138	137	123	103	42	17	3	743
Lynchburg, Va.	36	2	9	42	74	163	313	331	251	99	19	5	8	1316
Macon, Ga.	40	37	66	128	174	241	426	531	439	175	45	21	22	2305
Madison, Wis.	39	3	18	55	133	249	326	324	285	197	75	39	5	1709
Marquette, Mich.	40	0	2	24	38	117	215	251	195	113	35	10	0	1000
Medford, Oreg.	16	1	1	0	16	30	25	26	14	18	5	1	0	137
Memphis, Tenn.	40	61	77	161	225	261	338	362	307	175	74	62	51	2154
Meridian, Miss.	40	66	101	178	229	275	437	522	421	207	65	55	70	2626
Miami, Fla.	32	29	45	62	152	248	372	445	406	359	137	34	26	2315
Miles City, Mont.	38	0	0	3	29	119	285	257	197	50	10	2	1	953
Milwaukee, Wis.	40	7	18	53	113	198	272	242	238	182	69	35	3	1430
Minneapolis, Minn.	40	1	7	30	85	235	323	308	279	198	81	19	0	1566
Missoula, Mont.	8	0	0	1	8	33	42	57	41	26	2	0	0	218
Mobile, Ala.	40	64	104	154	196	263	483	650	582	287	83	48	68	2982
Modena, Utah	40	4	10	37	84	147	121	160	163	169	58	17	5	1575
Montgomery, Ala.	40	63	103	178	192	247	436	499	443	210	54	44	53	2522
Moorhead, Minn.	39	0	1	10	54	171	252	273	253	132	34	3	0	1183
Mt. Tamalpais, Calif.	17	6	3	4	1	0	1	1	1	7	1	2	5	29
Nantucket, Mass.	40	8	19	38	56	97	129	153	133	67	47	27	12	786
Narragansett Pier, R. I.	14	2	6	7	17	29	39	56	54	20	9	7	1	247
Nashville, Tenn.	40	36	67	160	212	294	403	441	336	190	68	39	39	2285
New Haven, Conn.	40	6	13	32	64	156	222	268	227	100	34	15	9	1146
New Orleans, La.	40	79	97	154	194	265	457	627	603	316	94	48	73	3007
New York, N. Y.	40	12	17	39	89	188	268	332	246	117	47	22	9	1386
Norfolk, Va.	40	10	32	78	118	222	310	390	293	124	38	21	9	1645
Northfield, Vt.	35	1	2	12	31	104	180	244	188	98	37	2	2	901
North Head, Wash.	40	8	11	4	1	5	7	8	16	27	25	24	19	155
North Platte, Nebr.	40	0	2	20	109	261	382	409	352	152	38	7	0	1732
Oklahoma City, Okla.	40	26	46	119	202	298	356	225	272	195	140	51	18	1948
Omaha, Nebr.	40	4	9	54	138	279	386	343	346	234	101	26	4	1924
Oswego, N. Y.	39	9	14	37	45	130	181	226	185	105	56	14	9	1011
Palestine, Tex.	40	64	82	151	255	286	265	290	258	190	112	76	69	2098
Parkersburg, Va.	40	10	41	96	141	268	388	402	299	162	53	16	11	1887
Pensacola, Fla.	40	79	111	138	197	270	462	635	598	335	94	47	77	3043
Peoria, Ill.	39	16	26	109	175	292	363	313	293	201	85	41	13	1927
Philadelphia, Pa.	40	4	16	39	83	167	244	322	238	102	36	15	5	1271
Phoenix, Ariz.	40	8	34	37	53	44	61	313	371	141	49	26	18	1155
Pierre, S. Dak.	28	0	1	6	31	132	217	233	188	81	22	2	0	913
Pittsburgh, Pa.	40	19	21	80	122	239	340	384	292	178	57	21	9	1762
Pocatello, Idaho	40	5	2	15	78	157	190	304	294	157	44	6	3	1255

Table 1 (contd)

Station	Yrs.	J	F	M	A	M	J	J	A	S	O	N	D	Ann.
Point Reyes Light, Calif.	23	9	7	4	1	0	1	1	4	6	4	6	5	48
Port Angeles, Wash.	14	0	1	0	1	1	2	7	12	0	0	0	0	24
Port Arthur, Tex.	26	55	62	81	119	159	228	363	332	189	76	53	61	1778
Port Crescent, Wash.	12	0	0	0	0	2	6	6	4	0	2	2	4	26
Port Huron, Mich.	29	4	15	38	72	133	183	198	174	110	40	12	3	982
Portland, Maine	40	8	4	26	35	93	184	238	167	93	42	11	8	909
Portland, Oreg.	40	4	7	9	22	46	40	22	31	41	19	5	2	248
Providence, R. I.	39	3	9	29	48	111	143	193	165	81	19	10	3	814
Pueblo, Colo.	40	1	4	14	76	223	345	484	418	146	28	4	2	1745
Raleigh, N. C.	40	11	28	75	116	221	342	420	311	141	40	18	8	1731
Rapid City, S. Dak.	40	0	0	7	57	209	414	459	351	109	29	3	0	1638
Reading, Pa.	31	2	7	37	76	152	232	294	190	90	29	10	6	1125
Red Bluff, Calif.	32	5	9	18	24	39	25	8	7	14	12	1	5	167
Redding, Calif.	8	3	7	11	15	14	15	8	2	13	4	4	4	100
Reno, Nev.	38	0	2	6	18	66	102	153	106	65	13	0	0	531
Richmond, Va.	40	9	19	69	120	227	337	388	300	126	28	13	5	1641
Rochester, N. Y.	40	4	9	39	67	143	208	288	217	120	40	8	5	1448
Roseburg, Oreg.	40	1	0	6	19	31	34	26	19	28	7	3	1	175
Roswell, N. Mex.	38	7	14	32	114	231	287	366	349	195	103	19	5	1722
Royal Center, Ind.	13	3	8	35	66	84	115	134	116	76	32	18	5	692
Sacramento, Calif.	40	11	27	21	26	15	10	6	5	17	21	8	6	173
Saginaw, Mich.	12	0	4	18	31	44	83	77	83	44	16	3	1	404
St. Joseph, Mo.	34	5	19	77	164	252	328	261	306	232	102	31	11	1788
St. Louis, Mo.	40	24	40	135	191	267	352	311	307	205	108	48	12	2000
St. Paul, Minn.	29	0	4	21	48	150	220	195	179	130	42	11	1	1001
Salt Lake City, Utah	40	13	22	43	95	166	195	301	327	169	60	21	4	1416
San Antonio, Tex.	40	32	53	117	201	279	175	222	159	176	92	49	32	1587
San Diego, Calif.	40	18	11	14	8	6	11	19	24	10	15	12	14	162
Sand Key, Fla.	16	28	23	26	59	103	142	190	208	187	79	28	32	1105
Sandusky, Ohio	40	9	19	69	104	225	292	314	242	149	67	18	4	1512
Sandy Hook, N. J.	25	2	11	19	59	110	175	205	162	65	35	9	7	859
San Francisco, Calif.	40	10	19	7	9	3	3	1	6	5	7	5	9	84
San Jose, Calif.	27	3	7	0	4	0	2	0	4	6	4	2	6	38
San Luis Obispo, Calif.	23	3	5	11	8	5	5	5	6	11	9	5	4	77
Santa Fe, N. Mex.	38	5	11	40	91	261	366	724	625	285	97	16	1	2522
Sault Ste. Marie, Mich.	40	1	2	26	55	101	166	180	168	142	73	18	1	933
Savannah, Ga.	40	26	54	85	137	227	428	562	470	226	46	17	13	2291
Scranton, Pa.	40	3	5	31	72	178	270	314	230	109	40	10	4	1266
Seattle, Wash.	40	3	4	14	17	31	45	28	31	34	12	7	0	250
Sheridan, Wyo.	36	0	0	1	41	177	333	361	220	79	15	0	0	1225
Shreveport, La.	40	87	93	161	272	257	296	337	281	156	81	74	85	2180
Sioux City, Iowa	40	2	2	33	109	255	360	359	335	201	70	19	3	1748
Spokane, Wash.	40	2	0	6	25	65	108	91	83	49	11	0	0	440
Springfield, Ill.	40	16	36	138	177	300	376	333	299	201	96	53	12	2037
Springfield, Mo.	40	39	45	152	214	329	402	326	316	187	135	70	23	2338
Syracuse, N. Y.	40	4	6	35	70	159	230	295	233	125	57	8	1	1223
Tacoma, Wash.	36	7	3	3	15	19	34	29	30	28	14	10	2	194
Tampa, Fla.	40	48	60	104	138	319	652	870	799	517	123	22	29	3681
Tatoosh Island, Wash.	39	19	7	8	5	9	6	20	12	17	25	30	32	190
Taylor, Tex.	29	33	49	95	163	202	146	158	135	77	39	43	1296	
Terre Haute, Ind.	31	14	29	95	131	217	283	253	239	154	65	43	10	1533
Thomasville, Ga.	27	31	65	88	126	200	365	498	408	230	53	19	26	2109
Toledo, Ohio	40	11	21	73	132	227	317	330	250	165	80	32	7	1645
Tonopah, Nev.	16	0	2	1	9	22	23	58	52	27	6	0	0	200
Topeka, Kans.	40	12	22	92	199	299	361	331	355	268	129	54	13	2135
Trenton, N. J.	30	4	8	32	66	131	215	289	202	82	33	12	6	1080
Valentine, Nebr.	40	0	0	14	84	226	370	392	350	138	30	6	0	1610
Vicksburg, Miss.	40	82	115	198	264	276	398	466	492	221	99	73	68	2682
Wagon Wheel Gap, Colo.	13	0	1	4	26	64	160	255	254	102	27	5	1	899
Walla Walla, Wash.	40	1	3	14	34	60	91	84	75	54	14	1	0	431
Washington, D. C.	40	7	24	53	105	207	300	346	253	138	39	17	10	1499
Wausau, Wis.	18	0	2	12	31	64	125	127	85	55	30	5	0	536
Wichita, Kans.	40	16	24	100	203	325	385	329	321	252	119	45	8	2127
Williston, N. Dak.	40	0	0	1	21	111	292	306	234	74	14	0	0	105
Wilmington, N. C.	40	24	52	92	144	235	378	497	417	213	46	16	17	2131
Winnemucca, Nev.	40	0	1	13	38	87	100	127	105	66	18	2	0	557
Wytheville, Va.	37	3	13	59	100	222	333	350	263	132	22	6	2	1505
Yakima, Wash.	15	0	1	4	3	19	20	21	11	10	1	0	0	90
Yankton, S. Dak.	29	0	1	16	71	166	247	244	231	128	36	9	0	1149
Yellowstone Park, Wyo.	35	1	0	1	24	130	272	376	319	138	20	2	0	1283
Yuma, Ariz.	40	5	10	14	13	6	14	94	138	67	24	9	5	399

Table 2 (contd)

Station	Yrs.	J	F	M	A	M	J	J	A	S	O	N	D	Ann.
Greensboro, N. C.	14	2	4	6	6	11	14	22	16	8	3	2	2	70
		0	0	0	0	3	7	7	3	2	0	0	0	39
Greenville, S. C.	21	4	4	9	7	11	17	20	16	11	4	3	2	73
		0	0	0	0	0	6	8	4	1	0	0	0	36
Groesbeck, Tex.	12	3	5	11	10	14	13	14	12	9	11	6	4	78
		0	0	1	3	3	0	0	1	3	1	0	0	32
Hannibal, Mo.	29	4	3	9	7	14	13	15	14	16	6	6	2	61
		0	0	0	1	2	4	3	2	2	0	0	0	26
Harrisburg, Pa.	40	1	2	3	8	11	12	14	16	7	4	2	1	46
		0	0	0	0	1	4	3	2	0	0	0	0	19
Hartford, Conn.	38	1	3	5	5	8	11	12	9	7	4	2	2	41
		0	0	0	0	0	2	3	1	0	0	0	0	21
Hatteras, N. C.	40	4	3	8	6	12	12	15	12	11	5	4	3	60
		0	0	0	1	1	2	3	1	1	0	0	0	25
Havre, Mont.	40	0	0	0	2	3	7	13	16	11	10	2	0	35
		0	0	0	0	0	4	1	2	0	0	0	0	14
Helena, Mont.	40	1	0	1	5	9	20	18	17	10	3	1	0	59
		0	0	0	0	0	4	1	2	0	0	0	0	15
Houghton, Mich.	29	0	2	3	4	8	8	11	9	8	3	1	0	36
		0	0	0	0	0	1	1	2	1	0	0	0	14
Houston, Tex.	34	6	6	7	9	14	13	21	17	16	7	5	5	78
		0	0	0	0	0	2	5	1	2	0	0	0	41
Huron, S. Dak.	40	0	2	3	5	11	16	15	14	10	4	1	0	51
		0	0	0	0	0	3	3	3	1	0	0	0	25
Independence, Calif.	20	0	0	1	2	3	6	15	18	4	3	1	0	31
		0	0	0	0	0	0	0	0	0	0	0	0	0
Indianapolis, Ind.	40	2	3	7	9	16	13	14	12	11	6	8	3	79
		0	0	0	1	0	3	3	4	0	0	0	0	31
Iola, Kans.	26	4	3	5	10	13	16	13	11	9	6	4	1	65
		0	0	0	1	5	4	2	3	3	1	0	0	35
Ithaca, N. Y.	35	1	3	2	4	8	9	11	11	8	5	2	1	41
		0	0	0	0	2	1	4	2	2	0	0	0	27
Jacksonville, Fla.	40	3	5	8	9	18	24	25	23	19	9	2	4	95
		0	0	1	0	0	6	13	9	2	0	0	0	59
Jupiter, Fla.	8	1	2	4	5	10	15	19	18	14	5	2	2	74
		0	0	0	2	5	6	11	9	3	2	0	0	58
Kalispell, Mont.	40	1	0	2	3	9	10	14	12	5	2	1	0	41
		0	0	0	0	0	0	2	0	0	0	0	0	8
Kansas City, Mo.	40	2	4	9	12	12	20	15	13	12	8	4	2	73
		0	0	0	2	4	3	1	3	0	0	0	0	35
Keokuk, Iowa	40	3	3	8	9	13	15	16	13	15	6	4	2	67
		0	0	0	1	3	3	4	2	0	0	0	0	34
Key West, Fla.	40	5	5	7	10	16	15	21	22	24	8	4	6	97
		0	0	0	0	0	3	6	5	4	1	0	0	39
Knoxville, Tenn.	40	4	6	7	8	13	18	18	18	13	3	3	3	71
		0	0	0	1	1	2	1	5	1	0	0	0	23
La Crosse, Wis.	40	2	1	4	7	14	15	16	15	12	5	4	1	62
		0	0	0	0	2	2	3	4	0	0	0	0	24
Lander, Wyo.	40	0	0	1	4	6	9	12	15	5	2	1	0	43
		0	0	0	0	0	0	1	1	0	0	0	0	3
Lansing, Mich.	33	1	2	5	9	12	13	15	12	11	8	5	1	57
		0	0	0	1	1	3	3	1	1	0	0	0	30
Lewiston, Idaho	29	1	2	3	3	6	8	9	7	5	4	1	1	31
		0	0	0	0	0	1	1	0	0	0	0	0	6
Lexington, Ky.	29	4	4	6	10	15	15	21	14	12	6	3	3	68
		0	0	0	0	1	6	6	3	0	0	0	0	31
Lincoln, Nebr.	40	1	2	4	8	11	15	15	13	12	6	2	1	65
		0	0	0	0	2	5	3	2	2	0	0	0	30
Little Rock, Ark.	40	5	7	12	12	12	15	17	15	9	6	6	4	88
		0	0	0	1	2	2	3	1	1	0	0	0	33
Los Angeles, Calif.	40	3	4	6	3	2	3	2	3	3	3	1	5	14
		0	0	0	0	0	0	0	0	0	0	0	0	0
Louisville, Ky.	40	6	6	8	10	17	14	18	12	11	4	6	2	66
		0	0	0	1	0	0	3	2	1	0	0	0	27
Ludington, Mich.	20	1	3	4	8	11	11	11	11	12	6	4	1	53
		0	0	0	0	0	4	2	1	0	0	0	0	20
Lynchburg, Va.	36	1	1	4	4	9	17	14	13	7	3	1	3	53
		0	0	0	0	0	2	2	2	0	0	0	0	19
Macon, Ga.	40	5	8	8	8	16	19	22	16	10	5	2	3	82
		0	0	0	1	0	5	8	3	1	0	0	0	37
Madison, Wis.	39	1	4	4	7	13	15	12	16	10	6	5	1	61
		0	0	0	0	1	2	3	1	2	0	0	0	32

Table 2 (contd)

Station	Yrs.	J	F	M	A	M	J	J	A	S	O	N	D	Ann.
Marquette, Mich.	40	0	1	3	3	9	11	12	8	6	3	2	0	34
Medford, Oreg.	16	0	0	0	0	0	1	2	0	0	0	0	0	15
Memphis, Tenn.	40	1	1	3	4	4	5	6	4	3	3	1	0	12
Meridian, Miss.	40	0	0	0	0	0	0	0	0	0	0	0	0	5
Miami, Fla.	32	5	6	10	14	12	15	15	14	11	5	6	6	86
Miles City, Mont.	38	0	0	2	1	1	2	4	1	1	0	0	0	36
Milwaukee, Wis.	40	6	7	10	12	16	18	22	18	10	7	6	5	84
Minneapolis, Minn.	40	0	0	0	1	2	2	7	5	1	0	0	0	43
Missoula, Mont.	8	4	5	7	10	16	19	22	22	21	10	5	3	90
Mobile, Ala.	40	0	0	0	0	1	3	4	3	4	0	0	0	52
Modena, Utah	40	0	0	1	4	7	16	14	16	5	2	1	1	49
Montgomery, Ala.	40	0	0	0	0	0	1	1	0	0	0	0	0	5
Moorhead, Minn.	39	2	3	4	7	13	12	12	11	11	5	3	1	50
Mt. Tamalpais, Calif.	17	0	0	0	0	0	2	2	1	0	0	0	0	22
Nantucket, Mass.	40	1	2	3	5	12	12	13	15	10	7	3	0	57
Narragansett Pier, R. I.	14	0	0	0	0	1	3	2	2	1	0	0	0	23
Nashville, Tenn.	40	0	0	1	4	7	8	12	7	5	1	0	0	37
New Haven, Conn.	40	0	0	0	0	2	3	2	0	0	0	0	0	15
New Orleans, La.	40	6	7	9	11	14	18	21	26	16	7	4	6	96
New York, N. Y.	40	0	0	0	1	2	5	10	7	0	0	0	0	53
Norfolk, Va.	40	1	2	5	8	13	10	22	20	12	5	2	1	54
Northfield, Vt.	35	0	0	0	0	0	0	0	3	1	0	0	0	29
North Head, Wash.	40	12	6	9	9	17	20	18	17	12	7	6	8	82
North Platte, Nebr.	40	0	0	0	0	0	0	0	0	0	0	0	0	45
Oklahoma City, Okla.	40	0	1	2	5	12	12	11	12	8	3	1	0	43
Omaha, Nebr.	40	0	0	0	0	0	2	4	1	1	0	0	0	17
Oswego, N. Y.	39	2	1	1	1	0	1	1	1	2	1	2	2	7
Palestine, Tex.	40	0	0	0	0	0	0	0	0	0	0	0	0	0
Parkersburg, Va.	40	2	3	4	5	5	8	8	7	4	4	3	2	30
Pensacola, Fla.	40	0	0	0	0	0	0	0	0	0	0	0	0	7
Peoria, Ill.	39	1	2	2	4	4	6	8	7	5	2	2	0	27
Philadelphia, Pa.	40	0	0	0	0	0	1	2	0	0	0	0	0	14
Phoenix, Ariz.	40	4	5	10	11	14	20	18	13	12	6	4	4	75
Pierre, S. Dak.	28	0	0	1	2	3	3	6	1	0	0	0	0	40
Pittsburgh, Pa.	40	0	0	0	0	0	2	2	10	6	6	2	2	41
Pocatello, Idaho	40	7	5	7	10	13	19	23	23	12	8	4	6	95
		0	0	0	0	2	1	2	7	6	1	0	0	60
		3	2	3	6	9	11	16	14	7	6	4	2	52
		0	0	0	0	1	2	1	2	0	0	0	0	15
		2	3	6	6	9	16	16	15	9	3	3	1	57
		0	0	0	0	1	1	4	3	0	0	0	0	27
		0	1	3	3	7	10	13	11	7	3	1	1	35
		0	0	0	0	1	2	3	2	0	0	0	0	17
		2	5	1	1	1	1	2	2	5	3	3	2	10
		0	0	0	0	0	0	0	0	0	0	0	0	0
		0	1	3	6	12	18	19	16	9	3	1	0	60
		0	0	0	0	2	5	5	2	1	0	0	0	26
		4	4	8	9	17	18	12	13	12	9	5	3	68
		0	0	0	1	2	3	2	2	1	0	0	0	29
		2	2	4	7	14	19	18	14	11	6	3	1	64
		0	0	0	0	1	4	3	4	1	0	0	0	33
		2	3	5	4	8	10	9	10	7	4	2	2	36
		0	0	0	0	0	0	0	0	0	0	0	0	15
		5	5	10	11	13	11	15	12	9	9	7	4	71
		0	0	0	3	3	1	0	1	2	0	0	0	32
		1	7	9	7	14	18	16	12	11	4	5	3	60
		0	0	0	1	1	3	6	1	0	0	0	0	31
		8	9	9	12	18	22	23	23	17	8	3	7	109
		0	0	0	1	1	5	8	7	2	0	0	0	41
		2	2	10	9	14	16	14	13	15	7	4	2	78
		0	0	0	1	3	4	3	3	1	0	0	0	31
		1	2	3	6	8	11	13	13	6	3	2	1	51
		0	0	0	0	2	2	3	0	0	0	0	0	18
		2	5	5	12	5	5	16	20	9	4	3	4	48
		0	0	0	0	0	0	2	3	0	0	0	0	11
		0	1	4	3	8	14	18	9	7	2	1	0	48
		0	0	0	0	1	2	4	4	0	0	0	0	20
		2	2	6	8	13	18	16	13	9	4	2	3	62
		0	0	0	0	1	3	4	2	1	0	0	0	28
		2	0	1	6	9	11	14	17	11	5	1	1	56
		0	0	0	0	0	0	4	0	0	0	0	0	14

Table 2 (contd)

Station	Yrs.	J	F	M	A	M	J	J	A	S	O	N	D	Ann.
Point Reyes Light, Calif.	23	2	2	2	1	0	1	1	2	2	2	1	2	5
Port Angeles, Wash.	14	0	0	0	0	0	0	0	0	0	0	0	0	0
Port Arthur, Tex.	26	5	5	7	9	14	15	24	21	14	6	6	8	94
Port Crescent, Wash.	12	0	0	0	0	0	4	2	5	3	0	0	0	46
Port Huron, Mich.	29	2	2	6	7	9	10	12	9	7	5	2	1	44
Portland, Maine	40	2	2	3	4	10	13	18	10	7	7	2	2	27
Portland, Oreg.	40	1	2	2	3	6	5	3	4	6	3	2	1	53
Providence, R. I.	39	1	2	3	4	5	8	9	9	6	2	1	1	7
Pueblo, Colo.	40	1	1	2	5	12	15	22	17	9	3	2	1	28
Raleigh, N. C.	40	2	3	5	8	13	17	15	15	8	3	2	2	10
Rapid City, S. Dak.	40	0	0	2	5	11	17	16	14	6	4	1	0	24
Reading, Pa.	31	1	2	5	7	11	12	14	14	9	4	2	1	60
Red Bluff, Calif.	32	1	2	3	4	6	4	2	2	4	0	0	2	24
Redding, Calif.	8	2	2	3	3	4	7	2	1	5	2	2	2	45
Reno, Nev.	38	0	0	0	0	0	0	0	0	0	0	0	0	25
Richmond, Va.	40	1	2	4	6	11	15	15	15	7	2	2	1	9
Rochester, N. Y.	40	2	2	4	5	11	11	15	9	6	3	1	2	5
Roseburg, Oreg.	40	1	0	2	3	6	4	3	3	4	2	1	1	51
Roswell, N. Mex.	38	4	2	7	15	17	15	14	14	12	12	3	2	25
Royal Center, Ind.	13	1	2	6	10	12	16	14	11	12	5	5	2	43
Sacramento, Calif.	40	3	3	3	4	2	2	1	1	3	3	3	2	16
Saginaw, Mich.	12	0	2	5	4	7	10	12	11	8	7	1	1	11
St. Joseph, Mo.	34	1	2	6	11	13	18	14	15	13	8	6	2	0
St. Louis, Mo.	40	2	3	9	10	14	17	12	12	7	5	2	2	38
St. Paul, Minn.	29	1	2	3	6	11	12	13	15	10	5	2	1	64
Salt Lake City, Utah	40	2	4	6	6	12	11	17	15	10	5	4	1	39
San Antonio, Tex.	40	6	4	8	13	19	11	14	11	9	7	5	4	9
San Diego, Calif.	40	3	2	4	3	2	3	3	3	3	2	2	2	63
Sand Key, Fla.	16	6	3	6	6	15	17	18	21	16	7	4	9	19
Sandusky, Ohio	40	2	3	7	5	11	12	12	12	8	4	3	1	1
Sandy Hook, N. J.	25	1	2	2	6	10	11	14	13	5	6	2	1	25
San Francisco, Calif.	40	2	4	2	2	1	1	1	2	3	2	2	2	47
San Jose, Calif.	27	1	2	0	1	0	1	0	1	1	1	1	1	50
San Luis Obispo, Calif.	23	2	2	1	5	4	3	2	1	4	3	1	1	25
Santa Fe, N. Mex.	38	2	2	5	7	16	21	31	24	17	6	3	1	47
Sault Ste. Marie, Mich.	40	1	1	3	4	6	11	11	9	8	5	2	1	24
		0	0	0	0	0	1	1	1	0	0	0	0	7

Table 2 (contd)

Station	Yrs.	J	F	M	A	M	J	J	A	S	O	N	D	Ann.
Savannah, Ga.	40	3	5	8	8	12	18	21	21	16	3	2	1	77
		0	0	0	0	0	5	9	4	0	0	0	0	42
Scranton, Pa.	40	1	1	3	6	11	13	13	11	9	4	2	1	46
		0	0	0	0	1	4	3	2	0	0	0	0	22
Seattle, Wash.	40	1	1	2	3	5	6	3	4	7	3	2	2	16
		0	0	0	0	0	0	0	0	0	0	0	0	1
Sheridan, Wyo.	36	0	0	1	4	13	15	17	13	5	3	0	0	46
		0	0	0	0	1	0	5	1	0	0	0	0	15
Shreveport, La.	40	5	8	8	12	13	13	16	16	9	8	7	7	78
		0	0	2	3	1	2	1	2	0	0	0	0	37
Sioux City, Iowa	40	1	1	4	6	12	15	18	15	13	4	3	1	57
		0	0	0	0	1	3	3	3	2	0	0	0	25
Spokane, Wash.	40	2	0	1	3	7	6	7	8	5	2	0	0	23
		0	0	0	0	0	0	0	0	0	0	0	0	2
Springfield, Ill.	40	3	4	9	8	17	16	14	13	12	11	6	2	70
		0	0	0	1	1	4	0	3	0	0	0	0	36
Springfield, Mo.	40	4	3	10	12	15	17	14	13	10	11	5	3	70
		0	0	0	2	3	3	3	3	0	0	0	0	45
Syracuse, N. Y.	40	1	2	4	5	10	11	12	11	8	5	1	1	43
		0	0	0	0	0	2	3	1	0	0	0	0	18
Tacoma, Wash.	36	2	1	1	2	3	3	4	3	5	2	2	1	12
		0	0	0	0	0	0	0	0	0	0	0	0	0
Tampa, Fla.	40	4	5	9	8	19	24	31	26	20	7	3	4	123
		0	0	0	1	0	9	13	10	5	0	0	0	65
Tatoosh Island, Wash.	39	4	3	2	1	2	2	4	2	4	3	3	4	10
		0	0	0	0	0	0	0	0	0	0	0	0	0
Taylor, Tex.	29	3	5	6	10	12	13	14	11	9	7	5	4	70
		0	0	0	2	3	0	0	2	2	0	0	0	23
Terre Haute, Ind.	31	2	3	8	10	13	14	13	15	11	7	7	2	71
		0	0	0	1	3	1	3	4	1	0	0	0	38
Thomasville, Ga.	27	3	5	8	10	18	19	25	24	18	5	6	4	90
		0	0	0	0	3	6	4	5	2	0	0	0	60
Toledo, Ohio	40	3	3	7	8	11	13	14	11	9	8	4	1	57
		0	0	0	0	2	1	3	2	0	0	0	0	26
Tonopah, Nev.	16	0	1	1	3	6	9	8	7	5	2	0	0	25
		0	0	0	0	0	0	0	0	0	0	0	0	1
Topeka, Kans.	40	2	3	8	12	16	16	14	14	15	8	6	3	76
		0	0	0	2	4	4	1	2	1	0	0	0	38
Trenton, N. J.	30	1	2	5	6	9	10	15	12	6	3	2	2	48
		0	0	0	0	1	4	6	3	1	0	0	0	27
Valentine, Nebr.	40	0	0	3	6	11	17	17	14	8	3	1	0	58
		0	0	0	0	0	0	0	0	0	0	0	0	2
Vicksburg, Miss.	40	9	8	11	12	13	17	18	20	12	7	5	8	93
		0	0	1	1	1	5	2	1	1	0	0	0	46
Wagon Wheel Gap, Colo.	3	0	0	1	2	6	22	24	21	11	4	1	0	79
		0	0	0	1	0	2	20	19	6	0	0	0	57
Walla Walla, Wash.	40	1	1	2	3	5	7	8	6	5	2	1	0	20
		0	0	0	0	0	0	0	0	0	0	0	0	4
Washington, D. C.	40	1	3	5	6	12	14	16	12	8	4	2	2	48
		0	0	0	0	1	3	4	2	0	0	0	0	25
Wausau, Wis.	18	0	1	3	5	12	14	11	9	8	5	2	0	41
		0	0	0	0	0	2	3	2	0	0	0	0	17
Wichita, Kans.	40	2	2	7	12	17	18	14	14	11	8	6	1	69
		0	0	0	1	4	6	2	2	2	0	0	0	30
Williston, N. Dak.	40	0	0	1	2	8	13	13	10	5	2	0	0	42
		0	0	0	0	0	2	3	1	0	0	0	0	14
Wilmington, N. C.	40	3	4	9	8	11	17	20	15	14	4	2	2	75
		0	0	0	0	1	2	5	4	0	0	0	0	37
Winnemucca, Nev.	40	0	1	2	5	7	8	11	10	9	3	1	0	29
		0	0	0	0	0	0	0	0	0	0	0	0	4
Wytheville, Va.	37	1	3	4	6	13	16	21	16	8	4	2	1	54
		0	0	0	0	2	3	4	1	1	0	0	0	24
Yakima, Wash.	15	0	1	2	1	5	4	3	2	6	1	0	0	10
		0	0	0	0	0	0	0	0	0	0	0	0	3
Yankton, S. Dak.	29	0	1	3	7	11	13	18	12	8	3	2	0	54
		0	0	0	0	0	0	3	4	0	0	0	0	29
Yellowstone Park, Wyo.	35	1	0	1	4	8	14	18	20	13	3	0	0	57
		0	0	0	0	1	1	4	4	0	0	0	0	25
Yuma, Ariz.	40	2	2	2	7	2	2	7	14	5	7	2	2	20
		0	0	0	0	0	0	0	0	0	0	0	0	0

lines of equal thunderstorm frequency ⁽⁸⁾, were then drawn and smoothed, consideration being given both to length of record and to major topographic differences, before reproduction in figures 28-31. It must be pointed out, however, that in these charts, as in all similar ones, neither the data nor the knowledge of topographic effects is sufficient to make the isoceraunics definite, particularly in the mountainous areas of the west. The orientation of the lines which cross the Canadian border was determined, when necessary, by considering Alexander's 1904-33 data from Canadian stations, since no further record was available. It should also be noted that the zero isoceraunics have been drawn to inclose or limit areas in which all stations have reported absolutely no thunderstorms during the period of record; these are, of course, smaller than the areas where the mean frequency is so small a fraction of unity that it would be plotted as zero.

140. The annual chart, figure 28, should be compared with several other similar charts which are available. It does not differ much in pattern from the chart which could be developed from the data used in figure 27, but most of the values are higher in figure 28. This supports Humphreys' objection to the record prior to 1904, although at Kansas City, as previously demonstrated, the difference was negligible. The 1904-43 pattern differs somewhat from Alexander's 1904-33 pattern - most significantly in Arizona and Florida where data from Flagstaff and Miami have been added to the tabulation. The later compilation extends the Rocky Mountain area of annual maximum occurrence westward and even shifts the maximum center on some monthly maps, as will be seen; in the Southeast it decreases the annual isoceraunic

gradient through southern Florida and also shows a migration of the maximum thunderstorm activity in that state on the monthly maps.

Another significant change is the emergence of the Lander minimum on the 1904-43 annual map; on Alexander's map Lander actually had a higher value than Pocatello. Another change is the elimination of the anomalous minimum area around St. Joseph, Missouri.

141. The annual map should also be compared with the most recently published annual chart on page 729 of "Climate and Man," the 1941 Department of Agriculture Yearbook. Since the periods of record are approximately the same, a close agreement is to be expected. However, there are some obvious differences which are due chiefly to errors in the basic data for the chart in "Climate and Man." Specifically, the most glaring discrepancy is in the orientation of, and the areas inclosed by, the isoceraunics over the Rocky Mountain region. It was found that for the Yearbook chart the average annual numbers of thunderstorms at Lander, Wyoming, and Pocatello, Idaho, had been erroneously reported as 49 and 41, respectively, figures which are inexplicably larger than the 20 and 29, respectively, of the comparative data, or the 22.9 and 31.4 of the 1904-43 data. The change in orientation in the vicinity of Santa Fe on the 1904-43 chart was caused by the addition of Flagstaff to the basic data. In southern Texas a similar discrepancy arose from the fact that Austin was incorrectly reported to have an average of 27 for the Yearbook chart instead of the correct value of 40 (from either comparative or 1904-43 data). The new chart shows a change in gradient between Miami and Key West because Key West's value was reported as 48 for the Yearbook chart

instead of 58 (comparative data) or 66.9 (1904-43 data). A questionable maximum of over 60 is indicated near Tulsa (at Broken Arrow) on the new chart, but the record is rather short. It is, however, supported by another short record at Bentonville, Arkansas. These records were not used for the Yearbook chart. On that chart, the isolated maximum at Birmingham was not drawn for, but it is supported by data from Anniston in the 1904-43 chart. Other differences are minor and attributable to differences in length of record and to the usual variability in isolines drawn by different persons.

142. The January pattern (figure 29) differs little from Alexander's except in a slight further contraction of the zero-occurrence area, natural enough in a lengthened record. The maximum of activity, defined as the geographical center of the maximum isoceraunic or its tongue-like protrusion, is still in central or northern Louisiana, though greater weight is now given to the Gulf Coast of northern Florida. The "rather significant isoceraunic over northern Utah," mentioned by Alexander, is now eliminated; its significance was already diminishing in 1933. An examination of the record at Salt Lake City, on which the "significant isoceraunic" depended, shows that although a total of ten thunderstorm days was reported for January during the period 1904-13, only one more day was added in each of the three following decades.

143. Although December seems to be the month of minimum thunderstorm activity by a small margin, January shows little more and has even less activity in a few places. Chronologically and from the standpoint of activity it may therefore be used as the beginning of a meteorological discussion of the spread of thunderstorm activity.

In any such meteorological exposition there are two difficulties. One is that mean flow patterns or any other mean distributions of meteorological factors cannot entirely explain thunderstorm activity when such activity is not the mean condition, just as mean-pressure charts fail to indicate migratory troughs or Lows. Nevertheless, it is possible to find some reasonable clues to the thunderstorm distribution. The other difficulty is that the available data usually offer a better, more specific explanation of the distribution and occurrence of rainfall than of thunderstorms and it is only assumed that thunderstorms will constitute a proportional part of the rainfall activity in the proper seasons. The assumption is often reasonable but there are times and places, as will become apparent, when the connection between the two phenomena is, at best, tenuous.

1144. The January isoceraunics indicate that at least two important factors fundamental to thunderstorm activity at this time are southerly latitude and source of moisture. Both factors could be included in the statement that the activity is proportional to the frequency of maritime tropical air at or near the surface. Showalter's study of American air-mass properties ⁽⁹⁾ shows the expected seasonal variation in the properties of maritime tropical air. The lapse rates of temperature and equivalent potential temperature and the moisture content are greatest in summer and least in winter. Equally important is the fact that, in winter, maritime tropical air moving over land surface is cooled from below and the lesser insolation of the season does not destroy the stabilization of lapse rate thus achieved ⁽¹⁰⁾. The insolation type of thunderstorm is therefore a rarity in winter.

Frontal or convergent action must be associated with the tropical maritime air in order to produce the thunderstorm in winter.

145. The mean position of the polar front at this time is just off the Atlantic and Gulf Coasts (11), a position resulting from the frequent incursions southward of the cold, polar, Canadian High formed over the snow-covered northern continent. The thrusts of cold air southward also induce a northward flow of warm moist air east of the cold current, and between the two a maximum of frontal and convergent activity is likely to occur. (It has been suggested that the sequence of currents is exactly the opposite; however, the effect is the same for the purposes of this discussion.) The mean position of the western wedge of the Atlantic or Azores High at 10,000 feet (12) is such that the intrusion northward of a deep layer of warm moist air is most likely west of the 90th meridian - approximately the longitude of New Orleans. Thus the northward extension of the isoceraunics in this region is probably an effect of this juxtaposition of opposing currents. In addition, Bigelow's (13) mean surface-pressure chart for the month shows some evidence of convergence in the region. In the vicinity of Vicksburg the isobars change from anticyclonic to geostrophic (and the wind from southeast to south), an indication of a downwind decrease of wind.

146. In January both Pacific and Atlantic anticyclones have reached approximately their easternmost and southernmost positions for the year. On the Atlantic side the effect is to confine practically all of the thunderstorm activity east of the 100th meridian - with a tendency for a decrease eastward toward the coast as the anticyclonic center, with its subsidence, is approached. On the Pacific side the seasonal shift

of the semipermanent centers of action has also brought the Aleutian Low closer to the American continent. While the High has been weakened, the Low has been strengthened. Between the two systems the Pacific polar front is at times displaced as far south as southern California. Cyclonic systems on the front in mid-Pacific occlude before they reach the mainland and each occlusion, as it crosses the coastline, is preceded by a movement northward of tropical Pacific air or of polar Pacific air rapidly becoming tropical. Although there is actually little thunderstorm activity at any time of year, these storm series make winter the peak thunderstorm season on the immediate coast. Because of the small numerical values involved, table 1 shows this better than the charts. The thunderstorms occur during the occluded-front passages and most often, experience indicates, with the final cold front which ends a sequence of occlusions. Although the topography is of extreme importance as a rainfall-producer in this region, given the winter southwest-flow pattern, it seems that a front is usually necessary to produce the winter thunderstorm.

147. The meteorological analysis of January thunderstorm activity may seem more detailed than the magnitude of the activity warrants but the analysis, modified by consideration of seasonal changes in factors and the continuing migration of the semipermanent circulations, will in general serve for other months as well.

148. The February chart (figure 29) differs in no important respect from Alexander's. Frequencies have increased somewhat, equaling almost three days per month at Vicksburg, and the area within the 2-day isoceraunic has spread, mostly eastward toward northern Florida. There

is a greater spread northward on the west side of the Appalachians than on the east. This can be attributed to the prevailing eastward component of the wind, which is up slope on the west side and down slope on the east side of the ridge. On the Pacific Coast the limited but nevertheless extreme activity for the region continues. There has been an appreciable increase of activity around Phoenix, which is shown by table 1 rather than by the isoceraunics. It may even be defined as a secondary maximum, as Alexander defined it, but its connection with the so-called significant isoceraunic of the previous month over Utah is doubtful. The 10,000-foot mean-pressure chart for the month offers some support for the increase by indicating a trajectory of air from a more southerly latitude off Lower California toward Arizona. It also shows a slight eastward displacement of the western wedge of the Atlantic High which may account for the extension of maximum activity toward Florida.

149. On the March chart (figure 29) the area of zero occurrence in the United States is finally eliminated, although Alexander still retained a small zero area around Yellowstone Park. The only other substantial change from Alexander's pattern is over Arizona and New Mexico, where the use of Flagstaff data altered the isoceraunic pattern. On the Pacific Coast there is a general diminution of thunderstorm activity associated with the northward and westward displacement of the Pacific centers of action. The similar displacement of the Atlantic cells accounts for the spread of activity in the eastern half of the country, the 1-day line now having moved into the western Plains States. The 1-day isoceraunic passing through Salt Lake, Santa Fe, and Phoenix may be, in part, also due to the influence of the Atlantic anticyclone on

the spread of maritime tropical air westward from the Gulf and Atlantic, aided by the mountainous topography. However, increased activity along the Mexican border from San Diego to El Paso, and affecting Los Angeles also, suggests that the Pacific may be another source of tropical maritime air for this region, as was indicated in the discussion of the February chart. As in February, the March 10,000-foot pressure chart shows a trajectory from the sea off Lower California.

150. On the April chart (figure 29) the maximum area has progressed farther northwestward and is now centered near Little Rock. Bigelow's sea-level pressure chart for April shows the center to be in a region where there is a change from anticyclonic to cyclonic curvature of isobars, also an indication of convergence. This convergence pattern, persisting in the region since January, is important in explaining the anomalous location of the maximum thunderstorm area during these months - a location which in March, April, and May seems to be separated from the source of the tropical maritime air by the isoceraunic gradient. A secondary maximum, with reversal of isoceraunic gradient indicated, appears for the first time near Miami. It is not shown on Alexander's chart because he did not use Miami data. It is possible that this increase in thunderstorm frequency is connected with a decrease of the anticyclonic curvature of the isobars over southern Florida as shown on Bigelow's chart. In any case, it is the first appearance of a new and rapidly growing thunderstorm center. On the eastern slopes of the Rockies increased thunderstorm activity is now more definitely associated with an Atlantic or Gulf source of moisture, as the Atlantic High continues to strengthen and expand and to migrate westward. There

is a leeward deficiency on the westernmost slopes of the Rockies, where an isoceraunic trough appears. The plateau increase of activity still farther west is probably linked to the Pacific source of moisture.

151. In May (figure 30) the maximum activity is in northwestern Arkansas. Southward through Texas this is the month of maximum thunderstorm activity, and it is possible to relate it to a mean 10,000-foot pressure trough over this region. The growing activity over Florida, now centered nearer Tampa, is a close secondary and the eastern ranges of the Rockies also show greatly increased values. The appearance of the 2-day isoceraunic in northeastern California indicates that the initial source of the tropical air for the westward advance is still the Gulf and the Atlantic, although it is not unlikely, considering the 10,000-foot pressure pattern, that the air moving westward across Mexico is recharged with moisture over the Gulf of California and over the Pacific off Lower California, before it turns northward. Over Florida it seems more definite that the emerging maximum results not only from the higher moisture values and greater insolation in the section but from the convergence indicated by the decreasing anticyclonic curvature of the isobars over the region. As a whole the May chart does not differ much from Alexander's except in an elongation of the isoceraunic over Florida.

152. By June (figure 30) the Arkansas maximum has moved to Missouri but it is exceeded both on the eastern slopes of the Rockies and over Florida and the Gulf Coast, with a country-wide maximum of 16.3 at Tampa. Over most of Texas, not including the Panhandle, there has been an actual decrease of activity. Over Texas there is now a

small anticyclonic circulation at 10,000 feet, where there was a slight trough during the previous month of maximum activity. This is Reed's ⁽⁶⁾ high-level anticyclone, in part thermally induced by the increased heating of the land surface at this time of year, but also an intensified extension of the dynamic Atlantic anticyclone of which it seems to be part. Reed has already shown how persistence of its center over a region coincides with drought conditions while on its western side the northward flow of tropical maritime air from the Gulf and Atlantic sources may bring thunderstorms as far west as California. On the eastern slopes of the Rockies the increased activity, basically due to the flow of such air against the barrier, is also enhanced by the summertime increase of valley-wind occurrences ⁽¹⁴⁾. This is an effect of greater heating of the slopes than of the free air at the same level during the hours of insolation, resulting in the diurnal up-slope wind which reaches maximum strength in the afternoon. It is less likely to occur in the winter and spring when the frozen and snow-covered slopes respond less to the insolational effects. The seasonal change in the diurnal variation of thunderstorm frequencies, to be discussed in a later section, is consistent with such an analysis. Convergence, which seems at least partially responsible for the activity in Florida, would also tend to decrease the diurnal variation and Norton ⁽¹⁵⁾ points out that in June showers in Florida are equally likely night or day. This is not confirmed by the statistics used in the current report which are, however, for very few stations. It is well to remember, though, that the convective instability of the air which the convergence acts upon does have a diurnal variation with a maximum in the afternoon, the

variation being an insolation effect. The June chart as a whole resembles Alexander's closely.

153. By July (figure 30) the lessening of thunderstorm frequency observable in Texas in June has spread, mostly northward and northeastward to Iowa, Illinois, and eastern Indiana. The 10,000-foot anticyclone, centered in June over southern Texas, is now over Louisiana with a much larger expanse. Elsewhere frequencies are still increasing, with maximum monthly values attained from Florida northward and over the eastern slopes of the Rockies. It is significant that the position of the high-level anticyclone now makes possible two main southerly currents over the United States, one west of the high-level anticyclone and the other east of it at the edge of the main body of the Atlantic anticyclonic cell. Within these two currents the maximum thunderstorm activity is now concentrated. In the mountain area Flagstaff now comes into secondary prominence, resulting in an isoceraunic change from Alexander's chart. The approximate curvature of the axis of maximum activity in the Rockies is about parallel to the orientation of the easternmost ridges from New Mexico to Montana, emphasizing the importance of the orographic lift. A slight increase in frequencies is still observable in California except on the Coast, where zero values now appear. There are no thunderstorms in the stabilized air flowing eastward out of the Pacific High; those which do occur in California are generated in the air flowing around the Atlantic High or its companion, the high-level anticyclone. Also noticeable in a comparison of the June and July charts is the inhibiting effect of the Great Lakes. Cooled from below, the stabilized air blowing inland off the Lakes makes its presence felt in the

persistence of the 8-day and 6-day isoceraunics in this region, which show little northward progression between June and July.

154. In August (figure 30) there is a general decline of thunderstorm activity throughout the country, with some significant exceptions. There is a slight increase over northern Missouri, northeastern Kansas, and southwestern Iowa. This is about the center of the region where, as Means has shown ⁽⁷⁾, there is in summer a type of advective warming at intermediate levels which is most effective in steepening the lapse rate at night. It is probably the cause of the excessive nocturnal thunderstorm activity in this region, which Means' figures indicate is at its maximum in August. The other slight increases in August appear at Key West and in the area from Flagstaff to the Mexican border. Both can be related to the expansion of the anticyclone at 10,000 feet, which pushes the northward current in the western part of the country farther west and forces the northward current around the Atlantic High farther east. Beneath the center of the expanding high-level anticyclone, the decline of thunderstorm activity continues. The August chart differs from Alexander's chiefly in the extension of the Rocky Mountain maximum isoceraunic from Santa Fe to Flagstaff. Flagstaff, indeed, now exceeds Santa Fe, 19.7 to 16.4.

155. September (figure 31) shows the very decided contraction Gulfward of the isoceraunics as both insolation and tropical-maritime flow northward decrease. The southeastward recession of the oceanic anticyclonic circulations begins at this time. While for practically all of the country this means a decrease in thunderstorm days, on the Pacific Coast it means a slight increase which is maintained into the

spring. The secondary maximum which persists around Kansas City on this chart may be due to the persistence of the nocturnal activity. Bigelow's sea-level pressure chart for the month also indicates convergent isobaric structure over the region.

156. It is the latter phenomenon which is the more important, because only its persistence through the following months can adequately explain the persistence of the maximum zone of activity approximately in the longitudinal center of the country, and appreciably removed from the Gulf. On the October chart (figure 31), for instance, the maximum point within the 2-day isoceraunic is about the geographical center of the four states: Kansas, Missouri, Oklahoma, and Arkansas. This is also the approximate location of the maximum decrease in curvature of the anticyclonic isobars on Bigelow's October chart. In general, of course, the decrease in thunderstorm activity and the pattern of recession toward the Gulf is maintained except along the Pacific Coast. Over southern Florida there is a change of isoceraunic gradient, Key West and Sand Key now having the maximum values on the map.

157. By November (figure 31) the midwinter pattern is closely approached, with isoceraunic gradient directed outward from Louisiana and Arkansas except in the Far West where the activity is maintained on the Coast. Bigelow's pressure chart also shows the southward recession of the convergence zone.

158. Between the December (figure 31) and January (figure 29) charts there is little difference. These are the months of minimum activity, the moderate concentration in Louisiana coinciding with a convergence zone of isobaric curvature and also with the longitude at

which the intrusion of tropical maritime air is most likely.

Associated wet-bulb temperatures

159. It was shown in the previous chapter that the wet-bulb temperature is a key to the thermodynamic analysis of the thunderstorm. It lies on the pseudo-adiabat which the rising surface air will follow and thus helps determine the magnitude of the conditional instability as well as the height of the condensation level. A decrease of the wet-bulb potential temperature with height signifies convective instability and the rate of the decrease also serves as an index of the lowest temperature to be expected in the thunderstorm downdraft. Furthermore, it was shown that the difference between the precipitable-water contents corresponding to the dew-point curve and the wet-bulb curve is equal to the amount that must be evaporated to cool the atmosphere to its wet-bulb temperature. It is of interest therefore to determine the wet-bulb temperatures that are commonly associated with thunderstorms.

160. Figure 32, taken from Albright ⁽¹⁶⁾, is a map of the distribution of surface wet-bulb temperatures which are exceeded not more than 5% of the total hours during June to September, inclusive, of a normal summer. Over the eastern half of the country there is some resemblance to the annual thunderstorm pattern (figure 28) and also, therefore, to the summer thunderstorm patterns (figure 30). In particular, the Gulfward increase characterizes all three charts. However, the temperatures in figure 32 are surface wet-bulb temperatures and therefore not directly comparable since, when air is lifted, its wet-bulb temperature is lowered pseudo-adiabatically while the air

is cooled dry-adiabatically. The relation of wet-bulb temperature to height can be obtained from figure 33, which also gives similar relations for the dew point and the dry-bulb temperature, the latter being reduced along the dry adiabat and the former along the mixing-ratio line. In all cases, sea level has been considered to be 1000 mb.

161. Pertinent to figure 32 is the fact that, in the summer, thunderstorms also occur on the average about 5% of the time. Allowing two clock hours for the average summer thunderstorm occurrence, thunderstorms may be said to occur during the summer from 1 to 6% of the time throughout the country except on the Pacific Coast. A check on this statement is provided by compilations of thunderstorm durations (time from first to last thunder heard) made by Fuller (17) for Peoria and by Bily (18) for Tampa.

Table 3

THUNDERSTORM DURATIONS AT PEORIA, ILL., 1905-31

	Jan	Feb	Mar	Apr	May	Jun	Jul	Aug	Sep	Oct	Nov	Dec
Hrs per month	0.4	0.5	5.3	10.2	18.5	21.5	20.1	16.5	14.7	4.3	1.9	0.1
% of total hrs	.05	.07	0.7	1.4	2.5	3.0	2.7	2.2	2.0	0.6	0.3	.01

Table 4

THUNDERSTORM DURATIONS AT TAMPA, FLA., 1890-1904

	Jan	Feb	Mar	Apr	May	Jun	Jul	Aug	Sep	Oct	Nov	Dec
Hrs per month	1.3	3.1	5.8	7.4	8.2	23.4	25.6	27.5	10.8	1.6	0.4	0.9
% of total hrs	0.2	0.5	0.8	1.0	1.1	3.2	3.4	3.7	1.5	0.2	.06	0.1

The frequencies would be slightly higher than those tabulated if based on clock hours rather than actual durations in hours and minutes.

162. It was thought that a closer approach to the values of the wet-bulb temperatures associated with thunderstorms could be obtained from a matching of the numerical frequencies of each. The wet-bulb frequencies were also obtained from Albright's book which includes tabulations of the total hours of occurrence of wet-bulb temperatures equaling or exceeding certain values during June to September, inclusive, of a normal year. The occurrences tabulated are those within 8-, 12-, and 24-hour periods each day. The 12-hour tables were used in this study, since the 12-hour periods were generally from 10 a.m. to 10 p.m., or from 1 p.m. to 1 a.m., and therefore most closely associated with the period in which the greatest number of thunderstorms occur. Because the higher wet-bulb temperatures are of the most interest, it was arbitrarily assumed, for the purposes of this study, that the duration of the wet-bulb temperature range associated with a thunderstorm day was equal to the normal duration of the wet-bulb temperatures within 2.5 F of the normal daily maximum wet-bulb temperature during the period June to September.

163. The normal diurnal variation of wet-bulb temperatures throughout the country is shown in figure 34, also from Albright. At Moline, Illinois, for instance, the average duration of the wet-bulb temperatures within 2.5 F of the normal maximum is 11 hours. In this analysis, then, 11 hours of wet-bulb duration were matched with one thunderstorm day at Moline (or, in this case, Davenport, which was the available station close by). The same practice was followed

at all other stations except those, such as Miami and San Antonio, where the average wet-bulb duration indicated was more than 12 hours. In such cases a 12-hour average duration was used. The selected average duration was then multiplied by the average number of thunderstorm days during the period June to September, obtained from the comparative data summaries. With this product used as a wet-bulb frequency, Albright's tabulations were entered to obtain the wet-bulb temperature corresponding to the frequency. Whenever the product did not closely match a tabulated frequency, the next larger frequency was used - in other words, the next lower temperature in whole degrees Fahrenheit. The wet-bulb temperatures thus obtained were reduced pseudo-adiabatically (by means of figure 33) to sea level (1000 mb) and plotted on a map. Figure 35 shows the distribution of these reduced wet-bulb temperatures throughout the country. They are also wet-bulb potential temperatures, by definition. The indicated gradient is less than in figure 32. It is also less than it would have been if the temperatures of figure 32 had been reduced to sea level. It can be seen that about two thirds of the country experiences wet-bulb potential temperatures of 74 to 77 F, inclusive, with a frequency directly proportional to the frequency of thunderstorm days.

164. A check on the validity of the relationship was made by determining the wet-bulb temperature frequencies during the thunderstorms indicated on the 1630 EST weather maps of July 1942, a month with considerable thunderstorm activity. The coincident surface wet-bulb potential temperature was determined for each indicated thunderstorm. There were 224 thunderstorm occurrences. Figure 36 shows the

distribution and cumulative curves of percentage frequencies of surface Θ_w observed at the time of these occurrences. The peak frequency is at 74 F which is within the narrow range of associated Θ_w values previously derived. Eighty-five percent of the thunderstorms occurred with Θ_w 70 F or higher, and all but one thunderstorm, which occurred on the California coast, were associated with a Θ_w of 66 F or higher.

165. Since a decrease of Θ_w with height signifies convective instability, it is of interest to note the values of Θ_w aloft. For convenience in such an analysis, the pseudo-adiabat associated with a particular Θ_w value may be identified by its Θ_E value. A Θ_w of 75 F or 24 C equals a Θ_E of 350.8 A. The pseudo-adiabat thus identified has a temperature of 12 C at 10,000 feet. In July 1942 only three cases were noted in which such a wet-bulb temperature was equaled or exceeded at that height - three cases, in other words, in which a Θ_w of 24 C or a Θ_E of 350.8 A was equaled or exceeded at 10,000 feet. In one of the cases, with a Θ_E of 355, a thunderstorm was in progress during the ascent. In another case, with a Θ_E of 353, the surface wet-bulb at the time was 82 F, giving a Θ_E of 371 and thus indicating exceptional convective instability. In the third case Θ_E at 10,000 feet was equal to 350.8 A.

166. Figure 37 shows distribution and cumulative curves of the percentage frequencies of Θ_E occurrences at 3 kilometers during the months June through September, 1936 and 1937, at four widely scattered stations: Omaha, Shreveport, Boston, and Billings. The highest Θ_E was 350, and there was only one case of that.

167. The conclusion can be reached that 75 F is a critical surface wet-bulb potential temperature anywhere in the United States, and especially in the northern portions. If exceeded, it almost always indicates convective instability as well as conditional instability. However, experience indicates that its occurrence does not guarantee the occurrence of the thunderstorm. A mechanism must be present to provide the trigger action. The instability, whether convective or conditional, is only potential and requires realization.

Comparison with average precipitation distribution

168. Figure 38 is an isohyetal map of average annual precipitation over the United States and the 12 succeeding charts in figures 39 to 41 are isohyetal maps of average monthly precipitation. The first chart is adapted from the annual precipitation chart on page 711 of "Climate and Man." The monthly charts are based on first-order-station averages obtained from the comparative-data summaries, plus averages selected from cooperative-station data published in the state climatic summaries of "Climate and Man." The latter maps are therefore not as accurate in detail as the annual map. They serve the purpose, however, of their reproduction here, which is a comparison with the distribution of thunderstorm days as shown by the red overprint. The comparison is general rather than detailed. No attempt is made to distinguish between snowfall and rainfall, the terms "precipitation" and "rainfall" being used interchangeably.

169. The annual map (figure 38) furnishes a few clues to the types of relationship which are best sustained in the monthly maps. East of

the 100th meridian both rainfall and thunderstorms decrease northward from the Gulf. Over the Plains States, however, the westward longitudinal gradient of rainfall is much steeper than the thunderstorm gradient and on the Atlantic Coast there is a tendency toward reversal of the thunderstorm gradient in the rainfall pattern. Over the Rocky Mountain area the relationships, if any, are not clear on the annual map. On the West Coast and in the Sierras the rainfall pattern is in sharp contrast to the thunderstorm pattern.

170. On the January map (figure 39), as on all the winter maps, an outstanding difference between the two types of activity is implied rather than demonstrated. As will be shown later, the number of days with rainfall far exceeds the number of days with thunderstorms in the winter months. Nevertheless, from the central Gulf States to the Ohio River Valley, isohyets and isoceraunics have approximately the same shape. The area of important rainfall in this region, however, extends farther northward and eastward than the thunderstorm activity. While the thunderstorms are confined mostly to the warm sector and the frontal zones, where tropical maritime air is deep and near the surface, the rain area spreads northward where the warm air overruns and where occlusion of the cyclone takes place. Along the Atlantic Coast, too, a new source of maritime tropical air is often drawn into the circulation, with consequent spread of coastal rainfall. On the Pacific Coast, although the heavy rainfall seems entirely excessive in proportion to the thunderstorm activity, it must be remembered that the latter, though rare at any time of year, actually decreases in the dry summer months. Also, as previously mentioned, while the orographic effect is sufficient

to cause heavy precipitation, it requires a particularly intense occluded front to produce a thunderstorm in that region.

171. In February (figure 39) a slight eastward shift and spread of the maximum isohyets toward the Atlantic Coast accompanies the slight eastward displacement to Mississippi of the maximum isoceraunic center. The thunderstorm spread northward to the Lakes and along the Atlantic Coast is not accompanied by any important increase in rainfall. The 4-inch isohyet, for example, has receded from northern to southern Kentucky. An increase of rainfall in Arizona, Utah, and Colorado is probably associated with the mild outbreak of thunderstorm activity indicated at Phoenix (table 1).

172. By March (figure 39) the 2-day isoceraunic has expanded more than the 2-inch isohyet in the same region but there is still a strong resemblance between the rain and thunderstorm patterns from the Gulf to the Lakes. The rainfall in the Plains States, though still under two inches, has increased somewhat with the movement of the 1-day isoceraunic into the area. Again, at least in the regions of the greatest activity (outside the West Coast area), the thunderstorm and rain maximum centers do not coincide, the thunderstorm center appearing south and west of the rain center.

173. In April (figure 39) the rains though still heavy, have diminished on the Pacific Coast while the thunderstorm activity has moved inland. The greatest increases in rainfall are in the Plains States west of the Mississippi River as shown by the spread of the 2-inch isohyet. The maximum thunderstorm activity, in Arkansas, is south and east of much of this spread, indicating a cyclonic flow of the warm,

moist air from the vicinity of the month's maximum thunderstorm activity.

In Florida, the first appearance of a 4-inch isohyet on the southeast coast coincides with the first appearance of a 4-day isoceraunic. The numerical similarity is, however, a coincidence.

174. In May (figure 40) the significant increases in rainfall are from Texas-Oklahoma northward and in Florida, where there are also the most significant increases in thunderstorm activity and where the latest maximum thunderstorm centers are located. Again there seems to be a northward and northwestward spread of increasing rain from the center of thunderstorm activity except in Arkansas, where thunderstorm and rainfall centers coincide. The rain spread is toward the Plains States and toward the Rockies, where a secondary thunderstorm maximum now begins to appear.

175. The shift of the maximum thunderstorm center westward across Florida by June (figure 40) has been accompanied by a shift of the maximum rainfall center and the increase in thunderstorm activity is also reflected in the rainfall. In most of Texas there has been a decrease of thunderstorm activity, and an accompanying isohyetal depression now extends across Louisiana and Mississippi to South Carolina. However, east of Texas thunderstorm activity has increased, and the isohyetal depression is only comparative east of Louisiana - the rainfall has actually increased. Along the eastern slopes of the Rockies the now visible thunderstorm centers are no longer reflected in any increase in rainfall. Except around Roswell, there has been an actual decrease in rainfall. The Missouri thunderstorm center, however, is still accompanied by increasing rainfall which has spread northward and northwestward.

176. By July (figure 40) the shift of the Florida thunderstorm maximum has finally brought the rainfall maximum to the west coast of the peninsula. Increasing rainfall accompanies the increase in thunderstorm activity along the immediate Gulf Coast and also in the Rockies, where there has been a significant extension of the rainfall zone westward into Arizona along with the extension to Flagstaff of the thunderstorm maximum. The high-level anticyclone has now erased the Arkansas-Missouri thunderstorm maximum and the flow of tropical maritime air toward the Rockies is entirely around the southern and western peripheries of the high-level circulation. Under its central portion the Texas decrease in activity has spread northward with rains diminished to the Canadian border. Along the Atlantic Coast from Georgia to Virginia there has been an important increase in rainfall, also accompanied by an increase in thunderstorm activity. But while the increase in rainfall is greater, the thunderstorm increase is less than on the Gulf Coast. This is probably due to the hurricane or tropical-storm frequency of this season ⁽¹⁹⁾, the hurricane being a heavy-rainfall producer, but causing little or no thunderstorm activity.

177. While there is not much change from July to August, the latter map (figure 40) gives the first evidence of the southward contraction of both isohyets and isoceraunics which, in the following months, becomes the general rule except on the West Coast. There is a slight decrease in most sections, the greatest decreases, both in rainfall and thunderstorms, being north of latitude 45.

178. In September (figure 41) the decrease in both activities continues throughout except in three locations. In the extreme northwest

the increase in rainfall is unaccompanied by any equivalent increase in thunderstorms. Over Missouri, Illinois, and Wisconsin rainfall has increased (probably associated with increased frontal activity in this region), the area being approximately coincident with a diminished center of thunderstorm frequency. Rainfall has increased over eastern Florida also, where thunderstorm activity has decreased, with the center of thunderstorm activity beginning to be displaced southeastward.

179. In October (figure 41) the southern Florida isoceraunic center corresponds to the isohyetal center in that region. There has been no increase in thunderstorm activity on the Pacific Coast except around Tatoosh (table 1), but the rainfall increase is important. Along the northeast Atlantic Coast rainfall values are still practically unchanged but thunderstorm days have dropped sharply. Elsewhere the decrease in both activities continues.

180. On the November map (figure 41) the general thunderstorm decrease is still accompanied by a decrease in rainfall except in Arkansas-Louisiana, in the Northeastern States, and on the West Coast. From Eureka northward Pacific Coast stations now show slightly increased thunderstorm activity (table 1) but the rainfall increase is much greater. In the Northeastern States, although thunderstorm activity has practically ceased, rainfall values are not much changed. The Arkansas-Louisiana rainfall center coincides with a diminished maximum thunderstorm center.

181. In December (figure 41) there is increased rainfall from East Texas to the Atlantic Coast, with the exception of southern Florida.

The rainfall values are maintained in the Northeast and further increased on the West Coast where the slight thunderstorm increase has extended southward to San Diego (table 1). Elsewhere in the country there is still a decrease in precipitation except in northern Louisiana, where a maximum rainfall center is located, coinciding approximately with the thunderstorm center.

182. The generally evident though not invariant relationship between rainfall and thunderstorm activity is further demonstrated in tables 5, 6, and 7. In table 5 the percentage of normal rainfall for a state or section during the wettest summer of record for the period 1904-43 is compared with the percentages of normal thunderstorm-day frequency at all the first-order stations which were available during the same season within the state or section. In table 6 a similar comparison is made for the driest summer of the 1904-43 period. The areal-rainfall values were obtained from a published Weather Bureau summary of normals and seasonal percentages of rainfall for the period 1886-1938 (20), to which have been added the seasonal percentages for the last five years. With few exceptions, the tables show mostly above-normal thunderstorm-day frequencies for the wettest summer and mostly below-normal frequencies for the driest summer.

183. For table 7, 47 stations were selected as geographically representative. The percentage of normal thunderstorm-day frequency and the percentage of normal rainfall are compared for each station, first, in the July with the maximum number of thunderstorm days (1904-43) and, second, in the July with the maximum rainfall (same period). On the whole the positive relationship indicated in tables 5

Table 5

COMPARISON OF PERCENTAGES OF NORMAL RAINFALL
WITH PERCENTAGES OF NORMAL THUNDERSTORM-DAY FREQUENCY
DURING THE WETTEST SUMMERS - 1904-43

State or Section	Year	Percentage of Normal Rainfall	Percentages of Normal Thunderstorm-Day Frequency at All Available First-Order Stations
Ala.	1916	165	110-101-93
Ariz.	1921	184	177-75
Ark.	1915	156	113-98-98
Calif.	1929	311	83-0-0-0-0-0-0
Colo.	1921	158	116-109-88
Fla.	1939	132	122-113-112-110-99-93
Ga.	1928	145	118-113-109-103-93
Idaho	1913	212	180-141-129
Ill.	1915	168	121-102-91-87
Ind.	1915	150	133-105-104-81
Iowa	1924	151	142-140-137-129-124-110
Kans.	1915	166	143-131-128-123-108
Ky.	1928	161	131-107
La.	1940	174	105-92
Md-Del.*	1906	155	138-105
Mich.	1905	135	110-106-102-99-96-82-79-70
Minn.	1905	142	171-135-123-120
Miss.	1940	151	93-76
Mo.	1915	170	142-136-136-133-119-115
Mont.	1915	173	165-137-123-101
Nebr.	1915	173	151-136-129-104-101
Nev.	1913	297	253-253-129
New Eng.	1922	151	139-139-133-127-110-109-108-108-95-81-78
N.J.	1928	153	124-105-94
N. Mex.	1921	175	144-133
N.Y.	1928	142	128-128-113-105-103-102-101-87-84
N.C.	1906	159	141-134-124-121-72
N. Dak.	1928	162	130-119-119-97
Ohio	1935	139	130-109-104-95-94
Okla.	1915	173	127
Oreg.	1941	238	263-244-165-125
Pa.	1928	142	128-119-112-106-103-91
S.C.	1906	148	139-138
S. Dak.	1915	167	134-118-109-96
Tenn.	1928	149	123-122-112-103
Tex.	1919	172	203-158-157-156-145-143-135-133-126-118-116-109-80-77
Utah	1936	211	189-153
Va.	1906	156	144-135-122-112-100
Wash.	1937	194	240-231-206-169-143-125-0
W. Va.	1907	133	110-99
Wis.	1905	145	163-143-111-108
Wyo.	1941	168	206-117-97

* including Washington, D. C.

Table 6

COMPARISON OF PERCENTAGES OF NORMAL RAINFALL
WITH PERCENTAGES OF NORMAL THUNDERSTORM-DAY FREQUENCY
DURING THE DRIEST SUMMERS - 1904-43

State or Section	Year	Percentage of Normal Rainfall	Percentages of Normal Thunderstorm-Day Frequency at All Available First-Order Stations
Ala.	1925	60	73-73-76-103
Ariz.	1924	59	48-48
Ark.	1930	36	64-82
Calif.	1940	20	0-0-0-0-0-32
Colo.	1924	42	49-50-55
Fla.	1931	68	71-82-82-88-95-104
Ga.	1925	52	66-83-86-93-104
Idaho	1919	24	50-75-89
Ill.	1936	53	53-85-87-102
Ind.	1936	57	86-88-120-133
Iowa	1927	59	58-63-66-67-68-70
Kans.	1936	31	38-45-64-67
Ky.	1930	44	45-111
La.	1924	43	48-100
Md-Del.*	1930	47	67-87
Mich.	1930	65	40-66-68-84-87-89-102-103-104-111-132
Minn.	1936	54	57-63-85
Miss.	1930	47	59-70
Mo.	1936	32	43-48-49-65-78
Mont.	1919	39	36-86
Nebr.	1936	45	56-64-89-90
Nev.	1919	27	12-84-85
New Eng.	1913	63	68-68-80-84-88-88-91-93-96-100-101-101
N.J.	1929	55	76-97-106
N. Mex.	1922	70	72-106
N.Y.	1913	60	65-81-82-86-89-101-101-102
N.C.	1925	60	75-86-92-109
N. Dak.	1936	44	55-97-106
Ohio	1930	56	65-76-76-83-86-108
Okla.	1936	30	42
Oreg.	1919	33	49-83-105
Pa.	1930	62	51-66-69-69-78-89
S.C.	1925	50	73-79-79-96
S. Dak.	1936	44	85-113
Tenn.	1930	50	43-61-81-100
Tex.	1934	50	21-39-43-49-58-65-67-69-83-86-89-94-95-96
Utah	1940	55	44-54
Va.	1930	52	44-51-51-52-71-74
Wash.	1919	38	0-38-80-99-125-127-133
W. Va.	1930	53	44-55
Wis.	1910	60	74-79-95
Wyo.	1924	49	12-65-69-86

* including Washington, D. C.

Table 7

COMPARISON OF MAXIMUM RAINFALL AND MAXIMUM THUNDERSTORM-DAY FREQUENCY
FOR JULY AT SELECTED STATIONS, 1904-43

Station	Year	July with Max. Thdrstm Days		Year	July with Maximum Rainfall	
		% Normal Th.Days	% Normal Rainfall		% Normal Rainfall	% Normal Th.Days
Abilene	1911	245	336	1938	418	94
Amarillo	1941	232	131	1908	211	82
Asheville	1934	159	104	1905	270	136
Atlanta*	1916	149	238	1916	238	149
Baker	1907	308	234	1908	442	128
Boston	1938	200	271	1921	335	140
Buffalo	1921	242	48	1927	188	136
Burlington	1933	152	16#	1932	226	114
Cairo*	1910	173	248	1910	248	173
Charles City	1942	183	198	1940	274	122
Charleston	1904	203	92	1935	256	154
Chicago	1935	180	96	1915	176	153
Cincinnati	1917	157	114	1926	283	93
Columbia, Mo.*	1924	155	146	1924	146	155
Del Rio	1938	218	115	1906	369	125
Denver	1918	160	184	1919	329	56
Dodge City	1904	214	60	1911	258	90
Duluth	1913	176	170	1909	298	132
Eastport	1917	186	62	1916	158	139
Elkins	1913	177	158	1911	189	93
El Paso*	1914	163	276	1914	276	163
Escanaba	1935	177	133	1922	221	51
Eureka	1935	1000	90	1916	1340	0
Fort Smith	1904	200	92	1905	251	133
Grand Junction*	1929	188	388	1929	388	188
Grand Rapids*	1912	176	256	1912	256	176
Havre	1935	228	94	1916	337	129
Huron	1939	170	59	1918	233	125
Los Angeles	1936	1000	100	1918	900	500
Modena	1906	192	173	1916	355	121
Nashville	1938	163	146	1936	206	127
New Orleans	1942	146	130	1940	179	134
New York	1938	193	151	1919	187	60
North Platte*	1907	186	264	1907	264	186
Omaha	1943	209	110	1915	219	151
Phoenix	1917	205	378	1911	616	141
Pittsburgh*	1943	167	197	1943	197	167
Pocatello*	1925	184	416	1925	416	184
Portland, Oreg.	1920	500	118	1916	418	0
Raleigh*	1931	143	220	1931	220	143
Reno*	1913	275	833	1913	833	275
Richmond	1913	155	77	1923	230	124
Santa Fe	1908	162	84	1911	216	115
Seattle*	1916	429	306	1916	306	429
Sheridan*	1923	149	522	1923	522	149
Tampa	1904	142	61	1906	175	124
Williston	1935	171	250	1928	311	158

*July of maximum thunderstorm days & maximum rainfall the same

#Minimum July Rainfall

and 6 is maintained. At 13 of the stations the July with the maximum number of thunderstorm days is also the July with the maximum rainfall. However, 13 stations had below-normal rainfall during the July of maximum thunderstorm-day frequency, and 10 had below-normal thunderstorm-day frequency during the July of maximum rainfall; Eureka and Dodge City are the only stations in both categories. Other rather startling exceptions may be noted. At Burlington, Vermont, the July of maximum thunderstorm-day frequency is actually the July of minimum rainfall. At Eureka and Portland (Oregon), the July of maximum rainfall is a month with no thunderstorms at all. At both Tampa and Santa Fe every day was a thunderstorm day during the July of maximum thunderstorm-day frequency but the associated monthly rainfall was below normal.

Comparison with precipitation-day distribution

184. It is apparent from the previous discussion that the existence of any relationship between rainfall and thunderstorm activity varies with time and place. A comparison of the distribution of thunderstorm days with the distribution of days with measurable precipitation discloses further interesting features of the variable relationship. Figures 42-45, based entirely on first-order-station records (primarily from comparative-data summaries) show the annual and monthly distribution of days with .01 inch or more of precipitation, the red overprints showing the corresponding isoceraunic patterns. The extent to which the lines of equal frequency have been smoothed by using only first-order-station data can be judged by comparison of figure 42 with the annual chart of the same type on page 723 of "Climate and Man." However, use

of first-order-station data makes the charts directly comparable with the thunderstorm charts which are based on the same data.

185. A dominant feature of most of these charts, first observable on the annual map (figure 42), is the sharp reversal of the gradient of activity. Except in Florida and along the Gulf Coast, the number of days with measurable precipitation decreases from north to south whereas the corresponding thunderstorm-day gradient is from south to north. Immediately west of the Mississippi, however, the westward gradient of rainfall* days is similar to the thunderstorm-day gradient. The highest rain-day values are on the northwest coast, where thunderstorm days are at about a minimum. Throughout, the numerical values of days with rain are higher than thunderstorm-day values but the ratio of days with rain to days with thunderstorms varies from about unity around Tampa and Santa Fe to a value 50 times as great on the Pacific Coast. Figures 46 to 49, to be discussed later, show the annual and monthly distribution of the ratios plotted as reciprocal percentages, i.e., as percentage ratios of thunderstorm days to rainfall days.

186. There is little variation from the annual over-all pattern in January, February, or March (figure 43) except that the comparatively high rainfall-day values in the Gulf and Florida are not yet visible. The latter maximum is a summertime contribution whereas the annual map is dominated by the winter contribution.

187. By April (figure 43) rainfall days have diminished and thunderstorm days increased to such an extent that the values are

* Used as synonymous with "precipitation" throughout this report.

actually equal at Roswell and fast approaching equality in that vicinity and in the Gulf States. In May (figure 44) the trend is continued, with Albuquerque and El Paso now joining Roswell in having more thunderstorm than rainfall days in that region. Another trend becoming discernible at this time is that stations in the Gulf region - Miami, in particular, this month - are now approaching northern stations in number of days with measurable rain. The gradient throughout has been slowly decreasing since January, and most rapidly along the West Coast.

188. By June (figure 44) continuation of the latter trend has established a northward gradient of rainfall days along all the Gulf Coast except the Texas portion. Days with thunderstorms now exceed days with measurable rain throughout Arizona, New Mexico, the eastern portions of Colorado and Wyoming, and at most stations along the Gulf Coast apart from Texas. Both trends are maintained in July and August (figure 44). From the Gulf States to New England the gradient of rain days has become almost entirely northward like the thunderstorm-day gradient, and thunderstorm days now either equal or exceed rain days almost everywhere except in the states bordering Canada.

189. September (figure 45) shows a return to the winter pattern. Except at stations in the Southwest, rain days again exceed thunderstorm days throughout and the rain-day gradient from the Canadian border southward shows signs of reestablishment. The pattern becomes steadily more definite in October, November, and December (figure 45).

190. As previously mentioned, figures 46 through 49 show the annual and monthly distribution of the percentage ratios of thunderstorm days to days with .01 inch or more of precipitation. These

ratios were obtained from the averages, to whole numbers, for which the isoceraunics of figures 28 to 31 and the isofrequency lines of figures 42 to 45 were drawn.

191. The annual chart, figure 46, shows all ratios but one (at Albuquerque) to be less than 100% and more than half to be under 50%. The monthly charts, however, demonstrate a wide seasonal variation of the ratio. In January (figure 47) the ratios are naturally small, mostly near zero except in the region of appreciable thunderstorm occurrence where no ratios, however, are much over 20%. The ratios increase in the following months until by April (figure 47) the near-zero values are confined to the West Coast. In the vicinity of Roswell thunderstorm days are now numerically equal to measurable-rainfall days.

192. The area of ratios equaling 100% or more grows rapidly until July and August (figure 48) and then declines rapidly, until by October (figure 49) it comprises only the vicinity of Yuma. The area in which the number of days with .01 inch or more approximately equals the number of thunderstorm days is thus at its maximum from June through August, but it is only a fair approximation to conclude that therefore nearly all rain is associated with thunderstorms during this period, especially within the area considered. An analysis of the record at Mobile in table 8 shows that even in the three months, June through August, when days with .01 and days with thunderstorms approach equality, the number of days that can be classified as both is only about 75% of either total:

Table 8

TOTAL THUNDERSTORM DAYS VS. TOTAL DAYS WITH .01 INCH OR MORE
AT MOBILE, ALA., 1914-36

	Jan	Feb	Mar	Apr	May	Jun	Jul	Aug	Sep	Oct	Nov	Dec
Days with .01 or more	229	219	198	181	191	237	331	301	191	155	154	234
Days with thdrstms	39	52	78	118	142	255	365	332	131	54	30	44
Days with both	38	50	75	111	113	186	265	243	85	44	30	44

During the other months the percentage of thunderstorm days that are also days with measurable rain at the station is often 100 or nearly so, but as few as 20% of the days with measurable rain may be thunderstorm days. In the wintertime, in other words, there are practically no thunderstorm days without measurable rain at the same station. A similar analysis, confined to the summer months, was made of 10-year records at Omaha and Oklahoma City:

Table 9

TOTAL THUNDERSTORM DAYS VS. TOTAL DAYS WITH .01 INCH OR MORE
AT OMAHA, NEBR., AND OKLAHOMA CITY, OKLA., 1933-42

	Omaha			Oklahoma City		
	June	July	August	June	July	August
Days with .01 or more	96	71	93	83	44	71
Days with thunderstorms	85	83	82	84	47	78
Days with both	71	63	63	65	31	56

At these two stations also, during the months when rain-day and thunderstorm-day frequencies approach equality, the occurrences actually coincide only about 75% of the time. While in the Gulf region the ratio of thunderstorm days to rain days during this period seldom exceeds 120%, at stations in the mountain regions of the West it often goes to 150

and 200% and even higher. This explains the ill-defined relationship between increased thunderstorm activity and increased average rainfall in the latter region. As the frequency of thunderstorms increases during the summer, more of the thunderstorms occur without rain at the reporting stations. It is not so well known that there is a similar effect, though less pronounced, in the Gulf States.

193. It does not follow from the above that there are necessarily a considerable number of thunderstorm situations in which there is no rain at all. Even when every thunderstorm event is accompanied by rain that does not evaporate before it reaches the rain gage, there are two important possibilities which would influence the comparative frequencies of thunder and of measurable precipitation as observed by individual stations. The first and more obvious possibility is that the area experiencing rainfall during the thunderstorm event may be smaller than the area in which thunder can be heard. This seems to characterize local or scattered thunderstorm occurrences. The result is that the station reports a number of thunderstorm days without measurable rain. However, there is the alternate possibility that the area experiencing rainfall during the thunderstorm even may be larger than the area in which thunder can be heard. This does not seem so likely, but examination of synoptic charts indicates that such circumstances are especially characteristic of the widespread or general thunderstorm situation. If the area of thunderstorm occurrence is defined solely on the basis of stations reporting thunder, the events often seem sporadic. But if the stations reporting only showers (or even only cumulonimbus clouds without showers) are also included, a continuous area of occurrence can be outlined,

an area which is homogeneously related to the frontal or dynamic flow pattern which appears to be the causal factor. An extreme case is the winter thunderstorm situation in which there is widespread rain but few and scattered reports of thunder; this type of situation may also occur in the summer. The result is that many stations will report measurable precipitation without thunder although the two phenomena are actually associated.

194. The data tabulated by Hamrick and Martin for Kansas City ⁽⁴⁾ make possible a comparison of the frequencies of days with .01 inch or more of precipitation with the frequencies of days of precipitation above a higher limiting magnitude. Figure 50 graphs the frequencies of several classes of such days. The monthly variations of the frequencies are similar and resemble the thunderstorm-day variation, also plotted in the figure. The principle cannot, however, be extended to other regions without a like analysis. A similar graph of frequencies by hours rather than by days is shown for Peoria, Illinois, in figure 51, based on data by Fuller ⁽¹⁷⁾. Here, the precipitation curves are completely out of phase with the thunderstorm curve, except in the higher intensities.

Comparison with daily-intensity distribution

195. The variable effectiveness of a thunderstorm regime as a rainfall-producer can be further analyzed by a comparison of the distribution of thunderstorm days (figures 28 to 31) with the distribution of the 24-hour rate of rainfall on calendar days having measurable rain. For convenience the latter value will be called the daily intensity.

These intensity values were obtained by dividing average annual or monthly rainfall (figures 38 to 41) by the average number of days with measurable rain for the period (figures 42 to 45). The isohyets of average daily intensity, for the year and for each month, are presented in figures 52 through 55. Not available in any form in the published literature until recently (21), the charts are of interest in themselves as well as for comparison with the thunderstorm distribution shown as a red overprint. Although the usual reservations concerning the accuracy of the isohyetal details should be made, the values can serve as a guide in the quantitative forecasting of rainfall. However, the values are necessarily compounded of a wide range of intensities of unequal frequencies. For the purposes of the current report it must be remembered that the daily intensity corresponds to the average thunderstorm-day intensity only when thunderstorm days and measurable-rainfall days are the same. However, there are periods and places when this coincidence is approached; and at other times and places the direction, if not the magnitude, of the effect of increased thunderstorm activity on the daily intensity may be seen. The effect is not always the expected one.

196. The annual map (figure 52) is representative of the charts which follow. East of the 100th meridian its resemblance in pattern to the thunderstorm-day pattern is striking. On both charts the value at New Orleans is about three times the value at Houghton, Michigan, and the relationship is roughly the same elsewhere in the vicinity of these stations. The Florida peninsula, particularly Tampa, has anomalously low intensities. The highest intensity values are in

northwestern Florida. Neglecting the Tampa thunderstorm maximum, this means that intensity and thunderstorm maxima are coincident in this region. The thunderstorm maximum over the eastern slopes of the Rockies, however, shows no apparent effect upon the intensity. On the West Coast, as usual, the intensities are in a class by themselves: high despite meagerness of thunderstorm activity and high despite the large number of rainfall days.

197. Compared with the annual map, the January chart (figure 53) displays lower intensity values almost everywhere except on the West Coast and on the Gulf Coast from New Orleans to Apalachicola. The 0.1-inch isohyet dipping southward over the Plains and Rocky Mountain States coincides approximately with the area of absolutely no thunderstorms. Most of the area within the 0.3-inch isohyet corresponds to the area within the 1-day isoceraunic. In February (figure 53) the intensity pattern is practically unchanged. A slight northward displacement of the 0.2-inch isohyet reflects the expansion of the 1-day isoceraunic and an eastward extension of the 0.4- and 0.5-inch isohyets corresponds to the spread of the 2-day isoceraunic. Except on the West Coast, intensities have increased. The same trend is continued in March and April (figure 53) but the percentage increase in daily intensity is only a small fraction of the percentage increase in thunderstorm days. The greatest increases are in the Gulf States, where 0.6- and 0.7-inch isohyets appear in April on the immediate coast, somewhat dissociated from the maximum thunderstorm center which persists northwest of the maximum isohyets. The April daily intensity of 0.77 inch at New Orleans, incidentally, is never exceeded in the months following,

despite the continuous thunderstorm increase through July. This is also true of many other stations in the same region.

198. In May (figure 54) there are definite breaks in the continuity of the intensity pattern. The high intensities of the West Coast are disappearing. The region of maximum intensity has been displaced to East Texas, the region where May is the month of maximum thunderstorm activity. There is also a notable isohyetal extension northward from this region, its axis corresponding approximately to the axis of the maximum thunderstorm center for the month. A new intensity maximum appears in southeastern Florida, lagging behind the appearance of the isoceraunic maximum in the same region the previous month. More or less symmetrical with the Appalachian Ridges, a sharpened isohyetal trough becomes evident, made more definite and elongated (as compared to the previous month) by an actual decrease of intensities in its southern portion, although throughout this area a seasonal increase in thunderstorm activity has occurred.

199. There is in June (figure 54), as there was in May, an overall decrease in intensities except in the general region from East Texas northward, in the states bordering Canada, and in Florida. Even on the eastern slopes of the Rockies, where a secondary thunderstorm maximum emerges in June, there is a slight decrease in intensity. One of the effects of this trend is to reduce the south-north gradient of intensity in the eastern half of the country. Whereas the decrease from Gulf to Canadian border was as high as 0.5 inch in April it is now about 0.1-0.2 inch. The ratio between Gulf and Canadian-border intensity, which was about 3:1 on the annual map and 4:1 in April, is

now reduced to about 3:2. This is the beginning of the season when thunderstorm days and rain days approach numerical equality over much of the country; thus the intensity pattern over the eastern half of the country may be taken as evidence that in midsummer there is no important variation in the intensity of thunderstorm rainfall throughout this region. Furthermore, even by strict interpretation, most of the summer rainfall is thunderstorm rainfall. The significant variation begins west of the 100th meridian.

200. The only important changes by July (figure 54) are a sharp decrease in intensity over the Florida peninsula (although thunderstorm days are still on the increase) and a substantial intensity increase along the Middle Atlantic Coast. The latter, an effect of the hurricane season, is continued in August (figure 54) and by September (figure 55) has also reached the Florida east coast. During these three months the isohyetal ridge from East Texas to Minnesota and Wisconsin is maintained and, by September, even strengthened. Only in the last month does it coincide with an isoceraunic ridge, and then only partially. Along the eastern slopes of the Rockies, during these months, neither the growth nor the decay of the thunderstorm maximum in the region shows any appreciable effect on the daily intensity.

201. During the last three months of the year (figure 55) there is the usual recession Gulfward characteristic of the winter pattern, while on the West Coast intensities increase. An appreciable area of intensity under 0.1 inch appears again in November and it is approximately the same as the area of zero occurrence of thunderstorms.

202. One of the weaknesses of the comparison between thunderstorm-day frequency and average daily intensity is that the latter is an average for both the days with and the days without thunderstorms. It seemed probable that the effect of thunderstorm frequency on daily intensity would be made more obvious if the two types of data could be separated. A pilot study was therefore made of the record at Mobile, Alabama, for the years 1914-36. Even with simplifying assumptions such as the association with the thunderstorm day of all the rainfall within the same calendar day, time did not permit the extension of the study to other representative stations in order to determine regional differences, if any. The results for Mobile, given in table 10, are sufficiently interesting to make such an extension worth while.

Table 10

THUNDERSTORM AND NON-THUNDERSTORM DAILY INTENSITIES
AT MOBILE, ALA., 1914-36

Month	Daily Intensities (inches) on Days with:				
	.01 inch Thunder- or more storms	Thunder- (2)	Thdrstms and (3)	.01 or more and no thdrstms (4)	T or more and no thdrstms (5)
January	.53	.91	.93	.45	.36
February	.52	1.01	1.06	.36	.27
March	.63	1.19	1.24	.25	.16
April	.57	.77	.82	.20	.11
May	.53	.54	.68	.32	.18
June	.46	.39	.53	.20	.11
July	.50	.39	.53	.38	.22
August	.47	.36	.51	.40	.20
September	.55	.40	.62	.49	.30
October	.59	.79	.96	.44	.30
November	.58	1.17	1.17	.44	.31
December	.50	.98	.98	.39	.29

203. A comparison of the first two columns yields a somewhat unexpected result. While the daily intensities are about doubled on thunderstorm days during the winter months, the difference between the two classes of intensity is decreased toward the summer months and finally reversed from June to September, inclusive. At first glance, this seems to say that more rain falls on individual thunderstorm days in winter than in summer and that, furthermore, while thunderstorm days have more intense rainfall than non-thunderstorm days in winter, they actually have less intense rainfall in summer. The latter statement, in particular, is contrary to popular experience and belief and is in fact not the truth, as further analysis will indicate.

204. In the first place, the actual duration or hourly frequency of the rainfall is not considered in this tabulation. Some material on that subject is presented in a later section on the diurnal variation of rainfall; at this time it is sufficient to recall the well-known fact that winter rainfall is usually of longer duration than summer rainfall. All-day rain is not unlikely in winter, whereas the summer type is more likely to have a duration of about one hour. The use of 24-hour intensities probably obliterates the important differences in actual or hourly intensities. It still remains true, however, that the winter thunderstorm day is by far a heavier rain-producer than the winter non-thunderstorm day.

205. The other fact to be recalled is that thunderstorm days are not necessarily days with appreciable rain or even days with any rain at all at the same station (paragraphs 190-93). While this is popularly known to be true of thunderstorms in the western part of the United

States, it is significantly true even in the Gulf States, as has been shown (table 8). At Mobile the monthly variation in the occurrence of thunderstorm days with less than .01 inch of rain (i.e., with trace or zero) is given in the following table:

Table 11

TOTAL THUNDERSTORM DAYS WITHOUT MEASURABLE RAIN
AT MOBILE, ALA., 1914-36

	Jan	Feb	Mar	Apr	May	June	July	Aug	Sept	Oct	Nov	Dec
Days	1	2	3	7	29	69	100	89	46	10	0	0

These occurrences are included in the thunderstorm-day intensities of column 2 of table 10 and their chief effect is to reduce the daily intensities for the summer months. The intensities of column 3 of table 10 are derived after eliminating the occurrences of table 11. The result is an increase over the values of column 2 in summer but no change, or practically none, in winter. For all months, now, the intensities on days with thunderstorms exceed the intensities on days with .01 inch or more of precipitation (with or without thunder).

206. A more appropriate comparison would be with the intensities of column 4, which are daily intensities on days with .01 inch or more but with no thunderstorms. The intensities of column 3 are all greater and by a greater margin than previously, but the difference is still greatest in winter months.

207. Another comparison can be made between the intensities of column 2 and those of column 5, the latter containing the values on days with a trace or more but with no thunderstorms. Between these

two, the differences are the greatest and are all in favor of the thunderstorm day.

208. From the data basic to the material in table 10, it is also possible to derive approximate values for the percentage of total rainfall associated with thunderstorm activity if the assumption is made that all the rain on a thunderstorm day is thunderstorm rain. Table 12 lists the percentages:

Table 12

PERCENTAGE OF RAINFALL ASSOCIATED WITH THUNDERSTORMS
AT MOBILE, ALA., 1914-36

	Jan	Feb	Mar	Apr	May	June	July	Aug	Sept	Oct	Nov	Dec
Percent	29	46	75	86	76	91	85	84	51	47	39	37

The summertime maximum and the wintertime minimum are well defined.

Comparison with distribution of selected intensities

209. A recent study by Dyck and Mattice ⁽²²⁾ contains tabulations of two classes of excessive rain occurrences: (1) rains with at least one hourly amount greater than 0.99 inch, and (2) rains with at least one 24-hour amount greater than 2.49 inches. Thirty years of record, 1908-37, were studied at 155 first-order stations, only two of which (Northfield, Vermont, and Lynchburg, Virginia) had less than the 30-year record. In this discussion, the occurrences will be referred to as 1.0"/hour and 2.5"/day occurrences, respectively. Their annual and monthly distributions are shown in figures 56-59 and 60-63, respectively, with the usual red overprint of the corresponding thunderstorm distribution. The charted values are all totals for the entire period of record.

The lines of equal frequency have not been excessively smoothed; they indicate the comparative non-uniformity of the data as well as the scattering of stations. The occurrence of such high intensities at a particular station (over a particular rain gage, to be exact) is relatively so infrequent that even 30 years of record does not give a uniform distribution in what is, as far as known, a meteorologically homogeneous region.

210. Nevertheless, the annual charts (figures 56 and 60) for both intensities show clearly enough the relation hitherto seen between distribution of intensities and distribution of thunderstorm days. East of the 100th meridian there is the usual similarity of pattern, with maximum values on the Gulf Coast. The Florida isoceraunic maximum is not reflected in due proportion but it is reflected more definitely on the 1.0"/hour chart than on the 2.5"/day chart. The Rocky Mountain thunderstorm maximum finds no corresponding feature on either of the charts. On the West Coast, the scarcity of 1.0"/hour rains corresponds to the thunderstorm scarcity, but the 2.5"/day rains have a comparatively high frequency. The highest frequency of 1.0"/hour rains is about 10% of the thunderstorm-day frequency, such a frequency occurring on the Gulf Coast. Elsewhere the ratio is between 5 and 10%, in general diminishing with increasing distance from the Gulf. Apart from the West Coast, the 2.5"/day frequency is, on the average, about one half of the 1.0"/hour frequency.

211. Along the Appalachian Ridge both annual intensity charts indicate an apparent inhibiting effect with greater emphasis than the thunderstorm chart. They indicate a similar effect in the region

of the Ozarks although there it is completely absent on the thunderstorm chart. The latter phenomenon is probably an example of the lesser frequency of rains of high intensity at higher elevations, a phenomenon noted elsewhere, specifically in the Hydrometeorological Section's report on the Sevier Basin (23). Although that report covers a region which shows scarcely any significant activity of the 1.0"/hour or 2.5"/day categories, the pertinent figure from the report is reproduced here as figure 64, to indicate the nature of the elevation effect. The obvious explanation is that at higher elevations the precipitable-water content of the atmosphere is generally less, just as the mass of air is always less. While this serves to decrease the frequencies of high intensities, it must be remembered that the number of occurrences of lower intensities is usually increased by the windward orographic effect.

212. A detailed discussion of the monthly charts would be largely a repetition of previous discussions of the rainfall-thunderstorm relationships. The charts are reproduced to complete the available record. They exhibit no radical changes in the basic annual pattern nor in the general resemblance between isoceraunic and frequency patterns. They show, of course, the West Coast 2.5"/day maximum to be entirely a winter phenomenon. In other regions also, it is noticeable that in January, February, and March, the area covered by 2.5"/day occurrences includes the area of 1.0"/hour occurrences and that even within the area of coincidence the 2.5"/day occurrences either equal or exceed the 1.0"/hour occurrences. By April the areal difference is diminished though still of the same

sign, but the 1.0"/hour occurrences are beginning to exceed the 2.5"/day occurrences, especially in the Gulf and Florida sections. In the following months this trend is continued, so that by midsummer occurrences of 1.0"/hour intensities exceed, by an average ratio of three to one, the 2.5"/day occurrences. The latter actually decrease in number except along the Atlantic Coast in the hurricane season, July to September, and from East Texas to Iowa in September. By November the return to the winter-type relationship again becomes visible.

213. It seemed probable that a more useful comparison could be made between thunderstorm-day frequency and the frequency of excessive rainfall for short periods since thunderstorm rainfall is better defined by such a class of intensities than by a class of specific intensities of rather low frequency such as discussed above. The Weather Bureau makes an annual tabulation of the occurrences of excessive rainfall* in the Meteorological Yearbook, formerly the Report of the Chief of the Weather Bureau. Using these tabulations, Yarnell has published monthly charts of the frequency distribution on pages 62-67 of his pamphlet ⁽²⁴⁾. A comparison between thunderstorm-distribution charts and Yarnell's charts of "excessive rainstorms", however, is misleading. Although the latter frequencies show the usual Gulf maximum, it is occasionally exceeded by maxima much

* Defined by the formula: $D = t + 20$, where D is accumulated depth in hundredths of inches and t is time in minutes, except in the Southern States, including North Carolina, South Carolina, Georgia, Florida, Alabama, Mississippi, Tennessee, Arkansas, Louisiana, Texas, and Oklahoma. In these the formula is: $D = 2t + 30$.

farther north. This would be extremely interesting, if real, but the fact is that the tabulations in the Meteorological Yearbook (or Report of the Chief) do not list all excessive-rain occurrences in the Southern States, as defined in the footnote. In these regions, generally, only those storms are listed in which one inch or more fell in one hour. The effect of this geographical discontinuity in criteria is not only to reduce the frequency gradient from the Gulf northward but also, apparently, to change the gradient occasionally in the vicinity of the discontinuity.

Comparison with areal-rainfall frequency

214. A compilation of the average depth of weekly precipitation over each climatic section of the United States made it possible to depart from the usual point-rainfall investigation. The compilation was made by a joint WPA-Weather Bureau project in 1937-38 and covered 30 years of record, 1906-35. The weeks were numbered consecutively beginning with January 1 and the depths for each climatic section were obtained from an arithmetical average of the point rainfall from a station network of one station for approximately 700 square miles.

215. For the present purpose the study was confined to the area of the United States east of the Rockies. This was necessary because of the variability of rainfall with topography in the western mountainous portion of the country. An arithmetical average computed from stations having radically different exposures and elevations would be of doubtful accuracy as an average depth over a climatic section. Further study is necessary before the western records can

be used for the determination of areal frequencies. Also, since the interest of a report on thunderstorms is primarily in summer rainfall, this study was restricted to the warm season, and the weeks numbered 14-39, April 2 - September 30, inclusive, were selected for analysis.

216. For each section a frequency tally was made for the selected weeks, using class intervals of 0.10 inch for the lower values of rainfall. In order to obtain sufficient points in the upper portion of the frequency curve, the extreme rainfall values were grouped in descending order of magnitude with a separate rank number assigned to each value. The second step was to compile a cumulative frequency array from the maximum weekly rainfall for the section down to a lower limit of one inch. Since the total number of years was 30, the return or recurrence interval was equal to $30/N$ where N is the rank number in weeks. The recurrence interval was plotted against rainfall depth on a 3-cycle semilogarithmic chart on which, it was found, the frequency curves were fairly straight. A smoothed curve was finally drawn through the plotted points, with greater weight being given to the lower rainfall values because of their greater reliability.

Figure 65 shows such a curve for southern Wisconsin.

217. Values of rainfall depth for selected recurrence intervals were taken from these curves and plotted at the center of the corresponding climatic section. Maps drawn for recurrence intervals of 1, 2, 3, 5, 10, 15, 20, 25, and 30 years or seasons are reproduced in figures 66 and 67, figure 66 including a map which gives the area in square miles for each of the sections in the compilation. The isohyets were drawn on the assumption that the value for each section

was representative of the center of the area. Some inaccuracy was probably introduced where the sections are long and narrow. The southern Alabama section, for example, is elongated in an east-west direction. Because its major axis thus tends to parallel the isohyets of greatest mean monthly rainfall along the Gulf Coast (see figure 40), it experiences greater rainfall. For the longer recurrence intervals, this produces a distortion of pattern in the isohyets that is probably not natural. It must also be remembered that the basic data for the analysis consist of depths for standard or calendar weeks; nonstandard 7-day periods would yield greater depths. However, the general isohyetal patterns of these charts furnish a useful guide to the probabilities of specific magnitudes of weekly areal precipitation for any locality in the eastern United States in the summer season.

218. The patterns show a consistent decrease in depth northward and westward from the Gulf source of moisture with some reversal of the gradient in mountainous areas such as western North Carolina. The greatest depth to be equaled or exceeded in any of the given intervals occurs along the Gulf Coast and varies from 3.8 inches in 1 year to 14.7 inches in 30 years. The patterns agree, in general, with the summer isoceraunic patterns and with the isohyetal pattern of warm-season precipitation on page 712 of "Climate and Man." Two differences, however, can be noted. As the recurrence interval increases above 10 years, the depths to be equaled or exceeded become anomalously low over Florida and Mississippi. These differences may be due in part to the distortion in the southern Alabama region discussed in the last paragraph.

However, there are also fewer points defining the curve for greater recurrence intervals.

219. The maps may be compared with the point-rainfall isopluvial charts prepared by the Miami Conservancy District (25). The general patterns are the same, except for the Mississippi and Florida minima, which are missing in the Miami charts. It is also not surprising that the 6-day isopluvial values of point rainfall for the same frequency are much higher than the weekly areal values. However, the areal values are also exceeded by the 3-day, and in some sections even by the 2- and 1-day, isopluvial values. In order to show a generalized version of the relation between rainfall frequency and area, three different frequency curves were developed for the Southwest Missouri section: (1) for the entire section of about 26,000 square miles, (2) for a 5,000-square-mile area centrally located within the section, and (3) for a point (Warsaw, Missouri) within the 5,000-square-mile area. Figure 68 shows the three curves.

Comparison with hail distribution

220. Although the occurrence of hail is generally associated with the occurrence of thunderstorms, it has long been known that the geographic distribution is not the same. The world-wide pattern of hail occurrence seems to be characterized by greater frequencies in the "continental interiors of middle latitudes, diminishing seaward, equatorward and poleward" (26). Locally and seasonally, as for instance in the United States in May (figure 30), a similar thunderstorm distribution is observed, but in the over-all pattern

only the poleward decrease of activity is also characteristic of the thunderstorm distribution.

221. To provide the material for a detailed comparison of the two distribution patterns in the United States, the hail-day data were collected in the same way as the thunderstorm-day data, that is, from the 40 years of record, 1904-43, published in the annual volumes of the Meteorological Yearbook (formerly Reports of the Chief of the Weather Bureau). The total number of days with hail at each of the stations and the length of station record within the period are given in table 13, which is thus comparable, station by station and month by month, with table 1. The lines of equal frequency based on the average annual and monthly values are reproduced in figures 69-72, with red overprints for the corresponding thunderstorm distributions.

222. For the same stations the maximum numbers of occurrences for each calendar month and for any year during the period of record are listed in table 14. The minimum numbers of occurrences have not been tabulated; they are all zero except the minimum annual numbers of occurrences at the following 23 stations:

Albuquerque, N. Mex.
 Cheyenne, Wyo.*
 Dallas, Tex.
 Dodge City, Kans.
 Drexel, Nebr.
 Dubuque, Iowa
 Ellendale, N. Dak.
 Eureka, Calif.
 Flagstaff, Ariz.*
 Groesbeck, Tex.
 Hannibal, Mo.
 Helena, Mont.

Huron, S. Dak.
 Kansas City, Mo.
 Lincoln, Nebr.
 Missoula, Mont.*
 Mt. Tamalpais, Calif.
 Mt. Weather, Va.
 Red Bluff, Calif.*
 Santa Fe, N. Mex.
 Wagon Wheel Gap, Colo.*
 Wichita, Kans.
 Yellowstone Park, Wyo.

Table 13
TOTAL DAYS WITH HAIL, 1904-43

Station	Yrs.	J	F	M	A	M	J	J	A	S	O	N	D	Ann.
Abilene, Tex.	40	2	4	16	38	60	11	6	1	4	6	6	2	156
Albany, N. Y.	40	1	0	3	4	14	9	11	5	3	1	1	0	52
Albuquerque, N. Mex.	12	1	1	7	8	8	2	3	4	3	4	1	3	43
Alpena, Mich.	40	0	0	5	4	13	8	8	6	8	4	4	1	61
Amarillo, Tex.	40	1	3	9	16	28	22	6	6	2	7	5	0	105
Anniston, Ala.	25	1	5	3	7	5	5	6	1	3	1	1	0	38
Apalachicola, Fla.	18	0	1	0	1	0	2	1	0	1	0	0	0	6
Asheville, N. C.	40	0	2	3	7	11	11	10	5	0	0	0	0	49
Atlanta, Ga.	40	1	4	9	6	9	7	10	5	0	3	1	5	60
Atlantic City, N. J.	40	0	2	4	1	4	4	1	2	1	1	2	1	23
Augusta, Ga.	40	0	3	4	7	2	1	1	1	1	0	1	1	23
Austin, Tex.	17	0	4	6	8	4	0	0	0	0	2	3	0	27
Baker, Oreg.	38	0	5	3	12	20	27	14	9	7	7	1	0	105
Baltimore, Md.	40	3	1	5	12	17	13	4	6	0	2	0	0	63
Bentonville, Ark.	14	3	10	5	5	8	4	1	1	0	3	3	5	48
Binghamton, N. Y.	40	2	0	3	4	9	15	17	11	5	5	3	0	74
Birmingham, Ala.	40	2	6	12	15	14	7	9	2	3	2	2	1	75
Bismark, N. Dak.	40	0	0	1	8	18	29	19	18	7	0	0	0	100
Block Island, R. I.	40	0	1	5	5	2	2	1	3	2	1	4	1	27
Boise, Idaho	40	2	10	29	26	27	15	2	2	4	7	12	7	113
Boston, Mass.	40	0	0	1	3	5	5	8	3	1	0	2	0	28
Broken Arrow, Okla.	12	1	3	8	16	12	9	1	1	1	2	0	0	54
Brownsville, Tex.	21	0	1	1	1	2	1	0	0	0	0	0	1	7
Buffalo, N. Y.	40	1	0	7	7	9	7	7	5	11	11	7	0	72
Burlington, Vt.	37	0	0	1	1	5	4	7	3	4	1	0	0	26
Cairo, Ill.	40	3	4	17	14	16	7	5	3	4	2	1	1	77
Canton, N. Y.	37	0	0	2	8	7	10	7	6	5	9	1	0	55
Cape Henry, Va.	35	0	0	5	7	6	5	1	3	0	4	1	0	32
Cape May, N. J.	18	6	1	5	1	0	1	1	1	0	0	2	3	21
Charles City, Iowa	39	0	0	5	16	24	21	10	7	9	5	1	0	98
Charleston, S. C.	40	0	3	4	3	3	2	3	2	1	0	1	0	22
Charlotte, N. C.	40	3	5	10	4	12	2	4	6	0	2	2	2	52
Chattanooga, Tenn.	40	3	4	9	13	17	10	5	4	1	0	2	1	69
Cheyenne, Wyo.	40	0	0	1	23	82	117	62	51	31	13	0	0	380
Chicago, Ill.	40	0	2	5	13	12	15	9	8	1	1	4	1	71
Cincinnati, Ohio	40	2	1	14	17	13	10	7	3	3	6	0	1	77
Cleveland, Ohio	40	2	2	7	9	6	10	8	6	8	16	4	0	78
Columbia, Mo.	40	7	2	12	29	18	14	4	3	14	5	6	3	117
Columbia, S. C.	40	1	1	0	8	10	4	6	2	0	0	1	3	36
Columbus, Ohio	40	1	4	18	11	16	10	7	9	2	2	5	0	85
Concord, N. H.	35	1	0	2	3	9	3	4	2	1	2	1	1	29
Concordia, Kans.	39	0	2	12	14	41	32	7	12	8	5	3	3	139
Corpus Christi, Tex.	40	0	4	6	10	11	0	0	0	1	1	2	2	37
Dallas, Tex.	35	6	20	27	27	31	7	2	3	5	2	3	3	136
Davenport, Iowa	40	1	1	14	23	23	19	8	3	5	3	5	1	106
Dayton, Ohio	29	4	3	8	12	10	11	7	5	2	1	1	0	64
Del Rio, Tex.	38	0	3	7	19	18	1	1	2	2	1	1	1	56
Denver, Colo.	40	0	0	2	17	45	33	11	13	9	6	1	0	137
Des Moines, Iowa	40	3	2	17	24	26	22	8	8	16	8	1	1	136
Detroit, Mich.	40	1	3	4	16	12	15	11	6	5	3	1	1	78
Devils Lake, N. Dak.	39	0	0	0	13	15	18	21	16	7	2	1	0	93
Dodge City, Kans.	40	0	3	13	29	41	14	16	10	9	7	5	0	179
Drexel, Nebr.	10	0	0	2	10	8	11	1	0	5	2	2	0	41
Dubuque, Iowa	40	0	1	12	29	25	18	6	7	5	5	4	0	112
Due West, S. C.	11	1	3	0	3	3	0	3	1	1	1	0	1	17
Duluth, Minn.	40	0	0	1	11	23	16	13	10	5	5	1	0	84
Eastport, Maine	40	4	1	2	5	4	7	3	1	1	2	2	1	33
Elkins, W. Va.	40	2	6	8	14	20	13	8	1	2	4	2	1	81
Ellendale, N. Dak.	15	0	0	0	6	9	9	8	6	2	0	0	0	40
El Paso, Tex.	40	6	3	11	9	10	8	3	3	5	4	4	4	70
Erie, Pa.	40	2	5	9	8	5	12	3	4	12	20	4	1	85
Escanaba, Mich.	40	0	2	6	9	14	14	12	12	5	7	0	0	81
Eureka, Calif.	40	57	49	61	17	9	1	0	0	1	4	15	32	246
Evansville, Ind.	40	1	4	16	16	23	10	7	6	3	2	2	2	92
Flagstaff, Ariz.	9	0	0	0	1	3	5	17	15	13	3	0	0	57
Ft. Smith, Ark.	40	4	6	15	22	17	11	5	1	0	0	1	6	88
Ft. Wayne, Ind.	32	0	3	6	16	10	7	10	5	2	3	0	0	62
Ft. Worth, Tex.	40	2	9	20	30	18	11	4	1	1	0	1	2	99
Fresno, Calif.	40	8	11	16	9	4	0	0	0	1	1	2	4	56
Galveston, Tex.	40	0	3	5	8	6	0	1	0	1	1	4	0	29
Grand Haven, Mich.	27	0	1	3	5	10	2	2	2	6	8	2	0	41
Grand Junction, Colo.	40	1	1	6	18	20	11	4	3	7	3	1	0	75
Grand Rapids, Mich.	40	2	1	8	17	19	9	7	2	9	10	5	0	89

Table 13 (contd)

Station	Yrs.	J	F	M	A	M	J	J	A	S	O	N	D	Ann.
Green Bay, Wis.	40	0	0	5	9	12	14	7	3	6	3	3	0	62
Greensboro, N. C.	14	2	0	1	2	3	2	1	1	1	0	0	1	14
Greenville, S. C.	21	1	2	1	5	5	4	4	1	1	0	1	1	26
Groesbeck, Tex.	12	1	2	5	5	6	2	2	0	0	0	3	1	27
Hannibal, Mo.	29	2	4	14	20	20	16	3	5	0	3	3	0	90
Harrisburg, Pa.	40	0	1	1	11	10	17	8	4	2	3	0	0	57
Hartford, Conn.	39	0	0	2	5	11	12	15	7	1	1	2	1	57
Hatteras, N. C.	39	0	0	1	3	7	0	1	0	0	0	0	2	14
Havre, Mont.	40	0	0	3	10	26	22	13	8	8	3	0	0	93
Helena, Mont.	40	0	0	1	10	35	66	42	20	12	4	3	4	197
Houghton, Mich.	29	0	0	2	4	7	6	8	5	8	2	0	3	42
Houston, Tex.	34	4	5	7	8	8	2	2	0	0	1	1	3	41
Huron, Dak.	40	0	0	3	8	28	29	19	20	8	3	1	0	119
Independence, Calif.	18	0	0	0	1	0	2	0	0	0	0	0	0	4
Indianapolis, Ind.	40	2	4	12	18	21	11	14	4	4	2	1	1	94
Iola, Kans.	26	0	4	15	18	18	12	2	0	2	3	3	2	79
Ithaca, N. Y.	15	0	0	1	0	3	5	6	4	1	0	0	0	20
Jacksonville, Fla.	40	0	1	2	5	7	13	2	2	1	1	0	1	35
Jupiter, Fla.	7	0	0	0	2	1	0	0	0	0	0	0	0	3
Kalispell, Mont.	40	0	0	3	4	19	25	19	11	8	3	0	0	92
Kansas City, Mo.	40	3	5	28	35	42	24	7	8	7	10	5	1	175
Keokuk, Iowa	38	0	4	15	18	26	10	7	8	8	6	7	2	111
Key West, Fla.	40	0	0	0	0	0	1	1	0	0	0	0	0	2
Knoxville, Tenn.	40	2	4	6	19	12	16	7	8	3	3	1	1	82
La Crosse, Wis.	40	1	0	6	23	19	15	9	10	4	7	4	0	98
Lander, Wyo.	40	0	0	1	11	21	17	7	6	1	0	2	0	66
Lansing, Mich.	33	0	5	11	18	13	6	3	6	2	6	1	1	72
La Salle, Ill.	8	0	1	1	4	4	1	1	0	3	1	1	0	17
Lewiston, Idaho	29	0	2	9	7	11	7	4	2	4	4	0	3	53
Lexington, Ky.	29	3	4	5	15	10	9	6	3	2	2	0	3	62
Lincoln, Nebr.	40	0	1	15	29	28	30	13	8	10	4	3	1	142
Little Rock, Ark.	40	2	13	16	24	17	11	5	2	3	1	2	2	98
Los Angeles, Calif.	40	8	10	17	3	2	0	0	0	1	0	0	2	43
Louisville, Ky.	40	3	3	16	16	18	9	7	5	2	0	4	4	87
Ludington, Mich.	20	1	1	6	2	2	3	4	1	7	10	2	1	40
Lynchburg, Va.	36	1	1	1	6	5	10	4	1	1	0	1	0	31
Macon, Ga.	40	2	3	5	8	7	4	7	4	2	0	0	2	44
Madison, Wis.	39	0	1	7	17	23	10	16	11	4	4	5	0	98
Marquette, Mich.	40	0	0	1	3	11	14	13	7	15	5	0	0	69
Medford, Oreg.	16	0	4	4	17	11	13	1	1	2	1	1	0	45
Memphis, Tenn.	40	3	10	11	23	10	10	1	0	3	1	0	4	81
Meridian, Miss.	40	2	6	7	16	5	3	3	2	0	1	0	0	45
Miami, Fla.	32	0	2	0	4	4	1	1	0	1	0	0	1	14
Miles City, Mont.	36	0	0	3	8	20	18	13	12	2	1	0	0	77
Milwaukee, Wis.	40	0	3	7	14	22	14	8	9	7	5	4	0	93
Minneapolis, Minn.	40	0	0	7	9	23	17	10	12	10	4	0	0	92
Missoula, Mont.	8	0	0	3	5	2	9	5	0	1	1	1	1	28
Mobile, Ala.	40	3	2	6	14	9	6	1	1	0	0	3	3	48
Modena, Utah	40	1	9	25	41	39	15	25	29	16	16	5	2	223
Montgomery, Ala.	40	3	6	12	12	5	8	3	0	1	0	1	0	51
Moorhead, Minn.	39	0	0	5	5	16	13	8	10	6	1	0	0	64
Mt. Tamalpais, Calif.	17	15	6	17	2	2	0	0	0	0	1	6	8	57
Mt. Weather, Va.	9	1	1	1	2	2	7	5	2	1	3	0	0	25
Nantucket, Mass.	40	0	0	4	5	3	1	0	0	1	1	4	2	21
Narragansett Pier, R. I.	14	5	6	6	7	0	1	1	0	1	0	1	6	34
Nashville, Tenn.	40	1	7	19	19	16	8	7	2	1	3	3	4	90
New Haven, Conn.	40	1	1	3	4	10	4	5	3	1	2	1	0	35
New Orleans, La.	40	2	5	7	14	7	1	5	1	1	1	1	2	47
New York, N. Y.	40	1	1	3	4	17	11	11	7	2	4	2	1	64
Norfolk, Va.	40	0	2	5	10	12	6	7	2	1	1	0	0	46
Northfield, Vt.	35	1	0	1	1	6	11	6	5	2	3	0	0	36
North Head, Wash.	40	42	50	65	32	18	2	0	0	4	19	40	40	312
North Platte, Nebr.	40	0	2	4	22	32	28	22	15	6	3	0	0	134
Oklahoma City, Okla.	40	2	7	27	32	34	16	2	3	4	4	4	3	138
Omaha, Nebr.	40	1	2	13	30	30	34	13	9	12	9	4	3	160
Oswego, N. Y.	39	1	0	2	3	3	5	6	5	11	25	18	0	79
Palestine, Tex.	40	3	3	10	19	13	3	0	2	2	1	1	2	59
Parkersburg, Va.	40	2	5	10	10	21	17	8	0	0	4	2	3	82
Pensacola, Fla.	40	1	6	7	10	5	2	3	0	0	0	1	3	38
Peoria, Ill.	38	0	2	13	15	21	9	7	4	4	3	3	0	81
Philadelphia, Pa.	40	0	2	3	2	7	3	3	6	0	0	1	0	27
Phoenix, Ariz.	40	3	12	7	7	4	0	2	3	1	3	1	4	47
Pierre, S. Dak.	26	0	0	1	5	13	13	9	6	1	1	0	0	49
Pittsburgh, Pa.	40	2	3	9	14	12	12	9	6	1	1	1	2	72
Pocatello, Idaho	40	0	6	20	36	42	25	25	18	15	7	2	4	200

Table 13 (contd)

Station	Yrs.	J	F	M	A	M	J	J	A	S	O	N	D	Ann.
Point Reyes Light, Calif.	23	18	13	12	2	0	0	0	0	1	0	0	8	54
Port Angeles, Wash.	14	1	0	8	5	1	0	0	1	0	0	0	1	17
Port Arthur, Tex.	26	1	3	3	9	5	1	0	0	0	0	0	1	23
Port Crescent, Wash.	12	0	1	1	1	1	0	0	0	0	1	2	1	8
Port Huron, Mich.	29	1	3	4	7	6	5	4	5	3	4	0	0	42
Portland, Maine	40	0	0	2	4	4	3	6	6	2	6	0	0	33
Portland, Oreg.	40	7	15	40	32	23	7	0	0	3	12	10	4	153
Providence, R. I.	39	0	0	2	3	6	5	9	3	3	0	0	0	31
Pueblo, Colo.	39	0	0	1	16	23	37	14	9	4	2	0	0	107
Raleigh, N. C.	40	0	4	3	7	13	1	6	4	0	0	2	3	43
Rapid City, S. Dak.	39	0	0	0	9	33	41	37	16	6	3	0	0	145
Reading, Pa.	31	0	2	1	7	13	5	14	10	1	3	0	1	57
Red Bluff, Calif.	32	6	7	19	7	10	4	0	0	1	1	0	5	60
Redding, Calif.	8	2	6	9	5	3	0	0	0	0	1	1	0	27
Reno, Nev.	38	1	0	2	5	14	9	6	8	4	2	1	0	52
Richmond, Va.	40	2	1	7	11	8	7	4	1	0	2	0	1	44
Rochester, N. Y.	40	0	0	2	3	9	7	4	5	9	4	0	1	44
Roseburg, Oreg.	40	6	4	15	32	20	6	0	0	2	2	6	4	97
Roswell, N. Mex.	39	1	2	6	21	24	16	5	3	6	9	3	1	97
Royal Center, Ind.	13	1	1	7	11	7	1	9	0	0	1	0	0	38
Sacramento, Calif.	40	7	9	19	10	2	0	0	0	0	1	1	3	52
Saginaw, Mich.	12	0	2	1	1	9	3	2	3	3	3	0	1	28
St. Joseph, Mo.	34	1	2	17	21	26	26	5	5	11	5	1	1	121
St. Louis, Mo.	40	4	4	19	23	24	9	8	8	4	2	3	0	108
St. Paul, Minn.	29	0	0	4	3	10	9	5	8	4	2	0	0	45
Salt Lake City, Utah	40	2	3	9	20	26	13	5	16	11	10	5	1	121
San Antonio, Tex.	40	3	6	23	30	23	6	3	1	1	1	2	1	100
San Diego, Calif.	40	10	9	12	8	1	0	0	0	0	1	3	7	51
Sand Key, Fla.	16	0	0	0	0	0	0	0	0	1	0	0	0	1
Sandusky, Ohio	40	0	3	8	14	15	13	13	9	2	4	0	0	81
Sandy Hook, N. J.	25	0	0	2	4	3	2	1	2	0	0	1	0	15
San Francisco, Calif.	40	30	24	29	5	1	0	1	0	2	9	6	13	120
San Jose, Calif.	27	5	5	7	2	0	0	0	0	0	1	0	3	23
San Luis Obispo, Calif.	23	6	5	10	0	0	0	0	0	1	0	2	2	26
Santa Fe, N. Mex.	38	2	1	13	19	46	27	36	23	13	27	3	1	211
Sault Ste. Marie, Mich.	40	0	0	4	3	6	7	5	7	7	13	4	0	56
Savannah, Ga.	40	1	3	1	4	13	5	3	3	1	1	0	0	35
Scranton, Pa.	40	3	0	6	6	12	21	8	5	3	12	1	1	78
Seattle, Wash.	40	4	9	23	17	8	5	1	1	3	7	10	9	97
Sheridan, Wyo.	36	0	0	2	14	30	42	14	11	10	0	0	0	123
Shreveport, La.	40	7	6	9	13	8	2	1	1	1	2	3	4	57
Sioux City, Iowa	40	0	2	4	18	27	28	9	10	13	3	1	0	115
Southeast Farallon, Calif.	9	10	5	5	0	1	0	0	0	0	0	0	0	21
Spokane, Wash.	40	1	2	26	25	42	14	4	7	6	9	2	2	140
Springfield, Ill.	40	0	5	30	24	21	15	4	4	4	0	4	3	114
Springfield, Mo.	40	6	8	24	26	25	14	9	4	0	2	7	3	128
Syracuse, N. Y.	40	0	1	1	0	7	12	11	3	3	5	1	0	44
Tacoma, Wash.	36	13	11	22	22	15	0	0	1	3	7	8	6	108
Tampa, Fla.	40	0	1	2	3	8	3	1	3	0	0	0	0	21
Tatoosh Island, Wash.	40	19	23	27	23	12	0	2	0	1	16	35	23	181
Taylor, Tex.	29	2	4	5	16	14	3	1	2	2	0	1	1	51
Terre Haute, Ind.	31	0	2	18	16	14	10	8	4	1	1	2	2	78
Thomasville, Ga.	27	0	1	0	4	3	3	1	1	1	0	0	0	14
Toledo, Ohio	40	0	1	5	11	11	11	7	3	0	4	2	0	55
Tonopah, Nev.	17	0	1	1	1	7	0	2	2	2	0	0	0	16
Topeka, Kans.	40	2	1	17	26	21	23	12	9	13	9	3	0	136
Trenton, N. J.	30	0	1	5	5	9	11	8	6	1	3	0	0	49
Valentine, Nebr.	40	2	2	3	9	25	34	24	23	7	4	1	0	134
Vicksburg, Miss.	40	3	10	13	20	5	6	2	2	3	0	3	1	68
Wagon Wheel Gap, Colo.	3	0	0	0	0	0	3	3	5	3	0	0	0	14
Walla Walla, Wash.	38	6	4	20	20	12	5	2	1	1	10	5	2	88
Washington, D. C.	40	0	2	4	10	12	10	7	3	1	2	1	0	52
Wausau, Wis.	17	0	1	0	3	9	10	4	2	3	0	1	0	33
Wichita, Kans.	40	2	6	17	31	43	26	8	5	6	7	4	3	158
Williston, N. Dak.	39	0	0	1	4	11	20	25	15	5	2	0	0	83
Wilmington, N. C.	40	0	1	3	5	8	4	2	2	0	0	0	0	25
Winnemucca, Nev.	40	3	8	12	12	16	12	5	2	3	6	3	0	82
Wytheville, Va.	37	1	1	6	10	11	5	4	3	2	0	0	0	43
Yakima, Wash.	15	0	1	1	2	4	2	0	0	0	0	0	0	10
Yankton, S. Dak.	29	0	0	6	11	20	12	11	11	3	2	1	0	77
Yellowstone Park, Wyo.	35	0	0	1	6	27	52	39	35	18	3	0	0	181
Yuma, Ariz.	40	2	2	3	0	0	0	0	1	0	0	1	1	10

Table 14

MAXIMUM NUMBER OF DAYS WITH HAIL, 1904-43

Station	Yrs.	J	F	M	A	M	J	J	A	S	O	N	D	Ann.
Abilene, Tex.	40	1	2	2	3	5	3	2	1	2	2	1	1	10
Albany, N. Y.	40	1	0	1	1	2	2	3	1	1	1	1	0	4
Albuquerque, N. Mex.	12	1	1	2	2	2	1	1	2	1	2	1	1	9
Alpena, Mich.	40	0	0	1	1	2	1	2	2	1	1	1	1	4
Amarillo, Tex.	40	1	1	1	2	3	2	1	1	1	2	1	0	5
Anniston, Ala.	25	1	1	1	1	1	2	1	1	1	1	1	0	4
Apalachicola, Fla.	18	0	1	0	1	0	1	1	0	1	0	0	0	2
Asheville, N. C.	40	0	1	1	1	2	2	1	2	0	0	0	0	4
Atlanta, Ga.	40	1	2	1	1	2	1	2	1	0	1	1	2	4
Atlantic City, N. J.	40	0	1	2	1	1	1	1	1	1	0	1	1	2
Augusta, Ga.	40	0	1	1	2	1	1	1	1	1	0	1	1	3
Austin, Tex.	17	0	2	1	2	1	0	0	0	0	1	1	0	4
Baker, Oreg.	38	0	2	1	1	2	3	3	3	2	1	1	0	6
Baltimore, Md.	40	1	1	1	2	2	3	1	2	0	1	0	0	5
Bentonville, Ark.	14	1	5	2	2	1	1	1	1	0	1	1	2	7
Binghamton, N. Y.	40	1	0	1	1	3	2	4	2	1	1	1	0	5
Birmingham, Ala.	40	1	2	2	2	2	2	2	1	1	1	1	1	5
Bismarck, N. Dak.	40	0	0	1	2	2	2	3	2	2	0	0	0	6
Block Island, R. I.	40	0	1	1	1	1	1	1	1	1	1	1	1	2
Boise, Idaho	40	1	4	5	3	4	2	1	1	2	1	3	2	10
Boston, Mass.	40	0	0	1	1	2	1	1	1	1	0	1	0	3
Broken Arrow, Okla.	12	1	1	2	4	3	2	1	1	1	1	0	0	8
Brownsville, Tex.	21	0	1	1	1	1	1	0	0	0	0	0	1	3
Buffalo, N. Y.	40	1	0	1	1	1	1	2	1	4	2	1	0	5
Burlington, Vt.	37	0	0	1	1	1	1	2	1	1	1	0	0	3
Cairo, Ill.	40	1	1	2	2	2	1	2	1	1	1	1	1	5
Canton, N. Y.	37	0	0	1	3	1	2	2	2	2	2	1	0	5
Cape Henry, Va.	35	0	0	1	2	1	1	1	1	0	2	1	0	3
Cape May, N. J.	18	2	1	2	1	0	1	1	1	0	0	1	1	4
Charles City, Iowa	39	0	0	1	3	3	3	2	1	2	2	1	0	8
Charleston, S. C.	40	0	1	1	1	1	1	1	1	1	0	1	0	2
Charlotte, N. C.	40	1	1	1	1	2	1	1	2	0	1	1	1	5
Chattanooga, Tenn.	40	1	1	1	1	2	2	1	1	1	0	1	1	5
Cheyenne, Wyo.	40	0	0	1	3	5	10	5	7	4	3	0	0	19
Chicago, Ill.	40	0	1	1	2	1	2	2	1	1	1	1	1	5
Cincinnati, Ohio	40	1	1	2	3	2	2	2	1	1	1	0	0	6
Cleveland, Ohio	40	1	1	1	2	2	2	1	2	2	3	1	1	6
Columbia, Mo.	40	2	2	3	4	2	2	2	1	8	1	1	1	8
Columbia, S. C.	40	1	1	2	1	2	1	1	2	0	0	1	1	3
Columbus, Ohio	40	1	3	2	2	1	1	1	2	1	1	1	0	6
Concord, N. H.	35	1	0	1	1	1	1	1	1	1	1	1	1	4
Concordia, Kans.	39	0	1	2	2	3	3	2	2	1	1	1	1	8
Corpus Christi, Tex.	40	0	2	1	1	3	0	0	0	1	1	1	1	5
Dallas, Tex.	35	2	3	3	4	4	1	1	1	1	2	1	2	10
Davenport, Iowa	40	1	1	3	3	3	2	1	1	1	1	2	1	8
Dayton, Ohio	29	1	2	2	2	2	2	2	1	1	1	1	0	6
Del Rio, Tex.	38	0	1	1	2	3	1	1	1	1	1	1	1	5
Denver, Colo.	40	0	0	1	2	4	4	2	2	2	1	1	0	8
Des Moines, Iowa	40	2	1	2	2	4	3	1	2	1	1	1	1	9
Detroit, Mich.	40	1	2	2	2	2	3	1	1	1	1	1	1	5
Devils Lake, N. Dak.	39	0	0	0	2	2	3	2	3	2	1	1	0	7
Dodge City, Kans.	40	0	1	2	3	4	5	2	1	2	1	1	0	12
Drexel, Nebr.	10	0	0	1	3	3	3	1	0	2	1	1	0	8
Dubuque, Iowa	40	0	1	2	5	3	2	1	1	1	1	1	0	8
Due West, S. C.	11	1	1	0	2	1	0	2	1	1	1	0	1	4
Duluth, Minn.	40	0	0	1	3	3	2	2	2	2	2	1	0	6
Eastport, Maine	40	2	1	1	1	1	3	1	1	1	1	2	1	4
Elkins, W. Va.	40	1	1	2	2	2	3	2	1	1	2	1	1	6
Ellendale, N. Dak.	15	0	0	0	2	3	2	2	2	1	0	0	0	6
El Paso, Tex.	40	1	1	3	2	3	1	1	1	2	1	2	1	5
Erie, Pa.	40	1	2	2	2	1	3	1	1	2	4	1	1	6
Escanaba, Mich.	40	0	1	2	3	4	2	2	2	1	2	0	0	8
Eureka, Calif.	40	5	5	4	2	2	1	0	0	1	1	1	4	16
Evansville, Ind.	40	1	2	2	2	2	2	1	2	1	1	1	1	6
Flagstaff, Ariz.	9	0	0	0	1	2	1	3	4	4	2	0	0	11
Ft. Smith, Ark.	40	1	2	2	3	2	2	2	1	0	0	1	1	5
Ft. Wayne, Ind.	32	0	1	1	3	1	1	2	1	1	1	0	0	6
Ft. Worth, Tex.	40	1	1	2	3	2	2	1	1	1	0	1	1	8
Fresno, Calif.	40	3	3	2	2	1	0	0	0	1	1	1	1	8
Galveston, Tex.	40	0	2	1	3	2	0	1	0	1	1	1	0	3
Grand Haven, Mich.	27	0	1	1	1	2	1	1	1	3	2	1	0	5
Grand Junction, Colo.	40	1	1	2	4	3	2	1	2	1	1	1	0	7
Grand Rapids, Mich.	40	1	1	1	2	2	1	1	1	2	2	1	0	6

Table 14 (contd)

Station	Yrs.	J	F	M	A	M	J	J	A	S	O	N	D	Ann.
Green Bay, Wis.	40	0	0	2	1	2	3	1	1	1	1	1	0	5
Greensboro, N. C.	14	1	0	1	1	2	1	1	1	1	0	0	1	4
Greenville, S. C.	21	1	2	1	2	1	1	1	1	1	1	1	1	3
Groesbeck, Tex.	12	1	1	1	2	2	2	1	0	1	0	1	1	4
Hannibal, Mo.	29	1	1	2	3	2	2	2	2	0	1	1	0	6
Harrisburg, Pa.	40	0	1	1	3	2	2	1	1	1	1	0	0	6
Hartford, Conn.	39	0	0	1	3	2	2	2	1	1	1	1	1	4
Hatteras, N. C.	39	0	0	1	1	1	0	1	0	0	0	0	0	2
Havre, Mont.	40	0	0	1	3	5	4	3	1	1	1	0	0	8
Helena, Mont.	40	0	0	1	3	3	5	4	3	2	1	2	2	11
Houghton, Mich.	29	0	0	1	1	2	1	1	1	1	1	0	0	4
Houston, Tex.	34	1	1	3	2	2	1	2	0	0	1	1	1	4
Huron, S. Dak.	40	0	0	2	1	4	4	2	3	1	1	1	0	7
Independence, Calif.	18	0	0	1	1	1	2	0	0	0	1	0	0	2
Indianapolis, Ind.	40	1	1	2	3	2	2	1	1	1	1	1	1	7
Iola, Kans.	26	0	1	2	3	2	2	1	0	1	1	1	1	8
Ithaca, N. Y.	15	0	0	1	0	1	2	2	2	1	0	0	0	5
Jacksonville, Fla.	40	0	1	1	2	1	2	1	1	1	1	0	1	3
Jupiter, Fla.	7	0	0	0	1	1	0	0	0	0	0	0	0	1
Kalispell, Mont.	40	0	0	1	1	2	3	3	2	1	1	0	0	5
Kansas City, Mo.	40	1	2	2	3	5	4	1	2	2	2	2	1	10
Keokuk, Iowa	38	0	1	2	3	5	2	2	2	2	1	1	1	7
Key West, Fla.	40	0	0	0	0	0	1	1	0	0	0	0	0	1
Knoxville, Tenn.	40	1	1	1	3	2	2	1	1	1	1	1	1	5
La Crosse, Wis.	40	1	0	2	2	3	2	2	2	1	2	1	0	6
Lander, Wyo.	40	0	0	1	4	4	2	1	2	1	0	1	0	6
Lansing, Mich.	33	0	1	2	3	2	2	1	1	1	3	1	1	6
La Salle, Ill.	8	0	1	1	3	2	1	1	0	1	1	1	0	4
Lewiston, Idaho	29	0	1	2	1	2	1	1	1	1	1	0	2	7
Lexington, Ky.	29	1	1	1	2	2	2	1	1	1	1	0	1	5
Lincoln, Nebr.	40	0	1	3	3	3	3	2	1	2	1	1	1	9
Little Rock, Ark.	40	1	2	2	3	2	2	1	1	1	1	1	1	5
Los Angeles, Calif.	40	1	1	3	1	1	0	0	0	1	0	0	1	4
Louisville, Ky.	40	1	1	2	1	3	2	2	1	1	0	2	1	6
Ludington, Mich.	20	1	1	2	1	1	2	2	1	2	4	1	1	5
Lynchburg, Va.	36	1	1	0	1	1	2	2	0	1	0	1	0	5
Macon, Ga.	40	1	1	1	2	1	1	1	1	1	0	0	1	4
Madison, Wis.	39	0	1	2	3	4	1	2	2	2	1	1	0	6
Marquette, Mich.	40	0	0	1	2	2	2	2	2	2	1	0	0	4
Medford, Oreg.	16	0	1	1	4	3	1	1	1	1	1	1	0	7
Memphis, Tenn.	40	1	2	2	2	2	2	1	0	1	1	2	1	5
Meridian, Miss.	40	1	2	1	3	1	2	2	1	0	1	0	0	3
Miami, Fla.	32	0	1	0	2	2	1	1	0	1	0	0	1	3
Miles City, Mont.	36	0	0	1	2	2	2	2	3	1	1	0	0	8
Milwaukee, Wis.	40	0	1	2	3	3	3	2	2	2	2	1	0	5
Minneapolis, Minn.	40	0	0	1	2	3	2	2	2	2	1	0	0	7
Missoula, Mont.	8	0	0	2	2	1	4	1	0	1	1	1	1	6
Mobile, Ala.	40	1	1	3	3	2	2	1	1	0	0	2	2	10
Modena, Utah	40	1	2	5	6	4	3	3	3	2	2	1	1	20
Montgomery, Ala.	40	1	1	1	2	1	1	1	0	1	0	1	0	4
Moorhead, Minn.	39	0	0	1	2	3	2	1	2	1	1	0	0	7
Mt. Tamalpais, Calif.	17	3	2	4	2	2	0	0	0	0	1	2	2	7
Mt. Weather, Va.	9	1	1	1	2	1	2	2	1	1	1	0	0	5
Nantucket, Mass.	40	0	0	1	2	1	1	0	0	1	1	1	1	2
Narragansett Pier, R. I.	14	2	2	2	2	0	1	1	0	1	0	1	2	6
Nashville, Tenn.	40	1	2	2	3	2	2	1	1	1	1	1	1	5
New Haven, Conn.	40	1	1	1	2	2	2	1	1	1	1	1	0	3
New Orleans, La.	40	1	1	1	2	2	1	1	1	1	1	1	2	4
New York, N. Y.	40	1	1	1	2	2	2	2	1	1	2	1	1	5
Norfolk, Va.	40	0	1	2	2	2	1	1	1	1	1	0	0	5
Northfield, Vt.	35	1	0	1	1	2	2	1	1	1	1	0	0	4
North Head, Wash.	40	5	7	7	3	3	1	0	0	2	5	4	6	26
North Platte, Nebr.	40	0	1	1	3	3	4	3	2	2	1	0	0	8
Oklahoma City, Okla.	40	1	2	3	4	4	2	1	1	1	1	1	3	9
Omaha, Nebr.	40	1	1	3	2	4	4	2	2	3	3	2	3	8
Oneego, N. Y.	39	1	0	1	1	1	1	1	1	2	3	3	0	5
Palestine, Tex.	40	1	1	2	3	2	1	0	1	1	1	1	1	4
Parkersburg, Va.	40	1	1	1	1	3	3	2	0	0	1	1	1	6
Pensacola, Fla.	40	1	2	2	2	1	1	1	0	0	0	1	1	5
Peoria, Ill.	38	0	1	2	3	3	1	1	2	1	1	1	0	7
Philadelphia, Pa.	40	0	1	1	1	1	1	1	1	0	0	1	0	4
Phoenix, Ariz.	40	1	2	2	1	1	0	1	1	1	1	1	1	5
Pierre, S. Dak.	26	0	0	1	1	2	3	2	1	1	1	0	0	6
Pittsburgh, Pa.	40	1	1	1	3	3	1	2	1	1	1	1	1	6
Pocahontas, Idaho	40	0	2	4	4	7	3	3	3	2	2	1	2	15

Table 14 (contd)

Station	Yrs.	J	F	M	A	M	J	J	A	S	O	N	D	Ann.
Point Reyes Light, Calif.	23	5	4	2	1	0	0	0	0	1	0	0	2	10
Port Angeles, Wash.	14	1	0	3	2	1	0	0	1	0	0	0	1	4
Port Arthur, Tex.	26	1	1	1	2	2	1	0	0	0	0	0	1	3
Port Crescent, Wash.	12	0	1	1	1	1	0	0	0	0	1	1	1	4
Port Huron, Mich.	29	1	2	1	2	2	2	1	2	1	2	0	0	5
Portland, Maine	40	0	0	1	1	1	1	2	1	1	2	0	0	4
Portland, Oreg.	40	1	2	3	3	3	1	0	0	2	3	1	1	9
Providence, R. I.	39	0	0	1	1	1	1	1	1	1	0	0	0	4
Pueblo, Colo.	39	0	0	1	2	2	3	2	3	1	1	0	0	10
Raleigh, N. C.	40	0	1	1	1	2	1	2	1	0	0	1	1	3
Rapid City, S. Dak.	39	0	0	0	2	3	1	4	3	1	1	0	0	9
Reading, Pa.	31	0	1	1	3	2	1	2	2	1	1	0	1	8
Red Bluff, Calif.	32	2	2	4	2	2	1	0	0	1	0	0	2	9
Redding, Calif.	8	1	2	3	2	2	0	0	0	0	1	1	0	5
Reno, Nev.	38	1	0	1	1	2	1	1	1	2	1	1	0	5
Richmond, Va.	40	1	1	1	1	2	1	1	1	0	1	0	1	3
Rochester, N. Y.	40	0	0	1	2	2	2	1	1	1	2	0	1	4
Roseburg, Oreg.	40	2	1	2	4	3	1	0	0	1	1	2	1	8
Roswell, N. Mex.	39	1	1	2	4	2	3	1	1	2	2	2	1	8
Royal Center, Ind.	13	1	1	1	3	2	1	2	0	0	1	0	0	7
Sacramento, Calif.	40	3	2	3	1	1	0	0	0	0	1	1	1	4
Saginaw, Mich.	12	0	1	1	1	2	1	1	1	2	1	0	1	7
St. Joseph, Mo.	34	1	1	2	2	4	3	1	2	2	1	1	1	10
St. Louis, Mo.	40	1	2	3	2	3	1	1	1	1	1	1	0	7
St. Paul, Minn.	29	0	0	2	1	2	2	1	2	1	1	0	0	5
Salt Lake City, Utah	40	1	2	2	3	3	2	1	2	2	2	2	1	8
San Antonio, Tex.	40	2	1	3	4	4	2	1	1	1	1	1	1	8
San Diego, Calif.	40	2	1	3	2	1	0	0	0	0	1	2	2	5
Sand Key, Fla.	16	0	0	0	0	0	0	0	0	1	0	0	0	1
Sandusky, Ohio	40	0	2	1	2	3	2	2	2	1	1	0	0	6
Sandy Hook, N. J.	25	0	0	1	1	1	1	1	1	0	0	1	0	3
San Francisco, Calif.	40	4	4	5	2	1	0	1	0	2	8	3	5	28
San Jose, Calif.	27	2	1	1	1	0	0	0	0	0	1	0	1	3
San Luis Obispo, Calif.	23	1	3	2	0	0	0	0	0	1	0	1	1	4
Santa Fe, N. Mex.	38	1	1	3	3	5	3	3	3	2	4	2	1	12
Sault Ste. Marie, Mich.	40	0	0	2	1	2	1	1	1	3	3	2	0	6
Savannah, Ga.	40	1	1	1	1	3	1	1	2	1	1	0	0	4
Scranton, Pa.	40	2	0	1	1	1	3	2	1	2	2	1	1	4
Seattle, Wash.	40	1	1	2	2	2	2	1	1	1	2	2	2	6
Sheridan, Wyo.	36	0	0	1	3	4	3	3	3	1	2	0	0	9
Shreveport, La.	40	1	2	2	2	2	1	1	1	1	1	1	2	4
Sioux City, Iowa	40	0	1	2	2	3	3	2	3	2	1	1	0	6
Southeast Parallon, Calif.	9	5	3	2	0	1	0	0	0	0	0	0	0	6
Spokane, Wash.	40	1	1	4	3	5	3	1	1	1	4	1	1	10
Springfield, Ill.	40	0	2	3	3	2	2	1	1	1	0	1	1	7
Springfield, Mo.	40	1	1	3	3	4	2	2	1	0	1	1	1	9
Syracuse, N. Y.	40	0	1	1	0	1	2	2	1	1	1	1	0	3
Tacoma, Wash.	36	2	3	3	4	2	0	0	1	1	3	3	1	9
Tampa, Fla.	40	0	1	1	1	2	1	1	2	0	0	0	0	3
Tatoosh Island, Wash.	40	3	5	7	6	3	0	1	0	1	3	7	5	19
Taylor, Tex.	29	1	2	2	3	3	1	1	1	1	0	1	1	6
Terre Haute, Ind.	31	0	1	2	2	2	2	2	1	1	1	1	1	6
Thomasville, Ga.	27	0	1	0	1	1	1	1	1	1	0	0	0	2
Toledo, Ohio	40	0	1	1	1	3	2	1	1	0	1	1	0	7
Tomopah, Nev.	17	0	1	1	1	2	0	1	1	1	0	0	0	4
Topeka, Kans.	40	1	1	3	3	2	2	4	1	3	2	2	0	10
Trenton, N. J.	30	0	1	1	1	1	2	2	1	1	1	0	0	3
Valentine, Nebr.	40	2	1	1	2	4	4	3	2	2	1	1	0	8
Vicksburg, Miss.	40	2	1	2	2	1	1	1	1	2	0	1	1	5
Wagon Wheel Gap, Colo.	3	0	0	0	0	0	3	2	2	2	0	0	0	9
Walla Walla, Wash.	38	2	1	3	3	2	1	1	1	1	2	1	1	6
Washington, D. C.	40	0	1	1	1	3	1	2	1	1	1	1	0	5
Wausau, Wis.	17	0	1	0	1	3	3	1	1	1	0	1	0	9
Wichita, Kans.	40	1	1	3	4	4	3	1	1	1	2	1	1	8
Williston, N. Dak.	39	0	0	1	1	1	3	3	2	1	1	0	0	6
Wilmington, N. C.	40	0	1	1	1	2	1	1	1	0	0	0	0	4
Winnemucca, Nev.	40	1	3	2	3	4	2	1	1	1	2	2	0	10
Wytheville, Va.	37	1	1	2	1	2	1	2	1	1	0	0	0	3
Yakima, Wash.	15	0	1	1	1	1	1	0	0	0	0	0	0	2
Yankton, S. Dak.	29	0	0	1	2	3	2	2	2	1	1	1	0	5
Yellowstone Park, Wyo.	35	0	0	1	2	5	5	4	4	3	1	0	0	11
Yuma, Ariz.	40	1	1	1	0	0	0	0	1	0	0	0	1	2

At five of these stations (marked with an asterisk) the minimum annual number of days with hail is two; at all the others in the list it is one.

223. Some of the differences between the annual chart of the average distribution of days with hail, figure 69, and the similar annual chart on page 730 of "Climate and Man" (2) should be explained before proceeding to a comparison with the thunderstorm distribution. The most obvious difference is on the West Coast, where the "Climate and Man" chart shows hail occurrence tapering off toward zero while figure 69 shows an increase to an important secondary maximum on the Coast. The difference arises from a disagreement in the interpretation of the basic data. Most of the Pacific Coast occurrences are of what is known as "small hail", a hydrometeor characteristic of the winter or cooler months but occurring, nevertheless, with surface temperatures above freezing and falling from cumulonimbus clouds. It is often, but not always, accompanied by thunder. It is smaller than the ordinary hailstone and is composed of fewer, if any, concentric shells of clear and opaque ice. Often it is a soft, snow-like nucleus surrounded by a thin crust of ice which gives it a glazed appearance (27). In climatological summaries no distinction is made between hail and small hail. For the "Climate and Man" chart the supposition has been that real hail occurrences on the West Coast are effectively zero while elsewhere there are no small-hail occurrences, so that the frequency of hail occurrences, as deduced from the climatological summaries, has been ignored for the West Coast and fully accepted elsewhere. In figure 69,

however, and also in the following monthly charts, the Hydrometeorological Section has used the data strictly as tabulated without other corrections than smoothing, since the tabulations themselves make no distinction between types of hail.

224. In other respects, the differences between the two charts are mostly minor. Most differences in point values can be attributed to differences in length of record used and to the fact that the basic averages used in the "Climate and Man" chart were usually in whole numbers rather than in tenths, as in the Hydrometeorological charts. Occasionally, also, the addition of another station affected the pattern; Flagstaff data, for instance, were used in the Hydrometeorological chart and forced a notable change in the region of northern Arizona by doubling the frequency in the vicinity of Flagstaff.

225. Excepting the Pacific Coast, the annual hail chart, figure 69, shows the characteristic continental concentration from which there is a diminution of activity in all directions: poleward, equatorward, and seaward. It might be described as a purely continental concentration (annual frequencies of three to four) in the region from Iowa-Nebraska to Texas with an orographic enhancement of activity in the mountains on the west. The midcountry maximum corresponds to the secondary isoceraunic maximum in that region seen in figure 28 and the orographic maximum corresponds roughly to the Rocky Mountain thunderstorm maximum. In the mountain region both charts also show a comparative minimum in western Wyoming. The thunderstorm maximum near the Gulf is not reflected in the hail

pattern. Also, the West Coast thunderstorm minimum does not correspond to the secondary hail (or small-hail) maximum in that region although the actual totals are not far apart.

226. Inspection of the over-all hail pattern indicates at least two influences that may be responsible for the higher frequencies. One is orographic and the other frontal. They are contributory rather than sufficient or invariable factors.

227. The orographic effect is probably twofold. Although the mechanical lift provides the stimulus to free convection, the height of the station above sea level also contributes to the possibility of hail occurrence because of the comparatively short distance between the zero-isothermal level (or, more accurately, the zero-wet-bulb level) and the surface. The extreme, country-wide difference in the mean height of the zero-isothermal surface above sea level in July, for instance, is about 1500 m and, for most of the country, about 500 m. Both are less than the difference in elevation between, for example, Cheyenne and Tampa. The consequent lesser height between the ground and the zero-isothermal level corresponds to a lesser opportunity for the melting of hail as it falls to the ground. Tropical regions, of which Key West is a good local example and where the zero-isothermal surface is in general high while the lower air is warm, are notoriously deficient in hail occurrences at or near sea level (26).

228. The extension of the non-orographic maximum area from Oklahoma-Kansas east-northeastward toward Pennsylvania coincides roughly with a region of strong frontal activity. The monthly

distributions, to be discussed later, also favor the plausibility of frontal origins. This should not be taken to mean that the hail occurrence is associated strictly with the frontal passage. Although no reliable study has been made of the synoptic causes in a sufficient number of cases, such evidence as has been noted strongly suggests that hail occurrences are usually closely associated with frontal situations and that the "local hailstorm," analogue of the local thunderstorm, is probably a rarity.

229. On account of the comparatively low number of occurrences on the monthly charts it has been necessary to draw for occurrences of less than one per month in order to show the seasonal change of pattern. In this class, values of 0.2 and 0.5 were chosen, that is, frequencies of one in five years and one in two years, respectively. Except for a few isolated points, the line of zero frequency sets off an area of actually zero occurrence during the period of record just as in the thunderstorm-frequency charts. There has, however, been no attempt to adjust the area of zero hail occurrence to the area of zero thunderstorm occurrence, a problem of the winter months. The zero lines were drawn independently of each other; this seemed the best solution since hail is known to occur without thunder. The phenomenon is not limited to the United States. Tabulations of climatological data for "the world known to the ancients" by Shaw (28) yield a number of places where, on the average, hail occurrences exceed thunderstorm occurrences in some months: specifically, at Jerusalem, at Richmond in southeast England, and in particular at Malta, where the January figures are actually 3.4 to 0.8.

Landsberg's data ⁽²⁹⁾ show similar relationships at some points in Japan.

230. The January hail pattern (figure 70) differs markedly from the January thunderstorm pattern except in the approximate coincidence of the areas of zero occurrence in the northern sections of the country. On the West Coast, during this month, hail actually exceeds thunderstorm frequency. Only in the region of the juncture of Arkansas, Louisiana, Oklahoma, and Texas does there seem to be a direct relation between thunderstorm and hail activity. There the hail occurrences are about one in five years and their ratio to thunderstorm occurrences is about one in ten. In February (figure 70), apart from the West Coast where maximum activity is maintained, the area of appreciable occurrence of hail (one in five years) has expanded to include the states from Oklahoma and eastern Texas to Alabama, and again it is roughly coincident with an area in which ten times as many thunderstorms occur. By March (figure 70) the hail activity is more than doubled over the Great Basin Plateau and also in midcountry with a maximum center, exclusive of the West Coast, in Oklahoma-Missouri. The general spread of the areas of hail and thunderstorm activity is now about the same but the continental hail centers are displaced northwest of the isoceraunic centers. However, average hail frequencies still do not average one per month except on the West Coast. By April (figure 70) a further general increase in hail activity except on the West Coast, where it has diminished, has now produced one-per-month frequency lines in both the midcontinental center over eastern Oklahoma and in the Nevada-Utah

plateau area. Both centers can be related to increases in thunderstorm activity, but the latter increases are of much greater magnitude. The emergent isoceraunic maximum in southeastern Florida is, however, unaccompanied by an increase in hail activity.

231. May (figure 71) is, in general, the month of maximum hail activity, although at a considerable number of stations April or March is locally the month of maximum activity. By May the 1-day centers have expanded appreciably, small new centers of the same magnitude have emerged, and a new center with a 2-day maximum now appears at Cheyenne. Both the increases and centers in these regions roughly reflect the isoceraunic patterns and centers but, as before, the latter intensification is greater. In Florida there is no such reflection at all. On the West Coast the 1-day line has now disappeared.

232. In June (figure 71) only a few stations, including Cheyenne which now has 2.9 hail occurrences per month, show any further increases. Mostly there have been marked decreases, and all but the Cheyenne-centered maximum area have disappeared. This does not correspond to the thunderstorm situation, in which there has been marked intensification of activity except in southern Texas. It is interesting to see that in the latter region the thunderstorm decrease is accompanied by the intrusion of an area of zero hail occurrence between Corpus Christi and Galveston. The Cheyenne hail center seems fairly well correlated with the eastern Rocky Mountain thunderstorm maximum. Otherwise, the patterns and frequencies of the two phenomena diverge - and continue to do so in July, when the hail map (figure 71) exhibits an area of significant increase only around Flagstaff while the thunderstorm chart

is a pattern of increased activity generally. The Flagstaff region however, shows increased activity on both charts and, all in all, it is still in the Rocky Mountains that the hail pattern resembles the thunderstorm pattern most closely. That is also true of the hail patterns for August (figure 71) and September (figure 72).

233. By October (figure 72) the winter and spring hail pattern is foreshadowed. West Coast activity is again on the increase and the midcontinental center (now over Kansas-Missouri) is associated with a secondary thunderstorm center. A notable item is the appreciable but temporary increase of hail activity at leeward stations in the region of the Great Lakes. Except for the disappearance of the latter effect, the November and December hail patterns (figure 72) can be similarly characterized.

The hail-thunderstorm ratio

234. The ratio of hail to thunderstorm occurrences is implicit in the foregoing discussion, but its variation in time and place, although possessing significant features, is not easily noted without special presentation. For this purpose the station values of table 13 were divided by the station values of table 1 and multiplied by 100 to obtain the percentage ratios of hail to thunderstorm days annually and monthly. The isopercental lines are shown in figures 73-76. Because of the changing gradient of values, the same isopercental lines were not necessarily used from chart to chart nor in different portions of the same chart. Particularly for the low percentage values, only

such lines were drawn as would adequately indicate the gradient and changes. The zero lines were drawn to coincide with the lines of zero hail occurrence on the previous charts (figures 69-72), although the true ratio at those places where there were also no thunderstorm occurrences is really indeterminate rather than zero. No lines were drawn for values over 100%; however, there are many such values, particularly in the Far West, and some of these values are infinite - that is, there are days with hail but no days with thunderstorms in the record. Tables 1 and 13 provide the basic data for those who are interested in the exact numerical ratios of particular stations. Occasional reference to them is suggested, in any case, because the smoothing involved in the construction of the isopercental patterns had to be somewhat more drastic than usual in order to eliminate the anomalous local variations. Only the large-scale patterns are of interest here and only those patterns showed important systematic variations.

235. The annual ratio chart (figure 73) shows the ratios increasing northwestward from below 2% within a Gulf and Atlantic Coastal strip in the Southeast. More than half the country has an annual hail-thunderstorm ratio of less than 10% and more than a third has a ratio under 5%. Percentages over 10 occur only from the Rocky Mountains westward. On the eastern slopes of the Rockies Cheyenne has a maximum value of 18.2. The Great Basin area shows a greater expanse of over 10% occurrence and some values over 20%, but close to the Pacific Coast the percentages rise rapidly to as high as 200% at North Head, Washington.

236. The north-south gradient of the ratio, east of the Rockies, is emphasized on the winter charts, of which January (figure 74) is typical. The decrease toward the Atlantic and Gulf Coasts is also notable. Many of the Far West percentages are over 100 and some, like Reno and Winnemucca, Nevada, infinite. The violent convolutions of the isopercental lines in this region and also along the Great Lakes could not be well related to topographic features since they varied too much from month to month. However, in the East there is a noticeable and fairly consistent correspondence between the location of the Appalachian system and an area of comparatively high ratios.

237. In general, a similar pattern is preserved in the following months except that by June and July (figure 75) the West Coast becomes mostly an area of zero ratios. There are similar changes in the country-wide values of the ratio. Considering the country as a whole, the values are probably highest in February (figure 74) because of the high West Coast ratios during that month. For the rest of the country, especially from the Rockies eastward, the eastward spread of the 10% line indicates that probably March (figure 74) is the month of maximum ratio. By May (figure 75), the westward retreat of the 10% line, the appearance of a 5% line, and the lack of even isolated 20% values east of the Rockies, indicate the country-wide diminution of the ratio. This diminution continues through September (figure 76) except on the West Coast, where the winter increase has already begun. Elsewhere the zero and the 2% lines bound considerable area. By October (figure 76) the winter pattern, with its greater northward and westward increases, is

being reestablished, and during the following months the gradient is intensified because of the comparative constancy of the ratio in the southeastern coastal states.

238. From the above data the conclusion should be drawn that at most stations the hail-thunderstorm ratio is quite small. Except in the Far West, it rarely exceeds 20% and in most places it is a much lower percentage. An examination of some of the monthly climatic summaries for states and sections within this region indicated, however, that the number of days on which hail occurred anywhere in a state was usually much higher than 20% of the number of days with thunderstorms in that state. Almost always the dates of occurrence were the same. The state and section data are based on reports from cooperative stations, newspapers, and other sources, as well as from first-order stations.

239.* To check this indication, the number of days with hail and also the number of days with thunderstorms were counted for the 25 years from 1916 to 1940, in Iowa and in the Maryland-Delaware-District of Columbia climatic section. Iowa was chosen because it had one of the best collections of climatic summaries and the other section was chosen because a comparison of its hail-thunderstorm ratio could be made with the detailed data for Washington, D. C. The data for Iowa were compared with the point data for Kansas City, Missouri, because a complete, lengthy record from the latter was

* The material contained in this and the following paragraphs of this section of the report has previously been published in the Monthly Weather Review (30).

also available ⁽⁴⁾. The 1904-43 summaries of both hail and thunderstorm frequencies had not as yet been compiled at the time this portion of the study was made but the differences do not affect the results in any important way.

240. Tables 15 and 16 show the frequency data for days with thunderstorms, hail, and tornadoes in the two sections. The tornado data are from a report on tornadoes ⁽³¹⁾ in which the Hydrometeorological Section cooperated. In figure 77 the data for the station and for the area are compared. However, although the tornado totals are included in the tables they are not plotted in the figure because the tornado values are too small for adequate representation. It can be pointed out that where the tornado occurrences are appreciable, as in Iowa, the monthly variation in average number of occurrences forms a curve which is a flattened version of the hail-variation curve. In the Maryland-Delaware-District of Columbia section the tornado occurrences are too few to make comparison worth while.

241. Both tables and figure show how the state-wide or section-wide days of occurrence of thunderstorms or hail exceed the occurrences as reported by the single station. That this should be so is obvious from the consideration that if a large enough area - for instance, the area of the earth - were used, then every day would be a thunderstorm day and a hail day, perhaps even a tornado day. However, this fact does not cancel the validity of the increase in occurrences observed in the state-wide data. The thunderstorm and, to a greater degree, the hailstorm are phenomena of small areal extent. Thunderstorms are officially reported only when thunder is heard and the audibility of

Table 15

AREAL THUNDERSTORM-HAIL-TORNADO FREQUENCIES - IOWA

Year	January			February			March			April			May			June			July			August			September			October			November			December		
	W	H	T	W	H	T	W	H	T	W	H	T	W	H	T	W	H	T	W	H	T	W	H	T	W	H	T	W	H	T	W	H	T	W	H	T
1940	0	0	0	1	0	0	10	6	1	12	7	0	18	10	0	24	12	4	23	13	2	27	8	0	12	2	0	12	1	0	5	3	0	1	0	0
1939	4	1	0	2	3	0	10	3	0	12	8	0	19	5	1	26	7	4	24	14	0	20	5	1	12	2	0	13	8	1	3	1	0	0	0	0
1938	2	0	0	8	9	0	13	14	2	16	10	1	25	11	1	21	5	0	28	13	1	23	6	0	12	3	0	11	6	0	5	1	0	0	0	0
1937	2	0	0	1	0	0	2	4	0	14	8	0	25	12	4	21	8	8	22	6	3	22	5	1	12	1	0	4	1	0	5	0	0	0	0	0
1936	1	0	0	2	0	0	8	11	0	7	4	0	25	10	0	20	6	0	19	5	0	25	9	0	17	5	0	12	4	0	2	1	0	4	1	0
1935	3	1	0	3	0	0	13	6	2	6	8	0	21	8	0	26	5	0	25	9	2	23	3	1	17	7	0	11	4	0	4	1	0	0	0	0
1934	0	0	0	0	0	0	5	3	0	5	7	0	13	5	0	22	13	4	22	9	3	24	3	0	23	2	0	9	1	1	7	1	0	0	0	0
1933	7	5	0	5	4	0	10	8	0	11	9	1	22	11	2	17	7	1	16	9	2	21	3	0	21	9	0	5	3	0	3	0	0	0	0	0
1932	0	0	0	4	1	0	3	2	0	11	6	0	17	13	1	28	13	5	23	10	2	18	7	0	10	5	1	10	3	0	1	0	0	1	2	0
1931	0	0	0	1	0	0	0	0	0	7	4	1	15	8	2	17	9	3	18	10	0	18	6	2	20	4	2	12	7	0	10	2	0	2	2	0
1930	0	0	0	5	5	0	5	5	0	12	4	0	19	10	1	16	18	0	13	8	0	19	2	0	14	10	2	11	1	1	4	1	0	0	0	0
1929	3	0	0	1	0	0	11	5	3	17	13	2	14	6	2	22	10	2	20	10	2	20	6	0	19	1	1	11	2	0	2	3	0	0	0	0
1928	1	0	0	5	1	0	10	3	1	6	3	2	16	5	1	20	13	3	23	14	4	20	10	2	14	3	2	11	1	1	5	1	1	1	0	0
1927	0	0	0	5	0	0	10	7	0	21	9	0	18	10	4	21	7	0	27	11	2	18	9	0	20	6	1	12	3	0	5	3	0	1	0	0
1926	1	0	0	2	3	0	3	0	0	4	1	0	21	8	0	20	11	2	24	10	0	24	12	0	25	6	1	9	3	1	7	3	0	0	1	0
1925	0	0	0	6	1	0	6	1	0	16	12	1	14	4	0	25	17	5	26	13	1	18	7	0	19	4	0	7	2	1	3	1	0	0	1	0
1924	0	0	0	0	1	0	6	4	0	20	10	0	13	8	0	27	14	0	23	11	0	25	10	1	12	3	1	14	1	1	7	4	0	2	1	0
1923	1	0	0	2	2	0	4	0	0	12	6	0	18	5	1	27	13	1	19	9	0	24	10	3	21	5	1	3	0	0	3	1	0	0	0	0
1922	2	2	0	3	4	1	7	6	0	11	10	5	23	17	3	21	10	0	27	10	2	23	11	0	16	2	0	12	1	0	9	1	0	1	1	0
1921	0	1	0	2	1	0	15	3	1	13	11	1	20	13	2	24	7	0	23	2	0	24	6	0	7	8	1	12	4	0	3	2	0	1	0	0
1920	0	0	0	0	0	0	11	7	0	16	10	0	19	6	2	23	13	2	26	16	1	20	4	0	18	6	0	10	5	0	2	0	0	3	2	0
1919	0	0	0	2	4	0	7	4	1	20	11	2	13	5	2	26	9	1	20	7	0	22	5	1	16	1	0	22	2	0	7	0	0	0	0	0
1918	0	2	0	4	4	0	5	2	0	14	7	0	23	15	4	22	12	0	20	5	1	24	5	0	13	5	0	4	0	0	6	4	0	3	2	0
1917	0	0	0	2	0	0	0	1	0	14	7	0	17	5	0	28	9	2	25	9	0	20	3	0	20	3	0	6	6	0	4	0	0	0	0	0
1916	4	0	0	1	0	0	8	0	0	10	7	1	29	14	1	28	9	0	23	6	0	26	2	1	11	6	1	11	0	0	2	0	0	4	0	0
Totals	31	12	0	67	43	1	182	105	11	307	192	17	477	224	34	572	257	47	559	239	28	548	157	13	401	109	14	243	69	7	114	34	1	24	13	0
Means (W)	1.24			2.68			7.28			12.28			19.08			22.88			22.36			21.92			16.04			9.72			4.56			.96		
Means (H)	.48			1.72			4.20			7.68			8.96			10.28			9.56			6.28			4.36			2.76			1.06			.52		
Means (T)	0			.04			.14			.68			1.36			1.88			1.12			.52			.56			.28			.04			0		
Percentage Ratios (H/W)	38.7			63.2			57.7			62.5			47.0			44.9			42.8			28.6			24.7			28.4			29.8			54.2		

W = Days with Thunderstorms. H = Days with Hail. T = Days with Tornadoes.

Table 16

AREAL THUNDERSTORM-HAIL-TORNADO FREQUENCIES - MARYLAND-DELAWARE-WASHINGTON, D. C.

Year	January			February			March			April			May			June			July			August			September			October			November			December		
	Ⓕ	H	T	Ⓕ	H	T	Ⓕ	H	T	Ⓕ	H	T	Ⓕ	H	T	Ⓕ	H	T	Ⓕ	H	T	Ⓕ	H	T	Ⓕ	H	T	Ⓕ	H	T	Ⓕ	H	T	Ⓕ	H	T
1940	1	0	0	1	0	0	5	0	0	7	2	0	19	7	0	16	3	0	16	4	1	*	0	0	*	*	0	4	1	0	*	*	1	1	0	0
1939	3	0	0	4	0	0	6	0	0	9	1	0	9	4	0	14	1	0	14	3	1	18	2	1	12	3	0	5	2	1	0	0	0	1	0	0
1938	1	1	0	4	0	0	10	0	0	4	1	1	16	5	0	14	3	1	22	0	1	16	3	2	8	0	0	3	1	0	2	0	0	3	0	0
1937	3	0	0	3	0	2	0	1	0	6	0	0	12	5	2	19	4	1	18	2	0	19	1	0	2	0	0	2	1	0	2	0	0	0	0	0
1936	2	0	0	0	0	0	10	0	0	7	3	0	8	4	0	13	5	0	19	4	0	18	1	0	7	0	0	6	0	0	0	0	0	0	0	0
1935	0	0	0	2	0	0	6	3	0	2	2	0	10	0	0	15	1	0	21	0	0	12	2	0	6	1	2	5	0	0	1	0	0	1	0	0
1934	1	0	0	0	0	0	3	0	0	6	1	0	4	2	1	12	1	0	19	5	0	13	1	2	8	0	0	3	0	0	3	0	0	2	0	0
1933	0	0	0	0	0	0	5	1	0	5	2	0	20	2	0	18	5	0	16	4	0	15	0	1	9	0	0	1	0	0	0	0	0	0	0	0
1932	0	0	0	2	0	0	4	0	0	5	2	0	15	2	0	14	3	0	14	5	0	9	0	0	7	0	0	4	0	0	1	0	0	0	0	0
1931	1	0	0	0	0	0	2	1	0	6	0	0	16	4	0	9	1	0	22	4	1	15	1	0	11	0	0	6	1	0	0	0	0	2	0	0
1930	1	0	0	4	2	0	2	2	0	5	2	0	11	3	0	8	3	0	14	4	0	5	1	0	9	1	0	4	1	0	1	0	0	0	0	0
1929	0	0	0	0	0	0	3	1	0	9	3	0	13	4	1	16	5	0	17	1	0	11	4	0	8	0	0	6	2	0	1	0	0	2	0	0
1928	1	1	0	2	1	0	4	1	0	3	0	0	9	5	0	17	5	0	16	2	1	14	0	0	5	0	0	5	0	0	1	0	0	0	0	0
1927	1	0	0	5	3	0	4	4	0	8	2	0	10	6	1	9	1	0	18	5	0	9	2	0	9	0	0	2	0	0	1	0	1	1	0	0
1926	1	0	0	3	0	0	3	0	0	3	3	0	12	1	0	11	4	0	16	2	0	14	0	0	8	0	0	9	2	0	2	1	1	0	0	0
1925	0	0	0	2	0	0	4	0	0	8	4	0	*	2	0	*	4	0	*	4	0	12	3	0	9	3	0	*	*	0	*	*	0	*	*	0
1924	2	0	0	1	0	0	4	0	0	6	1	0	7	1	0	14	5	0	12	0	0	10	0	0	6	0	0	*	*	0	*	*	0	*	*	0
1923	2	0	0	1	0	0	3	0	0	*	*	1	*	*	0	13	5	0	16	2	0	12	2	0	10	1	0	2	0	0	1	0	0	3	0	0
1922	0	0	0	6	0	0	8	1	0	5	2	0	11	0	0	15	0	0	15	4	0	17	3	0	7	0	0	2	0	0	*	*	0	1	0	0
1921	1	0	0	1	0	0	7	1	0	6	2	0	8	2	0	13	4	0	19	3	0	12	1	0	*	*	0	2	0	0	4	3	0	2	0	0
1920	0	0	0	2	0	0	6	0	0	8	2	0	5	1	0	14	6	0	15	4	0	17	2	0	9	0	0	2	2	0	2	0	0	3	0	0
1919	0	0	0	2	1	0	4	1	0	6	2	0	16	5	0	17	5	0	15	2	0	15	3	0	8	1	0	8	0	0	2	0	0	1	0	0
1918	2	0	0	4	0	0	3	0	0	12	0	0	21	4	0	17	2	0	20	3	0	17	3	0	7	0	0	2	1	0	3	2	0	2	0	0
1917	1	0	0	4	0	0	2	2	0	6	2	0	12	6	0	20	6	0	22	6	0	21	5	0	7	1	0	*	2	0	1	0	0	0	0	0
1916	1	0	0	0	0	0	8	4	0	8	5	0	14	3	0	22	5	0	18	0	0	19	4	0	12	1	0	5	0	0	3	1	0	1	1	0
Totals	25	2	0	53	7	2	116	23	0	150	44	2	278	78	5	350	87	2	414	73	5	340	44	6	184	12	2	88	16	1	31	7	3	26	1	0
Means (Ⓕ)	1.0			2.12			4.64			6.2			12.1			14.6			17.2			13.8			8.0			4.0			1.48			1.13		
Means (H)	.08			.28			.92			1.8			3.2			3.48			2.92			1.76			.52			.7			.33			.04		
Means (T)	0			.08			0			.08			.20			.08			.20			.24			.08			.04			.12			0		
Percentage Ratios (H/Ⓕ)	8.0			13.2			19.8			29.3			26.4			23.8			17.0			12.7			8.0			17.5			22.6			3.8		

Ⓕ = Days with Thunderstorms. H = Days with Hail. T = Days with Tornadoes. * = No Data.

thunder, according to C.E.P. Brooks ⁽⁵⁾, is 10 or 12 miles under favorable circumstances and only about 6 miles under normal circumstances, making the area within which thunder is normally heard about 100 square miles. An interesting corroboration of the latter figure has been made by R. L. Day ⁽³²⁾. Hence, if only first-order stations, widely spaced, are used to study frequency of occurrence, many occurrences of thunder will be missed. The observations made by a dense network of stations, intended for forest-fire protection in the State of Washington, increased the thunderstorm-day values of Alexander's isoceraunics for the period 1904-23 ⁽³⁾ twofold to fourfold ⁽³³⁾. Fewer would be missed by a sparse network if lightning were the phenomenon that had to be observed. Hail, on the other hand, is neither seen nor heard at any appreciable distance, its total area of occurrence being often of the order of 20 square miles. A sparse network will thus miss more hailstorms than thunderstorms. The use of occurrence over an area rather than over a single station corrects these faults although the exact area to be used for proper correction is problematical, and an academic question in this case since the areal data are limited to climatic sections or states.

242. In the two examples cited the frequencies of thunderstorms, as observed over the state or section, are about double the frequencies as observed by a single station; the hail occurrences are increased about tenfold. The result is an increase in the hail-thunderstorm ratios although the pattern of the monthly variation of the ratio is retained. At Kansas City the annual ratio is 8%, but for the State of Iowa it is 42%. The peak monthly ratios at the station are

22 and 24 in March and November; the peak state ratios are 63, 62, and 54 in February, April, and December, respectively. The minimum ratio is 2% in July-August at the station, and 25 in September in the state. At Washington, D. C. the annual ratio is 4% but for the climatic section it is 19%. The monthly peaks at the station are 12 in February and 45 in December (the latter being unusually out of line) and the section peaks are 29 in April and 22 in November. The station minima range between 0 and 2 in January and from June through September; the section minima are 4 in December and 8 in both January and September.

243. The evidence points to an error in the commonly held notion that hail occurrences in thunderstorms are comparatively infrequent. The notion is based on a comparison of point frequencies. Some indication of the greater validity of the areal count, when states of average size are used, is the following fact: while Iowa has an area of 56,000 and Maryland-Delaware-District of Columbia an area of only 12,700 square miles, the areal annual hail-thunderstorm ratio is in both cases about five times the point ratio. Further research in the matter is suggested, but most of it would have to be done at climatic-section centers since in most cases it would be necessary to use the original manuscript records of cooperative stations for the basic data needed in a summary of areal frequencies.

Comparison with tornado distribution

244. Charts of the annual and monthly distribution of tornado days per state are available in the "Preliminary Report on Tornadoes" (31), previously cited. They show the total number of occurrences for the

63 years from 1880 to 1942, the data having been collected from various published sources. In figure 78 the data are summarized in histograms that show the monthly variation of tornado frequency per state or section. The New England States (except Maine) are combined into one histogram as are Maryland, Delaware, and the District of Columbia. These exceptions were made because of the small areas of the individual members of these sectional units. It is obvious that the totals of figure 166 reflect not only tornado activity but also the size of the area in which the activity was observed. To correct for this, the frequencies were divided by the state or sectional area and new histograms constructed, in figure 79, showing the monthly variation of the total number of tornado days per unit area of 10,000 square miles. This unit is a fraction of the average state area. Only the area of New Jersey is exceeded by the unit area, where the tornado frequency per unit area therefore exceeds the frequency per state. The sectional combinations were made to avoid this inconsistency. In the case of Washington, D. C., which has had three tornadoes in the 63-year period but has an area of only 70 square miles, the conversion to tornado frequency per 10,000-square-mile area would have resulted in a terrifying value, indeed. Another important correction but one not easily applied, is for density of population. The chances of a tornado being reported at all vary with the population density, which itself has varied enormously during the period of record. A population factor would increase the theoretical tornado frequencies in the less populous states, the factor itself generally increasing toward the western part of the United States. The annual and monthly tornado totals used

in figures 78 and 79 are also given in tables 17 and 18. The monthly tornado totals of table 18 are also charted in figures 80-82, with red overprints for the corresponding thunderstorm distributions.

245. Although the pattern of the monthly variation is naturally unchanged in figure 79, the unit-area correction does rearrange the frequency ranking of the states. This is best demonstrated by table 19 in which the states and sections are ranked in the order of annual tornado frequency, per state or section in the first column and per 10,000-square-mile area per state or section in the second column. The latter frequency, which is the truer measure of activity, puts Iowa rather than Kansas first, drops Texas from 2d to 29th place, and raises Maryland-Delaware-D.C. from 29th to 4th - to cite a few examples. Table 20 shows the monthly variations of the ranking by frequency per unit area for each state or section.

246. The annual distribution of the tornado frequencies per unit area (figure 79) confines the totals over 10 to the area east of the Rockies, not including Maine and North Dakota. The maximum values extend northwestward from Alabama to Kansas and Iowa, with a center over 40 in Alabama and a center over 50 in Kansas and Iowa. There are secondary centers of about 35 over the New Jersey and Maryland-Delaware-D.C. areas and also over South Carolina. The pattern resembles the thunderstorm distribution (figure 28) in the extension of a zone of activity from Alabama toward Iowa, and the hail distribution (figure 69) in the approximate location of the midcontinental center.

Table 17

TOTAL TORNADO DAYS PER STATE OR SECTION

(1880-1942)

	J	F	M	A	M	J	J	A	S	O	N	D	Annual
Alabama	20	29	63	48	18	4	3	0	1	6	9	11	212
Arizona	0	0	0	0	0	0	0	1	1	0	0	0	2
Arkansas	6	10	38	49	29	12	9	2	6	9	18	15	203
California	2	0	3	5	0	0	1	0	0	1	2	1	15
Colorado	0	0	0	6	13	14	2	3	0	0	1	0	39
Florida	5	8	7	15	6	5	5	5	7	5	3	3	74
Georgia	6	11	35	31	6	8	7	1	3	1	1	5	115
Idaho	0	0	0	0	1	1	2	0	0	0	0	0	4
Illinois	1	2	23	27	40	27	13	9	12	3	6	0	163
Indiana	1	3	13	13	23	12	10	11	9	1	0	2	98
Iowa	0	1	15	36	60	80	43	17	24	13	5	1	295
Kansas	0	2	20	68	96	97	42	46	29	8	5	0	413
Kentucky	4	5	10	3	7	8	3	3	2	2	2	2	51
Louisiana	9	11	18	20	9	6	4	1	4	9	12	12	115
Maine	0	0	0	0	1	1	5	0	1	0	0	0	8
Md.-Del.-D.C.	0	3	0	2	8	4	12	13	2	2	3	0	49
Michigan	1	1	2	10	28	19	7	3	12	1	1	0	85
Minnesota	0	0	2	4	24	35	20	17	9	2	1	0	114
Mississippi	7	15	39	31	16	4	3	1	2	3	9	12	142
Missouri	4	8	20	39	31	27	11	4	14	6	6	1	171
Montana	0	1	0	1	5	9	13	6	0	0	2	2	39
Nebraska	0	0	3	20	44	53	20	8	9	2	1	0	160
Nevada	0	0	0	0	0	0	0	0	0	0	0	0	0
New Eng. (except Maine)	2	0	0	0	8	4	18	7	9	2	2	1	53
New Jersey	0	0	2	3	4	6	3	7	2	1	1	0	29
New Mexico	0	0	1	1	9	6	3	2	1	0	0	0	23
New York	1	0	1	1	7	18	13	7	8	2	3	0	61
North Carolina	2	4	10	13	11	9	6	5	1	4	1	3	69
North Dakota	0	0	0	1	7	18	20	9	1	0	0	0	56
Ohio	3	3	8	14	24	23	18	10	11	2	1	0	117
Oklahoma	6	5	14	44	53	26	4	5	8	8	8	2	183
Oregon	0	1	0	2	1	2	0	0	0	1	2	0	9
Pennsylvania	1	1	1	8	11	19	13	11	2	1	6	0	74
South Carolina	1	5	18	20	19	12	9	6	8	3	3	3	107
South Dakota	0	0	0	7	19	41	29	16	9	0	2	0	123
Tennessee	8	4	26	16	10	9	5	4	2	3	7	2	96
Texas	15	11	34	77	74	35	24	17	4	12	14	11	328
Utah	0	0	0	0	1	0	0	1	0	0	0	0	2
Virginia	1	3	2	6	12	6	10	13	9	1	2	0	65
Washington	0	0	0	0	2	1	0	0	2	0	0	0	5
West Virginia	0	0	0	1	4	3	1	1	0	0	0	0	10
Wisconsin	0	0	2	12	19	29	20	11	12	8	3	0	116
Wyoming	0	0	0	1	10	15	3	4	0	0	0	0	33

Table 18

TOTAL TORNADO DAYS PER 10,000-SQUARE-MILE AREA
PER STATE OR SECTION

(1880-1942)

	J	F	M	A	M	J	J	A	S	O	N	D	Annual
Alabama	3.9	5.6	12.2	9.3	3.5	0.8	0.6	0	0.2	1.2	1.7	2.1	41.1
Arizona	0	0	0	0	0	0	0	0.1	0.1	0	0	0	0.2
Arkansas	1.1	1.9	7.2	9.2	5.5	2.3	1.7	0.4	1.1	1.7	3.4	2.8	38.2
California	0.1	0	0.2	0.3	0	0	0.1	0	0	0.1	0.1	0.1	0.9
Colorado	0	0	0	0.6	1.2	1.3	0.2	0.3	0	0	0.1	0	3.7
Florida	0.8	1.4	1.2	2.6	1.0	0.8	0.8	0.8	1.2	0.8	0.5	0.5	12.6
Georgia	1.0	1.9	5.9	5.3	1.0	1.4	1.2	0.2	0.5	0.2	0.2	0.8	19.5
Idaho	0	0	0	0	0.1	0.1	0.2	0	0	0	0	0	0.5
Illinois	0.2	0.4	4.1	4.8	7.1	4.8	2.3	1.6	2.1	0.5	1.1	0	28.9
Indiana	0.3	0.8	3.6	3.6	6.3	3.3	2.8	3.0	3.5	0.3	0	0.6	28.0
Iowa	0	0.2	2.7	6.4	10.7	14.2	7.6	3.0	4.3	2.3	0.9	0.2	52.4
Kansas	0	0.2	2.4	8.3	11.7	11.8	5.1	5.6	3.5	1.0	0.6	0	50.2
Kentucky	1.0	1.2	2.5	0.7	1.7	2.0	0.7	0.7	0.5	0.5	0.5	0.5	12.6
Louisiana	1.9	2.3	3.7	4.1	1.9	1.2	0.8	0.2	0.8	1.9	2.5	2.5	23.7
Maine	0	0	0	0	0.3	0.3	1.5	0	0.3	0	0	0	2.4
Md.-Del.-D.C.	0	2.4	0	1.6	6.3	3.2	9.4	10.2	1.6	1.6	2.4	0	38.6
Michigan	0.2	0.2	0.3	1.7	4.8	3.3	1.2	0.5	2.1	0.2	0.2	0	14.6
Minnesota	0	0	0.2	0.5	2.8	4.2	2.4	2.0	1.1	0.2	0.1	0	13.6
Mississippi	1.5	3.1	8.2	6.5	3.4	0.8	0.6	0.2	0.4	0.6	1.9	2.5	29.8
Missouri	0.6	1.2	2.9	5.6	4.4	3.9	1.6	0.6	2.0	0.9	0.9	0.1	24.5
Montana	0	0.1	0	0.1	0.3	0.6	0.9	0.4	0	0	0.1	0.1	2.6
Nebraska	0	0	0.4	2.6	5.7	6.9	2.6	1.0	1.2	0.3	0.1	0	20.7
Nevada	0	0	0	0	0	0	0	0	0	0	0	0	0
New Eng. (except Maine)	0.6	0	0	0	2.4	1.2	5.4	2.1	2.7	0.6	0.6	0.3	15.9
New Jersey	0	0	2.6	3.8	5.1	7.7	3.8	9.0	2.6	1.3	1.3	0	37.2
New Mexico	0	0	0.1	0.1	0.7	0.5	0.2	0.2	0.1	0	0	0	1.9
New York	0.2	0	0.2	0.2	1.4	3.6	2.6	1.4	1.6	0.4	0.6	0	12.3
North Carolina	0.4	0.8	1.9	2.5	2.1	1.7	1.1	1.0	0.2	0.8	0.2	0.6	13.1
North Dakota	0	0	0	0.1	1.0	2.5	2.8	1.3	0.1	0	0	0	7.9
Ohio	0.7	0.7	1.9	3.4	5.8	5.6	4.4	2.4	2.7	0.5	0.2	0	28.4
Oklahoma	0.9	0.7	2.0	6.3	7.6	3.7	0.6	0.7	1.2	1.2	1.2	0.3	26.3
Oregon	0	0.1	0	0.2	0.1	0.2	0	0	0	0.1	0.2	0	0.9
Pennsylvania	0.2	0.2	0.2	1.8	2.4	4.2	2.9	2.4	0.4	0.2	1.3	0	16.3
South Carolina	0.3	1.6	5.8	6.4	6.1	3.9	2.9	1.9	2.6	1.0	1.0	1.0	34.4
South Dakota	0	0	0	0.9	2.5	5.3	3.8	2.1	1.2	0	0.3	0	16.0
Tennessee	1.9	1.0	6.2	3.8	2.4	2.1	1.2	1.0	0.5	0.7	1.7	0.5	22.8
Texas	0.6	0.4	1.3	2.9	2.8	1.3	0.9	0.6	0.2	0.4	0.5	0.4	12.3
Utah	0	0	0	0	0.1	0	0	0.1	0	0	0	0	0.2
Virginia	0.2	0.7	0.5	1.5	2.9	1.5	2.4	3.2	2.2	0.2	0.5	0	15.9
Washington	0	0	0	0	0.3	0.2	0	0	0.3	0	0	0	0.7
West Virginia	0	0	0	0.4	1.6	1.2	0.4	0.4	0	0	0	0	4.1
Wisconsin	0	0	0.4	2.1	3.4	5.2	3.6	2.0	2.1	1.4	0.5	0	20.6
Wyoming	0	0	0	0.1	1.0	1.5	0.3	0.4	0	0	0	0	3.4

Table 19

RANKING OF STATES OR SECTIONS
IN DESCENDING ORDER OF ANNUAL TORNADO FREQUENCY

(1880-1942)

Rank	Per State or Section	Rank	Per 10,000-Sq.-Mi. Area
1	Kansas	1	Iowa
2	Texas	2	Kansas
3	Iowa	3	Alabama
4	Alabama	4	Md.-Del.-D.C.
5	Arkansas	5	Arkansas
6	Oklahoma	6	New Jersey
7	Missouri	7	South Carolina
8	Illinois	8	Mississippi
9	Nebraska	9	Illinois
10	Mississippi	10	Ohio
11	South Dakota	11	Indiana
12	Ohio	12	Oklahoma
13	Wisconsin	13	Missouri
14	Georgia	14	Louisiana
14	Louisiana	15	Tennessee
16	Minnesota	16	Nebraska
17	South Carolina	17	Wisconsin
18	Indiana	18	Georgia
19	Tennessee	19	Pennsylvania
20	Michigan	20	South Dakota
21	Florida	21	Virginia
21	Pennsylvania	22	New England (except Maine)
23	North Carolina	23	Michigan
24	Virginia	24	Minnesota
25	New York	25	North Carolina
26	North Dakota	26	Florida
27	New England (except Maine)	27	Kentucky
28	Kentucky	28	New York
29	Md.-Del.-D.C.	29	Texas
30	Colorado	30	North Dakota
30	Montana	31	West Virginia
32	Wyoming	32	Colorado
33	New Jersey	33	Wyoming
34	New Mexico	34	Montana
35	California	35	Maine
36	West Virginia	36	New Mexico
37	Oregon	37	California
38	Maine	38	Oregon
39	Washington	39	Washington
40	Idaho	40	Idaho
41	Arizona	41	Utah
41	Utah	42	Arizona
43	Nevada	43	Nevada

Table 20

MONTHLY VARIATION OF STATE OR SECTION RANK
BY TORNADO FREQUENCY PER 10,000-SQUARE-MILE AREA

(1880-1942)*

	J	F	M	A	M	J	J	A	S	O	N	D	Annual
Alabama	1	1	1	1	14	33	31	*	29	7	5	4	3
Arizona	*	*	*	*	*	*	*	36	33	*	*	*	42
Arkansas	5	6	3	2	10	19	18	29	19	3	1	1	5
California	21	*	27	30	*	*	38	*	*	30	30	18	37
Colorado	*	*	*	27	29	26	37	30	*	*	32	*	32
Florida	9	8	19	18	30	31	27	20	15	12	19	9	26
Georgia	6	5	5	9	32	25	22	33	22	27	26	6	18
Idaho	*	*	*	*	38	39	35	*	*	*	*	*	40
Illinois	19	18	7	10	4	8	17	14	10	17	10	*	9
Indiana	16	12	9	14	5	15	12	5	3	22	*	8	11
Iowa	*	21	11	6	2	1	2	6	1	1	12	15	1
Kansas	*	19	14	3	1	2	4	3	2	9	14	*	2
Kentucky	7	9	13	26	26	21	29	21	23	18	20	10	27
Louisiana	3	4	8	11	25	29	28	32	21	2	2	3	14
Maine	*	*	*	*	36	36	20	*	27	*	*	*	35
Md.-Del.-D.C.	*	3	*	23	6	17	1	1	14	4	3	*	4
Michigan	20	22	23	22	12	16	21	25	11	28	27	*	23
Minnesota	*	*	24	28	18	10	16	11	20	25	31	*	24
Mississippi	4	2	2	4	16	32	30	31	26	15	4	2	8
Missouri	12	10	10	8	13	11	19	24	12	11	13	16	13
Montana	*	24	*	36	35	34	26	28	*	*	28	17	34
Nebraska	*	*	21	17	9	4	14	17	17	23	29	*	16
Nevada	*	*	*	*	*	*	*	*	*	*	*	*	43
New Eng. (except Maine)	11	*	*	*	22	30	3	9	4	16	16	13	22
New Jersey	*	*	12	12	11	3	6	2	7	6	8	*	6
New Mexico	*	*	28	35	34	35	36	34	34	*	*	*	36
New York	*	*	26	32	28	14	13	15	13	21	15	*	28
North Carolina	14	13	17	19	24	22	24	18	30	13	25	7	25
North Dakota	*	*	*	33	33	18	11	16	32	*	*	*	30
Ohio	10	15	16	15	8	5	5	8	5	19	23	*	10
Oklahoma	8	16	15	7	3	13	32	22	18	8	9	14	12
Oregon	*	23	*	31	40	37	*	*	*	29	24	*	38
Pennsylvania	18	20	25	21	21	9	10	7	25	26	7	*	19
South Carolina	15	7	6	5	7	12	9	13	6	10	11	5	7
South Dakota	*	*	*	25	20	6	7	10	16	*	22	*	20
Tennessee	2	11	4	13	23	20	23	19	24	14	6	11	15
Texas	13	17	18	16	19	27	25	23	31	20	18	12	29
Utah	*	*	*	*	39	*	*	35	*	*	*	*	41
Virginia	17	14	20	24	17	24	15	4	8	24	21	*	21
Washington	*	*	*	*	37	38	*	*	28	*	*	*	39
West Virginia	*	*	*	29	27	28	33	26	*	*	*	*	31
Wisconsin	*		22	20	15	7	8	12	9	5	17	*	17
Wyoming	*	*	*	34	31	23	34	27	*	*	*	*	33

* No occurrences, tied for last place with other states or sections.

247. In January (figure 80) the center of tornado occurrence is Alabama, where there are about four occurrences (per unit area) during the period. The area of any occurrence at all slightly exceeds the area included within the 1-day isoceraunic on the west and north and also includes all the Atlantic States but Maine. Except in New England and New York, where there have been no occurrences in February, the principal tornado occurrence area is slightly expanded in February (figure 80). Alabama remains the center, with a value of 5.6. In the region surrounding Alabama there is a resemblance to the hail (figure 70) and thunderstorm centers but the tornado center is farther east in both cases. The Alabama center grows to 12.2 in March (figure 80) with similar increases elsewhere, and its relation to both hail (figure 70) and thunderstorm centers is still about the same. By April (figure 80) Alabama's frequency has fallen to 9.3, which is now rivaled by the 9.2 value in Arkansas and 8.3 in Kansas. It is interesting to note that Mississippi falls from 8.2 to 6.5 from March to April - an indication of the passing of the maximum center through the state. In April Arkansas is the thunderstorm center, just east of the hail center in Oklahoma (figure 70).

248. By May (figure 81) there are decreases in the tornado frequency in all the Gulf States and also northward to Arkansas, Missouri, and Tennessee. The new center then is Kansas, with a value of 11.7, and Iowa is next with 10.7. Separated from this region by a zone of two occurrences per unit area paralleling the Appalachian Ridges, is a distinct secondary development with maximum values of 6.3 in Maryland-Delaware-D.C. and 5.1 in New Jersey. In the region of the primary

maximum there is an overlapping of the thunderstorm, hail (figure 71), and tornado centers. By June (figure 81) the increases in tornado frequency are confined mostly to the states north of the Potomac, Ohio, and Missouri Valleys but also include the Plains and Mountain States from Kansas and Colorado northward. The June maximum center is Iowa, with a value of 14.2. The eastern center is 7.7 in New Jersey. There is little resemblance now to the thunderstorm pattern, and the chief resemblance to the hail pattern (figure 71) is a progression of activity northward with diminishing activity behind. July (figure 81) shows diminution of tornado activity throughout except in North Dakota and Montana in the West and in New England and Maryland-Delaware-D.C. in the East. Iowa is still the maximum in its region with a value of 7.6, but the Maryland-Delaware-D.C. center is the highest with 9.4. The latter center is also maintained in August (figure 81) with a value of 10.2 but elsewhere there is a continued diminution of activity, the Iowa center retreating temporarily to Kansas where its value becomes 5.6. Alabama shows no occurrences at all in August, the only month of the year when this is true.

249. It is only by September (figure 82) that tornado frequencies begin to increase again in the region west of the Appalachians, at which time Iowa is again the maximum state with a value of 4.3. The Atlantic Coast maximum is again eliminated except by contrast with the area of minimum occurrence paralleling the Appalachian Highlands. It is during these months - June through September - that the most suggestive parallelism between the hail (figures 71 and 72) and tornado patterns can be found. Both have shown decreasing activity and their midcontinental

centers have both been located approximately over Kansas and Iowa. The thunderstorm charts have also shown a small secondary center in the region of Missouri during the period but, except for September, the tendency has been toward an over-all increase of activity. In October (figure 82) Iowa continues to have the maximum tornado value (2.3) but growing activity near the Gulf minimizes its importance. By November (figure 82) Arkansas is highest with a 3.4 value. Arkansas is still the leading state in December (figure 82) but with a value of only 2.8 against 2.5 for both Louisiana and Mississippi. By January (figure 80) it is thus not strange to find Alabama again in the lead. There is a roughly parallel retreat southward of both the hail (figure 72) and thunderstorm activity during this period.

The maximum thunderstorm month

250. It has already been noted that July is the month of maximum thunderstorm activity over the United States. However, even a casual inspection of the figures showing the monthly variation in frequency of thunderstorm days indicates a variation of the maximum month. In an effort to define this variation, if possible, the chart showing the months of the maximum average number of thunderstorm days (figure 83) was constructed. The pattern is definite; no smoothing was needed to separate the different months of maximum occurrence. When averages to whole days were used to determine the maximum month, the extent of the area included seemed to justify a delineation of the region where June and July are equally possible maxima; but use of averages to tenths of days eliminated this area. It is possible that

the August area near Key West should also hug the Gulf Coast of Florida since many of the coastal stations had a secondary maximum in August or even an equal maximum when averages to whole days were considered.

251. The result still shows July to be the dominant month, closely followed by June, in area covered. The actual maximum values in the July and August regions are the highest, however, as can be verified by consulting the monthly charts (figures 29-31), or the monthly variation chart (figure 27).

252. There is the same evidence of the progression of thunderstorm activity previously indicated: a movement from central Texas in May northward through the Mississippi Valley with a branching eastward and westward, followed by a return southward approximately along the Appalachian and Rocky Mountain Divides. Even a final return to Texas might be deduced from the small September area near Brownsville and Corpus Christi. The transition from low to high pressure at 10,000 feet over Texas, with the gradual progression northward and expansion of the high-level anticyclone in the following months, has already been adduced as a possible explanation (paragraphs 151-4). On the West Coast the maximum month moves southward with the southward retreat of the Pacific High and the cyclonic activity on its north side.

253. A comparison of this chart with one showing the months of maximum rainfall (also figure 83) was an obvious next step. All months having average rainfall within 0.20 inch of the maximum value were considered and where two or more were thus the "maximum months", the dividing lines were drawn to favor continuity of area. It was

not surprising to find important areas where the thunderstorm season did not include the month of maximum rainfall. The widest departures from the thunderstorm pattern are in the vicinity of the lower Mississippi, the lower Ohio, and the Tennessee Valleys; in the Lake region; and along the New England Coast. Otherwise, the May-June maximum-rain areas were expanded mostly at the expense of the July maximum-thunderstorm area. Between the Mississippi and the Rockies, the May and June areas are particularly well defined and the chart shows that June is the month when the largest area has its maximum month of rainfall. There is no clear sequence of rainfall maxima comparable to the sequence of thunderstorm maxima.

254. A further comparison was made with a chart (not shown) of the maximum months of rainfall chosen from the season of maximum thunderstorm activity, i.e., May, June, July, and August. Similarity to the thunderstorm chart is, of course, greater. The western spring and winter maximum months are all replaced by May. In the central region they are replaced by May and partly by July. May also replaces September in this region. On the New England Coast August replaces January, February, and March.

255. The distribution of the maximum hail month is also given in figure 83. As indicated in previous sections, it generally precedes the maximum thunderstorm month but there is a similar progression outward in time - from April in the Gulf States in this case, rather than from May in Texas. The chart is most comparable to the chart of the distribution of the maximum tornado months in the same figure. In the latter case, since the occurrences are within a state rather

than at a point, the dividing lines are simply smoothed state boundaries. In general, the close relation between tornado and hail occurrences is apparent.

Diurnal variation of thunderstorm frequency

256. From basic data gathered by W. R. Gregg, former Chief of the Weather Bureau, available only in manuscript form and thoughtfully suggested to the Hydrometeorological Section by L. P. Harrison of the Bureau, it was possible to make a more detailed study of the diurnal variations of thunderstorm frequency in the United States than had ever before been accomplished. There had been many earlier observations of such a variation but none had been areally defined except in the recent "Airway Meteorological Atlas for the United States" (34), which is based on a shorter period of record (though probably a better one) and on a lesser number of stations. Nevertheless, the latter shows no appreciable conflict with the results of the analysis of the Gregg data. Other observations of the variation have been mostly qualitative or based on single-station records.

257. The period of the Gregg data is from 1906 through 1925. The data were gathered from 192 stations in the United States, some of which have shorter periods of record, varying from 7 to 19 years. The shorter periods of record are indicated on the appropriate charts and also in table 21, which summarizes the data. The hour of thunderstorm occurrence in these data is the hour of beginning, defined as the hour in which thunder is first heard. Gregg made separate tabulations of occurrences recorded only as DNA (during a.m. hours of

Table 21
DIURNAL VARIATION OF THUNDERSTORM FREQUENCY
(PERIOD: 1906-1925)

Station and Years of Record	Season	00-06			06-12			12-18			18-24			ΣN
		N	%F	%P	N	%F	%P	N	%F	%P	N	%F	%P	
Abilene, Texas (20)	W	11	26.8	0.6	10	24.4	0.6	9	22.0	0.5	11	26.8	0.6	41
	Sp	71	22.9	3.9	51	16.4	2.8	99	31.9	5.4	90	29.0	4.9	311
	Su	61	16.1	3.3	39	10.3	2.1	186	49.1	10.1	93	24.6	5.0	379
	A	31	20.1	1.7	29	18.8	1.6	59	38.3	3.2	35	22.7	1.9	154
Albany, New York (20)	W	174	19.7	2.4	129	14.6	1.8	353	39.9	4.8	229	25.9	3.1	885
	Sp	3	42.8	0.2	1	14.3	0.1	2	28.6	0.1	1	14.3	0.1	7
	Su	21	15.7	1.1	12	8.9	0.6	61	45.5	3.3	40	29.8	2.2	134
	A	46	10.2	2.5	48	10.7	2.6	238	53.0	12.9	117	26.0	6.4	449
Alpena, Michigan (20)	W	15	16.5	0.8	7	7.7	0.4	35	38.5	1.9	34	37.4	1.9	91
	Sp	85	12.5	1.2	68	10.0	0.9	336	49.3	4.6	192	28.2	2.6	681
	Su	2	50.0	0.1	0	0	0	0	0	0	2	50.0	0.1	4
	A	32	20.5	1.7	32	20.5	1.7	50	32.0	2.7	42	26.9	2.3	156
Amarillo, Texas (20)	W	45	11.6	2.4	93	24.0	5.0	172	44.4	9.3	77	19.9	4.2	387
	Sp	30	26.3	1.6	12	10.5	0.7	49	43.0	2.7	23	20.2	1.3	114
	Su	109	16.5	1.5	137	20.7	1.9	271	40.9	3.7	144	21.7	2.0	661
	A	1	12.5	0.1	2	25.0	0.1	1	12.5	0.1	4	50.0	0.2	8
Anniston, Alabama (20)	W	14	7.3	0.8	17	8.8	0.9	78	40.4	4.2	84	43.5	4.6	193
	Sp	40	9.7	2.2	18	4.4	1.0	190	46.2	10.3	164	39.9	8.9	412
	Su	23	16.5	1.3	11	7.9	0.6	64	46.0	3.5	41	29.5	2.2	139
	A	78	10.4	1.1	48	6.4	6.6	333	44.3	4.6	293	39.0	4.0	752
Asheville, North Carolina (20)	W	17	20.0	0.9	22	25.9	1.2	26	30.6	1.4	20	23.5	1.1	85
	Sp	48	13.5	2.6	80	22.6	4.3	157	44.3	8.5	69	19.5	3.7	354
	Su	47	5.3	2.6	167	18.7	9.1	551	61.7	29.9	128	14.3	7.0	893
	A	14	7.1	0.8	39	19.7	2.1	115	58.1	6.3	30	15.2	1.6	198
Atlanta, Georgia (20)	W	126	8.2	1.7	308	20.1	4.2	849	55.5	11.6	247	16.2	3.4	1530
	Sp	6	26.1	0.3	4	17.4	0.2	9	39.1	0.5	4	17.4	0.2	23
	Su	32	13.2	1.7	30	12.4	1.6	132	54.4	7.2	49	20.2	2.7	243
	A	31	4.4	1.7	55	7.8	3.0	539	76.0	29.3	83	11.8	4.5	708
Atlantic City New Jersey (20)	W	8	5.4	0.4	6	4.1	0.3	110	74.4	6.0	24	16.2	1.3	148
	Sp	77	6.9	1.1	95	8.5	1.3	790	70.3	10.8	160	14.2	2.2	1122
	Su	7	15.2	0.4	17	37.0	0.9	11	23.9	0.6	11	23.9	0.6	46
	A	50	17.1	2.7	45	15.4	2.4	141	48.2	7.7	56	19.2	3.0	292
Augusta, Georgia (20)	W	5	0.7	0.3	99	13.3	5.4	521	69.8	28.3	122	16.3	6.6	747
	Sp	6	4.4	0.3	24	17.4	1.3	82	59.4	4.5	26	18.8	1.4	138
	Su	68	5.6	0.9	185	15.1	2.5	755	61.8	10.3	215	17.6	2.9	1223
	A	5	31.2	0.3	2	12.5	0.1	2	12.5	0.1	7	43.8	0.4	16
Baker, Oregon (15)	W	20	14.7	1.1	17	12.5	0.9	43	31.6	2.3	56	41.2	3.0	136
	Sp	63	15.8	3.4	46	11.5	2.5	151	37.8	8.2	140	35.0	7.6	400
	Su	14	15.9	0.8	15	17.0	0.8	22	25.0	1.2	37	42.0	2.0	88
	A	102	15.9	1.4	80	12.5	1.1	218	34.0	3.0	240	37.5	3.3	640
Baltimore, Maryland (20)	W	4	7.7	0.2	10	19.1	0.6	20	38.5	1.1	18	34.6	1.0	52
	Sp	26	12.4	1.4	37	17.7	2.0	90	43.0	4.9	56	26.8	3.0	209
	Su	16	2.5	0.9	44	6.9	2.4	429	67.7	23.3	144	22.7	7.8	633
	A	11	8.5	0.6	6	4.6	0.3	80	61.5	4.4	33	25.4	1.8	130
Birmingham, Alabama (20)	W	57	5.7	0.8	97	9.5	1.3	619	60.5	8.5	251	24.5	3.4	1024
	Sp	0	0	0	0	0	0	0	0	0	0	0	0	0
	Su	1	2.7	0.1	3	8.1	0.2	29	78.4	2.1	4	10.8	0.3	37
	A	12	6.2	0.9	31	16.1	2.2	114	59.1	8.3	36	18.6	2.6	193
Binghamton, New York (20)	W	2	7.1	0.2	3	10.7	0.2	18	64.3	1.3	5	17.9	0.4	28
	Sp	15	5.8	0.3	37	14.4	0.7	161	82.5	2.9	45	17.4	0.8	258
	Su	6	31.6	0.3	2	10.5	0.1	4	21.0	0.2	7	36.3	0.4	19
	A	23	11.7	1.2	10	5.1	0.5	87	44.4	4.7	76	38.8	4.1	196
Bismarck, North Dakota (20)	W	47	8.6	2.6	31	5.7	1.7	291	53.4	15.3	176	32.3	9.6	545
	Sp	8	10.3	0.4	6	7.7	0.3	31	39.7	1.7	33	42.3	1.8	78
	Su	84	10.0	1.2	49	5.8	6.7	413	49.3	5.6	292	34.8	4.0	838
	A	0	0	0	0	0	0	5	62.5	0.3	3	57.5	0.2	8
Birmingham, Alabama (20)	W	14	8.3	0.8	14	8.3	0.8	80	47.6	4.4	60	35.7	3.3	168
	Sp	33	6.6	1.8	42	8.5	2.3	292	58.8	15.9	130	26.2	7.1	497
	Su	13	12.3	0.7	14	13.2	0.8	54	51.0	3.0	25	23.6	1.4	106
	A	60	7.7	0.8	70	9.0	1.0	431	55.3	6.0	218	28.0	3.0	779
Bismarck, North Dakota (20)	W	26	28.0	1.4	18	19.4	1.0	24	25.8	1.3	25	26.9	1.4	93
	Sp	66	17.8	3.6	85	23.0	4.6	140	37.8	7.6	79	21.3	4.3	370
	Su	44	5.1	2.4	151	17.4	8.2	556	64.1	30.2	116	13.4	6.3	867
	A	24	11.2	1.3	34	15.9	1.9	128	59.8	7.0	28	13.1	1.5	214
Bismarck, North Dakota (20)	W	160	10.4	2.2	288	18.7	3.9	848	55.0	11.5	248	16.1	3.4	1544
	Sp	0	0	0	0	0	0	0	0	0	0	0	0	0
	Su	19	17.6	1.0	13	12.0	0.7	42	38.9	2.3	34	31.5	1.8	108
	A	93	18.9	5.0	84	17.1	4.6	157	31.9	8.5	158	32.1	8.6	492
Bismarck, North Dakota (20)	W	16	19.3	0.9	19	22.9	1.0	31	37.4	1.7	17	20.5	0.9	83
	Sp	128	18.7	1.8	116	17.0	1.6	230	33.7	3.1	209	30.6	2.9	683

W = Winter (Dec., Jan., Feb.)

Sp = Spring (Mar., Apr., May)

Su = Summer (June, July, Aug.)

A = Autumn (Sept., Oct., Nov.)

N = Number of thunderstorm beginnings.

%F = Frequency, % of ΣN

%P = Probability, % of total periods.

Table 21 (Contd)

Station and Years of Record	Season	00-06			06-12			12-18			18-24			ΣN
		N	%F	%P	N	%F	%P	N	%F	%P	N	%F	%P	
Blook Island, Rhode Island (20)	W Sp Su A	1 26 40 16 83	8.4 25.7 19.0 26.2 21.6	0.1 1.4 2.2 0.9 1.1	5 19 40 7 71	41.7 18.8 19.0 11.5 18.5	0.3 1.0 2.2 0.4 1.0	1 25 69 21 116	8.4 24.7 32.9 34.4 30.2	0.1 1.4 3.8 1.2 1.6	5 31 61 17 114	41.7 30.7 29.1 27.9 29.7	0.3 1.7 3.3 0.9 1.6	12 101 210 61 384
Boise, Idaho (20)	W Sp Su A	0 9 27 12 48	0 7.7 11.2 17.9 11.0	0 0.5 1.5 0.7 0.7	1 10 18 8 37	10.0 8.6 7.4 11.9 8.5	0.1 0.5 1.0 0.4 0.5	6 66 109 25 206	60.0 56.4 45.0 37.3 47.2	0.3 3.6 5.9 1.4 2.8	3 32 88 22 145	30.0 27.4 36.3 32.8 33.2	0.2 1.7 4.8 1.2 2.0	10 117 242 67 436
Boston, Massachu- setts (20)	W Sp Su A	2 14 28 17 61	25.0 17.5 11.0 29.8 15.3	0.1 0.8 1.5 0.9 0.8	2 10 27 3 42	25.0 12.5 10.6 5.3 10.5	0.1 0.5 1.5 0.2 0.6	1 25 139 21 186	12.5 31.2 54.7 36.9 46.6	0.1 1.4 7.5 1.2 2.5	3 31 60 16 110	37.5 38.8 23.6 28.1 27.6	0.2 1.7 3.3 0.9 1.5	8 80 254 57 399
Broken Arrow, Oklahoma (7)	W Sp Su A	4 46 52 22 124	23.5 25.3 23.2 23.9 24.1	0.6 7.1 8.1 3.4 4.8	5 40 55 21 121	29.4 22.0 24.5 22.6 23.5	0.8 6.2 8.5 3.2 4.7	3 58 82 25 168	17.6 31.8 36.6 27.2 32.6	0.5 9.0 12.7 3.9 6.6	5 38 35 24 102	29.4 20.9 15.6 28.1 19.8	0.8 5.9 5.4 3.7 4.0	17 182 224 92 515
Buffalo, New York (20)	W Sp Su A	3 33 83 26 145	17.6 17.8 18.1 20.6 18.4	0.2 1.8 4.5 1.4 2.0	2 27 74 15 118	11.8 14.5 16.1 11.9 15.0	0.1 1.5 4.0 0.8 1.6	5 60 159 39 263	29.4 32.3 34.7 31.0 33.4	0.3 3.3 8.6 1.6 3.6	7 66 142 46 261	41.2 35.5 31.0 38.5 33.1	0.4 3.6 7.7 2.5 3.6	17 186 458 126 787
Burlington, Vermont (20)	W Sp Su A	1 10 51 12 74	25.0 8.7 10.4 11.9 10.4	0.1 0.5 2.8 0.7 1.0	0 17 82 23 122	0.0 14.8 16.7 22.8 17.1	0.0 0.9 4.5 1.3 1.7	3 63 251 49 366	75.0 54.7 51.0 48.5 51.4	0.2 3.4 13.6 2.7 5.0	0 25 108 17 150	0.0 21.7 22.0 16.8 21.1	0.0 1.4 5.9 0.9 2.1	4 115 492 101 712
Cairo, Illinois (20)	W Sp Su A	26 76 90 37 229	27.1 17.9 12.9 17.0 15.9	1.4 4.1 4.9 2.0 3.1	16 78 117 33 244	16.7 18.3 16.7 15.1 17.0	0.9 4.2 6.4 1.8 3.3	25 150 339 85 599	26.0 35.2 48.5 39.0 41.6	1.4 8.1 18.4 4.7 8.2	29 122 152 63 366	30.2 28.7 21.7 28.9 26.4	1.6 6.6 8.2 3.5 5.0	96 426 698 218 1438
Canton, New York (20)	W Sp Su A	4 21 55 15 95	66.7 21.2 17.2 16.3 18.3	0.2 1.1 3.0 0.8 1.3	1 13 58 24 96	16.7 13.1 18.1 26.1 18.5	0.1 0.7 3.2 1.3 1.3	1 42 149 34 226	16.7 42.4 46.5 37.0 43.6	0.1 2.3 8.1 1.9 3.1	0 23 59 19 101	0 23.2 18.4 20.7 19.5	0 1.2 3.2 1.0 1.4	6 99 321 92 518
Cape Henry, Virginia (20)	W Sp Su A	6 34 62 7 109	27.3 13.7 10.9 7.5 11.7	0.3 1.8 3.4 0.4 1.5	5 27 43 11 86	22.7 10.9 7.6 11.8 9.2	0.3 1.5 2.3 0.6 1.2	7 98 305 49 459	31.8 39.5 53.6 52.7 49.2	0.4 5.3 16.6 2.7 6.3	4 89 159 26 278	18.2 35.9 27.9 28.0 29.8	0.2 4.8 8.6 1.4 3.8	22 248 569 93 932
Charles City, Iowa (20)	W Sp Su A	2 44 118 36 200	40.0 18.6 22.5 23.4 21.7	0.1 2.4 6.4 2.0 2.7	2 36 87 29 154	40.0 15.2 16.6 18.8 16.7	0.1 2.0 4.7 1.6 2.1	1 79 166 41 287	20.0 33.3 31.6 26.6 31.2	0.1 4.3 9.0 2.2 3.9	0 78 154 48 280	0 32.9 29.3 31.2 30.4	0 4.2 8.4 2.6 3.8	5 237 525 154 921
Charleston, South Carolina (20)	W Sp Su A	9 34 72 26 141	20.4 14.3 9.2 15.1 11.4	0.5 1.8 3.9 1.4 1.9	5 40 140 37 222	11.4 16.9 17.8 21.5 17.9	0.3 2.2 7.6 2.0 3.1	13 102 420 80 615	29.5 43.0 53.5 46.5 49.7	0.7 5.5 22.8 4.4 8.4	17 61 153 29 260	38.6 25.7 19.5 16.8 21.0	0.9 3.3 8.3 1.6 3.6	44 237 785 172 1238
Charlotte, North Carolina (20)	W Sp Su A	5 27 25 7 64	19.2 11.6 4.0 6.4 6.4	0.3 1.6 1.5 0.4 1.0	9 36 28 8 81	34.6 15.4 4.5 7.3 8.1	0.6 2.2 1.7 0.5 1.2	7 99 366 52 524	26.9 42.5 58.2 47.3 52.4	0.4 6.0 22.2 3.2 6.0	5 71 210 43 329	19.2 30.5 33.4 39.1 32.9	0.3 4.3 12.7 2.6 5.0	26 233 629 110 998
Chattanooga, Tennessee (20)	W Sp Su A	24 66 60 14 164	40.7 20.0 7.4 7.7 11.8	1.3 3.6 3.3 0.8 2.2	6 49 159 36 250	10.2 14.8 19.5 17.9 18.1	0.3 2.7 8.6 2.0 3.4	14 137 452 105 708	23.7 41.5 55.5 58.0 51.1	0.8 7.4 24.5 5.8 9.7	15 78 143 26 262	23.4 23.6 17.6 14.4 13.9	0.8 4.2 7.8 1.4 3.6	59 330 814 181 1384
Cheyenne, Wyoming (20)	W Sp Su A	0 8 14 3 25	0 4.1 1.7 2.1 2.1	0 0.4 0.8 0.3 0.3	0 19 81 9 109	0 9.8 9.7 6.2 9.4	0 1.0 4.4 0.5 1.5	0 125 585 96 806	0 64.8 70.4 66.2 69.3	0 6.8 31.8 5.3 11.0	0 41 151 37 229	0 21.2 18.1 25.5 19.7	0 2.2 8.2 2.0 3.1	0 193 831 145 1169
Chicago, Illinois (20)	W Sp Su A	5 47 97 41 190	22.7 17.7 20.4 27.1 20.8	0.3 2.6 5.3 2.2 2.6	4 42 73 21 140	18.2 15.8 15.3 13.9 15.3	0.2 2.3 4.0 1.2 1.9	8 88 175 45 316	36.4 33.1 36.8 29.8 34.6	0.4 4.8 9.5 2.5 4.3	5 89 131 44 269	22.7 33.5 27.5 29.1 29.4	0.3 4.8 7.1 2.4 3.7	22 266 476 151 915

W = Winter (Dec., Jan., Feb.)
 Sp = Spring (Mar., Apr., May)
 Su = Summer (June, July, Aug.)
 A = Autumn (Sept., Oct., Nov.)

N = Number of thunderstorm beginnings.
 %F = Frequency, % of ΣN
 %P = Probability, % of total periods.

Table 21 (contd)

Station and Years of Record	Season	00-06			06-12			12-18			18-24			ΣN
		N	F	P	N	F	P	N	F	P	N	F	P	
Cincinnati, Ohio (20)	W	8	19.0	0.4	6	14.3	0.3	15	35.7	0.8	13	31.0	0.7	42
	Sp	61	14.7	3.3	71	17.1	3.9	170	41.0	9.2	113	27.2	6.1	415
	Su	92	11.0	5.0	119	14.3	6.5	424	50.9	23.0	200	24.0	10.9	835
	A	46	22.5	2.5	38	18.6	2.1	76	37.2	4.2	44	21.6	2.4	204
Cleveland, Ohio (20)	W	207	13.8	2.8	234	15.6	3.2	685	45.9	9.4	370	24.3	5.1	1496
	Sp	6	37.5	0.3	1	6.2	0.1	4	25.0	0.2	5	31.2	0.3	16
	Su	38	15.9	2.1	39	16.3	2.1	85	35.5	4.6	77	32.2	4.2	239
	A	75	14.8	4.1	76	15.0	4.1	200	39.6	10.9	154	30.5	8.4	505
Columbia, Missouri (20)	W	34	24.8	1.9	14	10.2	0.9	46	33.6	2.5	43	31.4	2.4	137
	Sp	153	17.1	2.1	130	14.5	1.8	335	37.4	4.6	279	31.1	3.3	897
	Su	12	31.6	0.7	6	15.3	0.3	5	13.2	0.3	15	39.5	0.8	38
	A	71	17.9	3.9	80	20.2	4.3	146	36.8	7.9	100	25.2	5.4	397
Columbia, South Carolina (20)	W	133	21.8	7.2	132	21.6	7.2	215	35.3	11.7	129	21.2	7.0	609
	Sp	53	22.7	2.9	49	21.0	2.7	77	33.0	4.2	54	23.2	3.0	233
	Su	269	21.0	3.7	267	20.8	3.7	443	34.6	6.1	298	23.2	4.1	1277
	A	6	14.3	0.3	9	21.4	0.5	13	30.9	0.7	14	33.3	0.8	42
Columbus, Ohio (20)	W	31	10.5	1.7	51	17.4	2.8	151	51.3	8.2	61	20.7	3.3	294
	Sp	39	4.6	2.1	75	8.7	4.1	530	61.8	28.8	213	24.9	11.6	857
	Su	14	8.2	0.8	12	7.1	0.7	102	60.0	5.6	42	24.7	2.3	170
	A	90	6.6	1.2	147	10.8	2.0	796	58.4	10.9	330	24.2	4.5	1363
Concord, New Hamp- shire (20)	W	7	21.2	0.4	6	18.2	0.3	11	33.3	0.6	9	27.3	0.5	33
	Sp	50	16.5	2.7	58	19.1	3.2	98	32.3	5.3	97	32.0	5.3	303
	Su	90	13.9	4.9	96	14.8	5.2	301	46.4	16.3	162	24.9	8.8	649
	A	32	21.9	1.8	26	17.3	1.4	53	36.3	2.9	35	24.0	1.9	146
Concordia, Kansas (20)	W	179	15.8	2.5	186	16.4	2.5	463	40.9	6.3	303	26.8	4.2	1131
	Sp	0	0	0	0	0	0	1	25.0	0.1	3	75.0	0.2	4
	Su	8	11.3	0.4	11	15.5	0.6	35	49.3	1.9	17	24.0	0.9	71
	A	32	10.5	1.7	28	8.9	1.5	175	55.4	9.5	79	25.2	4.3	314
Corpus Christi, Texas (20)	W	5	9.3	0.3	5	9.3	0.3	27	50.0	1.5	17	31.5	0.9	54
	Sp	45	10.2	0.6	44	9.9	0.6	238	53.8	3.3	116	26.2	1.6	443
	Su	1	11.1	0.1	1	11.1	0.1	1	11.1	0.1	6	66.7	0.3	9
	A	39	20.6	2.1	21	11.1	1.1	51	27.0	2.8	78	41.3	4.2	189
Dallas, Texas (12)	W	115	24.0	6.2	50	10.4	2.7	123	25.7	6.7	191	39.9	10.4	479
	Sp	34	26.6	1.9	18	14.1	1.0	30	23.4	1.6	46	35.9	2.5	128
	Su	189	23.4	2.6	90	11.2	1.2	205	25.5	2.8	321	33.8	4.4	805
	A	17	34.0	0.9	12	24.0	0.7	11	22.0	0.6	10	20.0	0.6	50
Davenport, Iowa (20)	W	68	31.9	3.7	46	21.6	2.5	46	21.6	2.5	53	24.9	2.9	213
	Sp	59	22.2	3.2	97	36.5	5.3	95	35.7	5.2	15	5.6	0.8	266
	Su	55	28.9	3.0	53	27.9	2.9	63	33.1	3.5	19	10.0	1.0	190
	A	199	27.7	2.7	208	28.9	2.8	215	29.9	2.9	97	13.5	1.3	719
Dayton, Ohio (15)	W	18	24.7	1.7	16	21.9	1.5	18	24.7	1.7	21	28.8	1.9	73
	Sp	60	24.3	5.4	51	20.7	4.6	72	29.2	6.5	64	25.9	5.8	247
	Su	49	17.8	4.4	38	13.8	3.4	133	48.4	12.0	55	20.0	5.0	275
	A	22	19.8	2.0	8	7.2	0.7	52	46.9	4.8	29	26.1	2.7	111
Del Rio, Texas (20)	W	149	21.2	3.4	113	16.0	2.6	275	39.0	6.3	169	24.0	3.9	706
	Sp	4	22.2	0.2	4	22.2	0.2	4	22.2	0.2	6	33.3	0.3	18
	Su	64	23.6	3.5	35	12.9	1.9	91	33.5	4.9	82	30.2	4.4	272
	A	121	24.0	6.6	79	15.6	4.3	173	34.3	9.4	131	25.9	7.1	504
Denver, Colorado (20)	W	43	23.8	2.4	29	17.4	1.6	46	27.6	2.5	49	29.4	2.7	167
	Sp	232	24.1	3.2	147	15.3	2.0	314	32.7	4.3	268	27.9	3.7	961
	Su	3	13.0	0.2	5	21.7	0.4	10	43.5	0.7	5	21.7	0.4	23
	A	36	15.9	2.6	37	16.3	2.7	85	37.5	6.2	69	30.4	5.0	227
Denver, Colorado (20)	W	61	14.8	4.4	62	15.0	4.5	202	48.9	14.6	89	21.5	6.4	414
	Sp	19	17.3	1.4	22	20.0	1.6	44	40.0	3.2	25	22.7	1.8	110
	Su	119	15.4	2.2	126	16.3	2.3	341	44.0	6.2	188	24.3	3.4	774
	A	6	31.6	0.3	3	15.8	0.2	6	31.6	0.3	4	21.1	0.2	19
Denver, Colorado (20)	W	41	27.5	2.2	9	6.0	0.5	39	26.2	2.1	60	40.3	3.3	149
	Sp	30	21.0	1.6	14	9.8	0.8	61	42.6	3.3	38	26.6	2.1	143
	Su	19	26.4	1.0	8	11.1	0.4	19	26.4	1.0	26	36.1	1.4	72
	A	96	25.1	1.3	34	8.9	4.7	125	32.6	1.7	128	33.4	1.8	383
Denver, Colorado (20)	W	0	0	0	0	0	0	1	100.0	0.1	0	0	0	1
	Sp	12	7.7	0.6	18	11.6	1.0	103	66.4	5.6	22	14.2	1.2	155
	Su	20	2.7	1.1	41	5.5	2.2	498	67.2	27.0	183	24.7	9.9	742
	A	2	1.6	0.1	7	5.5	0.4	87	67.9	4.8	32	25.0	1.8	128
Denver, Colorado (20)	W	34	3.3	0.5	66	6.4	0.9	689	67.0	9.4	237	23.1	3.2	1026

W = Winter (Dec., Jan., Feb.)
 Sp = Spring (Mar., Apr., May)
 Su = Summer (June, July, Aug.)
 A = Autumn (Sept., Oct., Nov.)

N = Number of thunderstorm beginnings.
 F = Frequency, % of ΣN
 P = Probability, % of total periods.

Table 21 (contd)

Station and Years of Record	Season	00-06			06-12			12-18			18-24			ΣN
		N	FP	PP	N	FP	PP	N	FP	PP	N	FP	PP	
Des Moines, Iowa (20)	W	7	58.3	0.4	1	8.3	0.1	1	8.3	0.1	3	25.0	0.2	12
	Sp	66	21.6	3.6	142	13.0	2.3	89	29.2	4.6	108	35.4	5.9	505
	Su	143	25.2	7.8	89	15.7	4.8	162	28.5	8.8	174	30.6	9.4	568
	A	49	22.3	2.7	45	20.5	2.5	56	25.5	3.1	70	31.8	3.8	220
		265	24.0	3.6	177	16.0	2.4	308	27.9	4.2	355	32.1	4.9	1105
Detroit, Michigan (20)	W	4	22.2	0.2	1	5.6	0.1	7	38.9	0.4	6	33.3	0.3	18
	Sp	27	12.7	1.5	37	17.5	2.0	76	35.9	4.1	72	34.0	3.9	212
	Su	74	15.3	4.0	67	13.9	3.6	216	44.7	11.7	126	26.1	6.8	483
	A	27	22.1	1.5	21	17.2	1.2	41	33.6	2.2	33	27.1	1.8	122
		132	15.8	1.8	126	15.1	1.7	340	40.8	4.7	237	28.4	3.2	835
Devils Lake, North Dakota (20)	W	0	0	0	0	0	0	0	0	0	0	0	0	0
	Sp	15	15.3	0.8	13	13.5	0.7	34	34.7	1.8	36	36.7	2.0	98
	Su	91	18.2	4.9	90	18.0	4.9	155	31.0	8.4	165	33.0	9.0	501
	A	18	22.2	1.0	12	14.8	0.7	26	32.1	1.4	25	30.9	1.4	81
		124	18.2	1.7	115	16.9	1.6	215	31.6	2.9	226	33.2	3.1	680
Dodge City, Kansas (11)	W	1	25.0	0.1	1	25.0	0.1	0	0	0	2	60.0	0.2	4
	Sp	26	24.5	2.6	15	14.1	1.5	28	26.4	2.8	37	34.9	3.7	106
	Su	69	24.8	6.8	23	8.3	2.3	95	34.2	9.4	91	32.8	9.0	278
	A	17	19.8	1.7	11	12.8	1.1	23	26.7	2.3	35	40.7	3.5	86
		113	23.8	2.8	50	10.6	1.2	146	30.8	3.6	165	34.8	4.1	474
Dubuque, Iowa (20)	W	1	7.7	0.1	4	30.8	0.2	3	23.1	0.2	5	38.4	0.3	13
	Sp	58	25.9	3.2	39	17.4	2.1	63	28.1	3.4	64	28.5	3.5	224
	Su	122	24.4	6.6	97	19.4	5.3	169	33.8	9.2	113	22.6	6.1	501
	A	36	22.6	2.0	37	23.3	2.0	39	24.5	2.1	47	29.6	2.6	159
		217	24.2	3.0	177	19.7	2.4	274	30.6	3.8	229	25.5	3.1	897
Duluth, Minnesota (20)	W	0	0	0	0	0	0	1	50.0	0.1	1	50.0	0.1	2
	Sp	24	19.3	1.3	12	9.7	0.6	42	33.9	2.3	46	37.1	2.5	124
	Su	86	18.0	4.7	79	16.5	4.3	170	35.5	9.2	144	30.1	7.8	479
	A	29	26.6	1.6	19	17.4	1.0	31	28.4	1.7	30	27.5	1.6	109
		139	19.5	1.9	110	15.4	1.5	244	34.2	3.3	221	30.9	3.0	714
Eastport, Maine (20)	W	2	33.3	0.1	2	33.3	0.1	2	33.3	0.1	0	0	0	6
	Sp	9	18.4	0.5	7	14.3	0.4	22	44.9	1.2	11	22.4	0.6	49
	Su	38	15.4	2.1	37	15.0	2.8	109	44.3	5.9	62	25.3	3.4	246
	A	12	24.0	0.7	10	20.0	0.6	13	26.0	0.7	15	30.0	0.8	50
		61	17.3	0.8	56	16.0	0.8	146	41.6	2.0	88	25.1	1.2	351
Elkins, West Virginia (20)	W	7	35.0	0.4	0	0	0	7	35.0	0.4	6	30.0	0.3	20
	Sp	28	11.7	1.5	33	13.8	1.8	113	47.1	6.2	66	27.5	3.6	240
	Su	67	11.0	3.6	85	14.0	4.6	309	50.8	16.8	147	24.2	8.0	608
	A	14	11.4	0.8	18	14.6	1.0	59	48.0	3.2	32	26.0	1.8	123
		116	11.7	1.6	136	13.7	1.9	488	49.3	6.7	251	25.4	3.4	991
Ellendale, North Dakota (9)	W	0	0	0	0	0	0	0	0	0	0	0	0	0
	Sp	4	7.0	0.5	8	14.0	1.0	29	50.9	3.5	16	28.1	1.9	57
	Su	35	13.5	4.2	65	25.1	7.8	92	35.5	11.1	67	25.9	8.1	259
	A	13	21.7	1.6	16	26.7	1.9	19	31.7	2.3	12	20.0	1.5	60
		52	13.8	1.6	89	23.7	2.7	140	37.2	4.3	95	25.3	2.9	376
El Paso, Texas (20)	W	3	20.0	0.2	1	6.7	0.1	8	53.3	0.4	3	20.0	0.2	15
	Sp	3	4.6	0.2	8	12.3	0.4	32	49.2	1.7	22	33.8	1.2	65
	Su	34	6.7	1.8	12	2.4	0.6	266	52.1	14.4	197	38.6	10.7	509
	A	9	7.3	0.5	9	7.3	0.5	60	48.8	3.3	45	36.6	2.5	123
		49	6.9	0.7	30	4.2	0.4	366	51.4	5.0	267	37.5	3.7	712
Erie, Pennsylvania (20)	W	4	20.0	0.2	1	5.0	0.1	3	15.0	0.2	12	60.0	0.7	20
	Sp	29	12.7	1.6	34	14.9	1.8	86	37.8	4.7	79	34.7	4.3	228
	Su	75	16.4	4.1	72	15.7	3.9	175	38.2	9.5	136	29.6	7.4	458
	A	30	22.2	1.6	22	16.3	1.2	43	31.9	2.4	40	29.6	2.2	135
		138	16.4	1.9	129	15.4	1.8	307	36.5	4.2	267	31.8	3.7	841
Escanaba, Michigan (20)	W	0	0	0	1	25.0	0.1	0	0	0	3	75.0	0.2	4
	Sp	27	20.5	1.5	26	19.7	1.4	43	32.6	2.3	36	27.3	2.0	132
	Su	74	15.8	4.0	64	13.7	3.5	211	45.2	11.5	118	25.2	6.4	467
	A	21	16.0	1.2	31	23.6	1.7	44	33.6	2.4	35	26.7	1.9	131
		122	16.6	1.7	122	16.6	1.7	298	40.6	4.1	192	26.2	2.6	734
Eureka, California (20)	W	9	22.5	0.5	6	15.0	0.3	18	45.0	1.0	7	17.5	0.4	40
	Sp	2	22.2	0.1	0	0	0	4	44.4	0.2	3	33.3	0.2	9
	Su	2	33.3	0.1	0	0	0	2	33.3	0.1	2	33.3	0.1	6
	A	6	24.0	0.3	2	8.0	0.1	9	36.0	0.5	8	32.0	0.4	25
		19	23.8	0.3	8	10.0	0.1	33	41.2	0.5	20	25.0	0.3	80

W = Winter (Dec., Jan., Feb.)
 Sp = Spring (Mar., Apr., May)
 Su = Summer (June, July, Aug.)
 A = Autumn (Sept., Oct., Nov.)

N = Number of thunderstorm beginnings.
 FP = Frequency, % of ΣN
 PP = Probability, % of total periods.

Table 21 (contd)

Station and Years of Record	Season	00-06			06-12			12-18			18-24			ΣN
		N	FP	PP	N	FP	PP	N	FP	PP	N	FP	PP	
Evansville, Indiana (20)	W	20	29.4	1.1	9	13.2	0.5	23	33.8	1.3	16	23.5	0.9	68
	Sp	75	23.0	4.1	55	16.8	3.0	103	31.5	5.6	94	28.8	5.1	327
	Su	76	12.5	4.1	98	16.2	5.3	290	47.8	15.8	142	23.4	7.7	606
	A	39	21.7	2.1	27	15.0	1.5	71	39.5	3.9	43	23.9	2.4	180
Ft. Smith, Arkansas (20)	W	21	17.8	2.9	189	16.0	2.6	487	41.2	6.7	295	25.0	4.0	1181
	Sp	21	25.9	1.2	10	12.3	0.6	24	29.6	1.3	26	32.1	1.4	81
	Su	77	19.2	4.2	66	16.4	3.6	121	30.1	6.6	137	34.1	7.4	401
	A	83	16.8	4.5	75	15.2	4.1	241	48.7	13.1	96	19.4	5.2	495
Ft. Wayne, Indiana (20)	W	48	25.8	2.6	35	18.8	1.9	61	32.8	3.3	42	22.6	2.3	186
	Sp	229	19.7	3.1	186	16.0	2.5	447	38.4	6.1	301	25.9	4.1	1163
	Su	3	21.4	0.2	2	14.3	0.1	5	35.7	0.3	4	28.6	0.2	14
	A	38	19.5	2.1	33	16.9	1.8	76	39.0	4.1	48	24.6	2.6	195
Ft. Worth, Texas (20)	W	60	17.5	3.3	47	13.7	2.6	161	47.0	8.7	75	21.8	4.1	343
	Sp	20	19.2	1.1	24	23.1	1.3	30	28.9	1.6	30	28.9	1.6	104
	Su	121	18.4	1.7	106	16.2	1.5	272	41.5	3.7	157	23.9	2.1	656
	A	20	27.0	1.1	14	18.9	0.8	21	28.4	1.2	19	25.7	1.0	74
Fresno, California (20)	W	84	22.6	4.6	70	18.8	3.8	101	27.2	5.5	117	31.5	6.4	372
	Sp	71	15.9	3.9	60	13.4	3.3	223	50.0	12.1	93	20.8	5.0	447
	Su	36	18.5	2.0	24	12.3	1.3	88	45.1	4.8	47	24.1	2.6	195
	A	211	19.4	2.9	168	15.5	2.3	433	39.8	5.9	276	25.4	3.8	1088
Galveston, Texas (20)	W	1	66.7	0.1	1	66.7	0.1	10	66.7	0.6	3	20.0	0.2	15
	Sp	3	7.3	0.2	2	4.9	0.1	20	48.8	1.1	16	39.0	0.9	41
	Su	6	28.6	0.3	4	19.0	0.2	5	23.8	0.3	6	28.6	0.3	21
	A	0	0	0	2	10.0	0.1	12	60.0	0.7	6	30.0	0.3	20
Grand Haven, Michigan (20)	W	10	10.3	0.1	9	9.3	0.1	47	48.5	0.6	31	32.0	0.4	97
	Sp	29	25.7	1.6	30	26.6	1.7	32	28.3	1.8	22	19.5	1.2	113
	Su	68	28.1	3.7	56	23.1	3.0	72	29.7	3.9	46	19.0	2.5	242
	A	94	22.1	5.1	110	32.9	7.6	138	32.4	7.5	53	12.5	2.9	425
Grand Junction, Colorado (20)	W	64	27.1	3.5	79	33.5	4.3	55	23.3	3.0	38	16.1	2.1	236
	Sp	255	25.1	3.5	305	30.0	4.2	297	29.2	4.1	159	15.6	2.2	1016
	Su	2	11.8	0.1	6	35.3	0.3	2	11.8	0.1	7	41.2	0.4	17
	A	47	19.9	2.6	33	14.0	1.8	76	32.2	4.1	80	33.9	4.3	230
Green Bay, Wisconsin (20)	W	118	27.2	6.4	79	18.2	4.3	98	22.7	5.3	139	32.0	7.6	434
	Sp	34	20.4	1.9	37	22.2	2.0	51	30.5	2.8	45	27.0	2.5	167
	Su	201	23.5	2.8	155	18.1	2.1	227	26.6	3.1	271	31.7	3.7	854
	A	0	0	0	0	0	0	4	80.0	0.2	1	20.0	0.1	5
Grand Rapids, Michigan (20)	W	6	3.6	0.3	33	19.5	1.8	99	58.6	5.4	31	18.4	1.7	169
	Sp	28	3.8	1.5	161	21.6	8.7	423	56.7	23.0	133	17.8	7.2	745
	Su	16	7.8	0.9	50	24.2	2.7	96	46.6	5.3	44	21.3	2.4	206
	A	50	4.4	0.7	244	21.7	3.3	622	55.4	8.5	209	18.6	2.9	1125
Greenville, South Carolina (8)	W	4	23.5	0.2	3	17.6	0.2	4	23.5	0.2	6	35.3	0.3	17
	Sp	49	20.2	2.7	38	15.7	2.1	78	32.2	4.2	77	31.8	4.2	242
	Su	101	23.5	5.5	64	14.9	3.5	135	31.5	7.3	129	30.1	7.0	429
	A	39	24.8	2.1	24	15.3	1.3	39	24.8	2.1	55	35.0	3.0	157
Groesbeck, Texas (7)	W	193	22.8	2.6	129	15.3	1.8	256	30.3	3.5	267	31.6	3.7	845
	Sp	1	16.7	0.1	2	33.3	0.1	2	33.3	0.1	1	16.7	0.1	6
	Su	35	21.6	1.9	23	14.2	1.2	50	30.8	2.7	54	33.3	2.9	162
	A	87	19.1	4.7	75	16.4	4.1	180	39.4	9.8	114	25.0	6.2	456
Hannibal, Missouri (20)	W	34	26.6	1.9	29	22.6	1.6	35	27.3	1.9	30	23.4	1.6	128
	Sp	157	20.9	2.1	129	17.2	1.8	267	35.5	3.7	199	26.5	2.7	752
	Su	4	21.0	0.6	4	21.0	0.6	5	26.3	0.7	6	31.6	0.8	19
	A	25	17.5	3.4	11	7.7	1.5	72	50.3	9.8	35	24.5	4.8	143
Hannibal, Missouri (20)	W	10	3.4	1.4	13	4.4	1.8	199	67.4	27.0	73	24.7	9.8	295
	Sp	4	5.3	0.5	7	9.2	1.0	42	55.3	5.7	23	30.3	3.1	76
	Su	43	8.1	1.5	35	6.6	1.2	318	59.6	10.9	137	25.7	4.7	533
	A	14	34.1	2.2	9	22.0	1.4	10	24.4	1.6	8	19.5	1.3	41
Hannibal, Missouri (20)	W	24	19.2	3.7	29	23.2	4.5	49	39.2	7.6	23	18.4	3.6	125
	Sp	10	6.5	1.6	37	24.2	5.7	96	62.8	14.9	10	6.5	1.6	153
	Su	15	17.2	2.3	23	26.4	3.6	39	44.8	6.0	10	11.5	1.6	87
	A	63	15.5	2.5	98	24.1	3.8	194	47.7	7.6	51	12.5	2.0	406
Hannibal, Missouri (20)	W	8	22.2	0.4	8	22.2	0.4	5	13.9	0.3	15	41.7	0.8	36
	Sp	80	20.6	4.3	71	18.2	3.9	117	30.1	6.4	121	31.1	6.6	389
	Su	118	21.5	6.4	100	18.2	5.4	205	37.3	11.1	125	22.8	2.6	548
	A	51	23.9	2.8	38	17.8	2.1	76	35.6	4.2	48	22.5	2.6	213
Hannibal, Missouri (20)	W	257	21.7	3.5	217	18.3	3.0	403	34.0	5.5	309	26.0	4.2	1186

W = Winter (Dec., Jan., Feb.)
 Sp = Spring (Mar., Apr., May)
 Su = Summer (June, July, Aug.)
 A = Autumn (Sept., Oct., Nov.)

N = Number of thunderstorm beginnings.
 FP = Frequency, % of ΣN
 PP = Probability, % of total periods.

Table 21 (contd)

Station and Years of Record	Season	00-06			06-12			12-18			18-24			ΣN
		N	ΣP	ΣP	N	ΣP	ΣP	N	ΣP	ΣP	N	ΣP	ΣP	
Harrisburg, Pennsylvania (20)	W	2	16.7	0.1	1	8.3	0.1	3	25.0	0.2	6	50.0	0.3	12
	Sp	18	10.3	1.0	14	8.0	0.8	91	52.3	4.9	51	29.3	2.8	174
	Su	51	9.6	2.8	36	6.8	2.0	293	55.0	15.9	153	28.7	8.3	533
	A	8	9.0	0.4	5	5.6	0.3	41	46.1	2.2	35	39.3	1.9	89
Hartford, Connecticut (20)	W	79	9.8	1.1	56	6.9	0.8	428	53.0	5.8	245	30.3	3.4	808
	Sp	1	7.7	0.1	3	23.1	0.2	2	15.4	0.1	7	53.8	0.4	13
	Su	27	20.3	1.5	16	12.0	0.9	43	32.3	2.3	47	35.3	2.6	133
	A	61	13.9	3.3	43	9.8	2.3	220	50.1	12.0	115	26.2	6.2	439
Hatteras, North Carolina (20)	W	15	15.0	0.8	17	17.0	0.9	33	33.0	1.8	35	35.0	1.9	100
	Sp	104	15.2	1.4	79	11.5	1.1	298	45.5	4.1	204	29.8	2.8	685
	Su	16	28.6	0.9	8	14.3	0.4	19	33.9	1.0	13	23.2	0.7	56
	A	62	33.5	3.4	38	20.6	2.1	47	25.4	2.6	38	20.6	2.1	185
Havre, Montana (20)	W	99	28.4	5.4	58	16.6	3.2	125	35.9	6.8	67	19.2	3.6	349
	Sp	46	43.8	2.5	9	8.6	0.5	29	27.6	1.6	21	20.0	1.1	105
	Su	223	32.1	3.1	113	16.3	1.5	220	31.7	3.0	139	20.0	1.9	695
	A	0	0	0	0	0	0	0	0	0	0	0	0	0
Helena, Montana (20)	W	1	1.7	0.1	5	8.3	0.3	30	50.0	1.6	24	40.0	1.3	60
	Sp	43	10.5	2.3	52	12.7	2.8	157	38.3	8.5	157	38.3	8.5	409
	Su	3	9.1	0.2	4	12.1	0.2	15	45.4	0.8	11	33.3	0.6	33
	A	47	9.4	0.6	61	12.1	0.8	202	40.2	2.8	192	38.2	2.6	502
Houghton, Michigan (20)	W	0	0	0	1	33.3	0.1	1	33.3	0.1	1	33.3	0.1	3
	Sp	2	1.5	0.1	16	11.8	0.9	94	69.1	5.1	24	17.6	1.3	136
	Su	50	6.8	2.7	83	11.2	4.5	439	59.3	23.8	167	22.5	9.1	739
	A	6	7.6	0.3	7	8.9	0.4	46	58.2	2.5	20	25.3	1.1	79
Houston, Texas (20)	W	58	6.1	0.8	107	11.2	1.5	580	60.6	7.9	212	22.1	2.9	957
	Sp	1	50.0	0.1	0	0	0	0	0	0	1	50.0	0.1	2
	Su	31	28.2	1.7	20	18.2	1.1	28	25.5	1.5	31	28.2	1.7	110
	A	87	28.0	4.7	44	14.1	2.4	83	26.7	4.5	97	31.2	5.3	311
Ithaca, New York (20)	W	33	30.6	1.8	16	14.8	0.9	37	34.3	2.0	22	20.4	1.2	108
	Sp	152	28.6	2.1	80	15.1	1.1	148	27.9	2.0	151	28.4	2.1	531
	Su	26	28.3	1.4	25	27.2	1.4	22	23.9	1.2	19	20.7	1.0	92
	A	37	15.8	2.0	67	28.5	3.6	76	32.4	4.1	55	23.4	3.0	235
Jacksonville, Florida (20)	W	25	5.5	1.4	92	20.3	5.0	285	63.0	15.5	50	11.0	2.7	452
	Sp	21	11.5	1.2	56	30.6	3.1	85	46.4	4.7	21	11.5	1.2	183
	Su	109	11.3	1.5	240	25.0	3.3	468	48.7	6.4	145	15.1	2.0	962
	A	0	0	0	0	0	0	0	0	0	2	100.0	0.1	2
Kalispell, Montana (20)	W	26	16.9	1.4	14	9.1	0.8	54	35.0	2.9	60	38.9	3.3	154
	Sp	129	23.9	7.0	89	16.5	4.8	152	28.1	8.2	171	31.6	9.3	544
	Su	26	23.6	1.4	17	15.4	0.9	22	20.0	1.2	45	40.9	2.5	110
	A	181	22.4	2.5	120	14.9	1.6	228	28.3	3.1	278	34.5	3.8	807
KalisPELL, Montana (20)	W	8	26.7	0.4	7	23.3	0.4	7	23.3	0.4	8	26.7	0.4	30
	Sp	75	21.9	4.1	53	15.5	2.9	128	37.4	7.0	86	25.1	4.7	342
	Su	74	12.3	4.0	93	15.4	5.0	319	53.0	17.3	115	19.1	6.2	601
	A	38	20.6	2.1	29	15.7	1.6	73	39.5	4.0	45	24.3	2.5	185
Lima, Peru (20)	W	195	16.8	2.7	182	15.7	2.5	527	45.5	7.2	254	21.9	3.5	1158
	Sp	10	27.8	0.6	8	22.2	0.4	7	19.4	0.4	11	30.6	0.6	36
	Su	101	27.3	5.5	60	16.2	3.3	117	31.6	6.4	93	25.1	5.0	371
	A	157	28.4	8.5	92	16.7	5.0	177	32.0	9.6	126	22.8	6.8	552
Lima, Peru (20)	W	62	28.6	3.4	32	14.8	1.8	68	31.3	3.7	55	25.4	3.0	217
	Sp	330	28.0	4.5	192	16.3	2.6	369	31.4	5.1	285	24.2	3.9	1176
	Su	0	0	0	2	50.0	0.1	0	0	0	2	50.0	0.1	4
	A	10	6.5	0.5	15	9.7	0.8	80	51.9	4.3	49	31.8	2.7	154
Lima, Peru (20)	W	39	8.3	2.1	70	14.8	3.8	271	57.4	14.7	92	19.5	5.0	472
	Sp	10	9.6	0.6	12	11.5	0.7	54	51.9	3.0	28	26.9	1.5	104
	Su	59	8.0	0.8	99	13.5	1.3	405	55.2	5.5	171	23.3	2.3	734
	A	15	17.2	0.8	17	19.6	0.9	32	36.8	1.8	23	26.4	1.2	87
Lima, Peru (20)	W	19	5.3	1.0	70	19.6	3.8	210	58.8	11.4	58	16.2	3.1	357
	Sp	32	2.4	1.7	268	20.4	14.6	850	64.6	46.2	164	12.5	8.9	1314
	Su	22	8.3	1.2	49	18.5	2.7	154	58.1	8.5	40	15.1	2.2	265
	A	88	4.3	1.2	404	20.0	5.5	1246	61.6	17.1	285	14.1	3.9	2023
Lima, Peru (20)	W	0	0	0	0	0	0	0	0	0	0	0	0	0
	Sp	3	5.6	0.2	3	5.6	0.2	35	64.8	1.9	13	24.1	0.7	54
	Su	33	10.3	1.8	41	12.8	2.2	163	50.9	8.8	83	25.9	4.5	320
	A	8	20.5	0.4	5	12.8	0.3	17	43.6	0.9	9	23.1	0.5	39
Lima, Peru (20)	W	44	10.6	0.6	49	11.9	0.7	215	52.0	2.9	105	25.4	1.4	413

W = Winter (Dec., Jan., Feb.)
 Sp = Spring (Mar., Apr., May)
 Su = Summer (June, July, Aug.)
 A = Autumn (Sept., Oct., Nov.)

N = Number of thunderstorm beginnings.
 ΣP = Frequency, % of ΣN
 ΣP = Probability, % of total periods.

Table 21 (contd.)

Station and Years of Record	Season	00-06			06-12			12-18			18-24			ΣN
		N	%F	%P	N	%F	%P	N	%F	%P	N	%F	%P	
Kansas City, Missouri (20)	W	9	24.3	0.5	3	8.1	0.2	6	16.2	0.3	19	51.4	1.0	37
	Sp	114	29.4	6.2	52	13.4	2.8	101	26.1	5.5	121	31.2	6.6	388
	Su	185	28.7	10.0	78	12.1	4.2	185	28.7	10.0	198	30.7	10.8	646
	A	69	28.8	3.8	43	18.0	2.4	60	25.1	3.3	67	28.0	3.7	239
Keokuk, Iowa (20)	W	377	28.8	4.5	176	13.4	2.4	352	26.9	4.8	405	30.9	5.5	1310
	Sp	8	29.6	0.4	3	11.1	0.2	9	33.3	0.5	7	25.9	0.4	27
	Su	77	25.3	4.2	61	20.0	3.3	95	31.2	5.2	72	23.6	3.9	305
	A	127	24.6	6.9	85	16.5	4.6	182	35.3	9.9	122	23.7	6.6	516
Key West, Florida (20)	W	50	27.8	2.7	26	14.5	1.4	62	34.5	3.4	42	23.4	2.3	180
	Sp	262	25.4	3.6	175	17.0	2.4	348	33.8	4.8	243	23.6	3.3	1028
	Su	6	9.7	0.3	15	24.2	0.8	18	29.2	1.0	23	37.1	1.3	62
	A	20	10.3	1.1	43	22.1	2.3	65	33.5	3.5	66	34.0	3.6	194
Knoxville, Tennessee (20)	W	114	14.1	6.2	242	29.8	13.1	287	35.5	15.6	167	20.6	9.1	810
	Sp	57	14.8	3.1	95	24.7	5.2	158	41.2	8.7	74	19.3	4.1	384
	Su	197	13.6	2.7	395	27.3	5.4	528	36.4	7.2	330	22.8	4.5	1450
	A	11	26.8	0.6	6	14.6	0.3	12	29.3	0.7	12	29.3	0.7	41
La Crosse, Wisconsin (20)	W	59	18.8	3.2	42	13.4	2.3	132	42.2	7.2	80	25.6	4.3	313
	Sp	41	6.2	2.2	95	14.5	5.2	404	61.5	21.9	117	17.8	6.4	657
	Su	11	8.8	0.6	15	12.0	0.8	73	58.4	4.0	26	20.8	1.4	125
	A	122	10.7	1.7	158	13.9	2.2	621	54.7	8.5	235	20.7	3.2	1136
Lander, Wyoming (20)	W	2	33.3	0.1	2	3.3	0.1	0	0	0	2	33.3	0.1	6
	Sp	49	23.3	2.7	40	19.0	2.2	60	28.6	3.3	61	29.1	3.3	210
	Su	141	29.8	7.7	85	18.0	4.6	128	27.1	7.0	119	25.2	6.5	473
	A	37	25.5	2.0	20	13.8	1.1	41	28.3	2.2	47	32.4	2.6	145
Lansing, Michigan (16)	W	229	27.4	3.1	147	17.6	2.0	229	27.4	3.1	229	27.4	3.1	834
	Sp	0	0	0	0	0	0	0	0	0	0	0	0	0
	Su	3	4.7	0.2	6	9.4	0.3	44	68.8	2.4	11	17.2	0.6	64
	A	15	5.0	0.8	43	14.4	2.3	170	57.0	9.2	70	23.5	3.8	298
Lewiston, Idaho (20)	W	2	4.4	0.1	8	17.4	0.4	27	58.7	1.5	9	19.6	0.5	46
	Sp	20	4.9	0.3	57	14.0	0.8	241	59.0	3.3	90	22.0	1.2	408
	Su	1	12.5	0.1	0	0	0	3	37.5	0.2	4	50.0	0.3	8
	A	29	15.8	2.0	38	20.7	2.6	75	40.8	5.1	42	22.8	2.9	184
Lexington, Kentucky (20)	W	65	16.3	4.4	82	20.5	5.6	169	42.4	11.5	83	20.8	5.6	399
	Sp	32	27.8	2.2	18	15.7	1.2	39	33.9	2.7	26	22.6	1.8	115
	Su	127	18.0	2.2	138	19.5	2.4	286	40.5	4.9	155	21.9	2.7	706
	A	1	33.3	0.1	0	0	0	1	33.3	0.1	1	33.3	0.1	3
Lincoln, Nebraska (20)	W	4	6.1	0.2	4	6.1	0.2	48	72.7	2.6	10	15.2	0.5	66
	Sp	30	12.9	1.6	28	12.0	1.5	108	46.3	5.9	67	28.7	3.6	233
	Su	6	12.2	0.3	3	6.1	0.2	27	55.1	1.5	13	26.5	0.7	49
	A	41	11.7	0.6	35	10.0	0.5	184	52.4	2.5	91	25.9	1.2	351
Little Rock, Arkansas (20)	W	14	25.0	0.8	13	23.2	0.7	13	23.2	0.7	16	28.6	0.9	56
	Sp	53	17.6	2.9	49	16.3	2.7	117	39.0	6.4	81	27.0	4.4	300
	Su	80	12.2	4.3	118	17.9	6.4	332	50.5	18.0	129	19.6	7.0	659
	A	29	18.5	1.6	20	12.7	1.1	72	45.9	4.0	36	22.9	2.0	157
Los Angeles, California (20)	W	176	15.0	2.4	200	17.1	2.7	534	45.6	7.3	262	22.3	3.6	1172
	Sp	3	30.0	0.2	2	20.0	0.1	2	20.0	0.1	3	30.0	0.2	10
	Su	54	23.2	2.9	31	13.4	1.7	70	30.2	3.8	77	33.2	4.2	232
	A	157	26.9	8.5	89	15.3	4.8	148	25.5	8.0	189	32.5	10.3	583
Louisville, Kentucky (20)	W	47	23.2	2.6	24	11.8	1.3	63	31.1	3.5	69	34.0	3.8	203
	Sp	261	25.3	3.6	146	14.2	2.0	283	27.5	3.9	338	32.8	4.6	1028
	Su	24	22.8	1.3	18	17.2	1.0	24	22.8	1.3	39	37.2	2.2	105
	A	89	22.2	4.8	68	16.9	3.7	128	31.9	7.0	116	28.9	6.3	401
Los Angeles, California (20)	W	63	10.6	3.4	102	17.0	5.5	323	53.7	17.5	113	18.8	6.1	601
	Sp	37	18.5	2.0	35	17.5	1.9	93	46.5	5.1	35	17.6	1.9	200
	Su	213	16.3	2.9	223	17.1	3.1	568	43.5	7.8	303	23.2	4.2	1307
	A	5	29.4	0.3	4	23.5	0.2	5	29.4	0.3	3	17.6	0.2	17
Louisville, Kentucky (20)	W	7	24.1	0.4	3	10.3	0.2	16	55.2	0.9	3	10.3	0.2	29
	Sp	4	28.6	0.2	4	28.6	0.2	5	35.7	0.3	1	7.1	0.1	14
	Su	5	21.7	0.3	5	21.7	0.3	8	34.8	0.4	5	21.7	0.3	23
	A	21	25.3	0.3	16	19.3	0.2	34	41.0	0.5	12	14.5	0.2	83
Los Angeles, California (20)	W	16	25.8	0.9	12	19.4	0.7	13	21.0	0.7	21	33.9	1.2	62
	Sp	74	20.1	4.0	63	17.1	3.4	126	34.5	6.8	104	28.3	5.6	367
	Su	79	12.7	4.3	76	12.2	4.1	293	47.2	15.9	172	27.7	9.3	620
	A	38	23.2	2.1	30	18.3	1.6	67	40.9	3.7	29	17.7	1.6	164
Los Angeles, California (20)	W	207	17.1	2.8	181	14.9	2.5	499	41.1	6.8	326	26.9	4.5	1213

W = Winter (Dec., Jan., Feb.)
 Sp = Spring (Mar., Apr., May)
 Su = Summer (June, July, Aug.)
 A = Autumn (Sept., Oct., Nov.)

N = Number of thunderstorm beginnings.
 %F = Frequency, % of ΣN
 %P = Probability, % of total periods.

Table 21 (contd.)

Station and Years of Record	Season	00-06			06-12			12-18			18-24			Σ N
		N	%F	%P	N	%F	%P	N	%F	%P	N	%F	%P	
Ludington, Michigan (13)	W	1	11.1	0.1	2	22.2	0.2	3	33.3	0.3	3	33.3	0.3	9
	Sp	31	27.7	2.6	10	8.9	0.8	33	29.5	2.8	38	33.9	3.2	112
	Su	77	24.7	6.4	47	15.1	3.9	89	28.5	7.4	99	31.7	8.3	312
	A	29	25.0	2.4	21	18.1	1.8	36	31.0	3.0	30	25.8	2.5	116
Lynchburg, Virginia (20)	W	133	25.2	2.9	80	14.6	1.7	161	29.3	3.4	170	31.0	3.6	549
	Sp	1	14.3	0.1	1	14.3	0.1	4	57.1	0.2	1	14.3	0.1	7
	Su	17	11.1	0.9	14	9.2	0.8	68	44.4	3.7	54	35.3	2.9	153
	A	24	4.6	1.3	21	4.0	1.1	319	61.3	17.3	156	30.0	8.5	520
Macon, Georgia (20)	W	6	7.2	0.3	2	2.4	0.1	45	54.2	2.5	30	36.1	1.6	83
	Sp	48	6.3	0.7	38	5.0	0.6	436	57.2	6.0	241	31.6	3.3	763
	Su	15	21.1	0.8	15	21.1	0.8	27	38.0	1.5	14	19.7	0.8	71
	A	26	9.1	1.5	44	14.3	2.4	145	47.1	7.9	91	29.6	4.9	308
Madison, Wisconsin (20)	W	24	2.8	1.3	45	5.2	2.4	566	65.7	30.7	227	26.3	12.3	862
	Sp	10	6.5	0.6	8	5.2	0.4	95	62.1	5.2	40	26.2	2.2	153
	Su	77	5.5	1.1	112	8.0	1.5	833	59.7	11.4	372	26.7	5.1	1394
	A	1	10.0	0.1	2	20.0	0.1	6	60.0	0.3	1	10.0	0.1	10
Marquette, Michigan (20)	W	68	21.1	3.7	57	17.7	3.1	95	29.4	5.2	103	31.9	5.6	323
	Sp	118	18.3	6.4	138	21.4	7.5	221	34.3	12.0	168	26.0	9.1	645
	Su	39	22.9	2.1	35	20.6	1.9	51	30.0	2.8	45	26.5	2.5	170
	A	226	19.7	3.1	232	20.2	3.2	373	32.5	5.1	317	27.6	4.3	1448
Memphis, Tennessee (20)	W	0	0	0	0	0	0	0	0	0	0	0	0	0
	Sp	24	23.1	1.3	23	22.1	1.2	34	32.7	1.8	23	22.1	1.2	104
	Su	101	26.8	5.5	59	15.6	3.2	135	35.6	7.3	82	21.8	4.4	377
	A	29	30.9	1.6	17	18.1	0.9	29	30.9	1.6	19	20.2	1.0	94
Meridian, Mississippi (20)	W	154	26.8	2.1	99	17.2	1.4	198	34.4	2.7	124	21.6	1.7	575
	Sp	17	17.5	0.9	23	23.7	1.3	27	27.8	1.5	30	30.9	1.7	97
	Su	53	16.3	2.9	67	20.5	3.6	110	33.7	6.0	96	29.4	5.2	326
	A	51	9.0	2.8	97	17.1	5.3	308	54.4	16.7	110	19.4	6.0	566
Miami, Florida (14)	W	27	16.6	1.5	28	17.2	1.5	75	46.0	4.1	33	20.2	1.6	163
	Sp	148	12.8	2.0	215	18.7	2.9	520	45.1	7.1	269	23.3	3.7	1152
	Su	35	26.5	1.9	19	14.4	1.0	43	32.6	2.4	35	26.5	1.9	132
	A	83	22.2	4.5	67	18.0	3.6	142	38.1	7.7	81	21.7	4.4	373
Miles City Montana (20)	W	25	3.3	1.4	89	11.8	4.0	523	69.4	28.4	116	15.4	6.3	753
	Sp	16	8.6	0.9	15	6.1	0.8	114	61.2	6.3	41	22.0	2.2	186
	Su	159	11.0	2.2	190	13.2	2.6	822	57.0	11.2	273	16.9	3.7	1444
	A	6	16.2	0.5	5	13.5	0.4	11	29.7	0.9	15	40.5	1.2	37
Milwaukee, Wisconsin (20)	W	18	7.6	1.4	54	22.8	4.2	123	52.1	9.6	41	17.4	3.2	236
	Sp	144	7.1	3.4	205	33.0	15.9	262	42.1	20.4	111	17.6	8.6	622
	Su	18	7.0	1.4	49	19.2	3.8	123	48.2	9.7	65	25.5	5.1	255
	A	86	7.5	1.7	313	27.2	6.1	519	45.2	10.1	232	20.2	4.5	1150
Minneapolis, Minnesota (20)	W	1	100.0	0.1	0	0	0	0	0	0	0	0	0	1
	Sp	14	18.2	0.8	17	22.1	0.9	31	40.3	1.7	15	19.5	0.8	77
	Su	66	18.6	3.6	47	13.2	2.6	110	31.0	6.0	132	37.2	7.2	355
	A	7	25.0	0.4	11	39.3	0.6	5	17.9	0.3	5	17.9	0.3	28
Mobile, Alabama (20)	W	88	19.1	1.2	75	16.3	1.0	146	31.7	2.0	152	33.0	2.1	461
	Sp	3	33.3	0.2	2	22.2	0.1	3	33.3	0.2	1	11.1	0.1	9
	Su	55	27.4	3.0	24	12.0	1.3	64	31.9	3.5	58	28.9	3.2	201
	A	82	21.0	4.4	67	17.2	3.6	141	36.1	7.7	101	25.9	5.5	391
Modena, Utah (20)	W	36	26.1	2.0	20	14.5	1.1	42	30.4	2.3	40	29.0	2.2	138
	Sp	176	23.8	2.4	113	15.3	1.5	250	33.8	3.4	200	27.0	2.7	739
	Su	0	0	0	0	0	0	1	50.0	0.1	1	50.0	0.1	2
	A	45	23.8	2.4	24	12.7	1.3	51	27.0	2.8	69	36.5	3.8	189
Utah (20)	W	139	25.1	7.6	85	15.4	4.6	158	26.0	8.6	171	30.9	9.3	553
	Sp	38	25.7	2.1	28	18.9	1.5	34	24.0	1.9	48	32.4	2.6	148
	Su	222	24.9	3.0	137	15.4	1.9	244	27.4	3.3	289	32.4	4.0	892
	A	28	25.9	1.6	29	26.9	1.6	29	26.9	1.6	22	20.4	1.2	108
Utah (20)	W	68	21.4	3.7	81	25.5	4.4	109	34.2	5.9	60	18.9	3.3	318
	Sp	66	7.1	3.6	239	25.7	13.0	533	57.1	28.9	93	10.0	5.0	931
	Su	25	11.2	1.4	40	17.9	2.2	135	60.4	7.4	23	10.3	1.3	223
	A	187	11.8	2.6	389	24.6	5.3	806	51.0	11.0	198	12.5	2.7	1580
Utah (20)	W	2	22.0	0.1	1	11.0	0.1	5	56.3	0.3	1	11.0	0.1	9
	Sp	4	3.0	0.2	25	18.5	1.4	88	65.2	4.8	18	13.3	1.0	135
	Su	36	5.2	2.0	132	19.1	7.2	434	62.8	23.6	90	13.0	4.9	692
	A	18	12.2	1.0	29	19.7	1.6	83	56.5	4.6	17	11.0	0.9	147
		60	6.1	0.8	187	19.0	2.6	610	62.0	8.4	126	12.8	1.7	983

W = Winter (Dec., Jan., Feb.)
 Sp = Spring (Mar., Apr., May)
 Su = Summer (June, July, Aug.)
 A = Autumn (Sept., Oct., Nov.)

N = Number of thunderstorm beginnings.
 %F = Frequency, % of Σ N
 %P = Probability, % of total periods.

Table 21 (contd)

Station and Years of Record	Season	00-06			06-12			12-18			18-24			ΣN
		N	%F	%P	N	%F	%P	N	%F	%P	N	%F	%P	
Montgomery, Alabama (20)	W	36	30.5	2.0	21	17.8	1.2	33	28.0	1.8	28	23.7	1.6	118
	Sp	64	18.1	3.5	75	21.3	4.1	143	40.6	7.8	70	19.9	3.8	352
	Su	30	3.8	1.6	98	12.5	5.3	520	66.2	28.2	137	17.4	7.4	785
	A	17	8.8	0.9	20	10.4	1.1	116	60.0	6.4	40	20.7	2.2	193
Nantucket, Massachusetts (20)	W	147	10.1	2.0	214	14.8	2.9	812	56.0	11.1	275	19.0	3.8	1448
	Sp	8	38.1	0.4	8	38.1	0.4	0	0	0	5	23.8	0.3	21
	Su	32	30.8	1.7	22	21.2	1.2	27	26.0	1.5	23	22.1	1.2	104
	A	48	22.8	2.6	36	17.1	2.0	71	33.6	3.9	56	26.5	3.0	211
Nashville, Tennessee (20)	W	14	18.2	0.8	16	20.8	0.9	23	29.9	1.3	24	31.2	1.3	77
	Sp	102	24.7	1.4	82	19.8	1.1	121	29.3	1.7	108	26.2	1.5	413
	Su	24	28.6	1.3	17	20.2	0.9	20	23.8	1.1	23	27.4	1.3	84
	A	70	18.6	3.8	51	13.5	2.8	166	44.0	9.0	90	23.9	4.9	377
New Haven, Connecticut (20)	W	74	10.5	4.0	103	14.6	5.6	379	53.8	20.6	149	21.2	8.1	705
	Sp	30	16.4	1.6	28	15.3	1.5	93	50.8	5.1	32	17.5	1.8	183
	Su	198	14.7	2.7	199	14.7	2.7	658	48.7	9.0	294	21.8	4.0	1349
	A	2	18.2	0.1	2	18.2	0.1	3	27.3	0.2	4	36.4	0.2	11
New Orleans, Louisiana (20)	W	24	20.2	1.3	17	14.3	0.9	40	33.6	2.2	38	31.9	2.1	119
	Sp	48	13.1	2.6	32	8.7	1.7	173	47.3	9.4	113	30.9	6.1	366
	Su	9	11.2	0.5	10	12.5	0.6	32	40.0	1.8	29	36.3	1.6	80
	A	83	14.3	1.1	61	10.6	0.8	248	43.1	3.4	184	32.0	2.5	576
New York, New York (20)	W	27	22.7	1.5	27	22.7	1.5	32	26.9	1.8	33	27.7	1.8	119
	Sp	57	17.5	3.1	73	22.4	4.0	132	40.5	7.7	64	19.6	3.5	326
	Su	36	4.1	2.0	250	28.2	13.6	520	58.6	28.2	81	9.1	4.4	887
	A	19	7.6	1.0	64	25.5	3.5	141	56.1	7.7	27	10.7	1.5	251
Norfolk, Virginia (20)	W	139	8.8	1.9	444	26.1	5.7	825	52.1	11.3	205	12.9	2.8	1583
	Sp	4	26.7	0.2	5	33.3	0.3	1	6.7	0.1	5	33.3	0.3	15
	Su	31	19.1	1.7	12	7.4	0.6	63	38.9	3.4	56	34.6	3.0	162
	A	41	8.9	2.2	36	7.8	2.0	232	50.6	12.6	150	32.7	8.2	459
Northfield, Vermont (20)	W	14	15.0	0.8	9	9.7	0.5	35	37.6	1.9	35	37.6	1.9	93
	Sp	90	12.3	1.2	62	8.5	0.8	331	45.4	4.5	246	33.8	3.4	729
	Su	6	23.1	0.3	3	11.5	0.2	10	38.5	0.6	7	26.9	0.4	26
	A	29	12.6	1.6	23	10.0	1.2	97	42.0	5.3	82	35.5	4.4	231
North Head, Washington (20)	W	45	8.3	2.4	42	7.7	2.3	315	57.9	17.1	142	26.1	7.7	544
	Sp	6	7.5	0.3	10	12.5	0.6	39	48.8	2.1	25	31.2	1.4	80
	Su	86	9.8	1.2	78	8.8	1.1	461	52.3	6.3	256	29.1	3.5	881
	A	1	33.3	0.1	0	0.0	0.0	1	33.3	0.1	1	33.3	0.1	3
North Platte, Nebraska (20)	W	10	10.4	0.5	6	6.3	0.3	51	53.1	2.8	29	30.2	1.6	96
	Sp	37	8.4	2.0	55	12.6	3.0	241	55.0	13.1	105	24.0	5.7	438
	Su	10	11.4	0.5	7	8.0	0.4	45	51.2	2.5	26	29.5	1.4	88
	A	58	9.3	0.8	68	10.9	0.9	338	54.0	4.6	161	25.8	2.2	625
Oklahoma City, Oklahoma (20)	W	1	9.1	0.1	0	0	0	5	45.4	0.3	5	45.4	0.3	11
	Sp	0	0	0	0	0	0	0	0	0	0	0	0	0
	Su	1	12.5	0.1	0	0	0	2	25.0	0.1	5	62.5	0.3	8
	A	5	25.0	0.3	2	10.0	0.1	9	45.0	0.5	4	20.0	0.3	20
Omaha, Nebraska (20)	W	7	18.0	0.1	2	5.1	0.0	16	41.0	0.2	14	35.9	0.2	39
	Sp	0	0	0	0	0	0	1	100.0	0.1	0	0	0	1
	Su	25	13.6	1.4	19	10.3	1.0	70	38.0	3.8	70	38.0	3.8	184
	A	98	16.4	5.3	62	10.4	3.4	174	29.1	9.4	265	44.3	14.4	599
Oswego, New York (20)	W	24	27.6	1.3	8	9.2	0.4	23	26.4	1.3	32	36.8	1.8	87
	Sp	147	16.9	2.0	89	10.2	1.2	268	30.8	3.7	367	42.2	5.0	871
	Su	7	19.4	0.4	5	13.9	0.3	8	22.2	0.4	16	44.4	0.9	36
	A	88	24.8	4.8	58	16.4	3.2	110	31.0	6.0	98	27.6	5.3	354
Oswego, New York (20)	W	112	22.5	6.1	105	21.1	5.7	175	35.2	9.5	106	21.3	5.8	498
	Sp	53	26.7	2.9	36	18.1	2.0	61	30.7	3.4	49	24.6	2.7	199
	Su	260	23.9	3.6	204	18.8	2.8	354	32.6	4.8	269	24.7	3.7	1087
	A	2	18.2	0.1	1	9.1	0.1	4	36.4	0.2	4	36.4	0.2	11
Oswego, New York (20)	W	61	21.1	3.3	42	15.2	2.4	82	28.4	4.4	102	35.3	5.5	289
	Sp	177	29.6	9.6	92	35.4	5.0	143	23.9	7.8	186	31.1	10.1	598
	Su	41	21.5	2.2	27	14.1	1.5	61	32.0	3.3	62	32.5	3.4	191
	A	281	25.8	3.8	164	15.1	2.2	290	26.6	4.0	354	32.5	4.8	1089
Oswego, New York (20)	W	5	35.7	0.3	1	7.1	0.1	1	7.1	0.1	7	50.0	0.4	14
	Sp	14	10.4	0.8	28	20.9	1.5	53	39.5	2.9	39	29.1	2.1	134
	Su	65	18.2	3.5	52	14.6	2.8	147	41.2	8.0	93	26.0	5.0	357
	A	15	16.5	0.8	17	18.7	0.9	32	35.2	1.8	27	29.7	1.5	91
Oswego, New York (20)	W	99	16.6	1.4	98	16.5	1.3	233	39.1	3.2	166	27.9	2.3	596

W = Winter (Dec., Jan., Feb.)
 Sp = Spring (Mar., Apr., May)
 Su = Summer (June, July, Aug.)
 A = Autumn (Sept., Oct., Nov.)

N = Number of thunderstorm beginnings.
 %F = Frequency, % of ΣN
 %P = Probability, % of total periods.

Table 21 (contd)

Station and Years of Record	Season	00-06			06-12			12-18			18-24			Σ N
		N	%	%P	N	%	%P	N	%	%P	N	%	%P	
Palestine, Texas (20)	W	35	29.7	1.9	24	20.3	1.3	31	26.3	1.7	28	23.7	1.6	118
	Sp	73	20.2	4.0	83	22.9	4.5	105	29.0	5.7	101	27.9	5.5	362
	Su	39	9.3	2.1	45	10.8	2.4	256	61.2	13.9	78	18.7	4.2	418
	A	26	14.1	1.4	29	15.8	1.6	93	50.5	5.1	36	19.6	2.0	184
Parkersburg, West Virginia (20)	W	173	16.0	2.4	181	16.7	2.5	485	44.8	6.6	243	22.5	3.3	1082
	Sp	6	20.0	0.3	6	20.0	0.3	6	20.0	0.3	12	40.0	0.7	30
	Su	35	12.0	1.9	43	14.8	2.3	133	45.8	7.2	80	27.5	4.3	291
	A	81	12.1	4.4	90	13.4	4.9	345	51.4	18.7	154	22.9	8.4	670
Pensacola, Florida (20)	W	15	10.9	0.8	22	16.0	1.2	64	46.4	3.5	37	26.8	2.0	138
	Sp	137	12.1	1.9	161	14.3	2.2	548	48.6	7.5	283	25.1	3.9	1129
	Su	37	24.3	2.0	45	29.6	2.5	34	22.4	1.9	36	23.7	2.0	152
	A	65	18.4	3.5	92	26.0	5.0	131	37.0	7.1	66	18.6	3.6	354
Peoria, Illinois (20)	W	136	12.1	7.4	296	26.3	16.1	554	49.2	30.1	140	12.4	7.6	1126
	Sp	55	18.3	3.0	83	27.6	4.6	115	38.3	6.3	47	15.6	2.6	300
	Su	293	15.2	4.0	516	26.7	7.1	834	43.2	11.4	289	15.0	4.0	1932
	A	3	10.0	0.2	7	23.3	0.4	9	30.0	0.5	11	36.7	0.6	30
Philadelphia, Pennsylvania (20)	W	81	21.1	4.4	59	15.3	3.2	131	34.1	7.1	113	29.4	6.1	384
	Sp	132	21.4	7.2	93	15.1	5.0	242	39.2	13.1	151	24.5	8.2	618
	Su	42	20.7	2.3	36	17.7	2.0	72	35.5	4.0	53	26.1	2.9	203
	A	258	20.9	3.5	195	15.8	2.7	454	36.8	6.2	328	26.6	4.5	1235
Phoenix, Arizona (20)	W	3	18.8	0.2	2	12.5	0.1	3	18.8	0.2	8	50.0	0.4	16
	Sp	20	12.8	1.1	16	10.3	0.9	63	40.4	3.4	57	36.5	3.1	156
	Su	39	8.6	2.1	41	9.0	2.2	210	46.0	11.4	166	36.4	9.0	456
	A	11	15.5	0.6	7	9.9	0.4	28	39.4	1.5	25	35.2	1.4	71
Pittsburgh, Pennsylvania (20)	W	73	10.4	1.0	66	9.4	0.9	304	43.5	4.2	256	36.6	3.5	699
	Sp	3	16.7	0.2	2	11.1	0.1	7	38.9	0.4	6	33.3	0.3	18
	Su	6	10.9	0.3	5	9.1	0.3	28	50.9	1.5	16	29.1	0.9	55
	A	68	15.4	3.7	45	10.2	2.4	117	26.5	6.4	211	47.8	11.5	441
Pocatello, Idaho (20)	W	20	17.1	1.1	21	17.9	1.2	37	31.6	2.0	39	33.3	2.1	117
	Sp	97	15.4	1.3	73	11.6	1.0	189	30.0	2.6	272	43.1	3.7	631
	Su	5	20.0	0.3	4	16.0	0.2	8	32.0	0.4	8	32.0	0.4	25
	A	34	11.8	1.8	46	15.9	2.5	121	41.9	6.6	88	30.4	4.8	289
Point Reyes, California (20)	W	60	9.3	3.2	70	10.8	3.8	333	51.6	18.1	184	28.5	10.0	647
	Sp	29	18.6	1.6	16	10.3	0.9	60	38.5	3.3	51	32.7	2.8	156
	Su	128	11.4	1.8	136	12.2	1.9	522	46.7	7.2	331	29.6	4.5	1117
	A	1	16.7	0.1	1	16.7	0.1	2	33.3	0.1	2	33.3	0.1	6
Port Angeles, Washington (20)	W	10	6.4	0.5	22	14.2	1.2	105	67.7	5.7	18	11.6	1.0	155
	Sp	34	6.8	1.8	70	13.9	3.8	294	58.5	16.0	105	20.9	5.7	503
	Su	14	11.1	0.8	12	9.5	0.7	65	51.6	3.6	35	27.8	1.9	126
	A	59	7.5	0.8	105	13.3	1.4	466	59.0	6.4	160	20.2	2.2	790
Port Arthur, Texas (9)	W	3	15.0	0.2	3	15.0	0.2	7	35.0	0.4	7	35.0	0.4	20
	Sp	1	25.0	0.1	0	0	0	1	25.0	0.1	2	50.0	0.1	4
	Su	1	20.0	0.1	3	60.0	0.2	0	0	0	1	20.0	0.1	5
	A	2	20.0	0.1	2	20.0	0.1	2	20.0	0.1	4	40.0	0.2	10
Port Huron, Michigan (20)	W	7	17.9	0.1	8	20.5	0.1	10	25.6	0.1	14	35.9	0.2	39
	Sp	1	25.0	0.1	1	25.0	0.1	0	0	0	2	50.0	0.1	4
	Su	0	0	0	0	0	0	2	100.0	0.1	0	0	0	2
	A	0	0	0	1	25.0	0.1	1	25.0	0.1	2	50.0	0.1	4
Portland, Maine (20)	W	3	8.6	0.0	5	14.3	0.1	13	37.1	0.2	14	40.0	0.2	35
	Sp	9	19.1	1.1	8	17.0	1.0	16	34.0	2.0	14	29.8	1.7	47
	Su	27	19.7	3.3	30	21.9	3.6	49	35.8	5.9	31	22.6	3.7	137
	A	31	8.4	3.7	116	31.5	14.0	184	50.0	22.2	37	10.0	4.5	368
Portland, Maine (20)	W	17	12.4	2.0	45	32.8	5.4	56	40.9	6.8	19	13.9	2.3	137
	Sp	84	12.2	2.6	199	28.9	6.1	305	44.3	9.3	101	14.7	3.1	689
	Su	3	20.0	0.2	2	13.3	0.1	4	26.7	0.2	6	40.0	0.3	15
	A	43	23.8	2.3	22	12.2	1.2	56	30.9	3.0	60	33.2	3.3	181
Portland, Maine (20)	W	57	12.6	3.1	74	16.3	4.0	224	49.4	12.2	98	21.6	5.3	453
	Sp	19	18.2	1.0	17	16.3	0.9	35	33.6	1.9	33	31.7	1.8	104
	Su	122	16.2	1.7	115	15.3	1.6	319	42.4	4.4	107	26.2	2.7	753
	A	1	25.0	0.1	1	25.0	0.1	2	50.0	0.1	0	0.0	0.0	4
Portland, Maine (20)	W	7	17.1	0.4	6	14.6	0.3	19	46.4	1.0	9	22.0	0.5	41
	Sp	30	13.0	1.6	26	11.3	1.4	130	56.3	7.1	45	19.5	2.4	231
	Su	10	19.2	0.5	2	3.8	0.1	15	28.9	0.8	25	48.1	1.4	52
	A	48	14.6	0.7	35	10.7	0.5	166	50.6	2.3	79	24.1	1.1	328

W = Winter (Dec., Jan., Feb.)
 Sp = Spring (Mar., Apr., May)
 Su = Summer (June, July, Aug.)
 A = Autumn (Sept., Oct., Nov.)

N = Number of thunderstorm beginnings.
 % = Frequency, % of Σ N
 %P = Probability, % of total periods.

Table 21 (contd)

Station and Years of Record	Season	00-06			06-12			12-18			18-24			ΣN
		N	FP	PP	N	FP	PP	N	FP	PP	N	FP	PP	
Portland, Oregon (20)	W	0	0	0	0	0	0	2	50.0	0.1	2	50.0	0.1	4
	Sp	0	0	0	1	5.0	0.1	17	85.0	0.9	2	10.0	0.1	20
	Su	10	21.3	0.5	6	12.8	0.3	17	36.2	0.9	14	29.8	0.8	47
	A	2	6.7	0.1	1	3.3	0.1	20	66.7	1.1	7	23.3	0.4	30
Providence, Rhode Island (20)	W	12	11.9	0.2	8	7.9	0.1	56	55.4	0.8	25	24.8	0.3	10
	Sp	2	28.6	0.1	2	28.6	0.1	0	0	0	3	12.8	0.2	7
	Su	21	21.0	1.1	12	12.0	0.7	22	22.0	1.2	45	45.0	2.5	100
	A	30	10.5	1.6	35	12.2	1.9	140	48.9	7.6	81	28.3	4.4	286
Pueblo, Colorado (20)	W	12	20.7	0.7	10	17.2	0.6	13	22.4	0.7	23	39.7	1.3	58
	Sp	65	14.4	0.9	59	13.1	0.8	176	39.0	2.4	152	33.7	2.1	451
	Su	0	0	0	0	0	0	3	75.0	0.2	1	25.0	0.1	4
	A	9	5.3	0.5	13	7.6	0.7	120	70.6	6.5	28	16.5	1.5	170
Raleigh, North Carolina (20)	W	9	1.5	0.5	11	1.8	0.6	142	72.5	21.0	146	23.9	7.9	608
	Sp	2	2.1	0.1	2	2.1	0.1	58	59.8	3.2	35	36.1	1.9	97
	Su	20	2.3	0.3	26	3.0	0.4	623	71.0	8.5	210	23.9	2.9	879
	A	5	21.7	0.3	0	0	0	8	34.8	0.4	10	43.5	0.6	23
Rapid City, South Dakota (20)	W	22	11.0	1.2	25	12.4	1.4	86	42.8	4.7	68	33.9	3.7	201
	Sp	32	5.6	1.7	37	6.5	2.0	334	58.8	18.1	165	29.0	9.0	568
	Su	8	7.7	0.4	6	5.8	0.3	55	52.9	3.0	35	33.7	1.9	104
	A	67	7.5	0.9	68	7.6	0.9	483	53.9	6.6	278	31.0	3.8	896
Reading, Pennsylvania (20)	W	0	0	0	0	0	0	0	0	0	0	0	0	0
	Sp	10	6.4	0.5	22	14.2	1.2	74	47.7	4.0	49	31.6	2.7	155
	Su	62	8.7	3.4	113	15.8	6.1	347	48.6	18.8	191	26.7	10.4	713
	A	4	4.8	0.2	9	10.8	0.5	36	43.4	2.0	34	41.0	1.9	83
Red Bluff, California (20)	W	76	8.0	1.0	144	15.1	2.0	457	48.0	6.3	274	28.8	3.8	951
	Sp	2	15.4	0.1	2	15.4	0.1	3	23.1	0.2	6	46.2	0.3	13
	Su	25	15.8	1.4	20	12.6	1.1	72	45.6	3.9	41	26.0	2.2	158
	A	50	11.6	2.7	50	11.6	2.7	209	48.4	11.3	123	28.5	6.7	432
Reno, Nevada (20)	W	15	17.4	0.8	8	9.3	0.4	43	50.0	2.4	20	23.3	1.1	86
	Sp	92	13.4	1.3	80	11.6	1.1	327	47.4	4.5	190	27.6	2.6	689
	Su	5	38.5	0.3	0	0	0	6	46.2	0.3	2	15.4	0.1	13
	A	7	19.4	0.4	4	11.1	0.2	21	58.3	1.1	4	11.1	0.2	36
Richmond, Virginia (20)	W	4	22.2	0.2	4	22.2	0.2	3	16.7	0.2	7	38.9	0.4	18
	Sp	2	16.7	0.1	2	16.7	0.1	4	33.3	0.2	4	33.3	0.2	12
	Su	18	22.8	0.2	10	12.7	0.1	34	43.0	0.5	17	21.5	0.2	79
	A	0	0	0	0	0	0	1	100.0	0.1	0	0	0	1
Rochester, New York (20)	W	1	1.8	0.1	8	14.0	0.4	42	73.7	2.3	6	10.5	0.3	57
	Sp	4	1.8	0.2	19	8.3	1.0	174	75.9	9.4	32	14.0	1.7	229
	Su	0	0	0	8	16.0	0.4	38	76.0	2.1	4	8.0	0.2	50
	A	5	1.5	0.1	35	10.4	0.5	255	75.7	3.5	42	12.4	0.6	337
Roseburg, Oregon (20)	W	7	77.8	0.4	0	0	0	0	0	0	2	22.2	0.1	9
	Sp	24	12.0	1.3	12	6.0	0.6	86	43.0	4.7	78	39.0	4.2	200
	Su	44	7.7	2.4	23	4.0	1.2	331	57.7	18.0	176	30.7	9.6	574
	A	8	9.1	0.4	9	10.2	0.5	38	43.2	2.1	33	37.5	1.8	88
Roswell, New Mexico (20)	W	83	9.5	1.1	44	5.0	0.6	455	52.2	6.2	289	33.2	4.0	871
	Sp	1	16.7	0.1	1	16.7	0.1	2	33.3	0.1	2	33.3	0.1	6
	Su	30	20.3	1.6	22	14.9	1.2	54	36.5	2.9	42	28.4	2.3	148
	A	68	16.2	3.7	60	14.3	3.3	195	46.4	10.6	98	23.3	5.3	421
Royal Center, Indiana (8)	W	12	14.1	0.7	16	18.8	0.9	30	35.3	1.6	27	31.8	1.5	85
	Sp	111	16.8	1.5	99	15.0	1.4	281	42.7	3.8	169	25.7	2.3	660
	Su	0	0	0	0	0	0	0	0	0	0	0	0	0
	A	0	0	0	0	0	0	23	88.5	1.2	3	11.5	0.2	26
Rosalwell, New Mexico (20)	W	10	21.3	0.5	7	14.9	0.4	15	31.9	0.8	15	31.9	0.8	47
	Sp	4	21.1	0.2	0	0	0	11	57.9	0.6	4	21.1	0.2	19
	Su	14	15.2	0.2	7	7.6	0.1	49	53.3	0.7	22	23.9	0.3	92
	A	0	0	0	1	14.3	0.1	3	42.9	0.2	3	42.9	0.2	7
Royal Center, Indiana (8)	W	17	8.6	0.9	22	11.1	1.2	108	54.3	5.9	52	26.2	2.8	199
	Sp	44	7.8	2.4	20	3.6	1.1	322	57.3	17.5	175	31.2	9.5	561
	Su	22	12.6	1.2	9	5.1	0.5	89	50.8	4.9	55	31.4	3.0	175
	A	83	8.8	1.1	52	5.5	0.7	522	55.3	7.1	285	30.2	3.9	942
Royal Center, Indiana (8)	W	1	11.1	0.1	4	44.4	0.6	3	33.3	0.4	1	11.1	0.1	9
	Sp	19	14.5	2.6	32	24.4	4.4	57	43.5	7.8	23	17.5	3.1	131
	Su	32	11.5	4.3	63	22.6	8.6	142	50.8	19.3	42	15.0	5.7	279
	A	11	15.9	1.5	28	40.6	3.8	21	30.4	2.8	9	13.0	1.2	69
Roseburg, Oregon (20)	W	63	12.9	2.2	127	26.0	4.3	223	45.7	7.6	75	15.4	2.6	488

W = Winter (Dec., Jan., Feb.)
 Sp = Spring (Mar., Apr., May)
 Su = Summer (June, July, Aug.)
 A = Autumn (Sept., Oct., Nov.)

N = Number of thunderstorm beginnings.
 FP = Frequency, % of ΣN
 PP = Probability, % of total periods.

Table 21 (contd)

Station and Years of Record	Season	00-06			06-12			12-18			18-24			ΣN
		N	%F	%P	N	%F	%P	N	%F	%P	N	%F	%P	
Sacramento, California (20)	W	3	15.0	0.2	3	15.0	0.2	13	65.0	0.7	1	5.0	0.1	20
	Sp	0	0	0	7	25.9	0.4	18	66.7	1.0	2	7.4	0.1	27
	Su	2	28.6	0.1	0	0	0	4	57.1	0.2	1	14.3	0.1	7
	A	1	5.9	0.1	4	23.5	0.2	9	52.9	0.5	3	17.6	0.2	17
St. Joseph, Missouri (16)	W	6	8.4	0.1	14	19.7	0.2	44	62.0	0.6	7	9.9	0.1	71
	Sp	5	29.4	0.4	5	29.4	0.3	4	23.5	0.3	3	17.6	0.2	17
	Su	60	23.8	4.1	51	20.2	3.4	77	30.6	5.2	64	25.4	4.4	252
	A	136	29.9	9.2	80	17.6	5.4	145	31.9	9.8	93	20.5	6.3	454
St. Louis, Missouri (20)	W	48	26.5	3.5	36	19.9	2.5	56	30.9	3.8	41	22.6	2.8	181
	Sp	249	27.5	4.3	172	19.0	2.9	282	31.2	4.8	201	22.2	3.4	904
	Su	6	16.2	0.3	5	13.5	0.3	10	27.0	0.6	16	43.2	0.9	37
	A	73	21.5	4.0	65	19.1	3.5	106	31.2	5.8	96	28.2	5.2	340
St. Paul, Minnesota (20)	W	104	19.4	5.6	87	16.3	4.7	225	42.1	12.2	120	22.4	6.5	536
	Sp	31	16.6	1.7	40	21.4	2.2	60	32.1	3.3	56	30.0	3.1	187
	Su	214	19.5	2.9	197	17.0	2.7	401	36.4	5.5	288	26.2	3.9	1100
	A	1	33.3	0.1	1	33.3	0.1	0	0	0	1	33.3	0.1	3
Salt Lake City, Utah (20)	W	41	22.5	2.2	29	15.9	1.6	53	29.1	2.9	59	32.4	3.2	182
	Sp	133	24.0	7.2	84	15.2	4.6	164	29.6	8.9	172	31.1	9.3	553
	Su	43	27.7	2.4	35	22.6	1.9	36	23.2	2.0	41	26.4	2.2	155
	A	218	24.4	3.0	149	16.7	2.0	253	28.3	3.5	273	30.6	3.7	893
San Antonio, Texas (20)	W	3	16.7	0.2	0	0	0	8	44.4	0.4	7	38.9	0.4	18
	Sp	21	12.3	1.1	29	17.0	1.6	80	46.8	4.3	41	24.0	2.2	171
	Su	43	9.2	2.3	80	17.1	4.3	246	52.6	13.4	99	21.1	5.4	468
	A	26	18.3	1.4	32	22.5	1.8	68	47.8	3.7	16	11.2	0.9	142
San Diego, California (20)	W	93	11.6	1.3	141	17.6	1.9	402	50.3	5.5	163	20.4	2.2	799
	Sp	15	31.2	0.8	8	16.7	0.4	6	12.5	0.3	19	39.6	1.0	48
	Su	80	29.8	4.3	40	14.9	2.2	62	23.1	3.4	86	32.1	4.7	268
	A	20	7.5	1.1	28	10.6	1.5	140	52.8	7.6	77	29.1	4.2	265
Sandusky, Ohio (20)	W	19	12.3	1.0	17	11.0	0.9	69	44.5	3.8	50	32.3	2.7	155
	Sp	134	18.2	1.8	93	12.6	1.3	277	37.6	3.8	232	31.5	3.2	736
	Su	2	14.3	0.1	4	28.6	0.2	2	14.3	0.1	6	42.9	0.3	14
	A	3	27.3	0.2	2	18.2	0.1	4	36.4	0.2	2	18.2	0.1	11
Sandy Hook, New Jersey (11)	W	8	33.3	0.4	8	33.3	0.4	6	25.0	0.3	2	8.3	0.1	24
	Sp	2	13.3	0.1	3	20.0	0.2	6	40.0	0.3	4	26.7	0.2	15
	Su	15	23.4	0.2	17	26.6	0.2	18	28.1	0.2	14	21.9	0.2	64
	A	8	47.1	0.4	0	0	0	3	17.6	0.2	6	35.3	0.3	17
San Francisco, California (20)	W	45	16.6	2.4	52	19.2	2.8	96	35.5	5.2	77	28.5	4.2	270
	Sp	74	13.1	4.0	89	15.3	4.8	251	44.4	13.6	152	26.9	8.2	566
	Su	33	22.8	1.8	18	12.4	1.0	55	38.0	3.0	39	26.9	2.1	145
	A	160	16.0	2.2	159	15.9	2.2	405	40.5	5.5	274	27.4	3.8	998
San Jose, California (20)	W	2	28.6	0.2	1	14.3	0.1	0	0	0	4	57.1	0.4	7
	Sp	10	12.2	1.0	6	7.3	0.6	44	53.7	4.4	22	26.8	2.2	82
	Su	39	14.5	3.8	32	11.9	3.2	139	51.7	13.7	59	21.9	5.8	269
	A	7	13.7	0.7	10	19.6	1.0	19	37.3	1.9	15	29.4	1.4	51
San Luis Obispo, California (20)	W	58	14.2	1.4	49	12.0	1.2	202	49.4	5.0	100	24.4	2.5	409
	Sp	6	37.5	0.3	3	18.8	0.2	3	18.8	0.2	4	25.0	0.2	16
	Su	2	40.0	0.1	1	20.0	0.1	1	20.0	0.1	1	20.0	0.1	5
	A	0	0	0	3	75.0	0.2	0	0	0	1	25.0	0.1	4
Santa Fe, New Mexico (20)	W	3	37.5	0.2	1	12.5	0.1	3	37.5	0.2	1	12.5	0.1	8
	Sp	11	33.3	0.2	8	24.2	0.1	7	21.2	0.1	7	21.2	0.1	33
	Su	3	33.3	0.2	1	11.1	0.1	1	11.1	0.1	4	44.4	0.2	9
	A	1	50.0	0.1	0	0	0	1	50.0	0.1	0	0	0	2
San Jose, California (20)	W	0	0	0	2	50.0	0.1	0	0	0	2	50.0	0.1	4
	Sp	1	12.5	0.1	1	12.5	0.1	5	62.5	0.3	1	12.5	0.1	8
	Su	5	21.7	0.1	4	17.4	0.1	7	30.4	0.1	7	30.4	0.1	23
	A	4	40.0	0.2	2	20.0	0.1	4	40.0	0.2	0	0	0	10
San Luis Obispo, California (20)	W	3	15.0	0.2	6	30.0	0.3	8	40.0	0.4	3	15.0	0.2	20
	Sp	4	28.6	0.2	3	21.4	0.2	1	7.1	0.1	6	42.9	0.3	14
	Su	6	24.0	0.3	6	24.0	0.3	5	20.0	0.3	8	32.0	0.4	25
	A	17	24.7	0.2	17	24.7	0.2	18	26.1	0.2	17	24.7	0.2	69
Santa Fe, New Mexico (20)	W	0	0	0	1	9.1	0.1	6	54.5	0.3	4	36.4	0.2	11
	Sp	8	2.9	0.4	56	20.4	3.0	172	62.8	9.3	38	13.9	2.1	274
	Su	9	0.8	0.5	238	20.9	12.9	735	64.6	39.9	155	13.6	8.4	1137
	A	10	4.3	0.6	32	13.6	1.8	152	64.6	8.3	41	17.4	2.2	235
San Jose, California (20)	W	27	1.6	0.4	327	19.7	4.5	1065	64.2	14.6	238	14.4	3.3	1657

W = Winter (Dec., Jan., Feb.)
 Sp = Spring (Mar., Apr., May)
 Su = Summer (June, July, Aug.)
 A = Autumn (Sept., Oct., Nov.)

N = Number of thunderstorm beginnings.
 %F = Frequency, % of EN
 %P = Probability, % of total periods.

Table 21 (contd)

Station and Years of Record	Season	00-05			06-12			12-18			18-24			EN
		N	%F	%P	N	%F	%P	N	%F	%P	N	%F	%P	
Sault	W	0	0	0	2	100.0	0.1	0	0	0	0	0	0	2
Ste. Marie,	Sp	15	19.2	0.8	15	19.2	0.8	29	37.2	1.6	19	24.4	1.0	78
Michigan	Su	49	21.7	2.7	52	23.0	2.8	70	31.0	3.8	55	24.3	3.0	226
(20)	A	19	22.4	1.0	15	17.6	0.8	26	30.6	1.4	25	29.4	1.4	85
		83	21.2	1.1	84	21.5	1.2	125	32.0	1.7	99	25.3	1.4	391
Savannah,	W	12	22.2	0.7	8	14.8	0.4	12	22.2	0.7	22	40.7	1.2	54
Georgia	Sp	21	8.3	1.1	39	15.5	2.1	133	52.7	7.2	59	23.4	3.2	252
(20)	Su	29	3.6	1.6	93	11.4	5.0	525	64.6	28.5	165	20.3	9.0	812
	A	13	7.8	0.7	18	10.8	1.0	95	56.9	5.2	41	24.5	2.3	167
		75	5.8	1.0	158	12.3	2.2	765	59.5	10.5	287	22.3	3.9	1285
Seranton,	W	0	0	0	1	33.3	0.1	1	33.3	0.1	1	33.3	0.1	3
Pennsylvania	Sp	10	6.6	0.5	11	7.3	0.6	86	57.0	4.7	44	29.1	2.4	151
(20)	Su	31	6.3	1.7	43	8.7	2.3	231	56.8	15.3	140	28.3	7.6	495
	A	6	6.8	0.3	13	14.8	0.7	37	42.0	2.0	32	36.4	1.8	88
		47	6.4	0.6	68	9.2	0.9	405	55.0	5.5	217	29.4	3.0	737
Seattle,	W	0	0	0	0	0	0	0	0	0	2	100.0	0.1	2
Washington	Sp	1	3.6	0.1	1	3.6	0.1	20	71.4	1.1	6	21.4	0.3	28
(20)	Su	6	9.1	0.3	9	13.6	0.5	23	34.8	1.2	28	42.4	1.5	66
	A	2	6.5	0.1	4	12.9	0.2	19	61.3	1.0	6	19.4	0.3	31
		9	7.1	0.1	14	11.0	0.2	62	48.8	0.8	42	33.1	0.6	127
Sheridan,	W	0	0	0	0	0	0	0	0	0	0	0	0	0
Wyoming	Sp	4	3.8	0.2	11	10.5	0.6	65	61.9	3.7	25	23.8	1.4	105
(19)	Su	49	9.6	2.8	59	11.6	3.4	299	58.6	17.1	103	20.2	5.9	510
	A	8	17.0	0.5	8	17.0	0.5	20	42.6	1.2	11	23.4	0.6	47
		61	9.2	0.9	78	11.8	1.1	384	58.0	5.5	139	21.0	2.0	662
Shreveport,	W	24	19.0	1.3	25	19.8	1.4	34	27.0	1.9	43	34.1	2.4	126
Louisiana	Sp	82	23.4	4.4	65	18.6	3.6	115	32.9	6.3	88	25.1	4.8	350
(20)	Su	47	10.4	2.5	69	15.3	3.7	244	54.0	13.2	92	20.4	5.0	452
	A	25	17.0	1.4	16	10.9	0.9	67	45.6	3.7	39	26.5	2.1	147
		178	16.6	2.4	175	16.3	2.4	460	42.8	6.3	262	24.4	3.6	1075
Sioux City,	W	1	20.0	0.1	0	0	0	0	0	0	4	80.0	0.2	5
Iowa	Sp	45	20.2	2.4	34	15.2	1.8	76	34.0	4.1	68	30.5	3.7	223
(20)	Su	176	30.3	9.6	89	15.3	4.8	140	24.1	7.6	177	30.4	9.6	582
	A	39	26.2	2.1	22	14.8	1.2	33	22.1	1.8	55	36.9	3.1	149
		261	27.2	3.6	145	15.1	2.0	249	26.0	3.4	304	31.7	4.2	959
Spokane,	W	0	0	0	0	0	0	2	100.0	0.1	0	0	0	2
Washington	Sp	1	2.5	0.1	3	7.5	0.2	24	60.0	1.3	12	30.0	0.6	40
(20)	Su	34	22.7	1.8	18	12.0	1.0	50	33.3	2.7	48	32.0	2.6	150
	A	4	17.4	0.2	4	17.4	0.2	8	34.8	0.4	7	30.4	0.4	23
		39	18.1	0.5	25	11.6	0.3	84	39.1	1.2	67	31.2	0.9	215
Springfield,	W	8	21.6	0.4	7	18.9	0.4	12	32.4	0.7	10	27.0	0.6	37
Illinois	Sp	81	20.3	4.4	78	19.6	4.2	121	30.4	6.6	118	29.6	6.4	398
(20)	Su	130	20.2	7.1	88	13.6	4.8	268	41.5	14.6	160	24.8	8.7	646
	A	44	20.5	2.4	49	22.9	2.7	49	22.9	2.7	72	33.6	4.0	214
		263	20.3	3.6	222	17.1	3.0	450	34.7	6.2	360	27.8	4.9	1295
Springfield,	W	20	35.1	1.1	8	14.0	0.4	11	19.3	0.6	18	31.6	1.0	57
Missouri	Sp	75	22.4	4.1	70	20.9	3.8	99	29.6	5.4	90	26.9	4.9	334
(20)	Su	128	23.3	7.0	84	15.3	4.6	224	40.8	12.2	114	20.7	6.2	550
	A	46	25.9	2.5	26	14.6	1.4	70	39.3	3.8	36	20.2	2.0	178
		269	24.0	3.7	188	16.8	2.6	404	36.1	5.5	258	23.1	3.5	1119
Syracuse,	W	1	10.0	0.1	2	20.0	0.1	2	20.0	0.1	5	50.0	0.3	10
New York	Sp	20	11.2	1.1	28	15.7	1.5	84	47.2	4.6	46	25.9	2.5	178
(20)	Su	66	11.7	3.6	77	13.7	4.2	274	48.8	14.9	144	25.6	7.8	561
	A	19	13.6	1.0	17	12.1	0.9	64	45.7	3.5	40	28.6	2.2	140
		106	11.9	1.5	124	14.0	1.7	424	47.7	5.8	235	26.4	3.2	889
Tacoma,	W	1	16.7	0.1	1	16.7	0.1	4	66.7	0.2	0	0	0	6
Washington	Sp	0	0	0	2	10.5	0.1	15	78.9	0.8	2	10.5	0.1	19
(20)	Su	6	9.7	0.3	8	12.9	0.4	34	54.8	1.8	14	22.6	0.8	62
	A	0	0	0	8	33.3	0.4	9	37.5	0.5	7	29.2	0.4	24
		7	6.3	0.1	19	17.1	0.3	62	55.9	0.8	23	20.7	0.3	111
Tampa,	W	21	26.6	1.2	14	17.7	0.8	27	34.2	1.5	17	21.5	0.9	79
Florida	Sp	24	8.2	1.3	45	15.4	2.4	165	56.4	9.0	58	19.8	3.2	292
(20)	Su	52	3.7	2.8	235	16.8	12.8	890	63.5	48.3	226	16.1	12.3	1403
	A	9	2.5	0.5	36	10.0	2.0	241	67.2	13.2	73	20.4	4.0	359
		106	5.0	1.4	330	15.5	4.5	1323	62.1	18.1	374	17.5	4.4	2133

W = Winter (Dec., Jan., Feb.)
 Sp = Spring (Mar., Apr., May)
 Su = Summer (June, July, Aug.)
 A = Autumn (Sept., Oct., Nov.)

N = Number of thunderstorm beginnings.
 %F = Frequency, % of EN
 %P = Probability, % of total periods.

Table 21 (contd)

Station and Years of Record	Season	00-06			06-12			12-18			18-24			ΣN
		N	%F	%P	N	%F	%P	N	%F	%P	N	%F	%P	
Tatoosh Island, Washington (20)	W	6	25.0	0.3	5	20.8	0.3	6	25.0	0.3	7	29.2	0.4	24
	Sp	0	0	0	1	20.0	0.1	2	40.0	0.1	2	40.0	0.1	5
	Su	5	25.0	0.3	4	20.0	0.2	7	35.0	0.4	4	20.0	0.2	20
	A	5	14.3	0.3	7	20.0	0.4	6	17.1	0.3	17	48.6	0.9	35
Taylor, Texas (20)	W	16	19.0	0.2	17	20.2	0.2	21	25.0	0.3	30	35.7	0.4	84
	Sp	27	31.0	1.5	20	23.0	1.1	15	17.2	0.8	25	28.7	1.4	87
	Su	83	23.9	4.5	84	24.2	4.6	102	29.4	5.5	78	22.5	4.2	347
	A	22	6.2	1.2	35	9.8	1.9	231	64.9	12.5	68	19.1	3.7	356
Terre Haute, Indiana (8)	W	26	13.0	1.4	39	19.5	2.1	98	49.0	5.4	37	18.5	2.0	200
	Sp	158	16.0	2.2	178	18.0	2.4	146	45.0	6.1	208	21.0	2.8	990
	Su	7	33.3	1.0	4	19.0	0.6	6	28.6	0.8	4	19.0	0.6	21
	A	50	24.9	6.8	39	19.4	5.3	57	28.4	7.8	55	27.4	7.5	201
Thomasville, Georgia (20)	W	55	17.1	7.5	49	15.2	6.7	155	48.2	21.1	63	19.6	8.6	322
	Sp	18	15.7	2.4	14	12.2	1.9	58	50.5	7.9	25	21.8	3.4	115
	Su	130	19.8	4.4	106	16.1	3.6	276	42.0	9.4	117	22.3	5.0	659
	A	26	24.5	1.4	23	21.7	1.3	39	36.8	2.2	18	17.0	1.0	106
Toledo, Ohio (20)	W	46	12.3	2.5	70	18.6	3.8	200	53.6	10.9	57	15.3	3.1	373
	Sp	28	2.4	1.5	198	16.9	10.8	765	65.3	41.5	180	15.4	9.8	1171
	Su	8	3.2	0.4	24	9.6	1.3	180	71.6	9.9	39	15.5	2.1	251
	A	108	5.7	1.5	315	16.6	4.3	1184	62.3	16.2	294	15.5	4.0	1901
Topeka, Kansas (20)	W	7	33.3	0.4	3	14.3	0.2	5	23.2	0.3	6	28.6	0.3	21
	Sp	59	21.8	3.2	39	14.4	2.1	86	31.8	4.7	86	31.8	4.7	270
	Su	93	16.5	5.0	72	12.7	3.9	252	44.6	13.7	149	26.4	8.1	566
	A	32	21.3	1.8	22	14.7	1.2	52	34.7	2.9	44	29.3	2.4	150
Trenton, New Jersey (13)	W	191	19.0	2.6	136	13.5	1.9	395	39.2	5.4	285	28.3	3.9	1007
	Sp	6	26.1	0.3	2	8.7	0.1	9	39.1	0.5	6	26.1	0.3	23
	Su	85	25.9	4.6	47	14.3	2.6	67	26.5	4.7	109	33.2	5.9	328
	A	171	29.8	9.3	72	12.5	3.9	164	28.5	8.9	168	29.2	9.1	575
Valentine, Nebraska (20)	W	53	23.3	2.9	37	16.2	2.0	69	30.3	3.8	69	30.3	3.8	228
	Sp	315	27.3	4.3	158	13.7	2.2	329	28.5	4.5	352	30.5	4.8	1154
	Su	2	40.0	0.2	1	20.0	0.1	0	0	0	2	40.0	0.2	5
	A	12	11.1	1.0	12	11.1	1.0	47	43.5	3.9	37	34.3	3.1	108
Vicksburg, Mississippi (15)	W	29	8.1	2.4	32	8.9	2.7	184	51.3	15.4	114	31.8	9.5	359
	Sp	9	15.2	0.8	4	6.8	0.3	28	47.5	2.4	18	30.5	1.5	59
	Su	52	9.8	1.1	49	9.2	1.0	259	48.6	5.5	171	32.2	3.6	531
	A	0	0	0	0	0	0	0	0	0	0	0	0	0
Walla Walla, Washington (20)	W	22	15.3	1.2	20	13.9	1.1	42	29.1	2.3	60	41.6	3.3	144
	Sp	98	19.1	5.3	58	11.3	3.2	186	36.3	10.1	170	33.2	9.2	512
	Su	19	21.1	1.0	10	11.1	0.6	30	33.3	1.6	31	34.4	1.7	90
	A	139	18.6	1.9	88	11.8	1.2	258	34.6	3.5	261	35.0	3.6	746
Wichita, Kansas (20)	W	41	29.1	3.0	21	14.9	1.6	45	31.9	3.3	34	24.1	2.5	141
	Sp	62	19.9	4.5	48	15.4	3.5	121	38.9	8.8	80	25.7	5.8	311
	Su	43	7.7	3.1	63	11.3	4.6	352	63.1	25.5	100	17.9	7.2	558
	A	22	13.6	1.6	20	12.3	1.5	94	57.9	6.9	26	16.0	1.9	162
Wausau, Wisconsin (12)	W	168	14.3	3.1	152	13.0	2.8	612	52.2	11.2	240	20.5	4.4	1172
	Sp	0	0	0	0	0	0	0	0	0	1	100.0	0.1	1
	Su	1	2.0	0.1	5	10.0	0.3	33	66.0	1.8	11	22.0	0.6	50
	A	33	21.2	1.8	22	14.1	1.2	50	32.0	2.7	51	32.7	2.8	156
Washington, D. C. (20)	W	6	19.4	0.3	3	9.7	0.2	11	35.5	0.6	11	35.5	0.6	31
	Sp	40	16.8	0.5	30	12.6	0.4	94	39.5	1.3	74	31.1	1.0	238
	Su	9	40.9	0.5	1	4.5	0.1	4	18.2	0.2	8	36.4	0.4	22
	A	28	13.2	1.5	17	8.0	0.9	94	44.3	5.1	73	34.4	4.0	212
Wausau, Wisconsin (12)	W	146	8.6	2.5	35	6.5	1.9	285	53.3	15.5	169	31.6	9.2	535
	Sp	17	15.2	0.9	6	5.4	0.3	45	40.2	2.5	44	39.3	2.4	112
	Su	100	11.4	1.4	59	6.7	0.8	128	48.6	5.9	294	33.4	4.0	881
	A	0	0	0	0	0	0	1	100.0	0.1	0	0	0	1
Wichita, Kansas (20)	W	11	16.2	1.0	15	22.1	1.4	22	32.4	2.0	20	29.4	1.8	68
	Sp	42	18.1	3.8	50	21.6	4.5	89	38.4	8.1	51	22.0	4.6	232
	Su	11	19.0	1.0	13	22.4	1.2	18	31.0	1.6	16	27.6	1.5	58
	A	64	17.8	1.5	78	21.7	1.3	130	36.2	3.0	87	24.2	2.0	359
Wichita, Kansas (20)	W	6	18.8	0.3	9	28.1	0.5	7	21.9	0.4	10	31.2	0.6	32
	Sp	90	28.5	4.9	47	14.9	2.6	91	28.8	4.9	87	27.6	4.7	315
	Su	166	29.4	9.0	96	17.0	5.2	146	25.8	7.9	156	27.6	8.5	564
	A	50	23.2	2.7	36	16.7	2.0	68	31.5	3.7	62	28.7	3.4	216
		312	27.7	4.3	188	16.7	2.6	312	27.7	4.3	315	28.0	4.3	1127

W = Winter (Dec., Jan., Feb)
 Sp = Spring (Mar., Apr., May)
 Su = Summer (June, July, Aug.)
 A = Autumn (Sept., Oct., Nov.)

N = Number of thunderstorm beginnings.
 %F = Frequency, % of ΣN
 %P = Probability, % of total periods.

Table 21 (contd)

Station and Years of Record	Season	00-06			06-12			12-18			18-24			ΣN
		N	%F	%P	N	%F	%P	N	%F	%P	N	%F	%P	
Williston,	W	0	0	0	0	0	0	0	0	0	0	0	0	0
North	Sp	6	11.1	0.4	5	9.3	0.4	26	48.2	1.9	17	31.5	1.2	54
Dakota	Su	55	15.8	4.0	55	15.8	4.0	120	34.4	8.7	118	33.9	8.6	348
(15)	A	6	17.6	0.4	4	11.8	0.3	10	29.4	0.7	14	41.2	1.0	34
		67	15.3	1.2	64	14.7	1.2	156	35.7	2.8	149	34.1	2.7	436
Willmington,	W	12	26.1	0.7	6	13.0	0.3	12	26.1	0.7	16	34.8	0.9	46
North	Sp	46	19.2	2.5	36	15.0	2.0	86	35.9	4.7	71	29.7	3.9	239
Carolina	Su	78	10.8	4.2	106	14.6	5.8	349	48.2	19.0	192	26.5	10.4	725
(20)	A	24	16.6	1.3	27	18.6	1.5	66	45.5	3.6	28	19.3	1.5	145
		160	13.9	2.2	175	15.2	2.4	513	44.4	7.0	307	26.6	4.2	1155
Winnemucca,	W	0	0	0	0	0	0	0	0	0	0	0	0	0
Nevada	Sp	4	5.9	0.2	10	14.7	0.5	45	66.2	2.4	9	13.2	0.5	68
(20)	Su	6	3.6	0.3	25	14.8	1.4	114	67.4	6.2	24	14.2	1.3	169
	A	2	4.9	0.1	4	9.8	0.2	31	75.4	1.7	4	9.8	0.2	41
		12	4.3	0.2	39	14.0	0.5	190	68.2	2.6	37	13.3	0.5	278
Wytheville,	W	2	20.0	0.1	1	10.0	0.1	4	40.0	0.2	3	30.0	0.2	10
Virginia	Sp	16	9.0	0.9	33	18.5	1.8	92	51.7	5.0	37	20.8	2.0	178
(20)	Su	21	4.5	1.1	55	11.7	3.0	296	63.0	16.1	97	20.7	5.3	469
	A	4	4.9	0.2	7	8.5	0.4	54	65.9	3.0	17	20.7	0.9	82
		43	5.8	0.6	96	13.0	1.3	446	60.2	6.1	154	20.8	2.1	739
Yankton,	W	0	0	0	0	0	0	0	0	0	1	100.0	0.1	1
South	Sp	41	20.0	2.2	27	13.2	1.5	61	29.8	3.3	76	37.1	4.1	205
Dakota	Su	146	27.7	7.9	87	16.5	4.7	107	20.3	5.8	186	35.3	10.1	526
(20)	A	35	29.4	1.9	10	8.4	0.6	36	30.2	2.0	38	31.9	2.1	119
		222	26.1	3.0	124	14.6	1.7	204	24.0	2.8	301	35.4	4.1	851
Yellowstone	W	0	0	0	0	0	0	0	0	0	0	0	0	0
Park,	Sp	1	1.1	0.1	13	13.8	0.7	68	72.4	3.7	12	12.8	0.6	94
Wyoming	Su	26	3.8	1.4	101	14.6	5.5	430	62.4	23.3	134	19.4	7.3	691
(20)	A	6	5.7	0.3	17	16.2	0.9	66	62.8	3.6	16	15.2	0.9	105
		33	3.7	0.5	131	14.7	1.8	564	63.4	7.7	162	18.2	2.2	890
Yuma,	W	0	0	0	0	0	0	2	100.0	0.1	0	0	0	2
Arizona	Sp	0	0	0	1	7.7	0.1	5	38.1	0.3	7	54.1	0.4	13
(20)	Su	28	25.7	1.5	17	15.6	0.9	39	35.8	2.1	35	32.1	1.9	119
	A	11	14.9	0.6	8	10.8	0.4	41	55.4	2.2	14	18.9	0.8	74
		39	18.7	0.5	26	12.5	0.4	87	41.8	1.2	56	26.9	0.8	208

W = Winter (Dec., Jan., Feb.)
 Sp = Spring (Mar., Apr., May)
 Su = Summer (June, July, Aug.)
 A = Autumn (Sept., Oct., Nov.)

N = Number of thunderstorm beginnings.
 %F = Frequency, % of ΣN
 %P = Probability, % of total periods.

darkness) or DNP (during p.m. hours of darkness). In the breakdown of the data for the analysis that follows, DNA occurrences were placed in the first quarter of the day and DNP occurrences in the last quarter. The hours were, of course, local standard time. Although the occurrences were tabulated, in the original data, for each of the 24 hours of the day, the analysis was made on the basis of four 6-hour periods, marked 00-06, 06-12, 12-18, and 18-24 on the 24-hour clock and usually designated in the discussion as periods 1, 2, 3, and 4, respectively. This division was decided upon after a preliminary inspection of the nature of the diurnal variations and also favored because it agrees with common practice. As the work progressed, it became apparent that a breakdown on a 3-hourly basis would have added significant results; such a refinement is left to other investigations. The data are too few to justify an hourly breakdown.

258. In addition, the quarter-day data were analyzed on a seasonal basis, December, January, and February constituting the winter, etc. This analysis might profitably be refined on a monthly basis.

259. Table 21 lists in alphabetical order the 192 stations used in the analysis and contains all the data used in the charts following. The table also contains probability figures, in percent, pertaining to the various periods and seasons, in the column headed %P. For any quarter day and season the probability percentage was obtained by dividing the number of thunderstorm beginnings (i.e., occurrences) by the total number of such quarter days in the period

of record. At Abilene, Texas, for instance, there were 186 thunderstorm occurrences in the quarter day 12-18 in the summer during the period of record. There are 92 such quarter days each summer (June, July, and August) and in 20 years there are 1840. Dividing 186 by 1840 gives 10.1% as %P, which is thus the probability of the occurrence of a thunderstorm in Abilene in summer between the hours 12 and 18. The chance of occurrence is about 1 out of 10. The %P value on the fifth line of the tabulation for each station is the probability of an occurrence during the particular quarter day throughout the year - not as useful a probability as the seasonal probabilities.

260. The frequency percentage (%F) of the tabulations is obtained by dividing the total number of occurrences for one quarter day of any one season by the total number of occurrences during the same season. In the same Abilene quarter-day period, 12-18, the total number of occurrences (ΣN) for the summer is 379. The percentage frequency for the quarter day 12-18, summer season, thus becomes 186 divided by 379, or 49.1 (%F). This simply means that of all the thunderstorms that occur at Abilene during the summer months, 49.1% occur during the quarter day 12-18, period 3. The %F values in the fifth line of the station data give the same relation between the quarter-day occurrences and the total number of occurrences for the whole year (ΣN , fifth line).

261. Annual. Figure 84, "Annual Diurnal Variation of Thunderstorm Frequency," shows the distribution of the last-named values of %F. The dominance of the 3d period is clearly evident. A large area in which its dominance is greatly modified, however, or even completely suppressed, begins in Kansas and Missouri, spreads northward and,

fanwise, northwestward and northeastward. A similar suppression can be observed in the Great Lakes region, particularly on the eastern or southern shores (Chicago, Grand Haven, Ludington, Buffalo); in extreme southern Texas (Del Rio, Corpus Christi, Galveston); and at Atlantic Coastal stations from Hatteras to Nantucket. Phoenix also falls into this class. Variations from the dominant 3d period are also apparent at West Coast stations but cannot be considered too significant because of the small number of total occurrences.

262. A better view of the distribution of the diurnal variation (of all annual occurrences) can be obtained from the four subsidiary maps which are all included in figure 85. In this chart a map was used for each quarter-day period and on each were plotted the values of % F obtained from the fifth line of station data in table 21, the same values shown in the histograms of the chart of the annual diurnal variation, figure 84. If the variation were purely random, an equal number of thunderstorms would occur each quarter day, that is, each would show a 25% percentage frequency. In constructing the maps of figure 85 a percentage from 20 to 30 was considered to be one showing a random or "normal" distribution and areas containing these percentages have the lightest shading. No shading at all denotes an area of frequency below 20%, i.e., below normal. Two subdivisions are denoted of areas above normal, moderate shading being used for areas of frequency 31 to 50% and heavy shading for areas of frequency over 50%.

263. The map for the 1st period shows most of the country with subnormal frequency. The significant normal area is the Middle West from Texas to Minnesota and Wisconsin, with extensions across Lakes

Superior and Michigan. Slight areas of normal frequency also appear along the coasts but only two extreme coastal points, Hatteras and San Francisco, show above-normal frequencies.

264. The 06-12 map shows that this is the period of least thunder-storm activity, with a few scattered, small areas of normal frequency. The most notable increase from below-normal to normal frequency occurs along the Gulf Coast and the eastern and southern portions of Florida. The Middle West still preserves a scattered tendency toward normal, and an outbreak approaching normal is noticeable in the region of Santa Fe and Grand Junction. However, most of the so-called normal percentages on this map are actually below 25%.

265. The 12-18 map shows the frequency predominantly above normal and much of it even above 50%. In the Midwest region, however, which showed normal frequencies in the 1st period while most of the rest of the country showed below-normal, a normal frequency is maintained except for a small area of below-normal centered at Lincoln, Nebraska.

266. On the 18-24 map it is this area again which is outstanding. It shows an increase to above-normal frequencies while the rest of the country shows a rapid subsidence to normal and even below. The most rapid decrease from the 12-18 maximum frequencies is in the predominantly mountainous sections and in the Gulf region.

267. There are only a few small areas, practically points, that show up as normal throughout the four periods: a small area around San Luis Obispo, California; a point between La Crosse and Madison, Wisconsin; and a point on the Texas border a little west of Brownsville.

268. Winter. Figure 86 shows the histograms of the winter thunderstorm occurrences. No chart of the type of figure 85 is offered for this season although the basic data for such an analysis are contained in table 21. From an inspection of figure 86, if only stations with at least 20 occurrences (i.e., one per season) are considered, the important fact emerges that there is no predominating quarter day in the winter season. The one-per-season line would run from Cape Henry to Charlotte, then to Pittsburgh and Erie, and finally westward to include the southern portions of Ohio, Indiana, Illinois, and Iowa. It includes an area of three or more occurrences per season (60 or more for the period of record) which extends from the Gulf Coast to the Ohio River. The northern boundary of the latter region is an arc from Ft. Worth to Evansville and Louisville and then to Jacksonville. The maximum number is at Pensacola but Jacksonville exceeds all other Florida stations. There is a probable maximum at Vicksburg if the latter's 15-year record is extrapolated to 20 years. On the West Coast, Tatoosh Island, Point Reyes, and Sacramento show 20 or slightly more while Eureka shows 40.

269. Very few of the stations with at least 20 occurrences show any of the four periods with a frequency appreciably in excess of 30%. Among the few that do are Washington, D. C., with over 40% in the 1st period, Parkersburg with over 40% in the 4th period, Savannah with over 40% in the 4th period, Kansas City with over 50% in the 4th period, and Sacramento with over 50% in the 3d period. However, even within a limited region, there is no consistent maximum period. The characteristic minimum period of the annual chart, the 2d period, seems to be a fairly common minimum on the winter chart - more common, at any rate, than any

maximum period, but with many exceptions, even its appearance as the maximum period at Pensacola, Charlotte, and Atlanta, for example.

The tendency throughout is toward what has previously been called a random or normal distribution, that is, toward the equalization of the frequencies in all the four periods of the day, although the distribution is most nearly even along the Gulf Coast and in Texas.

270. The highest percentage probability of thunderstorm occurrence for the winter season is 3.3 at Vicksburg for the 3d period (see table 21), approximately a one-in-thirty chance of occurrence. There are a number of zero probabilities - for all four periods at some western and Rocky Mountain stations (also at Houghton, Michigan), and for scattered periods, even the 3d (at Nantucket), in the East. In only two of the latter cases does the total number of occurrences exceed 20 - at Nantucket and Raleigh; in all other cases showing any zero probability the total number of occurrences is less than 20.

271. It is evident that winter thunderstorms in the United States are mainly frontal in origin although convergent action not associated with fronts is also a cause. These phenomena have some diurnal variation, but the magnitude of the variation is not usually great enough to dominate the thunderstorm distribution, which remains fairly uniform or random throughout the four periods of the winter day. Since the thunderstorm is caused by frontal or convergent action upon unstable air, the diurnal variation of atmospheric instability must also be considered. Both conditional and convective instability have such a variation. It is largely a duplicate of the diurnal surface-temperature variation: a maximum in the 3d period

and a minimum in the 2d. However, in winter the temperature variation is less than in the other seasons and often, as previously cited (10), insufficient to produce instability in the lower layers, even strengthening the atmosphere's natural stability by formation of the surface inversion. The latter is steepest at the time of the minimum temperature, usually early in the 2d period.

272. Spring. On the spring diurnal-variation chart (figure 87) an actual maximum of 426 occurrences appears at Cairo and there are also over 400 at Ft. Smith, Little Rock, and Cincinnati, but extrapolation of a 12-year record at Dallas gives 412 and extrapolation of a 7-year record at Broken Arrow gives 520. Only West Coast stations and Yuma now show 20 occurrences or less and at practically all the stations on the immediate West Coast there has been a decrease of occurrences since the winter season. North Head is the only station with zero occurrences for the spring season.

273. The general 3d-period maximum now becomes definitely visible. Its percentage frequency climbs toward 50, and occasionally higher, at most East Gulf and inland Atlantic stations while in the Rocky Mountains it climbs to 60 and even 75. Its dominance is less in the states between the Lakes and the lower Ohio River Valley and disappears entirely within the Lake region and also in the region that fans out from East and Central Texas to Minnesota and North Dakota.

274. In the regions characterized by the dominant 3d period there is some variation in the order of the frequency magnitudes in the other three periods. If the periods, numbered 1 to 4 as previously explained, are arranged in the descending order of the magnitudes of their percentage

frequencies, then the type of variation in the Northeastern States (disregarding coastal stations), for instance, can be described as 3-4-1-2, meaning that the highest frequency occurs in the 3d period, the next highest in the 4th period, etc. Farther South, in the Carolinas, the variation is 3-4-2-1 and, when the Gulf is reached, it may be 3-4-2-1, 3-2-4-1, or 3-4-1-2. The characteristic Rocky Mountain sequence varies from 3-4-2-1 to 3-2-4-1.

275. The most even distribution occurs now in the Lake to Ohio River region, in Texas, at the Atlantic Coastal stations, and in the region roughly between the 90th and 100th meridians. The most consistent distribution in these areas can be described as 4-3-1-2, with the maximum value seldom exceeding 35%. More consistent here is the appearance of the 2d period as the minimum. It is because of this fact that the combined occurrences of periods 2 and 3 (roughly daylight periods) are always exceeded by the combined occurrences of periods 1 and 4 (roughly nighttime periods), producing the nocturnal maximum of thunderstorm activity in this area. Period 3 is often second in magnitude and even when third in magnitude it is not much exceeded by period 1 or 4; occasionally it may be first in magnitude - but not by much.

276. However, this analysis does not verify the observation sometimes made that the maximum activity in the Midwest is during the first quarter day. The maximum activity seems to be generally in the last quarter day and the third quarter is not far behind. It is possible that an analysis on a 3-hourly basis would alter these conclusions.

277. An odd distribution, 4-3-2-1, is found at both Key West and Yuma. At Key West the same sequence was observed in the winter.

278. The maximum probability of occurrence in the spring is at Jacksonville - 11.1% in the 3d period (see table 21); the chances are thus about one in ten that Jacksonville will experience an afternoon (12-18) thunderstorm in the spring. A few zero probabilities occur in the Far West.

279. It is evident that during the spring the insolational thunderstorm, or at least the thunderstorm in which insolation is an important factor, is coming into dominance. Its influence seems to be most effective in the mountain areas where the 3d period is definitely the most outstanding. In mountain areas insolation actually produces an added effect. By heating the mountain slopes more than the free air it produces an up-slope valley wind which aids in the production of the afternoon thunderstorm; at night the absence of insolation causes the mountain slope to cool more rapidly by radiation than the free air, thus producing the down-slope mountain wind which inhibits thunderstorm genesis. The up-slope valley wind usually begins during the 2d period and it may be this fact which is responsible for the displacement of the minimum frequency to the 1st period in the mountain area. In the eastern part of the country the only stations comparable to the mountain stations of the West are Asheville and Wytheville; it is noteworthy that at these stations the 3d-period frequency is in excess of 50%, even exceeding 75% at Asheville in the summer. The 3-4-2-1 variation can, in fact, be called the mountain or orographic type.

280. At Atlantic Coastal and Gulf stations the insolation effect is complicated and usually dampened by the sea breeze, itself a result of the unequal insolation heating of land and water surfaces. The sea breeze puts a stop to the rise of temperature of the land-surface air and also produces an inversion at a low level. In most cases this eliminates the thunderstorm possibility unless active dynamic features compel it. In some places like the Gulf Coast, however, where condensation levels and levels of free convection are low, the sea breeze may act as a cold front to set off an early thunderstorm, as early as the 2d period. The frictional retardation of the landward current (a downwind decrease of velocity) has also been adduced as a cause of coastal thunderstorms (35). These are possible explanations of the occasionally high frequency value of the 2d period in this region. However, comparably high frequencies also characterize the 1st and 4th periods at such stations, these periods constituting the land-breeze portion of the day. In part, the frequencies may be augmented by thunderstorms at sea which are observed from the land, since both theory and observations indicate maximum convective activity over sea surfaces at night. The diurnal variation in the Great Lakes region also represents a complexity of such effects. The so-called nocturnal maximum of thunderstorm activity over the Middle West, hardly explicable by either orographic or maritime influences, will be discussed in paragraphs 301-9.

281. Summer. On the summer chart (figure 88) the greatest number of occurrences is 1403 at Tampa, with Jacksonville, Thomasville, Santa Fe, and Pensacola, in that order, following. Each has over 1100 occurrences. There are no zero totals at all in summer and all stations with totals.

under 20 are confined to California and the Pacific Coast. At some of the latter points there has been a further decrease since the spring.

282. The chief feature of the diurnal variation in the summer is the further emergence of the 3d-period maximum. Its percentage frequency has now climbed to over 60 in the Southeast, to 75 in the Rockies and at topographically comparable stations in the East such as Asheville. In the Northeast, its percentage frequency is between 50 and 60 and it has definitely emerged as the dominant period for the first time in Texas, Arkansas, eastern Missouri, and in the region between the Lakes and the Ohio River. It has gained dominance even at places like Boston, Nantucket, Hatteras, Key West, and Buffalo; at these places, however, the 3d-period frequency is still mostly under 50%.

283. In the regions mentioned above there is thus overwhelming evidence of the importance of the insolation effect, whether direct or contributing. Its effect is still somehow counteracted, however, in a region spreading northward and fanwise from Oklahoma. Here the comparative frequencies, i.e., the sequences of the magnitudes, are still as they were in the spring. As before, the 3d period is occasionally highest but the 1st period seldom, and the differences between 1st, 3d, and 4th periods are not great. But the 2d period is always lowest. The result, to repeat, is that the combined number of occurrences in periods 1 and 4 always exceeds the combined number in 2 and 3, producing the so-called nocturnal maximum.

284. Along the Gulf Coast, a tendency that could be seen emerging in the spring becomes more evident. The 2d period now ranks second in frequency. At Galveston it is actually first by a narrow margin - 32.9% against 32.4 for the 3d period.

285. The highest probability of occurrence in the summer is at Tampa - 48.3% for the 3d period (see table 21). Thus, on any summer afternoon at Tampa there is practically a 50-50 chance of a thunderstorm occurrence. A few zero probabilities still show on the West Coast, some even for the 3d period.

286. In figure 89 the summer variations have been graphically analyzed in the manner of figure 85, which was for the annual variations. The main features of the two charts are much the same, as they should be since the annual totals are made up of summer occurrences predominantly. In the 1st period some above-normal areas appear in the Middle West on the summer chart which did not appear on the annual chart, indicating an intensification in the summer season of whatever phenomenon is responsible for the peculiar distribution. Greater frequencies appear on the Gulf Coast in the 2d period on the summer charts. The small area of below-normal frequency at Lincoln on the winter chart has moved to Yankton on the summer chart. In the 4th period, an above-normal area in Texas is eliminated on the summer chart. In that region, as has been seen, the diurnal variation changes from spring to summer, and spring contains the month of maximum occurrence, May.

287. Autumn. The autumn season (figure 90) shows, in general, a diminution of the strength of the 3d-period maximum. It is particularly evident in the Northeastern States where what is lost to the 3d period is transferred mostly to the 4th - possibly the maritime effect again coming to the fore as insolation decreases. At some stations like Portland (Maine), Eastport, Nantucket, and Atlantic City this change results in a definite 4th-period maximum. Also apparent,

particularly at the latter stations, is an increase in the percentage frequency for the 1st period. Similar changes are evident in Texas, and to a lesser extent, in the Southeast. The "nocturnal" region is still about the same as in the summer and shows about the same distribution of percentage frequencies.

288. The maximum number of occurrences for the autumn is 384 at Key West. There are no zero totals, and totals of 20 or less are still confined to California and the Pacific Coast. Most of the extreme coastal stations in the latter region show an increase of occurrences since the summer.

289. The highest probability of occurrence is 13.2% in the 3d period at Tampa and the few zero probabilities are confined to the 1st and 2d periods at some Far West stations (see table 21).

290. Numerical relations. All the charts of diurnal variation discussed thus far contain sufficient data to make possible the evaluation of the magnitudes involved in the diurnal variation. Table 21 lists the numerical values, as well as the percentage frequencies and probabilities. However, the numerical relations are not easily seen. In order to make them clear, the summer thunderstorm distribution (numerical) is repeated on a set of five charts. The first, figure 91, shows both the numerical averages and the isoceraunics for the entire day for the summer season of June, July, and August. The following four charts, figures 92-95, show the average numbers of occurrences and the isoceraunics for each of the quarter-day periods. It should be remembered that these charts are for thunderstorm occurrences and not thunderstorm days. They are also only roughly representative

of the annual distribution because the May maximum in Texas is excluded and also because more winter thunderstorms occur in the Gulf States than elsewhere.

291. However, on the total chart, figure 91, which includes the occurrences for all four periods, there appear the expected maxima over Florida and New Mexico, with a col or saddle over the Central States where the values increase from Del Rio to Kansas City and then decrease again toward Canada. Isoceraunics have been drawn for every eight occurrences on this chart. On the maps showing the numerical distributions for each quarter day the isoceraunics are drawn for every two occurrences so that, if exactly one-fourth the total number of occurrences occurred in a quarter period, the gradient over such a region would remain the same on the quarter-day map as on the total map. A steepened gradient would appear over a region where the quarter-day occurrences were in excess of 25% of the total and a weakened gradient where they were less.

292. The 00-06 map (figure 92) shows a startling change from the over-all pattern. The gradient has weakened throughout except in the Middle West, where it has strengthened. The area of maximum occurrence for the whole United States is now around Kansas City. Southeast of the Lakes region, along the Gulf Coast, and along the Atlantic Coast from New York to Georgia, the nocturnal maritime effect shows up in an increase of occurrences eastward, i.e., seaward - a tendency not observable on the over-all chart. The Santa Fe maximum has been replaced by a distinct minimum, one reason being that this is the period of the down-slope mountain wind. Away from the West

Coast the actual minimum point is at Atlanta - a total of only 5 occurrences in 20 years. In this connection it may be mentioned that, in an analysis of the ostensible causes of thunderstorms at St. Louis, Oklahoma City, Brownsville, and Atlanta, a cooperative project of the Weather Bureau and the University of Chicago ⁽³⁶⁾ found the insolation type of thunderstorm most predominant at Atlanta.

293. The 06-12 map (figure 93) restores the over-all maxima, with some displacement. The Florida maximum is now over Pensacola and on the peninsula itself Miami is the highest. A trough appears from Texas northward. Except for the West Coast, this trough contains the minimum values of the map in its southern half from West Texas to Eastern Colorado. It might be considered an eastward displacement of the Rocky Mountain trough of the previous period. The Appalachians appear as a divide between a secondary maximum on the west side and a secondary minimum on the east side - a condition attributable, in theory at least, to the windward and leeward effects of this ridge on the prevailing westerlies. In general, the gradient has steepened since the last map except in the Mississippi and Missouri Valleys, where it has weakened. That region has a comparatively moderate numerical frequency.

294. The 12-18 map (figure 94) shows an extraordinary steepening of gradient throughout. Neglecting the West Coast, the northern Lake region, and the Long Island Sound area, the areas of minimum occurrence are eastern Nebraska and extreme southern Texas - which could be interpreted as a displacement farther eastward of the Plains-Rockies trough of the previous map. The maximum value is now at Tampa with a very steep gradient toward Key West and Miami. The Santa Fe

maximum is retained, now definitely including other stations on the eastern slopes of the Rockies. A secondary maximum also appears at Helena, separated from the Santa Fe-Cheyenne isoceraunic ridge by low values at Lander and Salt Lake City. This trough, also seen on the previous map, is intensified by contrast with the adjoining maxima.

295. It is noteworthy, also, that the maximum value at Kansas City on the 00-06 map (9.2) is now equaled at the same station on this map. Kansas City, during this period, is on a line oriented SSW-NNE from southern Kansas to southern Minnesota, east of which there has been an increase of occurrences since the first period and west of which, up to the Nebraska trough, there has been a decrease of occurrences.

296. An interesting convolution of isoceraunics is evident over the Great Lakes. It can be described as a trough southeast of Lake Superior, a ridge west of Lake Michigan, a trough east of Lake Michigan, another ridge west of Lakes Huron and Erie, and then a trough east of the latter followed by a ridge which seems to parallel the Appalachian Highlands. The east-shore troughs are no doubt the effect of the stabilization of air in its eastward passage over the Lakes, whose surface temperatures are consistently lower than land-surface temperatures on summer afternoons. In Pennsylvania, Maryland, and Virginia, a trough appears again on the east or leeward side of the Appalachians.

297. On the 18-24 map (figure 95) the actual maximum, exceeding even values in the Southeast, is at North Platte, with reinforcement at Phoenix and El Paso. At Phoenix and North Platte the occurrences in

the 4th period exceed the occurrences in the 3d. A curved line from Dodge City to Kansas City to La Crosse now separates a region on the east where occurrences have decreased since the last map, from a region on the west where occurrences have increased since the last map. The Midwest trough has moved farther east, its axis now approximately from Corpus Christi to Dubuque. Part of the area formerly in the trough is, as previously indicated, under the influence of the North Platte maximum. Looked at differently, it is possible to say that the North Platte isoceraunic ridge moves eastward to Kansas City by 00-06 (the next period) and disappears, or merges with adjoining ridges, on the following two maps.

298. Along the Great Lakes during the 4th period there appear to be troughs on the west side and ridges on the east side of each Lake area. In the eastern part of the country the high points are Charlotte, Macon, and Tampa. A trough tendency still appears along, or slightly east of, the Appalachian Divide in Tennessee-North Carolina. An east-west ridge extends from Washington to Pittsburgh to Cincinnati.

299. A further expression of the magnitude of the activity in the nocturnal-thunderstorm belt can be obtained by plotting a chart of thunderstorm occurrences in the summer but excluding the occurrences during the hours 12-18, the 3d period. On such a chart (not reproduced) the area of, roughly, Kansas, Iowa, and Nebraska, which is a comparatively low area on the over-all summer chart, becomes the area of the secondary maximum. Its values are exceeded only by those in Florida. The Santa Fe maximum is lower. Additional maxima of the secondary order (20 plus) occur also at Wichita, Terre Haute, and Cincinnati.

300. Maximum hour. Although no analysis of the diurnal variation by hours has been made for this report, the hours of maximum thunderstorm occurrence have been investigated during each of the summer months, June, July, and August. The data showed too much scatter to allow the construction of isochrones connecting points with the same maximum hour. However, a predominance of early afternoon and even forenoon hours (11-14, inclusive) was found in the Gulf, northern Lake and Southeast Coastal region, a large number of 13-14 maximum hours in both the southern Appalachian and Rocky Mountain regions, and a scattering of maximum hours between 18 and 04 in the nocturnal-thunderstorm region of the Middle West as well as the lower Lake region and the southern New England Coast. Elsewhere the maximum hour is predominantly 17 or 18. There are no maximum hours between 07-10, inclusive, while 15, 16, and 18 are close behind the apparently predominant maximum hour of 17.

The nocturnal thunderstorm

301. The excessive occurrence of nocturnal thunderstorms is not peculiar to the United States. It is generally agreed, for instance, that nighttime thunderstorms are more common than daytime thunderstorms over oceans. C. E. P. Brooks (5) quotes Meinardus as stating that the period of maximum occurrence over the ocean is 00-04. The report of the H. M. S. Challenger quoted by Shaw (37) shows that of 235 occurrences of thunder and lightning over the open sea 44.6% were during the hours 00-06 and 48.5% during the hours 18-24. Shaw (38) also gives figures indicating nocturnal maxima of thunderstorm activity in the Caribbean and the open ocean near the West Indies, and the absence

of a nocturnal minimum in the Gulf of Mexico. The explanation usually accepted for this widespread phenomenon is the special nature of the diurnal variation of atmospheric instability over oceanic areas. Over land the time of maximum insolation and therefore maximum surface heating is also the time of maximum instability. The open sea surface, however, has a diurnal temperature range of only about 1 F while that of the atmosphere at a height of 500 to 1000 meters is several times as great ⁽⁵⁾, so that vertical temperature gradients favoring convection occur most frequently in the early morning hours when the atmosphere as a whole is cooling by radiation.

302. Coastal stations have also been found to have apparently anomalous periods of maximum thunderstorm activity. Over coastal Germany, for instance, there is a tendency toward a 06-09 maximum ⁽⁵⁾. This can be attributed to the instability of maritime air at that time and to the fact that it is also the time of the greatest temperature increase from land to sea, the resulting land breeze perhaps acting as a minor cold front.

303. No widespread continental area of maximum nocturnal thunderstorm activity is well known outside of the United States, although isolated station averages that may represent significant areas have been noted. One such case is that of Cordoba in the Argentine interior where the 1st and 4th periods each account for 29% of the total thunderstorm occurrences ⁽⁵⁾. Many explanations of the phenomenon have been offered. It is obvious that any factor tending to steepen the lapse rate or to realize potential instability can be the cause, and the only factor automatically ruled out in the consideration of the causes of nocturnal

thunderstorm activity is insolation heating. Fronts, topographic barriers, convergent-flow patterns, heating from below due to the higher temperatures of the surface traversed, cooling aloft due to radiational losses from moist to dry layers, convective instability attained by evaporation of rainfall, advection of warmer air in the lower layers or colder air in the upper layers -- any of these may cause the nocturnal thunderstorm. However, properly to explain the nocturnal maximum, a causative factor must be found which has a geographical distribution similar to that of the region of the nocturnal thunderstorm maximum and which also has a corresponding diurnal variation. Not until recently has an explanation fulfilling these requirements been found. This was done by Means in a paper previously cited (7). The author generously permitted the Hydrometeorological Section the use of his material while still unpublished. In the published version there have been some changes in charts and data that do not, however, affect their use in this report.

304. Means chose Omaha as a representative station because it was well located with reference to the general area of nocturnal thunderstorm occurrences and because radiosonde and upper-air wind data were available. Of 69 thunderstorm occurrences in 1941, he selected 51 as classifiable with respect to the principal factor contributing to the instability prior to the formation of the thunderstorm. These factors and the number of occasions each was considered to be the principal one are listed below:

Evaporation from precipitation.....	6 cases	
Frontal lifting.....	4	"
Surface heating or turbulence.....	8	"
Advection cooling aloft.....	5	"
Advection warming in lower layers....	28	"

Of the last type, most of the occurrences were at night, defined by Means as 8 p.m. to 8 a.m. Apparently this type contributed most to the nocturnal maximum.

305. In addition to the evidence of consecutive radiosondes, the fact of advective warming can also be indicated, as Means does, by the pattern of the isobars and isotherms on a fixed-level chart. On the assumption that the flow is approximately horizontal and gradient, any instance of isobars crossing isotherms means advective cooling or warming and a condition of closely packed isobars perpendicular to closely packed isotherms indicates the greatest advective effect. If the flow indicated by the isobars is from warm to cold, the advection is of warm air. In figure 96, taken from the Monthly Weather Review for the months indicated, the mean monthly isobars and isotherms at the 5,000- and 10,000-foot levels for July and August 1941 are shown. They indicate, first, a maximum warming effect over the main area of nocturnal thunderstorm activity. Second, they show the warming to be more rapid at the 5,000- than at the 10,000-foot level, which means a definite average steepening of the lapse rate due to that effect. These conditions are typical of mean summer charts.

306. The type of advection can also be demonstrated from the variation of the wind with height. It can be shown ⁽³⁹⁾ that the wind turns with height within a layer in such a way as to become more nearly parallel to the orientation of the mean isotherms of that particular layer. The vectorial difference between the wind at the bottom of the layer and the wind at the top of the layer is called the thermal wind, which is a vector that parallels the mean isotherms, directed so that the colder air is on the left, and with its magnitude directly proportional to the mean-temperature gradient in the vicinity. For the simplest illustration, a wind speed constant with height can be assumed. If, in such a case, there is a veering of wind direction with height (e.g., from south to west), the thermal wind, or vectorial difference, is directed from northwest to southeast. The warmer air is therefore southwest of the station (to the right of the thermal wind vector), southwest also being the mean wind direction of the layer. Thus a veering of wind with height indicates advective warming and, similarly, a backing with height indicates advective cooling.

307. A hodograph of the winds aloft (a plot of the wind vectors at various levels from a common origin) will therefore portray the variation of the advective effect with height. For any given layer the advective effect is proportional to "the area swept out by the wind vector," that is, the area of the triangle made by the lower wind vector, the upper wind vector, and the thermal wind vector, which is equal to $\frac{1}{2} V_1 V_2 \sin A$ where A is the angle between the lower and upper wind vectors, V_1 and V_2 . Twice the area of the triangle, or $V_1 V_2 \sin A$, can also be used for comparative purposes. In terms of

the area (or twice the area) a veering of wind with height is considered negative, a backing positive.

308. In figures 97 and 98, reproduced from his paper, Means has evaluated the quantity $V_1 V_2 \sin A$ from wind-resultant data for stations in the United States found in the Airway Meteorological Atlas (34). The negative areas indicate advective warming. Its maximum occurrence can be noted over the Midwestern area of interest. Also, comparison of the two figures shows that the warming is greater in the layer from the surface to 3 km (figure 97) than in the layer from 3 km to 5 km (figure 98), which is a type of variation of the advective effect with height favoring the production of instability.

309. Finally, in figure 99, also taken from Means, the same values for the Midwestern region are plotted separately for the four pilot-balloon observations of each day in order to demonstrate the diurnal variation of the advective factor in the layer, surface to 3 km. A sharp diurnal variation is evident, with the maxima at the 2300 and 0500 EST observations, which agrees with the diurnal thunderstorm variation in the region.

Days with more than one thunderstorm

310. The availability of two practically concurrent records, one of thunderstorm days and the other of thunderstorm beginnings, suggested the possibility of discovering the distribution of areas in which more than one thunderstorm per day was likely and an examination of the likelihood of such multiple occurrences within those areas. The period of record for the thunderstorm occurrences (or beginnings)

is the 20 years, 1906 to 1925 (Gregg's data), while the period of record for the thunderstorm days is 1904-23, from Alexander's second paper on the distribution of thunderstorms in the United States ⁽³⁾. Only the averages (to whole numbers), rather than the totals, were compared, making it unnecessary to extrapolate to 20 years any data that were for a shorter period. Considering the nature of the data and the final results, this method was sufficiently accurate.

311. It was surprising to find a number of stations which, in this comparison, had actually fewer thunderstorms than thunderstorm days. This cannot be attributed entirely to differences in periods of record, either. The day is, naturally, the calendar day and, therefore, a thunderstorm lasting through midnight makes one occurrence, but two thunderstorm days. However, no such negative differences were used; in such cases the difference was always called zero.

312. On such a basis, then, the annual number of thunderstorm occurrences in excess of thunderstorm days for each station was plotted on the map shown in figure 100 and lines of equal excess occurrence drawn. Assuming the occurrence of more than two thunderstorms per day to be unlikely enough to be negligible, the values indicated can be interpreted to mean the average annual number of days on which more than one thunderstorm occurs at the particular station. Actually each number is the excess of thunderstorm beginnings or occurrences over the number of calendar days with thunderstorms. Percentages, representing this excess as a percentage of the average number of calendar days on which thunderstorms occur, were also computed and plotted but the chart is not reproduced because it did not make the over-all pattern any more

comprehensible. The method resulted, in fact, in what seemed to be false emphasis when, as in the Pacific States, an excess of only one occurrence produced a percentage of 25 because of the low frequency of thunderstorm days. Such a percentage was exceeded at only a few other stations.

313. The Section had an opportunity to test the validity of the method used by examining the detailed record of thunderstorm occurrences at Detroit during the years 1906-1925. In these 20 years the excess of thunderstorm occurrences over thunderstorm days appeared to be 43 (835 - 792). The detailed record showed, however, that there were 109 occasions during the 20 years when a thunderstorm occurred on the same calendar day as another. This means that 66 (i.e., 109 - 43) of these occurrences were masked by the practice of designating two days with thunderstorms when one occurrence straddles midnight. Actually, though, there were more than 66 occurrences through midnight; there were 82, but 16 of them did not affect the record in the same way because another thunderstorm occurred later in the second day. The occurrence was counted an extra one only on the day that it began. By this analysis of the detailed data, then, the average annual excess of thunderstorm occurrences over thunderstorm days at Detroit is 4. By the method used in developing figure 100 it was 2.

314. There is also a distinct possibility that most of the 1906-25 records underestimate the number of thunderstorm occurrences. Observers will naturally differ in deciding whether prolonged thunderstorm activity consists of one or more distinct thunderstorms since the decision is often, at best, an uncertain one. The less conscientious

may decide that only one thunderstorm occurred because such a decision simplifies the written record. More important, however, is the fact that a station making continuous observations 24 hours a day will be more distinctly aware of multiple occurrences. There were no such stations in 1906-25. Means ⁽⁷⁾ made a count of thunderstorm occurrences at Omaha Airport for the period 1937-41. Comparison with the thunderstorm-day count for the same years shows an average excess occurrence of 13 while the value used in figure 100 is only 5. The data reported by the cooperative thunderstorm project of the Weather Bureau and the University of Chicago ⁽³⁶⁾ includes a tabulation of thunderstorm days and thunderstorm occurrences at Atlanta Airport for the years 1939-43. There were 405 thunderstorm occurrences against 299 thunderstorm days during this period, which gives an average excess occurrence of 21, while the value of figure 100 for Atlanta is just 1. On the other hand, through the courtesy of W. A. Mattice, a thunderstorm-occurrence count is available for the years 1905-43 for Washington, D. C. The count is 1623 compared with a thunderstorm-day total for the same period of 1459. The average excess occurrence thus becomes 4, which is exactly the value used in figure 100. Nevertheless, the fact that the recent Atlanta and Omaha records are from airports is of extreme importance in evaluating these comparisons. Only continuous observations can provide the true thunderstorm-occurrence record.

315. An examination of figure 100 does not readily reveal any important patterns, although it may be remarkable that isolines can be drawn to circumscribe any appreciable areas whatsoever. The larger numbers, except in Florida, are not confined to the regions of greatest

frequency of thunderstorms nor are the smaller numbers, except on the West Coast, confined to the regions of least frequency. The percentage pattern, as previously mentioned, changes all but the zero areas but does not offer a more comprehensible distribution. The comparatively large excess in Florida is, however, probably significant. Bily⁽¹⁸⁾ has mentioned the likelihood of recurrence in the normal or local thunderstorm situation at Tampa and the extreme unlikelihood of recurrence when the storm is frontal. A priori, it was also considered possible that a region in which quasi-stationary frontal activity was frequent would also be revealed as a region of maximum recurrence of thunderstorms. This seems to be confirmed by the pattern in the Lower Lakes and Ohio Valley region, a common location for quasi-stationary fronts. There is also an excess pattern which bears an approximately parallel relation to the Continental Divide, another characteristic location for a quasi-stationary front. But here the excess is chiefly a summertime phenomenon, while the front is a phenomenon of the cooler months.

316. The chart and the discussion are offered chiefly as a rough though inadequate guide to the distribution of the recurrence phenomenon and to avoid the waste of anyone's repetition of this particular technique. The proper approach must be through individual and detailed station data, preferably from airport stations keeping a 24-hour observational watch. In such an investigation the days with thunderstorms should be defined as days in which thunderstorms begin. This will avoid the midnight problem and also reduce the number of days. Whether any pattern will emerge from such a study is problematical.

Diurnal variation of rainfall

317. In previous sections it has been shown that the relation between thunderstorm activity and rainfall is not always direct and that the relation varies both geographically and temporally. A comparison of the diurnal variations of rainfall and of thunderstorm activity might also be made. Results of such a comparison are suggested in available tabulations of the diurnal variation of rainfall at various stations. Most of these tabulations have been published in the Monthly Weather Review. Wherever such tabulations were available, this report has reorganized the data to make the values comparable to the 6-hourly diurnal thunderstorm distribution. Because additional data were also available, comparisons of the monthly variations of thunderstorm and rainfall values have been included (figures 101-118).

318. The data for each station are charted on a separate figure which is divided into two parts, the upper showing the variation of the elements by months, the lower the variation of the elements diurnally and seasonally after the fashion of the investigation of the diurnal variation of thunderstorms. In so far as possible, the data were reduced to the same periods and units for all stations. For some months and some seasons, however, not all the rainfall data were available and in two cases there were no available diurnal-variation data. For the monthly variation, the thunderstorm-day monthly averages from the 1904-43 period of table 1 and figures 28-31 were used. For the diurnal variation the thunderstorm-occurrence values from the Gregg data were used (table 21). Three types of rainfall data are shown on the charts. One is average rainfall (R). The monthly values of R are

monthly averages of rainfall from comparative-data summaries. The seasonal 6-hourly values of R are from the diurnal-variation tabulations used, which are usually for periods of record from 10 to 20 years. Another rainfall value charted is frequency in hours (F). This usually means the average number of hours in which .01 inch or more of precipitation occurred. At some stations F was based on a count of hours with a trace or more, in one case on hours with 0.10 inch or more, and in two others on actual duration. The pertinent facts are always indicated on the charts. The third rainfall value charted is that of hourly intensity (I) which is simply R divided by F for the particular period considered. In the following discussion the abbreviations R, F, and I, will be used, and the thunderstorm curves will be referred to as T curves, although they are identified on the figures by the usual thunderstorm symbol.

319. At many of the stations, it will be seen, there is a definite tendency toward both higher intensities and longer durations of rainfall at night. This tendency has previously been noted in the literature. One of the theories explaining the effect has been that the higher relative humidity of the atmosphere during this period of lower temperatures reduces the evaporative capacity of the air. Rain can therefore fall through it without so much depletion by evaporation. Shipman ⁽⁴⁰⁾, in fact, offers that suggestion in explanation of the phenomenon at Ft. Smith, Arkansas. In a recent paper ⁽⁴¹⁾, R. V. Dexter suggests that the tendency toward a maximum in both the amount and in the width of the band of warm-front rainfall in the early morning hours may be accounted for by the radiational (insolational)

heating of the warm-sector air near the surface during the day. This increases the surface wet-bulb temperature more rapidly than the wet-bulb temperatures aloft; hence the convective instability of the surface layer is increased. By early morning the air ascending the warm-front surface has undergone sufficient lift to cause saturation and the realization of the convective instability of the layer. On the other hand, the air which ascends during the day has been cooled by radiation during the preceding night, resulting in a decrease in its convective instability.

320. There is still another possible explanation. Isobars in general make acute angles with a front and the front lies in the trough of low pressure. Any decrease of the component away from the front while the component toward the front remains unchanged or increases will thus produce convergence. Nongradient effects like friction cause a deflection of the wind toward lower pressure and therefore can cause an increase of the wind component against the front and a decrease of the wind component away from the front. Such a deflection is greatest when the wind is lightest and the air most stable, greatest therefore at night. At a cold front, friction produces convergence at any time. But with strong winds and a k-type air mass on the cold side and light winds (and stabilized air) on the warm side, the nocturnal effect will be to decrease the warm-air component away from the front while the cold-air component moving the front will tend to remain constant. The result will be added convergence in the lowest layers. At the warm front it is the cold air which is moving away from the front and, if its stability is sufficiently pronounced, the nocturnal effect will again be toward a decrease of its component away from the front and the production of added convergence.

321. Humphreys (42) has pointed out that, because of comparative cloudiness in the warm sector and comparative clearness in the cool sector of the extratropical cyclone, there is a tendency to develop an increased temperature contrast and therefore a greater cyclonic intensity at night. Also, because of thermal convection, there is a greater retardation of the flow of cold air by night than by day.

322. It has been suggested by Means (7) that, because nocturnal storms are not insolational in origin and the mechanism is dynamic (frontal, convergent, or advective) and therefore not self-liquidating like the insolational mechanism, the storm is likely to be of longer duration. The high F values of the 1st and 4th periods at many of the stations may be examples of this effect. Means found the average duration of daytime thunderstorms at Omaha to be about 85 minutes, while the average duration of nighttime thunderstorms was about 120 minutes.

323. Nevertheless, there is no pattern of the diurnal variation of rainfall that applies everywhere, as the analyses of the available station data demonstrate. Hann (43) realized this and therefore said:

Studies of available records do not warrant making a concise statement of the general characteristics of diurnal variation of intensity of rainfall; one can only present some of the more distinct types.... In the continental type of the temperate zone there is a principal maximum in the afternoon and a lesser maximum in the early morning hours, while the prominent minimum occurs between midnight and 4 a.m., and a secondary minimum between 8 a.m. and noon. In the oceanic type, the times of principal maxima and minima are the reverse of those in the continental type.

However, his types are contradicted by some of the station data that follow.

324. The most noteworthy exceptions to the continental pattern are Kansas City (44), Lincoln (45), and Topeka (46), figures 101-3, stations definitely continental but also definitely within the area of excessive nocturnal thunderstorm activity. Where the data are available, R, F, and I are highest in the 1st or 4th periods all seasons. Also, since the average number of thunderstorm occurrences in the 1st or 4th period is not much greater than the number of occurrences in the 3d period, the indications are that the nighttime thunderstorms in this region last longer, produce more rain, and are characterized by higher intensities than the daytime thunderstorms.

325. Similar but less extreme effects appear at the stations on the edges of the nocturnal thunderstorm zone: Oklahoma City (47), Fort Smith (40), Sault Sainte Marie (48), Lansing (49), Chicago (50), and Springfield, Illinois (51), figures 104-9. Though T often peaks in the 3d period of these stations, the peak is not as outstanding as at stations definitely outside the nocturnal thunderstorm region, and T for periods 1 and 4 combined usually exceeds T for periods 2 and 3 combined in all but the summer season. However, in all seasons R and F are at a maximum or nearly so in the nighttime periods 1 and 4, thus exceeding the total daytime R and F. Intensity values are also usually higher in periods 1 and 4. All the effects are more pronounced in the spring and autumn than in summer. Unusually consistent patterns of the diurnal variation of F through all seasons are shown at Oklahoma City (2-1-4-3) and Fort Smith (2-3-4-1). It should be noted that F values are low at Oklahoma City because they are based on actual duration, and even lower at Springfield because they are based on hours with 0.10 or more instead of the usual .01 or more.

326. The continental 3d-period maximum in all elements all seasons is shown best at New Orleans ⁽⁵²⁾, figure 110, and also indicated by the partial data available for Tampa ⁽⁵³⁾, figure 111, although these stations can reasonably be classified as maritime. However, a similar variation appears at the more definitely continental stations: Memphis ⁽⁵⁴⁾, Nashville ⁽⁵⁵⁾, Syracuse ⁽⁵⁶⁾, and Denver ⁽¹⁴⁾, figures 112-15. At these stations, and also at Portland, Maine ⁽⁵⁷⁾ and Baltimore ⁽⁵⁸⁾, figures 116-17, the available data show the continental type of variation most distinctly in the summer season. In other seasons, particularly spring and fall, although T still peaks in the 3d period with decided minima in the 1st and 4th periods, the R, F, and I values show an apparent nocturnal increase. The confinement of the nocturnal effect to these seasons emphasizes its connection with frontal rather than air-mass or local activity. At San Francisco ⁽⁵⁹⁾, figure 118, the maritime intensification of nocturnal activity becomes apparent in the high R and F values for the 1st and 4th periods during the rainfall season. A remarkable all-season consistency of the F variation is displayed by Baltimore - a 2-1-4-3 pattern. At this station a minimum F accompanies the 3d-period maximum in the other elements, while the much greater values of F in the 1st and 2d periods have apparently little effect on R.

327. The monthly-variation portions of the charts of rainfall-thunderstorm relations simply repeat for specific points the variation in thunderstorm frequency and average precipitation already indicated in the distribution charts previously described (figures 28-31 and 38-41). With some exceptions, the additional F and I curves, when

available, show a fairly consistent pattern, with maximum F in winter and minimum in summer, and a reversal of this pattern in I. From McDonald's data for New Orleans ⁽⁵²⁾, it has also been possible to compare monthly variations of F for various magnitudes of hourly intensity (figure 119).

328. A few other pertinent summaries of the diurnal variation of rainfall have appeared which have not been adapted for the type of graphical analysis used in this report. In a study at Los Angeles, French ⁽⁶⁰⁾ found that the hourly frequency of rains of .01 inch or more was 14% greater in the hours (all local standard time in this discussion) 6 p.m. to 6 a.m. than in the period 6 a.m. to 6 p.m. R was 23% greater in the first-mentioned period. The greatest F, almost 13% in terms of probability, occurred in the hour 5-6 a.m.; the least, less than 9%, in each of the hours 4-5 p.m. and 12-1 p.m. The greatest hourly total of rain, over 16 inches from 1905 to 1913, occurred also between 5-6 a.m. and the least, about 8.5 inches, in the hour 4-5 p.m. At Galveston, Tannehill ⁽⁶¹⁾ found the maximum hourly F to be at 9 a.m. for hourly rains of .01 inch or more, 0.10 inch or more, and 0.20 inch or more. Otherwise, however, the variation of the hourly frequency of the .01-inch-or-more amounts was only a rough, qualitative guide to the variations of the higher intensities. Tannehill explained the fall of frequency after 9 a.m. as due to the suppression of convection by the sea breeze at Galveston. Loveridge ⁽⁶²⁾ found maximum R and F occurring around 4 a.m. at Honolulu, with secondary maximum between 8 and 10 p.m., and minima between noon and 2 p.m. The variation was intensified in a summer month like July. Additional studies of the monthly

variation of F have been made at Philadelphia by Mindling ⁽⁶³⁾ and at Havre, Montana, by Math ⁽⁶⁴⁾.

329. Figure 120, after Kincer ⁽⁶⁵⁾, is an over-all picture of one aspect of the diurnal variation of rainfall during the months from April to September, inclusive. On it are shown the percentages of the total rainfall in these months occurring between the hours 8 p.m. and 8 a.m., EST. This period is approximately equivalent to periods 4 and 1 in the foregoing analysis; in the Middle West, in particular, there is only a one-hour discrepancy. The chart in general supports the conclusion of greater nocturnal R values, especially in the nocturnal-thunderstorm region where a 65% center can be observed. Values above 50% are also indicated near San Francisco and along the western portion of the Mexican border. Percentages less than 50 occur over the Rockies and in the East, the lowest values being on the Gulf Coast, with low centers around New Orleans and Tampa. No conclusions as to duration and therefore intensity can be drawn from this type of chart.

330. While data were lacking for a country-wide study of the diurnal variation of rainfall of selected intensities, there were data available for a class of intensities defined as "excessive"* by the Weather Bureau. These have been discussed in an earlier section where it was pointed out that Yarnell ⁽²⁴⁾ had published monthly charts of their frequency distribution although the available tabulated data were not comparable for northern and southern stations. However, the tabulations (in the annual Report of the Chief of the Weather Bureau

* See footnote page 128.

and later in the Meteorological Yearbook) included, through 1936, the time and date of each occurrence of excessive rain at every reporting station. These provided the basic material for a study of the diurnal variation. The occurrences thus investigated were for the same period of record as Yarnell's charts - 1904-33. It was reasoned that the discontinuity in criteria for tabulation, which mars the distribution charts, would probably not result in a discontinuity in diurnal variations. That such an assumption was valid is indicated by the results in figure 121, in which the distributions of the percentages of excessive-rain occurrences are shown for each quarter day, annually and for the summer. The resemblance to figures 85 and 89, which exhibit similar analyses of thunderstorm occurrences, is amazing. The same divisions and shadings are used on all four charts to facilitate comparison. It would be possible to substitute one of the excessive-rainfall charts for the corresponding thunderstorm chart with only slight loss in accuracy of detail. Within the limitations of the tabulated data, it can be said that the diurnal variation of excessive-rain occurrences is identical with the diurnal variation of thunderstorm occurrences in the same region and that therefore a region of pronounced nocturnal thunderstorm activity is also a region of equally pronounced nocturnal occurrence of excessive rain.

References

331. Abbreviations used in the list of references are explained in the Bibliography. See Appendix.

1. W. J. Humphreys, *Physics of the air*, 1940, p. 327-8.
2. USDA, *Climate and Man*, Yearbook, 1941.
3. W. H. Alexander, The distribution of thunderstorms in the United States, *MWR*, v. 43, 52, and 63, Jul. 1915, Jul. 1924, and May 1935 (for the years 1904-13, 1904-23, 1904-33, respectively).
4. A. M. Hamrick and H. H. Martin, Fifty years of weather in Kansas City, Mo., *MWR*, Supp. 44, 1941.
5. C.E.P. Brooks, The distribution of thunderstorms over the globe, *GBMO*, *Geoph. Mem.*, no. 24, 1925.
6. T. R. Reed, The North American high-level anticyclone, *MWR*, v. 61, Nov. 1933, p. 321-5. Further observations on the North American high-level anticyclone, *MWR*, v. 65, Oct. 1937, p. 364-6.
7. L. L. Means, The nocturnal maximum occurrence of thunderstorms in the Midwestern States, *Dept. of Met., Univ. of Chicago, Misc. Rpts.*, no. 16, Univ. of Chicago Press, 1944.
8. C. F. Talman, Terminological footnote to Alexander's second paper (3), p. 337.
9. A. K. Showalter, Further studies of American air-mass properties, *MWR*, v. 67, Jul. 1939, p. 204-18.
10. N. K. Johnson and G.S.P. Heywood, An investigation of the lapse rate of temperature in the lowest hundred metres of the atmosphere, *GBMO*, *Geoph. Mem.*, v. 9, no. 77, 1938.
11. S. Petterssen, *Weather analysis and forecasting*, 1940, p. 269.
12. J. Namias and K. Smith, Normal distribution of pressure at the 10,000-foot level over the Northern Hemisphere, *USWB*, June 1944. (Restricted).
13. F. H. Bigelow, Report on the barometry of the United States, Canada, and the West Indies, Report of the Chief of the Weather Bureau, 1900-1901, v. 2, p. 638 ff.
14. A. W. Cook, The diurnal variation of summer rainfall at Denver, *MWR*, v. 67, Apr. 1939, p. 95-8.
15. G. Norton, Some notes on forecasting for Atlanta and Miami districts, *USWB*, Research Paper no. 15, Feb. 1944.
16. J. C. Albright, Summer weather data, The Marley Co., Kansas City, Kansas, 1939.

17. M. L. Fuller, compiler, Annual Meteorological Summary with Comparative Data, 1941, for Peoria, Ill., WBO, Peoria.
18. J. Bily, Jr., Thunderstorms at Tampa, Fla., MWR, v. 32, Oct. 1904, p. 457-60.
19. I. R. Tannehill, Hurricanes, 1944, p. 120.
20. USWB, Maps of seasonal precipitation, percentage of normal by states, 1886-1938; Tables of normals and 10 wettest and 10 driest seasons and years; WB Pub. no. 1353, 1942.
21. W. F. McDonald, Average precipitation in the United States for the period 1906 to 1935 inclusive, USWB, 1944.
22. H. D. Dyck and W. A. Mattice, A study of excessive rainfall, MWR, v. 69, Oct. 1941, p. 293-301.
23. HMS, Off. of Hyd. Dir., USWB, A report on depth-frequency relations of thunderstorm rainfall on the Sevier Basin, Utah, in coop. with the Flood Control Office of Land Use Coordination, USDA, June 1941.
24. D. L. Yarnell, Rainfall intensity-frequency data, USDA, Misc. Pub. no. 204, Aug. 1935.
25. Miami Conservancy Dist., State of Ohio, Engineering Staff, Storm rainfall of eastern United States, Tech. Rpts., part V (rev.), Dayton, Ohio, 1936.
26. H. Lemons, Hail in high and low latitudes, BAMS, v. 23, Feb. 1942, p. 61-8.
27. S. Petterssen, Weather analysis and forecasting, 1904, p. 39.
28. W. N. Shaw, Manual of meteorology, v. 1, 1932, chap. II.
29. H. Landsberg, A climatic study of cloudiness over Japan, Inst. of Met. (Dept. of Met.), Univ. of Chicago, Misc. Rpts., no. 15, Univ. of Chicago Press, 1944.
30. A. L. Shands, The hail-thunderstorm ratio, MWR, v. 72, Mar. 1944, p. 71-3.
31. A. K. Showalter, The tornado, an analysis of antecedent meteorological conditions, in Preliminary report on tornadoes, HMS, Off. of Hyd. Dir., in coop. with WACM, USWB, 1943.
32. R. L. Day, Characteristics of thunderstorms at Portland, Maine, USWB, unpub. ms.

33. G. W. Alexander, Lightning storms and forest fires in the State of Washington, MWR, v. 55, Mar. 1927, p. 122-9.
34. USWB, Airway Meteorological Atlas for the United States, WB Pub. no. 1314, 1941.
35. R. H. Weightman, Forecasting from synoptic weather charts, USDA, Misc. Pub. no. 236, rev., 1940, p. 10.
36. A. V. Carlin, D. L. Jorgensen, R. H. Simpson, and L. L. Means, Analyses of thunderstorms in the South and Central United States, USWB, in coop. with Univ. of Chicago, 1944.
37. Ref. 28, v. 2, 1936, p. 29.
38. Ref. 28, v. 2, 1936, p. 409.
39. B. Haurwitz, Dynamic meteorology, 1941, p. 148-50.
40. T. G. Shipman, The east wind and its lifting effect at Fort Smith, Arkansas, MWR, v. 53, Dec. 1925, p. 536-9.
41. R. V. Dexter, The diurnal variation of warm-frontal precipitation and thunderstorms, QJMS, v. 70, Apr. 1944, p. 129-37.
42. W. J. Humphreys, The greater increase in size and intensity of the extratropical cyclone by night than by day, MWR, v. 55, Nov. 1927, p. 496.
43. J. von Hann and R. Suring, Lehrbuch der Meteorologie, 3d ed., 1915, p. 343.
44. H. H. Martin, Hourly distribution and intensity of precipitation at Kansas City, Mo., MWR, v. 70, Jul. 1942, p. 153-9.
45. H. G. Carter, Variations in hourly rainfall at Lincoln, Nebr., MWR, v. 52, Apr. 1924, p. 208-11.
46. S. D. Flora, Hourly precipitation at Topeka, Kans., MWR, v. 52, Apr. 1924, p. 211-12.
47. H. F. Alexander, A study of the hourly precipitation at Oklahoma City, Okla., MWR, v. 66, May 1938, p. 126-30.
48. C. L. Ray, Hourly rainfall probabilities at Sault Ste. Marie, Mich., MWR, v. 55, Jul. 1927, p. 323-5.
49. C. L. Ray, Hourly rainfall probabilities at Lansing, Mich., MWR, v. 53, June 1925, p. 256-8.

50. H. Cox and J. H. Armington, The weather and climate of Chicago, Geog. Soc. of Chicago, Bull. no. 4, 1914.
51. W. F. Feldwisch, The probabilities of 0.10 inch, or more, of rainfall at Springfield, Ill., MWR, v. 52, Dec. 1924, p. 581-3.
52. W. F. McDonald, Hourly frequency and intensity of rainfall at New Orleans, La., MWR, v. 57, Jan. 1929, p. 1-8.
53. W. J. Bennett, Some characteristics of the rainy season at Tampa, Fla., MWR, v. 57, Aug. 1929, p. 323-6.
54. A. R. Long, Hourly precipitation at Memphis, Tenn., MWR, v. 56, Feb. 1928, p. 58-9.
55. R. Nunn, Hourly precipitation at Nashville, Tenn., MWR, v. 50, Apr. 1922, p. 180-84.
56. M. R. Sanford, Hourly precipitation at Syracuse, N. Y., MWR, v. 51, Aug. 1923, p. 395-6.
57. R. L. Day, The diurnal distribution of precipitation at Portland, Maine, in winter and summer, USWB, unpubl. ms.
58. O. L. Fassig, Report on the climate and weather of Baltimore and vicinity, Maryland Weather Service, v. II, 1907.
59. R. C. Counts, Jr., Hourly frequency and intensity of rainfall at San Francisco, Calif., MWR, v. 61, Aug. 1933, p. 225-8.
60. G. M. French, Hourly rainfall at Los Angeles, Calif., MWR, v. 52, Dec. 1924, p. 583.
61. I. R. Tannehill, Frequency distributions of daily and hourly amounts of rainfall at Galveston, Tex., MWR, v. 51, Jan. 1923, p. 11-14.
62. E. F. Loveridge, Diurnal variations of precipitation at Honolulu, Hawaii, MWR, v. 52, Dec. 1924, p. 584-5.
63. G. W. Mindling, Hourly duration of precipitation at Philadelphia, MWR, v. 46, Nov. 1918, p. 517-20.
64. F. A. Math, Duration of rainfall at Havre, Montana, MWR, v. 57, Nov. 1929, p. 468-71.
65. J. B. Kincoer, Precipitation and humidity, in Atlas of American Agriculture, pt. II, Climate, USDA, Mar. 1922. (This is the first of three sections on climate.)

CHAPTER III

THE RELIABILITY OF AREAL RAINFALL DETERMINATION

Need for reliability determination

332. The results of cooperative storm studies by the U. S. Engineer Department and the Hydrometeorological Section are summarized in the form of duration-depth-area data. In the general field of hydrology, average depths of basin rainfall in individual storms, based on either arithmetic or weighted means of rainfall observations, are used to establish rainfall-runoff relations. It is important to know the limits of error involved in such use of rainfall data. The relation between the accuracy of the areal rainfall determination and the density of the observational network is also involved in the design of a rain-gage system for an experimental basin or a reporting network for the purpose of flood forecasting. The optimum number and spacing of the gages depends finally, however, on the precision desired.

333. Thunderstorm rainfall is especially characterized by extreme irregularity of areal pattern. The isohyetal map may feature a number of cells or centers produced by scattered outbreaks of local thunderstorms. Even when the rainfall is general throughout a large area for the entire period of storm activity, the total-storm isohyetal map often shows several intense centers with sharp rainfall gradients. The usual network of rain gages is too widely spaced to provide an adequate picture of the rainfall distribution in either type of storm. Consequently, the estimation of volumetric amounts for small areas may be subject to large inaccuracies. It is the purpose of this chapter

of the report to analyze these errors in volumetric determination of thunderstorm or convective type of rainfall.

Sources of error

334. The sources of error in areal rainfall estimates include instrumental deficiencies, nonrepresentativeness of gages, and inadequate sampling. An excellent analysis of the first two, namely, the inadequacies of rain gages and their exposures, can be found in articles by C. F. Brooks ⁽¹⁾, Riesbol ⁽²⁾, and J. C. Alter ⁽³⁾*.

335. Errors of instrumentation, or differences between the true rainfall at the gage site and the rain measured in the gage, are due to losses by blowing out, splashing, evaporation, etc. The major factor in such distortion of the rainfall measurement is the wind. At unshielded gages the movement of air past the gage creates an updraft which tends to carry raindrops away from the mouth of the gage and thus results in a systematic catch deficiency. The error is generally assumed to be small, however, when the precipitation is in the form of rain.

336. Local anomalies in the rainfall pattern may be produced by small-scale topographic influences or artificial obstructions which distort the wind pattern in the immediate vicinity of the gage. This makes the particular gage site nonrepresentative of the general region, introducing an error in the areal determinations.

337. In regions of flat topography these factors are usually of minor importance, and this study is restricted to such a region.

* References listed numerically at end of chapter.

However, sampling errors, or the errors due to the accidental position and orientation of the storm rainfall pattern with respect to the station network, have a pronounced influence. The two isohyetal maps in figure 122 illustrate this type of error. Section A of the figure shows an isohyetal pattern for a short-duration high-intensity summer storm, based on all the records at 449 stations within the Muskingum River Basin. Section B of the figure shows another isohyetal map for the same storm, based on the records of 21 stations uniformly spaced throughout the entire network. This network corresponds to the average spacing of official gages of all types in this country ⁽⁴⁾. The two isohyetal patterns differ considerably, as might be expected. The widely spaced gages, in this case, fail to catch any of the intense rainfall. In this type of storm, the intense-rainfall areas are so small compared to the average area controlled by each gage, that it is unusual for official gages to record maximum or even near-maximum rainfall depth for the storm.

Statistical theory

338. In general, the magnitude of errors of sampling is a function of two factors: variability of the phenomenon measured, and the number of measurements. By variability is meant the range of values, or their dispersion about the mean. In the case of a rainstorm, part of the variability of recorded rainfall amounts is due to the effects previously discussed: observational or instrumental errors and gage nonrepresentativeness. A greater effect is due to variations in storm activity over the area. The latter variation depends on the type of storm and the

position of the area under consideration relative to the storm. A large-scale, frontal type of storm is generally characterized by a more uniform rainfall pattern than a nonfrontal thunderstorm situation. The geographical position of the storm is important because, as the outer limits of the storm are approached, the rainfall decreases less rapidly. This effect produces a greater range of rainfall over a given size and shape of area near the center of the storm than along the edge.

339. Since the difference in rainfall amounts recorded within an area increases as the area increases, variability is also a function of the size of the drainage area. Disregarding shape or orientation of drainage area, to obtain the same accuracy for a large basin as for a small basin, a greater number of rain gages would be required but not necessarily as great a density of gages. Hence, any general determination of accuracy should take into account the factor of size of drainage area.

340. The statistical tool available for determining limits of error is the following formula:

$$SE = SD / \sqrt{N} \quad (3.1)$$

where SE is the standard error of means of samples drawn from a population whose standard deviation is SD, and N is the number of observations in the sample. In the case of rainfall, SD is the standard deviation of all the rainfall depths recorded within the area, and N is the number of rain gages. The formula is based on the assumption that the population is homogeneous, or that the individual observations are random deviations from the mean. For application to the problem of

rainfall the assumption is not perfectly valid, and the implications of this fact will be discussed later. This method, however, has been used by Wilm, Nelson, and Storey (5) and by Horton (6). The first-named authors determined the accuracy of storm-rainfall measurements for small, mountainous watersheds. Horton investigated the same problem in connection with annual rainfall.

341. Statistical measures of error are defined in terms of probability. That is, a given value of error can be associated with the percentage of cases in which that error is not exceeded. The frequency distribution of errors is, therefore, an important consideration. Theoretically, this distribution is normal for two conditions: for a normal frequency distribution of the population, and for any distribution of the population provided the size of the sample is large. In a normal distribution of errors, the standard error, or root-mean-square error, is the value of error that will not be exceeded in approximately two thirds (68.26%) of the cases. Other measures of error, having different values of probability, may be obtained from the standard error. The important measures are listed below together with their magnitudes and associated probabilities:

	<u>Ratio to Standard Error</u>	<u>Probability of Error Not Being Exceeded</u>
Probable error	0.67	0.50
Average error	0.80	0.58
Standard error	1.00	0.68
Twice standard error	2.00	0.95

342. The typical frequency distribution encountered in storm rainfall is the right or positively skewed distribution. An example of a frequency histogram of storm-rainfall depths is shown in figure 123. It can be seen that a large number of low rainfall values is balanced by a small number of extremely high values. This type of storm rainfall distribution has been noted and discussed by H.C.S. Thom (7), and is especially important in the case where one or only a few gages are used as a measure of rainfall volume. When the distribution of the population is skewed, as it usually is in storm rainfall, the error distribution of means of small-sized samples tends to be skewed in the same direction as the parent distribution. As a result, in successive samplings with only a few gages, a large number of small underestimates is balanced by a small number of large overestimates. As the number of gages used to determine the mean rainfall increases, the error distribution becomes normal, with equal numbers and magnitudes of negative and positive deviations from the true mean. A mathematical derivation of the characteristics of the frequency distribution of errors in terms of the parent distribution and sample size can be found in Shewhart (8), where it is shown that the error distribution converges rapidly toward a normal distribution as the number of observations in the sample increases.

Analysis of variability

343. The theory outlined above was employed in the determination of the reliability of storm-rainfall measurements, using data supplied by the Soil Conservation Service from the dense network of

recording gages in the Muskingum Basin. The rainfall record consisted of hourly and half-hourly tabulations at all stations in the 8000-square-mile area for the period 1937-41. The number of gages varied between 500 for the early record and 250 for the recent years. Thirty-eight relatively intense storms characterized by thunderstorm activity in the region were selected for study by examination of rain periods during the months of June, July, August, and September. The storms were not otherwise meteorologically classified.

344. In order to place the storms on a comparable basis it was decided to use a duration of six hours, covering the maximum-rain period, as the period of study. Since all or most of the rain from the type of storm selected usually falls within a 6-hour period, the results should apply to total-storm rainfall as well. A hyetograph, or time graph of average rainfall, as in figure 124, was plotted from data consisting of arithmetic averages of all the recorded rainfall amounts for successive hours (or half hours) during each storm. After selection of the maximum 6-hour period of the storm from the hyetograph values, the successive half-hourly or hourly rainfalls were summed to obtain the maximum average 6-hour depth over the basin. Because of the large number of observations used to determine this value, it was the best available estimate of the true average depth of rainfall and was used as the "true mean." In a few cases it was checked against the average depth obtained by planimetering the isohyetal map, but the results showed only very small differences. A frequency tally was then made of the individual rainfall amounts within each storm, and a standard deviation computed in each case.

In this way, an average depth and corresponding standard deviation of rainfall were determined for each of the 38 storms.

345. The investigation was extended to include sizes of area other than the 8000-square-mile Muskingum Basin in order to collect data on the effect of area on variability. Two arbitrary sub-areas of 375 and 1500 square miles were outlined within the Muskingum Basin. Since the sub-areas included a smaller number of gages it was decided that arithmetic averages were not sufficiently accurate; isohyetal maps were drawn as a basis for the computation of the mean rainfall. The procedure described above was then repeated and new statistics were derived for the same series of storms.

346. The results of this phase of the analysis are summarized in table 22 for the three areas concerned. The table shows a fluctuation of variability from storm to storm and with different values of areas. In order also to evaluate the effect of storm magnitude on variability the storms were subdivided into two classes: above and below 0.5-inch average depth of rainfall. Table 23 gives mean values of average depth of rainfall, standard deviation, and coefficient of variation (CV) for the breakdown of data in terms of rainfall magnitude and area. The coefficient of variation is a measure of relative variability and is equal to the standard deviation divided by the mean.

Table 22

AVERAGE DEPTHS AND STANDARD DEVIATIONS
OF RAINFALL MEASUREMENTS IN 6-HOUR STORMS
(MUSKINGUM BASIN)

Storm No.	Storm Date	375 SQ. MI.		1500 SQ. MI.		8000 SQ. MI.	
		AD	SD	AD	SD	AD	SD
1	Aug. 10, 1937	0.49	0.29	0.38	0.34	0.43	0.77
2	Aug. 3, 1939	0.44	0.80	0.28	0.57	0.22	0.45
3	Sept 12, 1938	0.27	0.23	0.61	0.53	0.93	0.77
4	June 18, 1939	1.15	0.34	1.01	0.43	0.72	0.52
5	July 4, 1939	0.74	0.19	0.70	0.21	0.73	0.47
6	June 4, 1941	0.79	0.29	0.61	0.34	0.46	0.36
7	June 12, 1941	0.33	0.58	0.34	0.87	0.30	0.37
8	June 15, 1941	0.12	0.09	0.20	0.09	0.30	0.32
9	June 29, 1941	0.51	0.27	0.49	0.29	0.36	0.42
10	July 15, 1941	0.48	0.50	0.56	0.41	0.32	0.57
11	July 29, 1941	0.40	0.39	0.71	0.63	0.51	0.58
12	Aug. 15, 1941	1.24	0.31	1.09	0.43	0.80	0.62
13	Aug. 18, 1941	0.79	0.70	0.68	0.63	0.54	0.57
14	Aug. 25, 1941	0.50	0.13	0.56	0.18	0.51	0.24
15	Aug. 26, 1941	0.08	0.16	0.16	0.21	0.29	0.47
16	Sept. 3, 1941	0.44	0.35	0.49	0.38	0.52	0.41
17	Sept. 5, 1941	0.62	0.35	0.66	0.42	0.56	0.26
18	Aug. 4, 1938	1.78	0.60	1.77	0.56	1.39	0.75
19	July 8, 1939	0.79	0.30	0.66	0.55	0.41	0.47
20	July 29, 1939	0.47	0.11	0.48	0.38	0.45	0.50
21	Aug. 7, 1939	0.20	0.12	0.40	0.50	0.49	0.52
22	July 23, 1940	0.48	0.26	0.41	0.38	0.32	0.36
23	Aug. 18, 1940	1.06	0.44	0.99	0.54	0.85	0.55
24	July 26, 1940	0.58	0.27	0.52	0.43	0.47	0.58
25	Aug. 27, 1940	0.48	0.38	0.54	0.59	0.49	0.54
26	June 7, 1940	0.26	0.17	0.30	0.25	0.29	0.37
27	June 11, 1940	0.18	0.14	0.23	0.18	0.36	0.50
28	June 18, 1940	0.72	0.36	0.55	0.47	0.38	0.44
29	June 28, 1940	0.98	0.28	0.91	0.28	0.80	0.43
30	Aug. 6, 1938	0.50	0.17	0.45	0.18	0.44	0.41
31	Sept. 4, 1937	0.46	0.27	0.40	0.34	0.68	0.66
32	Sept. 4, 1939	0.28	0.13	0.30	0.16	0.34	0.22
33	June 28, 1939	0.05	0.07	0.19	0.44	0.41	0.71
34	June 26, 1938	1.02	0.27	0.89	0.22	0.79	0.32
35	June 11, 1938	1.09	0.16	1.00	0.31	0.79	0.51
36	Aug. 9, 1938	0.32	0.08	0.38	0.13	0.37	0.25
37	June 9, 1939	0.16	0.05	0.21	0.24	0.33	0.41
38	Aug. 13, 1939	0.54	0.28	0.51	0.31	0.36	0.36

Table 23

EFFECTS OF AREAL SIZE AND STORM MAGNITUDE

ON 6-HOUR-STORM VARIABILITY

(MUSKINGUM BASIN)

	<u>No. of Storms</u>	<u>Mean Rainfall</u>	<u>Mean SD</u>	<u>Mean CV</u>
<u>375 Sq. Miles</u>				
All storms	38	0.574	0.286	0.498
Storms < 0.5 in.	20	0.320	0.258	0.806
Storms > 0.5 in.	18	0.856	0.318	0.372
<u>1500 Sq. Miles</u>				
All storms	38	0.569	0.379	0.666
Storms < 0.5 in.	18	0.338	0.329	0.974
Storms > 0.5 in.	20	0.776	0.424	0.546
<u>8000 Sq. Miles</u>				
All storms	38	0.519	0.474	0.913
Storms < 0.5 in.	23	0.374	0.451	1.206
Storms > 0.5 in.	15	0.741	0.511	0.689

347. The values of coefficient of variation indicate an increase of relative variability with increasing area and, for a constant area, a decrease with increasing rainfall. The effect of area as shown by the data is in line with the theory previously described. The effect of rainfall magnitude on the coefficient of variation agrees with the results obtained by Wilm, Nelson, and Storey ⁽⁵⁾ for small, mountainous watersheds. As a result of both studies it may be concluded that the percentage error of sampling increases with decreasing amounts of rainfall. The absolute value of the error can, however, be greater with greater rainfall. Figure 125 presents empirical relations, developed from the data of table 23, expressing the coefficient of variation as a function of areal size for the three storm categories. Since the

interest lies in storms producing heavy rainfall, the lowest curve is the important one.

348. Figure 125 may be used to evaluate sampling errors as a function of the number of rain gages (N) by means of the following equation:

$$100 \text{ SE} / \bar{X} = \% \text{ SE} = 100 \text{ CV} / \sqrt{N} \quad (3.2)$$

where CV is the coefficient of variation of the rainfall amounts within the area, and $\% \text{ SE}$ is the standard error expressed as a percentage of the average depth of rainfall (\bar{X}). This formula is based on the same assumption of homogeneity of data as equation 3.1. By means of the formula, values read off the graph can be converted into percent standard error for a given number of rain gages. Curves resulting from such a conversion are shown in figure 126.

349. A more useful relationship is one that expresses the errors in terms of station density. If we let G equal the average area per gage and A equal the total area included within the network, then

$$A = GN \quad (3.3)$$

$$\text{and} \quad \% \text{ SE} = 100 \frac{CV}{\sqrt{A}} \sqrt{G} \quad (3.4)$$

The quantity $\frac{CV}{\sqrt{A}}$ can be determined from figure 125 for a given size of area. Equation 3.4 will then give the percent standard error of estimate of rainfall volume for any gage density within the area.

Effects of uniform gage spacing

350. Up to this point, the relationships between error, gage density, and area have been developed without regard to the areal

pattern of storm rainfall. The values obtained apply to systems of rain gages superimposed at random on the rainfall pattern without regard to uniformity of spacing. The differences in rainfall depths at different points of an area are not, however, wholly chance variations but due in part to geographical variations of rainfall resulting from storm movement and development. This implies that a network of gages spaced uniformly so as to sample all parts of the area, will provide greater accuracy than an unrestricted network having the same number of gages.

351. In order to obtain equivalent reliability values for uniformly spaced gages an experimental procedure was adopted. A master network was constructed, as shown in figure 127, in which hypothetical gages are distributed at uniform intervals throughout the Muskingum area. The spacing of gages in the master network represents twice the average density of the present network of rainfall stations in this country, the latter being 1 gage per 375 square miles (4). Inscribed on transparency, the network was superimposed on each isohyetal map, a selection made of the stations nearest the numbered points, and their corresponding rainfall depths tabulated. Through the use of different gage arrangements, it was possible to obtain the hypothetical average rainfall corresponding to seven different networks sampling the area as a whole: one of twice normal density, two of normal density, and four of one-half normal density. The seven arrangements of gages are shown in figure 128.

352. The computation of errors involved the following steps:

For each storm, average depths for the seven networks were obtained from the arithmetic means of the appropriate gages. The errors were computed from the differences between the sample means and the "true" mean rainfall previously determined. The average and standard errors for each sample network were then derived from the set of 38 deviation values corresponding to the 38 storms analyzed.

353. To extend the results to smaller values of area it was necessary to repeat the procedure for the two sub-areas inside the Muskingum Basin, shown in figure 127. The various groupings of gages pertaining to these sub-areas are shown in figure 129. It is evident that, for a small area, the accident of basin location with respect to the gage system has a considerable effect on the number of gages controlling volumetric rainfall estimates. As an extreme case, consider the networks numbered 14 and 15. Both arrangements represent networks of the same density. In one case, a single gage, centrally located, controls the area while, in the other, four gages on the periphery of the area enter into the average depth determination. However, one centrally located gage should be a more accurate index than any one of the four peripheral gages, and possibly, than all four peripheral gages combined. Advantages in location may, therefore, compensate for a smaller number of measurements.

354. The computation of small-area reliability differed somewhat from the computation for the whole area. In actual practice, where data from only a few rain gages are available within a drainage area, weights are generally assigned to each gage in accordance with its

areal representativeness. A weighted average is then obtained which is more accurate than an arithmetic average. In the current study the Thiessen method of weighting ⁽⁹⁾ was used and a weight assigned to each hypothetical gage, before averaging to obtain a mean rainfall value from the sample network.

355. The results of this analysis are shown in figure 130 where the errors for 38 successive samplings are plotted for each of the 15 networks. It may be noted that the points become more dispersed with increased spacing of gages for the same size of area and with decreased area for the same degree of spacing.

356. In evaluating the results, the storms yielding rainfall amounts in excess of 0.5 inch were selected and their standard errors computed. The values are given in table 24. The results of this testing procedure could now be related to the results of the previous analysis of variability. By means of figure 125 and equation 3.4 errors were computed for each of the 15 networks. In terms of the values indicated for each of the networks in figures 128 and 129, the computation was as follows: The total area of the network was multiplied by the gage density (or divided by the average area per gage) and the square root of the result then divided into the coefficient of variation (as taken from figure 125 or table 23) for the particular area and a storm magnitude in excess of 0.5 inch. Multiplied by 100, the result is percent standard error. These errors may be termed random-gage errors, that is, deviations from true rainfall when random systems of gages are extracted from a dense network. The errors derived by the testing procedure, on the other hand, result

Table 24

STANDARD AND PERCENT STANDARD ERRORS
OF UNIFORMLY SPACED NETWORK

(STORMS > 0.5 IN., MUSKINGUM BASIN)

Network No.	Area (Sq. Mi.)	Area Per Gage (Sq. Mi.)	Number of Gages	Mean Rainfall	Standard Error	% Standard Error
1	8000	187.5	45	.741	.049	6.6
2	8000	375	22	.741	.097	13.1
3	8000	375	23	.741	.086	11.6
4	8000	750	12	.741	.101	13.6
5	8000	750	10	.741	.120	16.2
6	8000	750	13	.741	.120	16.2
7	8000	750	10	.741	.153	20.6
8	1500	187.5	13	.776	.099	12.8
9	1500	375	9	.776	.186	24.0
10	1500	375	4	.776	.219	28.2
11	1500	750	4	.776	.213	27.4
12	1500	750	5	.776	.230	29.7
13	375	187.5	5	.856	.145	16.9
14	375	375	4	.856	.237	27.7
15	375	375	1	.856	.251	29.3

from gages spaced uniformly over the area in question.

357. In figure 131 the uniform-gage errors (from table 24) are plotted against corresponding computed random-gage errors. This graph offers both a check on the values obtained by either procedure and a means of obtaining a reduction coefficient for uniformity of gage spacing to be applied to equation 3.4. It may be noted that, with the exception of one point, the errors of a uniformly spaced network are less than those of a random network. This is in conformity with theory. It is apparent that the greater accuracy in the regions of greater density in the random distribution is more than compensated by the greater error in the regions of lesser density. This is true no matter what type of uniformity is imposed on the network, as long as the average density remains the same.

358. The solid line of figure 131 was drawn to pass through the origin and have the least root-mean-square deviation from the plotted points. It is thus an average line which establishes an empirical relation for obtaining accuracy values of uniformly spaced networks. On the basis of available data there is little indication that the size of area considered or the gage density has any effect on the ratio between uniform and random-gage errors. It is also doubtful whether other patterns of uniformity that might have been used would substantially alter the relation here established, if the same basic data were employed.

359. To generalize the results and present them in useful form, the density-area-error graph of figure 132 is shown. This graph, derived from equation 3.4 modified by the coefficient determined by

the testing procedure, relates percent standard error of rainfall-volume estimates to size of drainage area and density of rain gages. The results are partly empirical and are subject to the limitations of the available data and the assumption of random distribution of errors. They should apply to regions resembling the Muskingum Basin in topography and summer rainfall characteristics. Although several storms have been studied where point rainfall has exceeded Yarnell's (10) 100-year frequency value for the Muskingum region, intense storms of the type considered in upper-limit rainfall investigations have not occurred during the five years of available record. Therefore, further study should be given to the variability of rainfall within the rare "cloudburst" type of storm, although here the obstacle is the lack of sufficient and reliable data.

The experimental network

360. In designing a rain-gage network for research purposes primary consideration must be given to the desired time units of precipitation. For basin analyses where an accurate areal distribution of storm totals or comparatively long-period rainfall amounts is required, a particular station density may be necessary. However, if the purpose of the project is a study of infiltration, rainfall intensities for very short periods are needed and for such an analysis a much closer spacing of gages is required. The same is true of a network designed for thunderstorm research where it is planned to obtain instantaneous areal patterns of rainfall intensities.

361. The result and methods described in the areal-reliability determination are not adequate in dealing with the new problem where

the interest is not in the sampling errors of mean rainfall over an area but in the accuracy of the isohyetal pattern of total-storm rainfall or of short-period rainfall intensity. Because the Muskingum spacing, roughly one rain gage per four or five linear miles, is not close enough to yield the significant features of the small-scale isohyetal pattern, it was necessary to use data from a denser network of gages. The available networks suitable for the purpose, however, cover areas considerably smaller than the average rainfall "cell" resulting from a thunderstorm. Hence, the data are not adequate for other purposes, such as determinations of the areal extent and total distribution of rain within the thunderstorm cell. The study was therefore limited to two objectives. One was to evaluate the accuracy of a given station spacing for plotting isohyets. The other objective, a by-product of the first, was to develop methods for best estimations of rainfall from nearby gages, and to evaluate the accuracy of these estimates.

362. In order to obtain information on the magnitude of rainfall gradients within intense summer storms, a number of profiles were plotted from 24-hour rainfall data collected by the Soil Conservation Service at the Little Mill Creek drainage basin in Ohio. Figure 133 is a map of this basin showing the location of recording and nonrecording gages. The average distance between gages is approximately one-third mile within an area of seven square miles. As shown in figure 133, a section along the major axis of the basin was taken as the axis of the profiles. All amounts recorded at stations within the narrow strip shown in the figure were plotted against distance

from station 56 at the extreme southwest tip of the basin. To obtain data on intense short-duration storms, 18 isolated one-day storms producing more than 0.5 inch of precipitation were selected for analysis from the period of available record, 1937-1942.

363. Smooth curves were drawn through the plotted points as shown in figures 134, 135, and 136. The assumption is that these curves represent the true profiles and that deviations from the curves are due to observational errors and local exposure anomalies. The results show a pronounced nonlinear variation of rainfall within a distance of 4 miles in 6 cases out of 18. This implies that 33% of the time a gage spacing of 4 miles would be grossly inadequate for plotting isohyetal maps of intense summer rains. The August 14, 1939, profile (figure 135) shows an extreme slope of about a half inch per mile on either side of a rainfall peak. This situation is probably characteristic of the distribution of rain near a storm center. The uniformity of rain in other cases might be due either to the type of storm or to the location of the profile along the fringe of the storm area where the rainfall gradient is less.

364. A quantitative evaluation of the effect of gage spacing on accuracy can be obtained through a statistical analysis of simultaneous rainfall amounts at a group of stations. Mutual correlations of rainfall within the station group will yield separate values of linear regression coefficients, correlation coefficients, and errors of estimate for each station pair. These values can then be plotted against the corresponding distance between stations. If a sufficient number of well-distributed values are available, a general relationship

can be derived expressing the rainfall correlation between two adjacent points in a region as a function of the distance of separation.

365. The rainfall correlation described above was accomplished in the following manner: A group of five well-distributed stations within the Little Mill Creek Basin was selected. Distances between stations varied from one-third mile to four miles, as shown in figure 137. The data used in correlations between each pair of stations consisted of one-day rainfall amounts for 41 selected dates of heavy rainfall. A value of 0.5 inch recorded at a single station within the group was chosen as the lower limit of heavy rainfall in selecting storm dates. Correlations were made between the five series of 24-hour rainfall amounts, and the results are presented in the following tables:

Table 25

MEANS AND STANDARD DEVIATIONS OF 24-HOUR RAINFALLS

(Unit = 1 inch)

Station	1	2	3	4	5	Average
Mean Rainfall	1.02	1.03	1.09	1.00	0.99	1.02
Standard Deviation	0.64	0.64	0.67	0.62	0.62	0.64

Table 26

CORRELATION COEFFICIENTS BETWEEN 24-HOUR RAINFALLS

Station	2	3	4	5
1	0.93	0.93	0.77	0.78
2	--	0.95	0.85	0.73
3	--	--	0.86	0.73
4	--	--	--	0.64

366. The values shown in table 26 were plotted against distance between stations, as shown in figure 138. A straight line has been fitted to the plotted points, representing the variation of 24-hour rainfall correlation with gage spacing. The slope of this line indicates the great reduction in correlation with increased distance of 24-hour depths of summer precipitation in the Little Mill Creek Basin. It should not be inferred that a straight line adequately represents this relation, nor that a curve fitted to these points can reasonably be extrapolated. The degree of correlation between precipitation catch at variously spaced stations is greatly influenced not only by the station spacing, but also by duration, depth, type of storm, location, topography, and season.

367. The curve for estimating the error of a single gage (figure 139) is computed from the curve of figure 138. The lower curve in figure 139 represents the reliability of the estimate (by multiple linear correlation) of rainfall midway between two gages. It gives the interpolation error involved in drawing isohyets of summer rainfall by mechanical interpolation between pairs of adjacent gages. The study of the geometry of interpolation among three or more gages is not relevant to this report. In any case, the drawing of isohyetal maps by mechanical interpolation is not dependable. Consideration should be given to orographic influence, storm configuration, and other factors. The Little Mill Creek example indicates the order of magnitude of error in estimating, by mechanical interpolation, the distribution of depth of short-duration summer rainfall over small areas.

368. The discussion thus far has dealt with storm totals for durations under 24 hours or 24-hour amounts for longer durations. There should not be any appreciable difference in the station density required for the ordinary short-duration summer storm. However, as pointed out previously, a closer network is necessary for rainfall-intensity patterns which are based on extremely short intervals. To obtain visual information on the nature of this problem, a number of rainfall intensity patterns were plotted for adjoining stations, using data supplied in Hydrologic Bulletins Nos. 1 and 4 of the Hydrologic Division, Office of Research, Soil Conservation Service. A set of typical charts for two gages one-half mile apart is shown in figure 140. It will be noted that considerable differences in magnitude and timing exist between the two stations. Some of the variation in pattern may be attributed to imperfect clock synchronization or other instrumental errors. However, the differences are too acute to be explained entirely on this basis, and the evidence of rapid fluctuation of intensity with time and geographical position indicates the necessity for a spacing closer than one-half mile per gage. The available recording-gage network was thus too sparse for the proper statistical study of short-period intensities.

369. The evidence furnished leads to several conclusions. One is that the original Muskingum network of approximately one gage per four linear miles is inadequate for small-basin studies and for obtaining detailed isohyetal patterns of thunderstorm situations. Optimum station density depends on the permissible error and the purpose of the rain-gage network. For total or 24-hour rainfall

amounts of summer storms and a tolerance of 20% standard error, a spacing of about one gage per linear mile seems to be necessary. Another conclusion of the study is that an even closer spacing would be required to obtain the areal distribution of short-period rainfall intensities. The required density would make it extremely costly to instrument an area the size of an ordinary thunderstorm cell in order to obtain isohyetal patterns at intervals of a few minutes.

370. The results obtained are applicable within the range of data used in the study, and to non-orographic rainfall. Further investigation is necessary to evaluate the effect of rainfall magnitude on the accuracy of a given station spacing. The study should also be extended to other regions where topography may influence the distribution of summer rainfall.

371. There is no reason for supposing that instrumental networks less dense would be required for the accurate delineation of the distribution of the other meteorological elements in the thunderstorm situation. The simultaneous study of conditions aloft only multiplies the difficulties and the problems. Furthermore, the purposes of even the most dense network would be defeated by the lack of precise synchronization of the recording equipment. A recorder-synchronizing system has been recently described by Hamilton (11).

372. In planning the geographical location of an experimental network for thunderstorm sampling, consideration should be given to other factors in addition to the frequency of thunderstorms. Since the primary interest is in intense rainfall, the United States west

of the 100th meridian is eliminated as a proper location because in that region the high thunderstorm frequencies are not accompanied by comparable frequencies of intense or even measurable rains. The major region of high thunderstorm frequency - the Gulf Coast - fulfills that need but fails to meet other possible requirements. The thunderstorms of this region are largely of the same type - nonfrontal. They are rarely accompanied by hail. However, only in this region is there a good probability of activity throughout all the months of the year. For that reason alone, the location of a network in such a region might be worth while. In table 32 (chapter IV) it can be seen that, of the four storms producing the maximum observed United States rainfall values tabulated, two occurred within an approximately 15,000-square-mile elliptical area between Uvalde and Temple, Texas. In the same region there have been other occurrences of "cloudburst" proportions. There being no such concentration of record rainfall values elsewhere in the United States, this area is indicated as of special interest to any project for the establishment of an experimental rain-gage network to determine the morphology of the maximum-type storm.

373. However, if it is desired to sample all the thunderstorm types and also the important accompanying phenomena, it is necessary to sacrifice the requirements of the highest frequencies of thunderstorms and intense rainfall. In the central region of the country - roughly eastern Kansas, Arkansas, Missouri, and Iowa - there is only moderately high thunderstorm frequency but the thunderstorms may be air-mass or frontal, daytime or nocturnal. In addition, the frequency

of hail is as high as it is anywhere in the country east of the 100th meridian and the tornado frequency is highest. For the observation of a variety of thunderstorm types, then, the network should be established in this region.

374. If mobile observational units are to be added to the fixed network, the available highway system should also be considered. It was such a consideration, though one not based on exhaustive study, that prompted the recommendation of an area north of Des Moines, Iowa, as a suitable location for the experimental thunderstorm network recently proposed by the Weather Bureau for the approval of Congress.

References

375. Abbreviations used in the list of references are explained in the Bibliography. See Appendix.

1. C. F. Brooks, Need for universal standards for measuring precipitation, snowfall, and snowcover, Int. Assoc. of Hyd., Bull no. 23, 1938. 52 p.
2. H. S. Riesbol, Results from experimental rain-gages at Coshocton, Ohio, TAGU, 1938, pt. I, p. 542-50.
3. J. C. Alter, Shielded storage precipitation gages, MWR, v. 65, Jul. 1937, p. 262-5.
4. M. Bernard, Precipitation, in Hydrology (no. IX, Physics of the earth, National Research Council), ed. by O. E. Meinzer, 1942, p. 32-55.
5. H. G. Wilm, A. Z. Nelson, and H. C. Storey, An analysis of precipitation measurements on mountain watersheds, MWR, v. 67, June 1939, p. 163-72.
6. R. E. Horton, Accuracy of areal rainfall estimates, MWR, v. 51, Jul. 1923, p. 348-53.
7. H.C.S. Thom, On the statistical analysis of rainfall-data, TAGU, 1940, pt. II, p. 490-99.

8. W. A. Shewhart, Economic control of quality of manufactured product, 1931, p. 230-41.
9. A. H. Thiessen, Precipitation averages for large areas, MWR, v. 39, Jul. 1911, p. 1082-4.
10. D. L. Yarnell, Rainfall intensity-frequency data, USDA, Misc. Pub. no. 204, Aug. 1935.
11. E. L. Hamilton, A system for the synchronization of hydrologic records, TAGU, 1943, pt. II, p. 624-31.

CHAPTER IV

HYDROLOGIC ASPECTS OF THUNDERSTORM RAINFALL

The typical mass curve

376. Although conclusions derived from point-rainfall data fail to satisfy the hydrologist's need for areal relations, a collection of mass curves of point rainfall is the necessary basis of a proper storm-rainfall analysis. It is with this in mind that an effort is here made to present the typical mass curve of thunderstorm rainfall, i.e., high-intensity short-duration rainfall.

377. Three sources of data were utilized. From the automatic tipping-bucket records of 11 stations, 207 storms, occurring in June, July, and August of 1940-42, were selected. The stations were chosen to represent a diversity of climatic regimes; they are listed below with the number of storms chosen from each:

Albuquerque, N. Mex.	16
Atlanta, Ga.	20
Cheyenne, Wyo.	20
Chicago, Ill.	20
Modena, Utah	11
Nashville, Tenn.	20
New Orleans, La.	20
Oklahoma City, Okla.	20
Omaha, Nebr.	20
Tampa, Fla.	20
Washington, D. C.	20

This storm list will hereinafter be referred to as the Hydromet list.

The two other sources of data were Meyer's tabulation of "Data for 100 Typical Intense Rainstorms, 1896-1914" (1)*, yielding 60 storms,

* References listed numerically at end of chapter.

and Yarnell's tabulation of the "Most intense rainstorm recorded at each station through 1933" (2), yielding 107 storms. Duplications were eliminated.

378. For the Hydromet list the criteria of selection were: thunder officially recorded within two hours of rain commencement and total precipitation exceeding 0.15 inch. At the western stations the magnitude limit was lowered to 0.10 inch in a few cases because of the infrequency of heavier thunderstorm rainfall. The beginning of rainfall was defined as the first tip* followed by an accumulation of at least 0.05 inch in the ensuing half hour and the rain was considered ended when the accumulation during any half-hour period was less than 0.05 inch. The total rainfall in these storms varied from 0.10 to 4.76 inches and the durations from 10 minutes to 3 hours. From Meyer's and Yarnell's lists the selection was limited to the storms for which complete data, tabulated by 10-minute increments, were available. This limited the number selected because for storms exceeding a 60-minute duration the rainfall data had been compiled by longer than 10-minute increments after the first hour. However, a few storms lasting 80 minutes were chosen when their last 20 minutes' rainfall was a small percentage of the total fall. Beginnings and endings in these two lists were considered to be exactly as tabulated, storms being excluded in which more than one or two percent of the total fell before the tabulation started. It is to be noted that the Meyer and Yarnell storms are not necessarily

* A tip is recorded after the accumulation of .01 inch of rainfall by a tipping-bucket gage.

thunderstorms but the intensity of rainfall involved is certainly the thunderstorm type.

379. Percentages of total rainfall in consecutive 10-minute periods were tabulated for all 374 storms. Tables 27 and 28 summarize the results.

Table 27

AVERAGE PERCENTAGE OF TOTAL THUNDERSTORM RAINFALL BY 10-MINUTE INCREMENTS

	Hydromet (207 storms)	Yarnell (107 storms)	Meyer (60 storms)	All (374 storms)
Highest 10-min.	54	53	48	53
2d highest 10-min.	25	29	26	26
3d highest 10-min.	14	15	16	15

Table 28

HIGHEST PERCENTAGE FREQUENCY OF EACH RANK FOR

10-MINUTE INCREMENTS IN THUNDERSTORM RAIN

	Hydromet (207 storms)	Yarnell (107 storms)	Meyer (60 storms)	All (374 storms)
1st 10-min. inc. ranking 1st	43	50	37	44
2d 10-min. inc. ranking 2d	46	59	35	48
3d 10-min. inc. ranking 3d	44	61	66	52

380. It is apparent that the average mass curve derived from these data would also be a depth-duration curve, since the time distribution of thunderstorm rainfall at a station is such that the highest intensity occurs at the beginning, with decreasing intensity

throughout the storm. This is a well-known characteristic of point rainfall in a thunderstorm but it is not, in most cases, true of areal rainfall, as will be demonstrated later in this chapter.

381. On account of the variation in the duration of the storms used in the analysis above (tables 27 and 28), it was decided to derive a mass curve (and depth-duration curve) on the basis of a single total-storm duration. One hour was chosen for the duration because it is the typical thunderstorm duration, and the 1-hour values used were the maximum observed (up to 1945) 1-hour rainfalls at 204 Weather Bureau recording gages. The amounts used for smaller time increments were the maximum observed at the same stations for 5, 10, 15, and 30 minutes. Not all the amounts at each station necessarily occurred in the same storm nor were all the occurrences necessarily reported as thunderstorms. However, it was felt that, at least within the limits of one hour, enveloping depth-duration values could occur in a single storm and that the intensities justified their classification as thunderstorm-type rainfall. Finally, the practical equivalence, as shown above, of mass curve and depth-duration curve made the data usable for both purposes.

382. Experimentation with the data revealed that any averaging of all the cases would mask a significant variation of curve slope with 1-hour amount. The data were therefore stratified by 1-inch (per hour) increments and the resulting smoothed curves are shown in figure 141. Because 1-hour amounts less than one inch or greater than five inches were so few, no curves were drawn for these classes, but in general these classes show continuation of the trend displayed by the figure.

Comparison of the percentages shown in figure 141 with the corresponding

percentages derived from the world's record rainfall amounts (mostly unofficial) which are shown in figure 112 indicates that, for a critical time distribution, higher-than-average percentage values should be used in the consideration of the maximum possible storm. The Opid's Camp 1-minute value shown in figure 112 was reduced from the originally reported 1-inch amount to 0.65 inch on the basis of a study made in the Hydrometeorological Section (3).

Area-depth relations

383. The usual engineering approach to the problems of small-area or thunderstorm-type rainfall results in empirical statements that take the form of intensity-duration-frequency relations based on point-rainfall data, or enveloping duration-depth-area curves developed from areal-rainfall analyses. Since the hydrologist is primarily interested in the simultaneous rainfall over a whole drainage area while the area of applicability of point-rainfall data remains uncertain, the first type of relation and others like it are deficient for the purpose. The duration-depth-area curves for small-area, short-duration, high-intensity storms are more useful hydrologically but are often unreliable because of the sparse network of gages upon which the analysis depends; furthermore, when based on official rainfall measurements, the curves may be limited by a minimum area of about 500 square miles and a minimum duration of 6 hours. Nevertheless, since the physical processes governing the growth, movement, and decay of individual thunderstorms or thunderstorm groups are not well understood, the

empirical approach remains the fruitful one. Applied to a dense rain-gage network like the Muskingum network, its possibilities are enhanced.

384. A detailed knowledge of the rainfall distribution with time and area is particularly required for surface-runoff determinations based on the infiltration theory. When rainfall is uniformly distributed and falling at a steady rate, a large proportion of the precipitation may be lost by infiltration. An equivalent volume of rainfall, concentrated over a small area or within a short period of time, will produce much more surface runoff. In a thunderstorm the heavy rainfall may cover a very small area, and within that area the total duration of the storm may be one hour or less. The Muskingum network of recording gages presents the opportunity for the study of the distribution of such rainfall in terms of small units of area and time. Because of the gage density the mean areal rainfall can be computed, with some degree of confidence, for areal units as small as 50 square miles; and the available half-hourly or hourly tabulations of station data permit corresponding short-period breakdowns of the rainfall volume.

385. For the purpose of this study, which is to develop useful empirical area-depth and duration-depth relations for thunderstorm rainfall, the Muskingum data are deficient in certain respects, but not insurmountably so. The Muskingum network is not large enough to include the entire area of the usual storm. Consequently, the area-depth curves developed from these data are not entirely comparable to the usual type of curves developed in storm studies. Even when the heaviest rainfall is wholly concentrated within the Muskingum Basin, appreciable rain may fall outside the basin. As a result,

the area-depth values for the upper range of area are representative of partial storm areas. However, because of the manner in which the storms were selected, the storm center usually falls within the basin limits. For that reason the portion of the area-depth curve at the lower limits of area bears a close resemblance to the type of curve desired. Since the paramount interest is in areas under 500 square miles, the data are thus not seriously deficient in these respects.

386. Lack of synchronization of clocks and the accidents of the clock intervals chosen also introduce some error in the calculations. A duration-depth curve based on storm data tabulated by clock hours or other standard intervals will underestimate the short-period values although the errors naturally decrease progressively with increased duration. To avoid this source of error it was necessary to examine the original recorder charts and tabulate rainfall depths for shorter increments. Attempts to do so were effectively balked by a deplorable lack of knowledge concerning the individual clock errors and, in any case, restrictions imposed by time and available personnel made such a procedure impossible. However, it is believed that the errors are of minor significance for the sizes of area and the durations considered here.

387. In analyzing the vast amount of available data it was decided to adopt short-cut procedures which did not involve any important sacrifice of accuracy. A numerical procedure was devised to reduce the amount of labor required to compute area-depth curves from the several hundred rainfall measurements in each of the 38 storms listed in the preceding chapter (table 22). This procedure made use

of the frequencies of storm-rainfall amounts tabulated in the reliability study (chapter III).

388. The usual method of computing an area-depth curve from an isohyetal map is based on the following equation:

$$\bar{D} = \frac{\sum (\Delta A \cdot D)}{\sum (\Delta A)} = \frac{\sum (\Delta A \cdot D)}{A} \quad (4.1)$$

where \bar{D} is the average depth for a particular value of area A on the area-depth curve, ΔA is an increment of area between two successive isohyets, D is the value midway between the two isohyets, and the summation signs represent accumulations in descending order of magnitude of rainfall. With a uniform distribution of rain gages, the increment of area enclosed between two isohyets is proportional to the number of gages enclosed between the same isohyets. Areal values can thus be closely approximated by such a procedure where there is a large number of stations distributed at roughly uniform intervals, as in the Muskingum. Substituting f , the frequency or number of stations in a particular class interval, for ΔA , the corresponding increment of area, we obtain

$$\bar{D} = \frac{\sum (fD)}{\sum f} \quad (4.2)$$

where D is now the midpoint of the class interval.

389. Equation 4.2 became the basis for the computation procedure. Figure 143 shows an example of an area-depth curve derived from the frequency histogram of figure 123 of chapter III. The curve is plotted with area on a logarithmic scale and depth on a linear scale. Each

individual point corresponds to a separate block of the frequency histogram. Each storm was analyzed in this manner. The area-depth values obtained by this procedure for the 38 storms are presented in table 29, where the storm of figures 123 and 143 is number 30. They can be checked against the average depths obtained by arithmetical averaging of observations, by comparing the 8000-square-mile values of tables 22 and 29. The differences are small.

390. From table 29 general relations for small areas were derived. The values for 50, 100, 200, and 350 square miles were plotted against corresponding depths for 500 square miles and the resulting graphs are shown in figure 144. Regression lines through the origin were drawn to represent average ratios between depths for various sub-areas and the depth for 500 square miles. Examination of the plotted points indicates that in 6-hour storms the percentage increase for smaller areas is independent of the observed magnitude of the average depth of the rainfall over 500 square miles. This justifies the use of an average percentage relation between depths for successive areas, which is shown in figure 145. The accuracy of this relation naturally decreases with reduction of area, as evidenced by the increasing scatter of points for decreasing values of area in figure 144.

391. The general relationship found lends some support to the practice of straight-line extrapolation (on semilog paper) of area-depth relations, as suggested in an earlier report ⁽⁴⁾. A similar plotting of the area-depth relation, using the United States maximum observed rainfall values (table 32)

Table 29

AREA-DEPTH VALUES, 6-HOUR STORMS
(MUSKINGUM BASIN)

Storm No.	AREA (SQUARE MILES)								
	50	100	200	350	500	1000	2000	5000	8000
1	5.58	5.00	4.15	3.40	2.92	2.06	1.34	0.64	0.45
2	4.28	3.25	2.40	1.87	1.56	1.09	0.74	0.36	0.20
3	3.70	3.61	3.41	3.20	3.04	2.63	2.13	1.38	0.95
4	1.83	1.77	1.71	1.65	1.61	1.52	1.39	1.06	0.74
5	3.32	3.02	2.67	2.40	2.22	1.85	1.48	0.98	0.74
6	1.86	1.72	1.56	1.43	1.35	1.19	0.99	0.68	0.48
7	2.07	1.90	1.70	1.50	1.37	1.12	0.85	0.50	0.31
8	1.72	1.62	1.48	1.33	1.23	1.00	0.75	0.44	0.30
9	2.53	2.32	2.06	1.82	1.66	1.34	1.01	0.58	0.33
10	3.50	3.14	2.70	2.30	2.05	1.60	1.14	0.51	0.32
11	3.23	3.02	2.70	2.40	2.20	1.76	1.35	0.81	0.54
12	2.74	2.65	2.48	2.32	2.20	1.95	1.67	1.20	0.80
13	2.55	2.42	2.22	2.03	1.90	1.65	1.34	0.84	0.56
14	1.24	1.17	1.10	1.04	1.00	0.92	0.84	0.65	0.51
15	2.93	2.65	2.32	2.03	1.84	1.45	1.08	0.59	0.34
16	2.67	2.28	1.94	1.68	1.55	1.32	1.07	0.72	0.51
17	1.44	1.39	1.30	1.22	1.16	1.06	0.94	0.72	0.56
18	4.78	4.31	3.84	3.45	3.20	2.75	2.30	1.70	1.41
19	2.78	2.53	2.25	1.99	1.82	1.46	1.10	0.62	0.41
20	2.32	2.21	2.06	1.88	1.75	1.46	1.14	0.69	0.45
21	2.70	2.52	2.26	2.04	1.89	1.58	1.25	0.75	0.50
22	2.13	1.85	1.60	1.40	1.26	1.02	0.77	0.48	0.32
23	3.24	3.05	2.78	2.51	2.35	1.98	1.60	1.10	0.85
24	3.02	2.73	2.42	2.14	1.97	1.64	1.30	0.78	0.46
25	3.40	3.05	2.68	2.37	2.16	1.75	1.33	0.79	0.54
26	2.71	2.19	1.70	1.41	1.26	0.98	0.70	0.34	0.15
27	2.72	2.45	2.10	1.78	1.59	1.24	0.90	0.50	0.29
28	2.10	2.04	1.89	1.72	1.60	1.32	1.02	0.60	0.38
29	2.18	2.09	1.95	1.83	1.75	1.60	1.40	1.06	0.80
30	2.78	2.40	2.05	1.77	1.60	1.28	0.97	0.58	0.40
31	3.42	3.12	2.81	2.55	2.40	2.05	1.65	1.03	0.69
32	1.31	1.20	1.07	0.95	0.90	0.76	0.64	0.44	0.34
33	3.00	2.91	2.70	2.50	2.34	1.99	1.52	0.80	0.43
34	2.23	2.10	1.92	1.77	1.67	1.47	1.22	0.93	0.80
35	3.09	2.84	2.54	2.27	2.10	1.77	1.45	1.02	0.80
36	1.91	1.70	1.48	1.27	1.15	0.92	0.70	0.47	0.39
37	2.14	2.00	1.85	1.70	1.60	1.35	1.02	0.58	0.32
38	2.01	1.85	1.66	1.48	1.35	1.12	0.87	0.57	0.39
Average	2.71	2.48	2.20	1.96	1.80	1.50	1.18	0.75	0.55

for a 6-hour duration and areas of 50 to 500 square miles, produced a similar straight-line relationship but a lesser slope.

Storm profiles

392. In theoretical studies it is useful to express a complex rainfall pattern in terms of a simpler picture or to develop a "synthetic" isohyetal map from the area-depth characteristics of a theoretical storm. Some work along these lines has been done in connection with the Caddoa Report ⁽⁵⁾. In that study, by a graphical process, ellipses of a given eccentricity were constructed to represent successive isohyets. The resultant isohyetal map possesses the same area-depth characteristics as the enveloping area-depth curve of the design storm. The object of such a study, in general, is to synthesize a storm from known volumetric rates of precipitation, in terms of a reasonable rainfall pattern.

393. The following treatment extends the concept of a synthetic rainfall pattern to one where the rainfall depth at any point in the area is expressed as a mathematical function of the space coordinates. For this purpose, equation 4.1 is put into integral form, so that \bar{D} is the value of minimum rainfall encompassed within area A :

$$\bar{D} = \frac{\int_0^A D \, dA}{A} \quad (4.3)$$

or

$$\int_0^A D \, dA = \bar{D} A \quad (4.4)$$

As before, the integration is from high values of rainfall, beginning with maximum rainfall, to low values of rainfall. Differentiating both sides of equation 4.4 with respect to A,

$$D = \bar{D} + A \frac{d\bar{D}}{dA} \quad (4.5)$$

This is the general solution for a minimum-rainfall curve, i.e., a curve similar to an area-depth curve, but where the depth represents the minimum instead of the average depth of rainfall included within the area. The term, minimum-rainfall curve, was assigned to this type of relation by Kroeger and Stewart (6). It also corresponds to the isohyet-area curve introduced in the Caddoa Report. If an isohyetal map with a single center and progressively decreasing rainfall outward is assumed, the same relation gives the value of each encompassing isohyet as a function of the total area enclosed by the isohyet.

394. A more useful form of equation 4.5 can be obtained by developing a functional relation for the area-depth curve. In most storms, a large portion of the area-depth curve can be approximated by a simple logarithmic expression of the form:

$$\bar{D} = a \log A + b \quad (\text{where } a < 0, b > 0) \quad (4.6)$$

where a and b are the parameters of a straight line on semilogarithmic paper, a being the negative slope and b the intercept on the Y axis. If it is assumed that this relation holds true for all values of area from a very small value up to A_0 , where the corresponding value of average depth is \bar{D}_0 , then equation 4.6 can be put in a more convenient form:

$$\bar{D} = a \log \frac{A}{A_0} + \bar{D}_0 \quad (0 < A \leq A_0) \quad (4.7)$$

Differentiating the above expression and substituting in equation 4.5,

$$D = \bar{D} + a \quad (4.8)$$

$$\text{or} \quad D = a \log \frac{A}{A_0} + \bar{D}_0 + a \quad (4.9)$$

395. In order to obtain a synthetic isohyetal map from the above relation, some general relation between rainfall depths and the space coordinates must be postulated. The simplest case is a single-celled rainfall pattern with concentric circles as isohyets. Letting r = the radius of any isohyet, and r_0 = the radius of the outermost isohyet corresponding to the area A_0 , equation 4.9 becomes

$$D = 2 a \log \frac{r}{r_0} + \bar{D}_0 + a \quad (0 < r \leq r_0) \quad (4.10)$$

396. Equation 4.10 shows that, for the particular pattern assumed, rainfall decreases logarithmically with distance from the storm center. This derivation applies to a simple circular pattern and a particular form of area-depth curve, but can be extended to include other conditions. An elliptical pattern bears a close similarity to most rainfall patterns and can be derived in the same fashion, although it involves greater mathematical difficulties.

397. Similarities between equations 4.7, 4.9, and 4.10 suggest the possibility of a simple graphical solution, as shown in figure 146. If the area-depth curve is plotted as a straight line on semi-logarithmic paper, the minimum-rainfall curve is a parallel line displaced downward a distance equal to the slope a of the area-depth

curve. With radius plotted on the same scale as area, then, the curve of depth against radius has twice the slope of the area-depth curve and terminates at a point defined by the radius r_0 of the outermost isohyet and the minimum rainfall depth D of area A_0 (which equals the rainfall value along the outermost isohyet).

398. Since the depth-radius curve for a circular storm corresponds to a storm profile or cross-section outward from the storm center, the graphical procedure outlined above was used to derive generalized storm profiles for all the Muskingum summer storms studied. First, the area-depth values for the 38 storms were grouped according to storm magnitude, and group means obtained for the areas from 50 to 500 square miles. The results, as fitted straight lines on semi-logarithmic paper, are shown in figure 147. The family of curves represents typical or average area-depth relationships arranged according to storm magnitude. Developed from the same data, the values are consistent with the ratios indicated by the percentage area-depth curve of figure 145. The corresponding storm profiles based on a circular pattern were then derived graphically and are displayed in figure 148. The portions of the curves shown as dashed lines represent extrapolated values based on an extension of the straight-line relationship below 50 and above 500 square miles. These curves can be visualized either as profiles for hypothetical circular storms or as average profiles through actual storms.

Duration-depth relations

399. The effect of storm movement is to make the mass curves of rainfall at successive points in the direction of movement out of

phase. Generally, each curve will show a steep rise near the beginning of rain, with the major portion of the rainfall occurring in a fraction of an hour, as in figure 141. The mass curve of rainfall for a basin, however, because of non-synchronization over the area, will show a more symmetrical and also more uniform time pattern of rainfall. The duration of rain will be longer and the maximum intensity less than shown by individual point-rainfall mass curves.

400. The time pattern or hyetograph of rainfall volume over a basin will be influenced by basin characteristics of size, shape, and orientation. The effect of basin size is to reduce short-duration rainfall intensity with increase of area. If the basin deviates considerably from a circular shape, the hyetograph will be influenced by the orientation of the basin relative to storm direction. A long, narrow basin parallel to the storm path will have a long, uniform pattern of average rainfall. The same basin shape oriented normal to the storm path will show the early, steep rise of rainfall intensity that is characteristic of the individual station.

401. It is readily seen that the form of the duration-depth curve is related to the velocity and direction of storm movement and to the basin characteristics described above. An attempt was made in this study to isolate the effect of basin size on the shape of the duration-depth curve of thunderstorm rainfall. Because sufficient time was not available for a thorough study of the problem, it was decided to make evaluations for two sizes of area: 375 and 8000 square miles. The lower limit was selected because previous calculations had been made for that value of area and because smaller

Table 30

DURATION-DEPTH VALUES, 375 SQUARE MILES
(MUSKINGUM BASIN)

Storm No.	DURATION (HOURS)											
	1/2	1	1-1/2	2	2-1/2	3	3-1/2	4	4-1/2	5	5-1/2	6
1	.179	.315	.388	.449	.467	.480	.485	.487	.488	.488	.489	.489
2	.106	.186	.239	.284	.321	.356	.427	.434	.440	.442	.443	.443
3	.053	.105	.131	.155	.161	.184	.186	.194	.235	.269	.271	.273
4	.161	.317	.447	.563	.714	.820	.906	.981	1.051	1.095	1.139	1.150
5	.392	.639	.698	.729	.736	.736	.736	.736	.736	.736	.736	.736
6		.510		.679		.735		.767		.780		.793
7		.165		.295		.326		.329		.329		.329
8		.087		.108		.111		.115		.120		.122
9		.283		.389		.478		.496		.509		.509
10		.284		.565		.707		.733		.763		.770
11		.217		.239		.289		.373		.399		.400
12		.561		1.066		1.151		1.187		1.230		1.245
13		.294		.547		.660		.733		.784		.790
14		.199		.385		.426		.449		.485		.495
15		.071		.072		.085		.085		.085		.085
16		.238		.422		.433		.436		.436		.436
17		.484		.582		.624		.625		.625		.625
18	.689	1.086	1.476	1.637	1.694	1.725	1.763	1.778	1.789	1.790	1.790	1.790
19	.439	.590	.702	.761	.779	.788	.789	.789	.792	.792	.793	.793
20	.092	.183	.252	.302	.341	.373	.418	.435	.449	.469	.471	.471
21	.067	.132	.158	.187	.192	.194	.195	.195	.195	.195	.195	.195
22		.391		.400		.424		.429		.473		.475
23		.691		.848		.874		.928		1.049		1.055
24		.352		.474		.577		.577		.584		.584
25		.322		.423		.450		.473		.477		.481
26		.205		.248		.256		.259		.259		.259
27		.128		.167		.178		.180		.181		.181
28		.191		.343		.443		.617		.702		.725
29		.425		.699		.952		.974		.978		.978
30	.207	.374	.414	.460	.482	.502	.503	.503	.503	.503	.503	.503
31	.123	.227	.326	.372	.389	.404	.433	.458	.459	.461	.461	.461
32	.216	.260	.271	.277	.282	.282	.282	.282	.282	.282	.282	.282
33	.020	.036	.052	.052	.052	.052	.052	.052	.052	.052	.052	.052
34	.256	.483	.682	.741	.774	.828	.941	.995	1.009	1.016	1.017	1.018
35	.437	.663	.723	.772	.825	.884	.937	.972	1.010	1.044	1.079	1.089
36	.065	.125	.181	.244	.286	.313	.317	.321	.321	.321	.321	.321
37	.032	.064	.090	.117	.128	.134	.146	.153	.157	.159	.161	.162
38	.117	.217	.260	.287	.292	.306	.419	.500	.533	.540	.543	.543
Means		.318		.456		.514		.553		.575		.582

Table 31

DURATION-DEPTH VALUES, 8000 SQUARE MILES
(MUSKINGUM BASIN)

Storm No.	DURATION (HOURS)											
	1/2	1	1-1/2	2	2-1/2	3	3-1/2	4	4-1/2	5	5-1/2	6
1	.048	.092	.132	.169	.208	.242	.280	.318	.351	.383	.412	.432
2	.032	.063	.085	.107	.122	.139	.168	.182	.192	.201	.210	.215
3	.137	.270	.391	.501	.597	.667	.732	.778	.821	.861	.900	.929
4	.104	.185	.265	.338	.406	.466	.523	.570	.611	.650	.685	.716
5	.147	.283	.419	.520	.598	.663	.715	.721	.726	.730	.730	.730
6		.121		.211		.292		.362		.413		.463
7		.101		.183		.232		.271		.296		.297
8		.093		.162		.210		.253		.278		.296
9		.102		.202		.258		.311		.345		.357
10		.079		.143		.188		.232		.282		.321
11		.190		.308		.397		.460		.496		.508
12		.229		.446		.581		.704		.761		.803
13		.119		.216		.293		.374		.474		.544
14		.180		.350		.400		.440		.490		.510
15		.134		.197		.249		.277		.286		.291
16		.192		.322		.414		.496		.508		.520
17		.231		.433		.504		.535		.546		.557
18	.224	.414	.597	.780	.927	1.053	1.163	1.245	1.297	1.334	1.364	1.390
19	.107	.212	.282	.346	.376	.393	.403	.412	.419	.422	.425	.426
20	.085	.163	.240	.294	.344	.384	.413	.440	.454	.463	.469	.474
21	.084	.155	.226	.294	.359	.403	.441	.459	.471	.478	.483	.487
22		.083		.162		.204		.244		.282		.319
23		.263		.453		.618		.696		.782		.848
24		.106		.188		.280		.339		.421		.468
25		.117		.223		.325		.406		.454		.491
26		.106		.162		.204		.238		.266		.291
27		.097		.171		.227		.265		.322		.357
28		.114		.225		.281		.325		.360		.383
29		.331		.628		.743		.788		.801		.802
30	.057	.104	.149	.196	.252	.302	.337	.369	.395	.417	.431	.445
31	.076	.146	.217	.274	.332	.387	.451	.500	.546	.593	.637	.677
32	.091	.172	.227	.281	.309	.324	.330	.334	.336	.337	.337	.337
33	.038	.075	.106	.142	.178	.209	.245	.278	.316	.349	.382	.409
34	.121	.233	.350	.461	.553	.624	.667	.710	.737	.759	.776	.792
35	.172	.317	.448	.540	.623	.671	.707	.737	.755	.770	.784	.794
36	.074	.142	.199	.251	.290	.316	.336	.352	.361	.367	.370	.373
37	.043	.084	.121	.157	.190	.219	.246	.269	.290	.305	.318	.327
38	.068	.110	.148	.181	.207	.244	.280	.305	.325	.342	.355	.363
Means		.163		.297		.384		.447		.490		.520

areas would have included an inadequate number of rainfall stations.

402. The basic data consisted of tabulations of half-hourly rainfall during 1937, 1938, and 1939, and hourly observations during 1940 and 1941. The computation procedure involved arithmetical averaging of station-rainfall amounts for successive time increments in each of the thirty-eight 6-hour storms. The arithmetic means for the smaller area were adjusted to agree with the isohyetal mean for the total period. No adjustments were required for the 8000-square-mile area, the hyetograph values being the same as those developed for the selection of the maximum 6-hour period in the reliability study (paragraphs 343-9). Duration-depth values for each storm were determined in the usual manner: by selecting maximum periods and computing total rainfall for those periods.

403. The effect of area on the time pattern of rainfall is shown in figure 149 in the form of an average mass curve of basin rainfall expressed as a percentage of total 6-hour precipitation. A comparison of figure 149 with figure 141, the characteristic point-rainfall curve, shows that the effect of area is to increase the duration of rainfall and to transfer the maximum intensities to the middle of the storm period.

404. The duration-depth values of each storm are presented in tables 30 and 31. These data were used to develop general duration-depth relations applicable to thunderstorm rainfall. Values for durations under 6 hours were plotted against total 6-hour depth, as shown in figures 150 and 151, and regression lines fitted to represent average ratios between depths for the shorter durations and the

6-hour depth. Some of the storms plot consistently below the lines, indicating greater uniformity of rainfall intensity through the 6-hour period. However, there is no evidence of any definite trend toward abnormal time distribution for the larger values of rainfall. With this in mind, figure 152 presents the results in the form of average percentage duration-depth curves for the two values of area, 375 and 8000 square miles. The two curves verify the theory discussed previously: increasing uniformity of rates with increasing basin area. A similar plotting, using the United States maximum observed rainfall values presented in the next section, produces curves with generally less curvature, i.e., with more uniform rates.

Maximum thunderstorm rainfall

405. Because the scope of the present report is, by assignment, thunderstorm rainfall, it is primarily concerned with areas less than 1,000 square miles and durations less than 12 hours. The problem of computing the maximum possible rainfall over larger areas, usually greater than 10,000 square miles, and for durations of 24 hours or more, has been discussed in previous reports of the Hydrometeorological Section, particularly numbers 2 (7) and 3 (8), but in these and subsequent reports it was carefully noted that the basic techniques employed cannot with equal facility or security be applied to the smaller areas and the shorter durations.

406. The factors that must control the magnitude of rainfall intensity are known. They are, essentially, available moisture and the rate and height of lift. The first has been defined as

precipitable water, W_p , in previous reports where it has been shown that the justifiable assumptions of a pseudo-adiabatic lapse rate and saturation in major storms make W_p a function of the dew point at 1000 mb. Figure 153 is a chart for the computation of W_p , based on these assumptions. The limiting values are thus dependent on the limiting dew points, and sufficient data are available on the latter for reasonably accurate geographical and seasonal definition. The possible duration of the dew point should also be known. The Hydrometeorological Section is now engaged in a statistical study of dew-point persistence -- specifically the regional and seasonal variation of the highest dew point that can be equaled or exceeded within a given duration. The study is sufficiently advanced to indicate definitely that the country-wide gradient of this maximum dew point is least when short durations are considered, greatest when the longest durations are considered. A high dew point that can persist for days at New Orleans, for example, can persist only for hours at Chicago. The possible geographical extent of simultaneously high dew points is another factor, but it is obvious that the importance of this factor decreases with decrease of area. The indications are, then, that the shorter the duration and the smaller the area, the less variation there is in the W_p that must be used in the computation of the maximum possible rainfall.

407. The height of lift is another factor which, though it has a wide seasonal and geographic variation, becomes practically a constant when maximum possible values for short durations and small areas are to be computed. Its maximum value may be safely

stated as the maximum height of the tropopause, which is at a pressure of about 100 mb, thus allowing a maximum of about 900 mb of lift or an outflow column stretched to that depth. Even 10 to 20% variations in the depth have negligible effects on the possible precipitation because of the very small values of mixing ratio at pressures near 100 mb at atmospheric temperatures.

408. The rate of lift is the factor whose unreliability increases as the durations and the areas involved in the computation decrease. The rate of lift obviously cannot be very great over large areas, so that its possible variations under such circumstances are confined within narrow limits. Furthermore, these limits over large areas are determinable indirectly by construction of simplified convergent-flow models which not only resemble reality but which have definite and important features that can be checked from observed data ⁽⁹⁾. The mean rate of lift, or vertical velocity, for instance, is a function of the mean downwind decrease of wind in such a flow model, as explained in chapter I (see paragraph 93). The maximum possible velocity of the inflow wind can be approximated by envelopment and adjustment of observations of pressure, temperature, and wind. The optimum velocity at outflow is determined by the optimum ratio of inflow to outflow mass, $\Delta p_1 / \Delta p_2$ ⁽¹⁰⁾, which varies within the narrow limits of about 1/3 and 1/2, depending on the dew point. When the linear dimensions of the area under consideration are great enough, both the maximum inflow velocity and the velocity drop across the area can be reasonably verified by observation.

409. Over very small areas and for very short durations, however, both theory and observation indicate vertical velocities of very great magnitude. There are insufficient data on their variation in time and space and no flow model that could produce such vertical velocities can have its important dynamic features confirmed from any available network of meteorological observations, either surface or aloft. The matter is further complicated by the fact that no raindrops can fall through upward currents exceeding 9 mps at normal air density and that the horizontal transport of the raindrops that do fall may far exceed the linear dimension of the small area being considered for computation.

410. Pending the necessary refinements in observational network, techniques, and data, the closest approach to the maximum possible thunderstorm rainfall is by envelopment of recorded rainfall. The bases for such an envelopment are contained in table 32, which lists the record rainfall amounts in the United States for durations up to 24 hours and areas up to 1000 square miles. These data were developed from storm studies cooperatively made by the Hydrometeorological Section and the U.S. Engineers, and the storms producing the record values are also listed in the table. Many of the controlling rainfall amounts were determined largely from unofficial rainfall observations collected by survey of the storm area. Some of these observations were as much as 50 miles from available recording gages and indicated values five to six times those reported by official stations. However, all possible care has been taken to verify the data used. A further consideration, as indicated in figure 132 (chapter III), is that the percent standard error of rainfall determinations over areas of 1000 square miles or less, with average gage

density, is over 20%. Though caution is naturally indicated, it seems rash to ignore the possibility of the rainfall rates shown in table 32.

411. For a first approximation of limiting thunderstorm rainfall rates the values of the table should be considered. They can occur in one storm; most of them actually did occur in one storm.

412. For project basins, these values, enveloped for the size of the project area, should be adjusted on the basis of moisture content or dew point. This type of adjustment has been discussed in previous reports (7) (8). In the present case, the dew-point adjustment is based on thunderstorm-flow models which are modifications of the radial-inflow model shown in figure 22 (chapter I). These models all have the following features:

- (a) Continuity of mass flow is obtained by specifying equal mass (equal vertical pressure differences) in convergent and divergent layers; in the case of any inequality, the outflow velocity is adjusted by the ratio of the inflow Δp to the outflow Δp .
- (b) Cell-top height is varied linearly with surface vapor pressure, from 300 mb at a 1000-mb dew point of 50 F to 100 mb at a 1000-mb dew point of 78 F.

The depth of the convergent or inflow layer was varied from one-third to two-thirds the pressure height of the total cell; the divergent or outflow layer from one-third to one-half the same height; and the middle layer from one third of the height to zero. Each of these models produced a different value of effective precipitable water or W_E for a specific dew point but the percentage variation of W_E with dew point in each model was very nearly the same as the variation of precipitable water or W_p with dew point, W_p being computed from 1000 mb to the top of the cell. This fact permits a moisture adjustment of thunderstorm rainfall without

Table 32

MAXIMUM OBSERVED U.S. RAINFALL

(Revised October 1946)

Area (square miles)	Duration (hours)					
	1	3	6	12	18	24
Station	10.0a	21.5b	30.7d	34.3d	36.4c	38.2c
25	8.0b	16.8b	22.4d	28.6c	33.7c	35.1c
50	7.1b	15.6c	20.8c	27.5c	32.4c	33.7c
100	6.0c	14.7c	19.6c	26.2c	30.7c	31.9c
250	5.3c	13.3c	17.3c	23.6c	27.9c	29.0c
500	4.7c	11.8c	15.4c	21.4c	25.6c	26.6c
1000	3.9c	10.0c	13.4c	18.8c	22.9c	24.0c

Storm	Date	Location of Center	U.S.E.D. No.
a	1819, July 26	Catskill, N. Y.	NA 2-17
b	1935, May 31	D'Hanis, Tex. *	GM 5-20
c	1921, Sept. 8-10	Thrall, Tex.	GM 4-12
d	1942, July 17-18	Smethport, Pa. *	OR 9-23

* tentative data

reference to a specific flow model or specific values of W_E .

413. The W_p or W_E ratios to be used in the adjustment, as a function of the 1000-mb dew point and in terms of the W_p or W_E at a 1000-mb dew point of 78 F, are given by the curve of figure 154. The curve can be used in two ways. Assuming that the upper limits of thunderstorm rainfall in the United States are reasonably well defined by an envelopment of the values of table 32, adjustment can start with those values as a base. The dynamic intensities involved (the rate of lift, etc.) in the production of these rainfall rates can be assumed to be the optimum; thus only a moisture adjustment is necessary. The 1000-mb dew point which can be considered common to the enveloping values is 78 F. To estimate the limiting thunderstorm rainfall rates in a specific region, then, it is necessary only to obtain the maximum possible dew point for the region and to apply the ratio indicated in figure 154 to the enveloped values of table 32. A region whose highest 1000-mb dew point is determined to be 70 F will thus, as a first approximation, have limiting rainfall rates that are 67.7% of the envelopment. There may be some variation of the percentage with duration, but that variation is often small and therefore ignored in this presentation. Another approach is to adjust known storm values which have occurred in the project region, or are transposable to the region, by the percentages indicated in figure 154. For example: if the actual storm occurred at a 1000-mb dew point of 70, while the maximum possible dew point for the region is determined to be 78, the storm values would be increased by the ratio of $100/67.7$. An envelopment of such adjustments is an approximation of the maximum possible rain. If both types of adjustment yield the same result, there is greater assurance in using

the result as an estimate of the maximum possible. If the values do not agree, they can be used as upper and lower limits between which the final values should fall. The second type of adjustment will usually yield the lower value.

4.14. Since the enveloped values of table 32 can be considered as occurring at sea level (defined as 1000 mb), a further adjustment is required for project basins at higher elevations. The assumption is that there is no orographic intensification of the limiting thunderstorm-rainfall rates but that there is an orographic depleting effect. The higher the level at which the storm occurs the less the total W_p that can be processed and therefore the less the rainfall. To compute this depleting effect, each of the radial-inflow models previously described was varied so that its base was put at successively higher levels (lower pressures) while its top remained constant (for a particular 1000-mb dew point) and its ratio of inflow Δp to outflow Δp and to the middle-layer Δp was retained. The result was that the depleting effect, expressed as a percentage, approximately equaled the ratio of the W_p computed for the layer between 1000 mb and the basin elevation to the W_p computed for the entire cell (1000 mb to the top of the cell). The residual percentages, or the percentages of the limiting thunderstorm-rainfall rates at sea level that are possible at higher elevations, are given in figure 155. The chart is to be used after rainfall values (regional storm or enveloped U.S.) have been adjusted by comparison of the 1000-mb (sea-level) values of actual and maximum possible dew point. (A chart for the pseudo-adiabatic reduction of dew point involved is given in figure 33, chapter II.) Figure 155 is to be entered with the

maximum possible regional dew point at 1000 mb and the height of the barrier to inflow of the optimum moisture into the basin. The height of the barrier is defined as the mean height of the topographic barrier over which the air must flow in order to enter the basin. The correction applied is simply for the removal of moisture by lifting before the top of the barrier is reached (8). In the two examples of adjustment cited in the last paragraph, the existence of a 3000-ft barrier, as defined, would call for the application of a factor of 76% in the first case (1000-mb dew point of 70) and a factor of 80% in the second case (1000-mb dew point of 78).

415. Because of the possibility - even probability - of translation of rainfall from the region of formation to the region of fall, it follows that in regions of abrupt topographic slope the air convectively processed could originate at elevations lower than the elevation of the barrier to the project basin. If the slope upward to the edge of the basin on the windward side is very steep, the proper percentage adjustment for basin elevation in such a case may be larger than indicated in figure 155 - as large a percentage, in the extreme case, as for the elevation of the base of the windward slope. Though special study of the topography may be required in some cases, it is recommended as a practical and generally applicable expedient, where steep slopes are concerned, that the possible rainfall intensities be considered the same for all elevations from the base of the slope to 3000 feet above the base. The base elevation to be considered should not be more than five miles from the barrier to the project area and should be open to comparatively unobstructed air flow. For basins more than 3000 feet above the base of

the slope the percentage of base rainfall should be allowed to decrease linearly with height to 12,000 feet above sea level (1000 mb). The final percentage to be used at 12,000 feet should be taken, for the appropriate dew point, from figure 155.

416. The use of transposed depth-area values, without adjustment other than for moisture charge and elevation, presupposes the possibility of reorientation of isohyetal patterns to fit the project basin. Consideration must therefore be given to the application of special reduction factors, based on basin configuration, if estimates are to be made for basins of shape or orientation radically different from known storm isohyetal patterns. For example, most of the intense storms that provide the maximum rates of rainfall in the United States over large areas have typically elongated elliptical isohyetal patterns with major axis normal to the direction of the inflowing air from the south. However, closer examination of these and also small-area isohyetal patterns discloses that over the small sizes of area considered as subject to thunderstorm-type rainfall, the isohyetal pattern can have almost any orientation and shape, although the large-scale pattern has definitely restricted orientation and shape. In other words, for the estimate of maximum thunderstorm rainfall, a basin-configuration factor may usually be neglected.

References

417. Abbreviations used in the list of references are explained in the Bibliography. See Appendix.

1. A. E. Meyer, The elements of hydrology, 2d ed. rev., 1928.
2. D. L. Yarnell, Rainfall intensity-frequency data, USDA, Misc. Pub. no. 204, Aug. 1935.

3. G. N. Brancato and W. E. Remmele, Record one-minute rainfall at Opid's Camp, California, April 5, 1926, HMS, Off. of Hyd. Dir., USWB, Jan. 23, 1946.
4. HMS, Off. of Hyd. Dir., USWB, Maximum possible precipitation over the Ompompanoosuc Basin above Union Village, Vermont, Rpt. no. 1, in coop. with Eng. Dept., Corps of Eng., War Dept., Mar. 1940, p. 55-62.
5. HMS, River and Flood Division (Off. of Hyd. Dir.), USWB, Supplement to the report on the maximum possible rainfall over the Arkansas River Basin above Caddoa, Colorado, in coop. with Eng. Dept., Corps of Eng., War Dept., May 1939.
6. H. Kroeger and H. I. Stewart, Depth-area relationship for an unusual storm in St. Louis, in Studies of a near-maximum storm at St. Louis, CE, v. 10, Apr. 1940, p. 230-3.
7. HMS, Off. of Hyd. Dir., USWB, Maximum possible precipitation over the Ohio River Basin above Pittsburgh, Pennsylvania, Rpt. no. 2, in coop. with Eng. Dept., Corps of Eng., War Dept., June 1941.
8. HMS, Off. of Hyd. Dir., USWB, Maximum possible precipitation over the Sacramento Basin of California, Rpt. no. 3, in coop. with Eng. Dept., Corps of Eng., War Dept., May 1942.
9. HMS, Off. of Hyd. Dir., USWB, Revised report on maximum possible precipitation, Los Angeles area, California, in coop. with Eng. Dept., Corps of Eng., War Dept., Dec. 1945.
10. A. K. Showalter, An approach to quantitative forecasting of precipitation, pt. II, Formulas for quantitative rainfall forecasting, BAMS, v. 25, Sept. 1944, p. 276-88.

APPENDIX

2000-01

SYMBOLS AND ABBREVIATIONS

A	degrees Absolute, area
AD	average depth of precipitation
a	acceleration, slope
b	intercept on Y axis
C	degrees Centigrade
CCC	ceiling of convection above CCL
CCL	convective condensation level
CICL	convective ice-crystal level
cm	centimeter
CV	coefficient of variation
D	depth of precipitation
E	efficiency
e	partial pressure of water vapor
e_s	partial pressure of water vapor at saturation
F	degrees Fahrenheit, frequency
f	frequency
fps	feet per second
ft	foot, feet
G	area per rain gage
g	acceleration of gravity, gram
gm	gram
H	height
h	height
hr	hour
I	intensity of precipitation

ICL	ice-crystal level
in	inch
K	constant
kg	kilogram
km	kilometer
LCC	ceiling of convection above LCL
LCL	lifting condensation level
LFC	level of free convection
LICL	lifting ice-crystal level
m	meter
mb	millibar
mm	millimeter
mph	miles per hour
mps	meters per second
N	number
NACA	National Advisory Committee for Aeronautics
P	pressure, probability
p	pressure
P_c	condensation pressure
R	gas constant, rainfall
r	radius
RH	relative humidity
S	superior air
SD	standard deviation
SE	standard error
sec	second

T	temperature, thunderstorm, trace
t	time
T_c	critical temperature, condensation temperature
T_d	dew-point temperature
T_E	equivalent temperature
T_G	tropical Gulf air
T_w	wet-bulb temperature
V	velocity
V_1	inflow velocity
V_2	outflow velocity
V_z	vertical velocity
w	mixing ratio
W_E	effective precipitable water
W_p	precipitable water
w_s	saturation mixing ratio
X	dimension normal to inflow
\bar{X}	arithmetical average
Y	dimension parallel to inflow
ρ	air density
θ	potential temperature
θ_d	partial potential temperature of the dry air
θ_E	equivalent potential temperature
θ_w	wet-bulb potential temperature
\mathcal{R}	thunderstorm

GLOSSARY

absolute instability - Thermodynamic state of atmosphere characterized by lapse rate greater than the dry-adiabatic, hence unstable for both saturated and unsaturated air.

absolute stability - Thermodynamic state of atmosphere characterized by lapse rate less than the pseudo-adiabatic, hence stable for both saturated and unsaturated air.

adiabat - Curve of thermodynamic change taking place without addition or subtraction of heat. On adiabatic chart or pseudo-adiabatic diagram: a line showing pressure and temperature changes undergone by air rising or sinking in the atmosphere without exchange of heat with its environment or condensation of its water vapor; a line, thus, of constant potential temperature. Also called a dry adiabat.

adiabatic - Referring to process described by adiabat.

adiabatic chart - Diagram in which temperature is plotted against pressure ($\log p$ or $p^{0.288}$) and on which adiabats are constructed.

adiabatic lapse rate - Lapse rate equal to the rate of change of temperature with height of unsaturated air adiabatically raised or lowered in the atmosphere; indicated by the adiabat, and equal to 1 C/100 m, approximately. Also called the dry-adiabatic lapse rate.

advection - Horizontal air transport.

air mass - Extensive body of air approximating horizontal homogeneity, identified as to source region and subsequent modifications.

anticyclone - A circulation around relatively high pressure at the center, clockwise in the Northern and counterclockwise in the Southern Hemisphere.

area-depth curve - Curve showing, for a given duration, the relation of maximum average depth to size of area within a storm or storms. Also called depth-area curve.

average depth - Mean depth of precipitation over an area, obtained from the arithmetical or weighted mean of the depths at points within the area.

average error - The arithmetical mean of all errors or deviations, regardless of sign, measured as departures from an accepted "true" value or mean.

backing - Counterclockwise change of wind direction, e.g., from west wind to south wind.

center of action - Semipermanent cyclonic or anticyclonic system characterizing the large-scale circulation of the atmosphere.

cirrus - High cloud composed of ice crystals; delicate, fibrous, transparent in appearance.

coefficient of variation (CV) - A measure of relative variability, equal to the standard deviation expressed as a percentage of the mean.

col - Region of saddle-shaped isobaric surfaces between two regions of high pressure and two regions of low pressure, alternately arranged. By analogy, any region bounded by such an arrangement of isolines of high and low values.

cold front - Front at which relatively colder air displaces warmer air.

colloid - Substance in a state of such fine dispersion that it can remain in suspension, without marked settling, indefinitely.

comparative data - Periodic summary of the annual and monthly means or normals of various meteorological elements at a station.

conditional instability - Thermodynamic state of atmosphere which is stable for lifting of unsaturated air particles but unstable for lifting of saturated air particles; characterized by a lapse rate between the dry and the pseudo-adiabatic.

conditionally neutral - Possessing a pseudo-adiabatic lapse rate, hence neither conditionally stable nor unstable.

convection - Atmospheric motion thermally induced; chiefly the vertical component of such motion and, by analogy, any vertical component of motion. Also heat transfer by means of mass motion within the medium.

convective condensation level (CCL) - Atmospheric level at which rising air will become saturated after insolation has established a dry-adiabatic lapse rate from the surface to that level.

convective ice-crystal level (CICL) - Level at which the isotherm of freezing temperature is reached by saturated air rising above CCL.

convective instability - Thermodynamic state of a layer of air which can become unstable after lift or after evaporation of moisture into it; characterized by a decrease of θ_E or θ_W with elevation, or a lapse rate of T_W exceeding the pseudo-adiabatic.

convectively neutral - Neither convectively unstable nor convectively stable; characterized by constancy of θ_E or θ_W with height, or a lapse rate of T_W equal to the pseudo-adiabatic.

convergence - Horizontal shrinking and vertical stretching of a volume of air, accompanied by net inflow horizontally and internal upward motion vertically.

Coriolis force - Apparent deflecting force, on a particle in motion, due to the earth's rotation.

correlation coefficient - A measure of the proportion of one variable's variation which is associated with the variation in another variable.

critical points (or levels) - The levels in an aerological sounding (and the values at these levels) which separate markedly different rates of change of temperature or of relative humidity with height. Also called significant points or levels.

critical temperature (T_C) - Surface temperature that must be exceeded for free convection beyond CCL.

cumulonimbus - Massive cloud with great vertical development, upper part having fibrous texture and spreading out in shape of anvil; the thunderstorm cloud.

cumulus - Cloud type showing vertical development, upper surface dome-shaped with rounded protuberances, base nearly horizontal, seldom covering sky completely.

cumulus congestus - Distended, sprouting cumulus, with dome showing cauliflower appearance; the thunderhead.

cyclone - A circulation around relatively low pressure at the center, counterclockwise in the Northern and clockwise in the Southern Hemisphere.

deepening - Decreasing pressure at the center of a pressure system.

depth-area-duration data - Combination of area-depth and duration-depth relations. Also called time-area-depth data.

dew-point temperature - The temperature at which saturation is attained when air is cooled at constant pressure without the addition or subtraction of water vapor.

diurnal variation - Change in the value of an element during each day.

divergence - Horizontal stretching and vertical shrinking of a volume of air, accompanied by net outflow horizontally and internal downward motion vertically.

duration-depth curve - Curve showing, for a given size of area, the relation of maximum average depth to duration within a storm or storms. Also called depth-duration curve.

dynamic anticyclone - Anticyclone of primarily dynamic origin, warm relative to the surrounding air, with anticyclonic circulation maintained to high levels almost directly above the surface position.

eddy transfer - Transfer by turbulence.

effective precipitable water (W_E) - The greatest amount of precipitable water that can be removed from a column of air by a specifically defined process.

equivalent potential temperature (Θ_E) - The potential temperature of air after all the latent heat of condensation of the contained water vapor has been realized.

equivalent temperature (T_E) - The temperature of air after all the latent heat of condensation of the contained water vapor has been realized without net change of pressure.

first-order station - Meteorological observatory making continuous records or hourly readings of pressure, temperature, wind, sunshine, and precipitation, and also eye observations of clouds at fixed hours.

front - Surface of discontinuity or transition zone between two air masses, intersecting the ground (or another frontal surface) as a line or transition zone.

geostrophic wind - The wind resulting from a balance of the force due to the pressure gradient and the apparent deflecting force due to the earth's rotation. Neglecting friction, the theoretical wind accompanying and paralleling straight, parallel isobars in a steady state.

gradient - Vector measuring the direction and magnitude of the rate of decrease of a value.

gradient wind - The wind resulting from a balance between the force due to the pressure gradient, the apparent deflecting force due to the earth's rotation, and the centrifugal force due to the curvature of path. Neglecting friction, the theoretical wind accompanying and paralleling curved, concentric isobars in a steady state.

High - Anticyclone.

histogram - Block diagram with blocks having bases representing a class interval and heights proportional to the class frequency.

hodograph - A diagram of wind vectors at successive levels drawn from a common origin; more specifically, the curve connecting the ends of these vectors.

hurricane - Specifically, a storm producing wind speeds in excess of 75 mph; generally, a cyclone of tropical origin.

hydrometeor - Form of condensed water vapor in the atmosphere, such as rain, fog, cloud, etc.

hydrostatic pressure - Pressure due to weight.

hyetograph - Bar chart of increments of rainfall arranged chronologically.

hygroscopic - Possessing the property of absorbing and condensing water vapor.

ice-crystal level (ICL) - Level at which the temperature of freezing occurs in the atmosphere.

infiltration - Process whereby rainfall passes through the ground surface.

insolation - Solar radiation absorbed by the earth and atmosphere.

instability - Thermodynamic state favoring vertical displacements.

inversion - Increase of temperature with height.

isentropic - Adiabatic; at constant potential temperature.

isobar - Line of equal atmospheric pressure.

isoceraunic - Line of equal thunderstorm frequency (or thunderstorm-day frequency).

isochrone - Line of simultaneous time of beginning or ending.

isohyet - Line of equal depth of precipitation.

isohyet-area curve - See minimum-rainfall curve.

isoline - Line connecting equal values.

isotherm - Line of equal temperature.

kinematic viscosity - Measure of the viscosity or resistance of fluids or gases to shear, divided by the density.

k-type air mass - Air mass colder than the surface over which it is passing, with stability consequently decreasing in the lower layers.

land breeze - Offshore wind resulting from the greater nocturnal radiational cooling of the land surface than of the sea surface.

lapse rate - Rate of change of temperature with height.

level of free convection (LFC) - Atmospheric level above which the saturated air particle, in conditionally unstable air, is warmer than its environment and can therefore ascend freely.

lift - Upward vertical motion. Also the upward vertical displacement required to saturate air by dry-adiabatic lift.

lifting condensation level (LCL) - Atmospheric level at which saturation takes place after forced dry-adiabatic lift.

lifting ice-crystal level (LICL) - Level at which the isotherm of freezing temperature is reached by rising saturated air after forced lift past LCL.

local (shower or thunderstorm) - Occurring sporadically; not general.

Low - Cyclone.

mass curve - Curve of cumulative values through time.

mean (\bar{X}) - The sum of a group of values divided by their number.

mean deviation - Mean of the deviations (disregarding sign) from an average value, usually the mean.

millibar (mb) - Unit of atmospheric pressure equal to 1000 dynes/cm², standard atmospheric pressure being 1013.2 mb.

minimum-rainfall curve - Similar to area-depth curve, except that ordinates represent minimum instead of average depths within the areas; also called isohyet-area curve.

mixing ratio (w) - Ratio of the mass of water vapor to the mass of dry air in a given sample.

mountain wind - Down-slope wind resulting from the greater nocturnal radiational cooling of the air in contact with the mountain slope than of the free air at the same level above the valley.

multiple correlation - Measurement of the proportion of one variable's variation which is associated with the variations in two or more other variables.

negative area - Area, on a thermodynamic chart, below LFC and bounded by lapse rate curve and curve of hypothetical ascent of air particle, which is a measure of the energy to be contributed before free convection from conditional instability is attained.

normal - Average value of a meteorological element over a period of years sufficiently long to make the average acceptable as a standard from which to measure departures from normal.

normal distribution - A frequency distribution of observations of a variable determined by random causes.

occluded front - Portion of the frontal surface (warm or cold) remaining in contact with the ground after the cold front has overtaken the warm front and lifted the air in the warm sector aloft.

occlusion - Formation of occluded front; a cyclonic system which has undergone the process.

orographic - Caused by topographic slope.

parcel method - Analysis of conditional instability by assuming ascent of an infinitesimal particle of air.

partial potential temperature of the dry air (θ_d) - Potential temperature of the air after its pressure is reduced by the vapor pressure.

percentage-depth-area curve - An area-depth curve, with depths plotted as percentages of depth over a specified area, usually the largest.

percentage frequency ($\%F$) - Ratio, expressed in percent, of items or occurrences in one class or interval to total of items or occurrences in all classes or intervals compared.

percentage probability ($\%P$) - Probability expressed in percent; percentage of certainty of occurrence; the number of occurrences out of 100 chances.

percent standard error (% SE) - Ratio of standard error to the mean, expressed as a percentage.

pilot-balloon observation (pibal) - Wind-aloft measurement by observation, from surface, of drift of free balloon.

planimeter - Mechanical integrator for measuring plane area.

point rainfall - Rainfall recorded by one gage.

polar front - Surface of discontinuity or transition zone separating air masses of polar origin from those of tropical origin.

positive area - Area, on a thermodynamic chart, above LFC or CCL and bounded by lapse-rate curve and curve of hypothetical ascent of air particle, which is a measure of the energy realizable from conditional instability.

potential instability - Attainable instability, either conditional or convective, or both.

potential temperature (θ) - Temperature of the air if expanded or compressed dry-adiabatically to a standard pressure of 1,000 mb.

precipitable water (W_p) - Total water vapor contained in an atmospheric column of unit cross-section, expressed in terms of the depth of an equivalent mass of liquid water of the same cross-section.

probability - Ratio of the average or expected number of occurrences to the total number of mathematically possible occurrences.

probable error - The value of error which divides all the observational errors into two classes of equal frequency and therefore of equal probability.

pseudo-adiabat - Line on thermodynamic diagram showing the pressure and temperature changes undergone by saturated air rising in the atmosphere, without ice-crystal formation and without exchange of heat with its environment other than that involved in assuming that the liquid water, formed by condensation, drops out.

pseudo-adiabatic - Referring to the process described by the pseudo-adiabat.

pseudo-adiabatic diagram - Adiabatic chart to which pseudo-adiabats and lines of constant saturation mixing ratio have been added.

pseudo-adiabatic lapse rate - Lapse rate equal to the rate at which an ascending body of saturated air will cool, as represented by the pseudo-adiabat.

quasi-stationary front - Front along which displacement of warm by cold air, or vice versa, is slight and accompanied by minor wave action along the front.

radiosonde - Sounding by balloon-lifted instrument transmitting observations of weather elements (p, T, RH) automatically by radio; also refers to the instrument.

reduction (of meteorological observations) - Conversion of observed values to more comparable values by reference to a standard base by computation.

regression coefficient - The rate of change of the dependent variable with respect to the independent variable; the slope of the regression line.

regression line - A line expressing the relation between two variables.

relative humidity (RH) - Ratio of actual water-vapor content to saturation content or total water-vapor capacity, expressed as a percentage.

ridge - V- or U-shaped isolines bounding relatively high values, usually of pressure.

right (or positively) skewed distribution - An asymmetrical distribution of observations about a central value, characterized by high frequencies of the lower values.

root-mean-square - The square root of the arithmetical mean of the squared items.

Rossby diagram - Diagram for identifying air masses and determining convective instability, consisting of lines of constant θ_d , θ_E , and w , plus an overprint of lines of adiabatic condensation temperatures and pressures in some versions.

runoff - The contribution from precipitation to streamflow.

saturation - Upper limit of water-vapor content in a given space, a function of the temperature solely.

saturation vapor pressure (e_s) - The pressure or partial pressure of water vapor at saturation.

scattering - Reflection of radiation in all directions by very small particles in the atmosphere.

scud - Low, ragged clouds.

sea breeze - Onshore wind resulting from the greater daytime insolation heating of the land surface than of the sea surface.

sounding - Measurement (by pibal, radiosonde, airplane, etc.) of vertical structure of the atmosphere above a station. Also the graph of the distribution of the elements with height or pressure.

stability - Thermodynamic state in which vertical displacements are resisted.

standard deviation (SD) - The average deviation from the mean computed by taking the square root of the arithmetical mean of the squares of the individual deviations. (For small samples, it is the square root of the quotient obtained by dividing the sum of the squared deviations by one less than the number of deviations.)

standard error of the mean (SE) - The standard deviation of a distribution of means of samples.

steepen - Usually, to increase the rate of decrease of temperature with height; referring to an inversion: to increase the rate of increase of temperature with height.

storm profile - Vertical section through an isohyetal pattern, with distance from center as abscissa and corresponding depth of precipitation as ordinate.

stratiform - Referring to clouds arranged in unbroken horizontal sheets or layers.

stratosphere - The portion of the atmosphere, characterized by an isothermal lapse rate or inversion, above the tropopause.

strengthening - Increase of pressure gradient.

sublimation - Condensation of vapor directly to the solid form, or evaporation from the solid directly to vapor.

subsidence - Sinking of air.

superadiabatic - Steeper than the dry-adiabatic lapse rate.

supercooled - Existing as a liquid below its freezing temperature.

superior air (S) - Air mass of low relative humidity, originating from subsidence aloft.

synoptic - Showing the distribution of meteorological elements over an area at a given moment, e.g., a synoptic chart.

tephigram - Alternate for pseudo-adiabatic diagram, in which equal areas represent equal energy values.

thermal wind - The vectorial difference between the geostrophic winds at the top and bottom of a layer of air. Its direction (in the Northern Hemisphere) is cyclonic or counterclockwise around the colder air, its magnitude proportional to the mean horizontal temperature gradient of the layer.

Thiessen method of weighting - Method for determining the average depth of precipitation over an area by the construction of Thiessen polygons, by means of which the individual observations are areally weighted.

Thiessen polygon - Geometrical figure drawn by plotting perpendicular bisectors between adjacent precipitation stations. These bisectors form closed areas around each station and together form a network of contiguous polygons, for each of which the enclosed station's precipitation is considered representative.

trace - Half or less of .01 inch of precipitation.

triple-phase state - Coexistence of the gaseous, liquid, and solid forms of the same substance.

tropical storm - Cyclone of tropical origin; hurricane.

tropopause - Surface or zone within the atmosphere marking the upper limit of convection, and identified by a transition from the normal decrease of temperature with height to isothermal or inversion conditions.

troposphere - The portion of the atmosphere between the tropopause and the earth's surface, normally characterized by the effects of convection and therefore a steady decrease of temperature with height.

trough - V- or U-shaped isolines bounding relatively low values, usually of pressure.

turbulence - Irregular gaseous or fluid motion resulting from flow past solid surfaces or flow of neighboring currents past or over each other.

valley wind - Up-slope wind resulting from the greater daytime insolation heating of the air in contact with the mountain slope than of the free air at the same level above the valley.

vapor pressure - Pressure of the water vapor in a sample of air.

veering - Clockwise change of wind direction, e.g., from south wind to west wind.

virgae - Streamers formed by precipitation evaporating between cloud base and ground surface.

vorticity - Rotational component of motion.

warm front - Front at which relatively warmer air replaces colder air.

warm sector - Sector of warm air bounded on two sides by the cold and warm fronts extending from a center of low pressure.

wave - Localized deformation of a front, resembling a warm-sector formation, usually traveling along the front and sometimes developing into a mature cyclone.

wave crest - Apex of warm sector of wave formation on a front.

weighted mean - The sum of the items, each multiplied by its respective weight, then divided by the sum of the weights.

wet-bulb potential temperature (θ_w) - Wet-bulb temperature reduced along the pseudo-adiabat to 1000 mb.

wet-bulb temperature (T_w) - Lowest temperature to which air can be cooled by evaporating water into it at constant pressure; the temperature at which saturation is attained when water is evaporated into air at constant pressure.

A SELECTED THUNDERSTORM BIBLIOGRAPHY

For abbreviations used see Abbreviations and Publication Information following the Bibliography.

Synoptics and Dynamics

- Abercromby, R. On the barometric fluctuations in squalls and thunderstorms. *QJRMS*, v. 1, Oct. 1875, p. 449-54.
- Alexander, G. W. Lightning storms and forest fires in the state of Washington. *MWR*, v. 55, Mar. 1927, p. 122-9.
- Alexander, W. H., C. E. Brooks, and G. H. Burnham. Thunderstorms in Ohio during 1917. *MWR*, v. 52, Jul. 1924, p. 343-8.
- Barlow, E. W. Thunderstorms at sea. *Marine Observer*, v. 12, Apr. 1935, p. 49-52.
- Beers, N. R. Atmospheric stability by slice method. *USNA*, 1944. (Mimeo no. 2989).
- von Bezold, W. On the thermodynamics of the atmosphere (Supersaturation and subcooling. Formation of thunderstorms). Chap. XII in *Mechanics of the earth's atmosphere*, ed. by Cleveland Abbe (Third Collection). *Smithsonian Misc. Coll. (Hodgkins Fund)*, v. 51, no. 4. Washington, 1930.
- von Bezold, W. "Über gesetzmässige Schwankungen in der Häufigkeit der Gewitter während langjähriger Zeiträume. *Sitzungsb., Akad., München*, v. 4, 1874, p. 289-322.
- Bohme, G. Der aerologische Zustand der Atmosphäre bei Gewitterlagen, *ZAM*, v. 51, Sept. 1934, p. 273-81.
- Boswell, R. W., and W. J. Wark. Relation between sources of atmospherics and meteorological conditions in southern Australia during October and November 1934. In *Discussion on thunderstorm researches*. *QJRMS*, v. 62, Oct. 1936, p. 499-527.
- Brancato, G. N. Meteorological behavior and characteristics of thunderstorms. *HMS, Off. of Hyd. Dir., USWB*, Apr. 1942. (Also, in *Aviation*, Oct.-Nov. 1942; and repr. by Dept. of Transport, Air Services Branch, Dominion of Canada.)
- Brooks, C. F. The local, or heat, thunderstorm. *MWR*, v. 50, June 1922, p. 281-4.

- Brooks, C. F., and others. Effect of winds and other weather conditions on the flight of airplanes. *MWR*, v. 47, Aug. 1919, p. 523-32.
- Browne, J. A. Thunderstorm characteristics and flight procedures. TWA, Met. Dept., Tech. Note no. 5. 1942. (Mimeo) Also, *Aeronautical Eng. Rev.* (New York, Inst. of Aeronautical Sciences), v. 1, no. 9, Dec. 1942, p. 5-19.
- Brunt, D. Convective circulation in the atmosphere. *Met. Mag.*, v. 60, Feb. 1925, p. 1-5. Also, *Physical and dynamical meteorology*. 2d ed. Cambridge Univ. Press, 1939. P. 213-16. (Benard Cell)
- Buell, C. E. The determination of vertical velocities in thunderstorms. *BAMS*, v. 24, Mar. 1943, p. 94-5.
- Bunch, S. The rain-bearing winds at Knoxville, Tennessee. *MWR*, v. 65, Jul. 1937, p. 269-70.
- Byers, H. R. Nonfrontal thunderstorms. *Inst. of Met. (Dept. of Met.)*, Univ. of Chicago, Misc. Rpt. no. 3. June 1942.
- Calwagen, E. G. Zur Diagnose und Prognose lokaler Sommerschauer. *Geophys. Pub.*, v. 3, no. 10. 1926.
- Carlin, A. V., D. L. Jorgensen, R. H. Simpson, and L. L. Means. Analyses of thunderstorms in the South and Central United States. USWB, in coop. with Univ. of Chicago, 1944. (Mimeo)
- Cook, A. W. The diurnal variation of summer rainfall at Denver. *MWR*, v. 67, Apr. 1939, p. 95-8.
- Devereaux, W. C. Records at the Abbe Meteorological Observatory compared with those at the Government Building, Cincinnati. *MWR*, v. 45, May 1917, p. 224-33.
- Douglas, C.K.M. A problem of convection. *Met. Mag.*, v. 64, Oct. 1929, p. 214.
- Douglas, C.K.M. Summer thunderstorms. *Met. Mag.*, v. 68, Apr. 1933, p. 53-60.
- Evans, E. A., and K. B. McEachron. The thunderstorm. *General Electric Rev.*, Sept. 1936, p. 413-25.
- Fairgrieve, J. Suggestions as to the conditions precedent to the occurrences of summer thunderstorms, with special reference to that of June 14, 1914. *MWR*, v. 47, June 1919, p. 394-5. (Abstr. from *QJRMS*, v. 44, 1918, p. 245-52.)

- von Ficker, H. "Über die Entstehung lokaler Wärmegewitter. SPAW. 1931-4. (In four parts.)
- Forrest, J. S. The determination of the location and frequency of thunderstorms by a radio method. QJRMS, v. 69, Jan. 1943, p. 33-46.
- Gisborne, H. T. A five-year record of lightning storms and forest fires. MWR, v. 59, Apr. 1931, p. 139-50.
- Gockel, A. Das Gewitter. 3d ed. Berlin, 1925. 316 p.
- Gregg, W. R. Aeronautical meteorology. 2d ed. New York, Ronald Press, 1930. P. 201-31.
- Günther, S. Ein Beitrag zur Vorgeschichte der modernen Gewitterkunde. SBAW. 1910. 22 p.
- Guilbert, G. Forecasting thunderstorms. MWR, v. 43, Nov. 1915, p. 556-62.
- Gupta, P. K. Sen. Kalbaishakhis (thundersqualls) of Bengal. BAMS, v. 24, Mar. 1943, p. 96-102. (Repr. from Science and Culture, v. 7, Sept. 1941, p. 134-9.)
- Hallenbeck, C. The topographic thunderstorm. MWR, v. 50, June 1922, p. 284-7.
- Haughton, W. R. Thunderstorms in eastern Bengal. QJRMS, v. 51, Oct. 1925, p. 406-8.
- Hellman, G. Beitrag zur Gewitterkunde. Veröff. PMI, no. 320, 1924, p. 43-51.
- Henry, A. J., F. H. Bowie, and others. Weather forecasting in the United States. Washington, GPO, 1916. P. 274-8.
- Hildebrandson, H. H., and L. Teisserenc de Bort. Les bases de la météorologie dynamique. Paris, Gauthier-Villars, 1900, v. 2, chap. V, Orages et grains, p. 243-78.
- Horton, R. E. A double-breasted thunderstorm. BAMS, v. 5, Aug.-Sept. 1924, p. 130-31.
- Horton, R. E. The beginning of a thunderstorm. MWR, v. 49, Apr. 1921, p. 193-4.
- Humphreys, W. J. Physics of the air. 3d ed. New York, McGraw-Hill, 1940.

- Jensen, J. C. Further studies on the electrical charges of thunderstorms. MWR, v. 58, Mar. 1930, p. 115-16.
- Kaplan, H. G. On the mechanism of thunderstorm downdrafts. BAMS, v. 24, Feb. 1943, p. 54-9.
- Kassner, C. Zur Wochenperiode der Gewitter. Das Wetter, v. 13, Aug. 1896, p. 178-84.
- Kaufmann, H. Beitrag zur Gewitterkunde Sachsens in Hinblick auf die hydrographischen Verhältnisse. Dresden, 1929.
- King, A. The great fireball of 1934, October 11, and an instance of streak-drift. QJRMS, v. 62, Jan. 1936, p. 33-40.
- Krebs, A. Beiträge zur Kenntnis und Erklärung der Gewitter-Erscheinungen auf Grund der Aufzeichnungen über die Gewitter Hamburgs in den Jahren 1878-1887. Inaugural Dissertation, Univ. Marburg, 1889. 31 p.
- Lenard, P. On waterfall electricity and on the surface conditions of liquids. MWR, v. 43, Oct. 1915, p. 509-10. (Also, Science Abstracts, Sec. A, Oct. 25, 1915, par. 1446.)
- Levin, G. Thunderstorm mechanics. CIT, 1941. 41 p.
- Levine, J. The effect of vertical accelerations on pressure during thunderstorms. BAMS, v. 23, Feb. 1942, p. 52-61.
- Linke, F. An account of Prof. Mugge's film "Clouds in motion; the thunderstorm." QJRMS, v. 63, Jan. 1937, p. 73-5.
- Loisel, J. Squalls and thunderstorms. MWR, v. 37, June 1909, p. 237-9.
- McAdie, A. The principles of aerography. New York, Rand McNally, 1917. Chap. XIV, Thunderstorms, p. 167-204.
- McAuliffe, J. P. Morning showers over the Gulf, and afternoon showers in the interior near Corpus Christi, Tex. MWR, v. 61, Aug. 1933, p. 229.
- McNeal, D. Some Observations on a free-balloon flight made from Aberdeen Proving Ground, Md., June 3, 1920. MWR, v. 48, June 1920, p. 334-5.
- Mal, S., and B. N. Desai. The mechanism of thundery conditions at Karachi. QJRMS, v. 64, Jul. 1938, p. 525-37.

- Meisinger, C. L. Balloon race from Fort Omaha through thunderstorms. MWR, v. 47, Aug. 1919, p. 533-4.
- Namias, J. Thunderstorm forecasting with the aid of isentropic charts. BAMS, v. 19, Jan. 1938, p. 1-14.
- Neiburger, M. Vorticity analysis of a thunderstorm situation. BAMS, v. 22, Jan. 1941, p. 1-5.
- Newnham, E. V. On the formation of thunderstorms over the British Isles in winter. GBMO, Prof. Notes, no. 29. 1922.
- Orkin, A. W. Thunderstorms, their causes and aids in forecasting. CIT, 1942. 10 p.
- Payne, F. F. Ground markings by lightning. MWR, v. 56, June 1928, p. 216.
- PCA. Thunderstorms. Met. Bull. no. 5. May 21, 1940.
- Peppler, W. Temperatur und Feuchtigkeit in der freien Atmosphäre an Gewittertagen. BPFA, v. 21, 1934, p. 121-8.
- Pernice, E. Der Spreewald als Gewitterherd. (Ein Beitrag zur Erklärung der Vorgänge in Gewitterherdgebieten.) Inaugural Dissertation, Friedrich Wilhems Univ., Berlin, 1930.
- Petterssen, S. Contribution to the theory of convection. Geofys. Pub., v. 12, no. 9, 1939.
- Petterssen, S., and J. M. Austin. Fronts and frontogenesis in relation to vorticity. MIT Papers, v. 7, no. 2, Jan. 1942.
- Pigot, E. F. Pressure fluctuations during a thunderstorm. MWR, v. 47, June 1919, p. 396.
- Reed, T. R. Thermal aspects of the high-level anticyclone. MWR, v. 67, Jul. 1939, p. 201-4.
- Renner, R. Über die Abkühlung unter Gewittern. AH, v. 66, Sept. 1938, p. 455-9.
- Rossmann, F. Bemerkungen zu einigen Gewittererscheinungen. ZAM, v. 56, Oct. 1939, p. 322-7.
- Scherhag, R. Über die atmosphärischen Zustände bei Gewittern (unter besonderer Berücksichtigung der Estgewitter und mehrtagiger Gewitterperioden). Inaugural Dissertation zur Doctorwürde, Univ. Berlin, 1931. 96 p.

- Schmidt, W. On thunder. MWR, v. 42, Dec. 1914, p. 665-71.
- Simpson, G. C. Electricity of rain and its origin in thunderstorms. MI, v. 20, pt. 8. 1910.
- Simpson, G. C. On the formation of cloud and rain. QJRMS, v. 67, Apr. 1941, p. 99-133.
- Sreenivasaiah, B. N., and N. K. Sur. A study of the duststorms of Agra. MI, v. 27, pt. 1. 1939.
- Sreenivasaiah, B. N., and N. K. Sur. The thermodynamics of dust storms. Current Science, v. 6, no. 5, Nov. 1937, p. 209-12.
- Starr, V. P. The readjustment of certain unstable atmospheric systems under conservation of vorticity. MWR, v. 67, May 1939, p. 125-34.
- Stearns, H. D. Effect of proximity to the sea on thunderstorm periods. MWR, v. 26, Oct. 1898, p. 452-4.
- Stevens, W. R. Lightning storms and fires on the national forests of Oregon and Washington. MWR, v. 62, Oct. 1934, p. 370-75. (Summarization of article by W. G. Morris.)
- Stevens, W. R. Meteorological conditions preceding thunderstorms on the national forests. MWR, v. 62, Oct. 1934, p. 366-70, and MWR, v. 63, June 1935, p. 183-4.
- Stickley, A. R. An evaluation of the Bergeron-Findeisen precipitation theory. MWR, v. 68, Oct. 1940, p. 272-9.
- Suckstorff, G. A. Die Ergebnisse der Untersuchungen an tropischen Gewittern und einigen anderen tropischen Wettererscheinungen. BG, v. 55, no. 1, 1939, p. 138-85.
- Suckstorff, G. A. Kaltluftherzeugung durch Niederschlag. MZ, v. 55, Aug. 1938, p. 287-92.
- Süring, R., and A. Mey. Über den Zusammenhang zwischen Gewitterzügen und Niederschlagsgebieten. Abhandl. Kön. PMI, v. 3, no. 5. 1910.
- Terada, K. Thunderstorm as a forerunner of typhoon. Jour. Met. Soc. Japan, Ser. 2, v. 13, no. 11, 1935, p. 505-12.
- Thornthwaite, C. W. The life history of rainstorms. Geog. Rev. (New York), v. 27, Jan. 1937, p. 92-111.
- TWA. Thunderstorms. Tech. Note no. 3. Mar. 15, 1941.

- Tray, F. Beitrag zur Erklärung der langen Dauer und der mehrfachen Schläge des Donners. *MZ*, v. 42, June 1925, p. 231-4.
- UATC. Met. Circulars, nos. 6, 16, 17 (Thunderstorms, June 15, 1939; Pre-coldfrontal squall lines, Mar. 1, 1941; Thunderstorms, Apr. 18, 1941).
- Wall, E. Was Man vom Gewitter weiss. *ZAM*, v. 56, Nov. 1939, p. 344-50.
- Ward, R. A. Pressure distribution in relation to thunderstorm occurrence on Oregon and Washington national forests. *MWR*, v. 64, Feb. 1936, p. 37-45.
- Warren, L. A. Wind stratification near a large thunderstorm. *MWR*, v. 47, June 1919, p. 395-6.
- Weeks, J. R. Mammato-cumulus clouds and thunderstorm at Binghamton, N. Y., June 24, 1914. *MWR*, v. 47, June 1919, p. 397.

Climatology

- Alexander, W. H. The distribution of thunderstorms in the United States, 1904-33. *MWR*, v. 63, May 1935, p. 157-8.
- Arendt, T. Ergebnisse zehnjähriger Gewitterbeobachtungen in Nord- und Mitteldeutschland. *Veröff. Kön. PMI*, v. 2, no. 2. 1908.
- Bily, J., Jr. Thunderstorms at Tampa, Fla. *MWR*, v. 32, Oct. 1904, p. 457-61.
- Brooks, C.E.P. Distribution of thunderstorms over the globe. *GBMO*, *Geoph. Mem.*, v. 3, no. 24, p. 147-64. 1925.
- Cornthwaite, H. G. Panama thunderstorms. *MWR*, v. 47, Oct. 1919, p. 722-4.
- Crestani, G. Temporali e groppi in Italia. *L'Aeronauta* (Rome), v. 1, no. 2, Mar. 1918.
- Davis, W. M. Notes on studies of thunderstorms in Europe (First and second papers). *Amer. Met. Jour.*, 1886.
- Davis, W. M. Thunderstorms in New England in the summer of 1885. *Proc., American Academy of Arts and Sciences* (Boston), v. 22, Jul. 1886, p. 14-58.
- Eredia, A. Sui temporali in Italia. *Elettrotecnica*, v. 19, no. 6, Feb. 25, 1932.

- India Met. Dept. Frequency of thunderstorms in India. Scientific Notes, v. 1, no. 5. Calcutta, 1929.
- Jurwitz, L. R. Thunderstorm frequencies for 6-hour periods at Miles City, Mont. MWR, v. 65, June 1937, p. 237-8.
- Kallio, N. Die Erstreckung des Gewitters nach dem Nord- und Südpol. Commentationes Physico-Mathematicae, Societas Scientiarum Fennica (Helsingfors), v. II, no. 10. 1924.
- Kidson, E., and A. Thomson. The occurrence of thunderstorms in New Zealand. Jour. Sci. and Tech. (Wellington, New Zealand), v. 12, no. 4, Feb. 1931, p. 193-206.
- Kincer, J. B. Precipitation and humidity. In Atlas of American Agriculture, Pt. II, Climate. USDA, Mar. 1922. (This is the first of three sections on climate.)
- Knoche, W. Über die Zahl der Gewitter in Chile. Mitteilungen Deutsch-Chilenischen Bundes, no. 3. Santiago, 1919.
- Koppen, W. Jährliche Häufigkeit der Gewitter zwischen Felsengebirge und Ural. AH, v. 55, Nov. 1927, p. 355-6.
- Marshall, W. A. L. The mean frequency of thunder over the British Isles and surrounding areas. QJRMS, v. 60, Oct. 1934, p. 413-24.
- Noto, H. Statistical investigations on thunderstorms in Japan. Japanese Jour. of Astronomy and Geophysics, v. 9, 1931-1932, no. 3, Transaction no. 14, p. 207-43; also, v. 10, 1932-33, p. 51-79.
- Riggenbach, A. Resultate aus 112 jährigen Gewitteraufzeichnungen in Basel. Verhandlungen der Naturforschenden Gesellschaft zu Basel, pt. 8. Basel, 1889.
- Russell, H. C. Thunder and hail storms in New South Wales. Jour. of Roy. Soc. of New South Wales (Sydney), v. 14, 1880.
- Schou, G. Gewitter in Norwegen. Geofys. Pub., v. 9, no. 7. 1932.
- Serra, A. B. Trovoadas locais no Rio de Janeiro. Rio de Janeiro, Departamento de Aeronautica Civil, Divisão de Meteorologia, 1937. (Repr. from Boletim Mensal, Divisão de Meteorologia, Sept. 1934.)
- Sohni, V. V. Temperature changes in Calcutta thunderstorms. India Met. Dept., Scientific Notes, v. 4, p. 19. Calcutta.

Sohoni, V. V. Thunderstorms of Calcutta 1900-1926. India Met. Dept., Scientific Notes, v. 1, no. 3, p. 25-36. Calcutta, 1928.

Sutton, J. R. Some statistics of thunder and lightning at Kimberley. Trans. of Roy. Soc. of South Africa (Capetown), v. 9, pt. 2. 1921.

Thomson, A. Thunder and lightning in the South Pacific Ocean. MWR, v. 58, Aug. 1930, p. 327-9.

Tinn, A. B. Local distribution of thunder rains round Nottingham. QJRMS, v. 66, Jan. 1940, p. 47-65.

USWB. Airway Meteorological Atlas for the United States. WB Pub. no. 1314. 1941.

Ward, R. D. The climates of the United States. New York, Ginn, 1925. Chap. XIV, Thunderstorms.

Hail

Arenberg, D. L. The formation of irregularly shaped hailstones. MWR, v. 66, Sept. 1938, p. 275-7.

Arenberg, D. L. The formation of small hail and snow pellets. BAMS, v. 22, Mar. 1941, p. 113-16.

Arenberg, D. L. Turbulence as the major factor in the growth of cloud drops. BAMS, v. 20, Dec. 1939, p. 444-8.

Arendt, T. Die Hagelgefahr in Nord- und Mitteldeutschland. Zeitschrift für wissenschaftliche Landwirtschaft (Berlin), v. 54, p. 539-61. 1920.

Bilham, E. G., and E. F. Relf. The dynamics of large hailstones. QJRMS, v. 63, Apr. 1937, p. 149-62.

Blair, T. A. Hailstones of great size at Potter, Nebr. MWR, v. 56, Aug. 1928, p. 313.

Brooks, C.E.P. Formation of hail. Discovery (London), v. 10, Sept. 1929, p. 305-8.

Canaday, G. L. Hail and windstorm over southeastern Louisiana, February 26, 1939. MWR, v. 67, Oct. 1939, p. 365-6.

Carey, F. Hailstorm of 1881 stands as a record. BAMS, v. 10, Nov. 1929, p. 204-5.

- Dyke, R. A. Heavy hailstorm and local squall at New Orleans, La., with a summary of the previous records of hail. *MWR*, v. 52, Apr. 1924, p. 205.
- Greening, G. K. Hailstones of July 6, 1932. *USWB, Climatological Data*, 1932, pt. 3, Jul., Iowa Section, p. 62-3.
- Grimminger, G. The upward speed of an air current necessary to sustain a hailstone. *MWR*, v. 61, Jul. 1933, p. 198-200.
- Grohmann, E. Hagelfälle und Blitzschlag auf Gebäude innerhalb des Königreichs Sachsen während der Jahre 1886-1905. Dresden, 1910. 16 p.
- Henry, A. J. Hail in the United States. *MWR*, v. 45, Mar. 1917, p. 94-9.
- Hoxmark, G. Granizo en la Republica Argentina. Dirección de Meteorología, Ministerio de Agricultura de la Nación, Republica Argentina. Buenos Aires, 1927. 35 p.
- Humphreys, W. J. The uprush of air necessary to sustain the hailstone. *MWR*, v. 56, Aug. 1928, p. 314.
- Johnson, R. P. The structure of hailstones. *MWR*, v. 66, Sept. 1938, p. 277. (Abstr. from *Nature*, v. 142, July 23, 1938, p. 172.)
- Koch, A. A. The dynamics of raindrops and hailstones. *Proc. Eng. Conf., S. Pacif. and N. Pacif. Div., Corps of Eng., War Dept.*, San Francisco, Feb. 1940, p. 241-68.
- Koch, G. D. Meteorological aspects of hailstorms in Nebraska. *MWR*, v. 65, June 1937, p. 236-7.
- Lemons, H. Hail as a factor in the regional climatology of the United States. *Geog. Rev. (New York)*, v. 32, no. 3, Jul. 1942, p. 471-5.
- Lemons, H. Hail in high and low latitudes. *BAMS*, v. 23, Feb. 1942, p. 61-8.
- Lemons, H. Semimonthly distribution of hail in the United States. *MWR*, v. 71, Jul. 1943, p. 115-22.
- Little, E.W.R. Observations on hail. *QJRMS*, v. 66, Jan. 1940, p. 21-2.
- Lloyd, F. E. Structure of hailstones of exceptional form and size. *McGill Univ., Dept. of Met., new series*, no. 1. Montreal, 1916. p. 47-50. (Repr. from *Trans. Roy. Soc. of Canada*, sec. 3, Sept. 1916.)

- Martinuzzi, L. Sulla possibilità della formazione della grandine a quota relativamente bassa. Atti della Pontificia Accademia della Scienze Nuovi Lincei, v. 84, session 7, June 21, 1931. Rome, 1931. 12 p.
- Milham, W. I. Note on the hailstones of August 9, 1938, at Williams-town, Mass. MWR, v. 66, Sept. 1938, p. 277.
- Reed, C. D. Dry hailstorms. BAMS, v. 18, Jan. 1937, p. 27-8.
- Reed, C. D. Hail damage in Iowa. USWB, Climatological Data, 1939, pt. 2, June, Iowa section, p. 50-51.
- Reed, C. D. Hail, wind and rain on June 18. USWB, Climatological Data, 1940, pt. 2, June, Iowa section, p. 48-9.
- Reed, C. D. Maps of hail losses of each individual year including 1925, the greatest hail loss of record. WBO, Des Moines, Iowa.
- Rohrbeck, W. Hagel, Hagelschadenbeurteilung und Hagelversicherung. Berlin, Paul Parey, 1913. 36 p.
- Russell, R. On hail. London, Edward Stanford, 1893. 224 p.
- Sarrazin, F. Acht Jahre Hagelstatistik des Kgl. Preuss. statistischen Büreaus unter Berücksichtigung der Naturgesetze des Hagels. Breslau, Morgenstern, 1892. 26 p.
- Schumann, T.E.W. The theory of hailstone formation. QJRMS, v. 64, Jan. 1938, p. 3-21.
- Seeley, D. A., and R. B. Dole. Hailstorms in Michigan, 1920-1923. MWR, v. 52, Apr. 1924, p. 195-205.
- Selga, M. Hail in the Philippines. Govt. of Philippine Islands, WB, Manila Central Observatory. Manila, 1929.
- Shaw, W. N. Manual of meteorology, v. III. Cambridge Univ. Press, 1930. P. 336-8.
- Slocum, G. Unusual fall of large hailstones at Washington, D. C. MWR, v. 66, Sept. 1938, p. 275.
- UATC. Thunderstorms. Met. Circular no. 6. June 15, 1939. P. 1-6 (section on hail). Mimeo.
- Visher, S. S. Hail in the tropics. BAMS, v. 3, Jul-Aug. 1922, p. 117-18.

Williford, C. C. Black dust with hail, snow and rain. BAMS, v.22, Mar. 1941, p. 122-4.

Tornadoes

Abbe, C. The prediction of tornadoes and thunderstorms. MWR, v. 27, Apr. 1899, p. 159-60.

Baier, J. Wind pressures in the St. Louis tornado. Proc. ASCE, v. 23, no. 1. Jan. 1897.

Belden, W. S. Tornadoes in Missouri. MWR, v. 58, May 1930, p. 208.

Bigelow, F. H. Atmospheric circulation and radiation. New York, Wiley, 1915. P. 196-215.

Bigelow, F. H. Studies on the thermodynamics of the atmosphere, MWR, v. 34, Jul., Aug., Oct., and Nov., 1906. Study no. VI, The waterspout seen off Cottage City, Mass., in Vineyard Sound, on August 19, 1896, p. 307-15; nos. VII, VIII, and IX, The meteorological conditions associated with the Cottage City waterspout, p. 360-70, p. 470-78, p. 511-17. Also, see Report of the Chief of the Weather Bureau, USWB, 1898-9, v. II, p. 632-3; and MWR, v. 29, Sept. 1901, p. 419.

Blackstock, I. B. The Hardtner (Kans.) tornado of June 2, 1929. MWR, v. 58, Aug. 1930, p. 325.

Brooks, C. F. Three observations of air sinks. BAMS, v. 23, Apr. 1942, p. 184-6.

Brown, C. W. A study of time-, areal-, and type-distribution of tornadoes in the United States. TAGU, 1933, p. 100-106.

Brown, C. W., and W.O.J. Roberts. The distribution of tornadoes in the United States from 1880 to 1931. TAGU, 1935, pt. I, p. 151-8.

Brunt, D. Tornadoes started by an oil fire. Met. Mag., v. 61, Jan. 1927, p. 292-4. Also, MWR, v. 55, Jan. 1927, p. 24-5.

Christensen, A. H. Tornadoes in Iowa during June, 1925. MWR, v. 53, Jul. 1925, p. 314.

Cole, H. S. Tornadoes in Arkansas, 1879-1926. MWR, v. 55, Apr. 1927, p. 176-82.

Condre, G. E., and G. A. Loveland. The Iowa-Nebraska tornadoes of Easter Sunday 1913. Bull. Amer. Geog. Soc. (New York), v. XLVI, Feb. 1914, p. 100-107.

- Dice, M. E. Tornado at Vernon, Calif., March 15, 1930. *MWR*, v. 58, Aug. 1930, p. 324-5.
- Dines, W. H. Experiment illustrating the formation of the tornado cloud. *QJRMS*, v. 22, Jan. 1896, p. 71-4.
- Espy, J. P. Philosophy of storms. Boston, Little and Brown, 1841. Sec. 7, Tornadoes, p. 304-74.
- van Everdingen, E. The cyclone-like whirlwinds of August 10, 1925. *Proc. Kon. Akad. Wetensch.*, v. 28, no. 10, p. 871-89. 1925.
- Fassig, O. L. Bibliography of meteorology. Signal Off., War Dept. Washington, 1891. Pt. IV, Storms, p. 177-99; p. 200-210.
- Ferrel, W. A popular treatise on the winds. New York, Wiley, 1898. Chap. VII, Tornadoes, p. 347-449.
- Finley, J. P. Report of the tornadoes of May 29 and 30 in the States of Kansas, Missouri, Nebraska, and Iowa. U. S. Signal Service, War Dept., Prof. Papers, no. 4. Washington, 1881.
- Finley, J. P. Report on the character of six hundred tornadoes. U. S. Signal Service, War Dept., Prof. Papers, no. 7. Washington, 1882.
- Finley, J. P. Tornado studies for 1884. U. S. Signal Service, War Dept., Prof. Papers, no. 16. Washington, 1885.
- Frankenfield, H. C. The tornado of May 27 at St. Louis, Mo. *MWR*, v. 24, Mar. 1896, p. 77-81. See also, Julius Baier, Low pressures in St. Louis tornado, *MWR*, v. 24, Sept. 1896, p. 332-3.
- Fujiwhara. The great earthquake in Japan. *Met. Mag.*, v. 58, Dec. 1923, p. 247-9. (Letter to Sir Napier Shaw concerning tornadoes formed by fire.)
- Gaigerov, S. S. Six tornadoes in the central areas of the European part of the (Soviet) Union, and their synoptic conditions. *Meteorologia and Hydrologia (Moscow)*, no. 5, May 1939, p. 44-54. (Tr. from Russian by Lt. Jacob Chaitkin, U. S. Army Air Corps.)
- Gaigerov, S. S. Synoptic conditions accompanying tornadoes in the United States during 1884. *BAMS*, v. 21, June 1940, p. 229-36.
- Giblett, M. A. Line squalls. *Jour. Roy. Aeronautical Soc.*, v. 31, no. 198, June 1927, p. 509-49.
- Giles, A. W. A Virginia tornado. *MWR*, v. 46, Oct. 1918, p. 460-64.
- Giles, A. W. Tornadoes in Virginia, 1814-1925. *MWR*, v. 55, Apr. 1927, p. 169-75.

- Gray, R. W. A tornado within a hurricane area. *MWR*, v. 47, Sept. 1919, p. 639.
- Greening, G. K., Jr. The Middle Missouri Valley tornadoes, September 13, 1928. *MWR*, v. 56, Sept. 1928, p. 353-4.
- Haines, W. C. Waterspout observed at San Juan, Porto Rico, September 10, 1919. *MWR*, v. 47, Oct. 1919, p. 727.
- Hale, P. G. Pensacola waterspout of June 14, 1929. *MWR*, v. 57, Aug. 1929, p. 338-9.
- Hawke, E. L. The tornado of July 7, 1938 in the Chiltern Hills. *QJRM*, v. 64, Oct. 1938, p. 616-18.
- Henry, A. J. Climatology of the United States. *USWB, Bull. Q.* 1906. P. 76-80.
- Hildebrandson, H. H., and L. Teisserenc de Bort. Les bases de la météorologie dynamique. Paris, Gauthier-Villars, 1900. V. 2, chap. VI, Trombes et tornades, p. 279-308.
- Hissong, J. E. Whirlwinds at oil-tank fire, San Luis Obispo, Calif. *MWR*, v. 54, Apr. 1926, p. 161-3.
- Hovde, M. R. The Champlin-Anoka, Minnesota, tornado. *MWR*, v. 67, June 1939, p. 176-7.
- Hunter, H. C. The Lorain, Ohio, tornado, June 28, 1924. *Eng. News Rec.*, v. 93, no. 5, Jul. 31, 1924, p. 190-91. Also, *MWR*, v. 52, June 1924, p. 309-10.
- Hunter, H. C. Tornadoes of the U. S., 1916-1923. *MWR*, v. 53, May 1925, p. 198-204.
- Hurd, W. E. Waterspouts. *MWR*, v. 56, June 1928, p. 207-11.
- Hurd, W. E. Waterspout on Hillsborough Bay, Tampa, Fla., April 2, 1929. *MWR*, v. 57, June 1929, p. 249-50.
- Justice, A. A. Seeing the inside of a tornado. *MWR*, v. 58, May 1930, p. 205-6.
- Kolobkov, N. V. Thunderstorms and squalls. Moscow, Hydromet. Inst., 1939. Chap. 40, 41, and 42, p. 161-75. (Tr. from Russian by Lt. Jacob Chaitkin, U. S. Army Air Corps.)
- Lemons, H. Some meteorological aspects of Nebraska tornadoes. *MWR*, v. 66, Jul. 1938, p. 205-8.

- Letzmann, J. Fortschreitende Luftwirbel. MZ, v. 42, no. 2, Jan. 1925, p. 41-52.
- Linney, C. E. Tornado in New Mexico. MWR, v. 58, June 1930, p. 254-6.
- Lloyd, J. R. The development and trajectories of tornadoes. MWR, v. 70, Apr. 1942, p. 65-75.
- Loveland, G. A. Tornadoes in eastern Nebraska, April 6, 1919. MWR, v. 47, Apr. 1919, p. 234-6.
- McClurg, R. J. Tornado strikes swiftly-moving train. MWR, v. 59, May 1931, p. 198-9.
- Martin, R. J. Tornadoes in the United States 1916-1937. USWB. May 24, 1940. (Mimeo)
- Mitchell, C. L. The tropical cyclone of September 18-October 4, 1929. MWR, v. 57, Oct. 1929, p. 418-20.
- Murphy, J. J. Meteorological features and history of tornado at Norfolk, Va., Sept. 5, 1935. BAMS, v. 16, Nov. 1935, p. 252-5.
- Norton, G. The New Orleans, La., tornado of March 26, 1934. MWR, v. 62, Mar. 1934, p. 96-7.
- Nunns, T. A waterspout in latitude 53° N. MWR, v. 53, Sept. 1925, p. 381.
- Oliver, A. R. The Gothenburg, Nebr., tornadoes, June 24, 1930. MWR, v. 59, June 1931, p. 228-9.
- Papers on tornadoes (The thirteen tornadoes of March 20, 1920; the four tornadoes of April 20, 1920). MWR, v. 48, Apr. 1920, p. 191-213.
- Randall, F. G. Waterspouts in the Strait of Malacca. MWR, v. 57, June 1929, p. 249.
- Root, C. J. Some outstanding tornadoes. MWR, v. 54, Feb. 1926, p. 58-60.
- Samuels, L. T. Washington, D. C., tornado of May 14, 1927. MWR, v. 55, May 1927, p. 227.
- Schlomer, W. B. Tornado at Cincinnati, Ohio, January 19, 1928. MWR, v. 56, Jan. 1928, p. 15.
- Seeley, D. A. Tornadoes in Michigan in May, 1930. MWR, v. 58, May 1930, p. 207.

- Sen, S. N. Mechanism of Bengal tornadoes in the Nor'wester season. *Nature* (London, Macmillan), v. 127, Jan. 24, 1931, p. 128-9.
- Shaw, W. N. Manual of meteorology, v. II. Cambridge Univ. Press, 1936. Chap. VIII, Transitory variations of pressure - cyclones and anticyclones, p. 356-60, Tornadoes. Also, chap. X, Notes and supplementary tables, note 22, p. 427-30.
- Shipman, T. G. An underdeveloped tornado. *MWR*, v. 54, Apr. 1926, p. 168.
- Shipman, T. G. Observing a tornado's life. *MWR*, v. 55, Apr. 1927, p. 183-4.
- Showalter, A. K., and J. R. Fulks. Preliminary report on tornadoes. HMS, Off. of Hyd. Dir., in coop. with WACM, USWB. 1943.
- Simpson, H. E. Tornado insurance. *MWR*, v. 33, Dec. 1905, p. 534-9.
- Some photographs of tornadoes. *QJRMS*, v. 63, Apr. 1937, p. 162.
- Stevens, W. R. Tornadoes in Alabama. *MWR*, v. 53, Oct. 1925, p. 437-43.
- Talman, C. F. Principal publications containing statistics of tornadoes in the United States. (A bibliography) *MWR*, v. 48, Apr. 1920, p. 212-13.
- Tornadoes of Oct. 8, 1919. *MWR*, v. 47, p. 728. (Editor).
- Tracy, W. H. Tornado at Grand Rapids, Mich., May 2, 1930. *MWR*, v. 58, May 1930, p. 206.
- Unger, E. E. Tornadoes in Lauderdale County, Miss., Sunday, February 25, 1934. *MWR*, v. 62, Feb. 1934, p. 59-61.
- Varney, B. M. Aerological evidence as to the causes of tornadoes. *MWR*, v. 54, Apr. 1926, p. 163-5. (Based on E. van Everdingen's paper, The cyclone-like whirlwinds of August 10, 1925.)
- Walker, G. T. On the mechanism of tornadoes. *QJRMS*, v. 56, Jan. 1930, p. 59-66.
- Ward, R. D. The climates of the United States. New York, Ginn, 1925. Chap. XV, Tornadoes.
- Weck, F. H. The Rockford, Ill., tornado, September 14, 1928. *MWR*, v. 56, Sept. 1928, p. 354-5.
- Wenstrom, W. H. Papagayo of March 7, 1939. *BAMS*, v. 20, Mar. 1939, p. 119-21.

Wenstrom, W. H. Waterspout off south coast of Costa Rica, April 1939. BAMS, v. 21, Feb. 1940, p. 77-8.

Wobus, H. B. Tornado from cumulonimbus. BAMS, v. 21, Nov. 1940, p. 367-8.

Atmospherics and Lightning

Allibone, T. E. The physics of lightning. QJMS, v. 67, Oct. 1941, p. 327-32.

Banerji, S. K. Does thunderstorm rain play any part in the replenishment of the earth's negative charge? QJMS, v. 64, Apr. 1938, p. 293-9.

Banerji, S. K. Potential gradient inside thunderclouds. QJMS, v. 64, Apr. 1938, p. 221-2.

Banerji, S. K. The electric field of overhead thunderclouds. QJMS, v. 56, Jul. 1930, p. 305-34.

Bellaschi, P. L. Lightning strokes in field and laboratory. Trans. Amer. Inst. of Electrical Engineers, v. 60, 1941, p. 1248-56; Discussion, p. 1392-3.

Boys, C. V. Progressive lightning. Nature (London, Macmillan), v. 118, Nov. 20, 1926, p. 749-50; v. 122, Sept. 1, 1928, p. 310-11.

Brand, W. Der Kugelblitz. Probleme der Kosmischen Physik, ed. by C. Jensen and A. Schwassmann, v. I and II (combined). Hamburg, Henri Grand, 1923. 170 p.

Bruce, C.E.R., and R. H. Golde. The lightning discharge. Jour. Institution of Electrical Engineers (London), pt. 2, Power Engineering, v. 88, no. 6, Dec. 1941, p. 487-524.

Bureau, R. Centres of thunderstorms and "centres" of sources of atmospherics. QJMS, v. 64, Apr. 1938, p. 331-5.

Byers, H. R. General meteorological aspects of thunderstorm electricity. BAMS, v. 20, May 1939, p. 181-6.

Cannon, J. B. Spectrum of lightning. Jour. Roy. Astronomical Soc. of Canada, v. 12, Mar. 1918, p. 95-7.

Chalmers, J. A. A note on theories of the electric fields below clouds. QJMS, v. 65, Apr. 1939, p. 237-43.

Chalmers, J. A. Cloud and earth lightning flashes. Phil. Mag., ser. 7, v. 32, Jul. 1941, p. 77-83.

- Chalmers, J. A. Electricity of cloud and rain. *Nature* (London, Macmillan), v. 149, June 13, 1942, p. 659-61.
- Chapman, F. W. Atmospheric disturbances due to thundercloud discharges, pt. I. *Proc. Phys. Soc. of London*, v. 51, 1939, p. 876-94.
- Dorsey, N. E. Lightning. *Jour. Franklin Inst.*, v. 201, Apr. 1926, p. 485-96.
- Dufay, J. Spectres des éclairs. *Comptes Rendus de l'Academie des Sciences*, v. 182, May 31, 1926, p. 1331-3.
- Fleming, J. A., ed. Terrestrial magnetism and electricity. *Physics of the earth* (National Research Council, Washington, D. C.), v. VIII. New York, McGraw-Hill, 1939. 778 p.
- Flint, H. T. On the problem of ball lightning - a note on a theory proposed by Th. Neugebauer. *QJRMS*, v. 65, Oct. 1939, p. 532-5.
- Flowers, J. W. The direct measurement of lightning current. *Jour. Franklin Inst.*, v. 232, Nov. 1941, p. 425-50.
- Gott, J. P. On the electric charge collected by water drops falling through a cloud of electrically charged particles in a vertical electric field. *Proc. Roy. Soc. of London, ser. A*, v. 151, no. 874, p. 665-84. Oct. 1, 1935.
- Halliday, E. C. On the propagation of a lightning discharge through the atmosphere. *Phil. Mag.*, ser. 7, v. 15, Feb. 1933, p. 409-20.
- Halliday, E. C. The polarity of thunderclouds. *Proc. Roy. Soc. of London, ser. A*, v. 138, p. 205-29. Oct. 1, 1932.
- Halliday, E. C. The thundercloud as a source of penetrating particles. *Phys. Rev.*, ser. 2, v. 60, no. 2, Jul. 15, 1941, p. 101-6.
- Halliday, E. C. Thunderstorms and the penetrating radiation. *Proc. Cambridge (England) Phil. Soc.*, v. 30, p. 206-15. Jan. 22, 1934.
- Humphreys, W. J. *Physics of the air*. 3d ed. New York, McGraw-Hill, 1940. Pt. 1, Mechanics and thermodynamics of the atmosphere, chap. XVIII, Lightning, p. 361-95; pt. II, Atmospheric electricity and auroras, chap. I, Atmospheric electricity, and chap. II, Aurora polaris, p. 395-413.
- Hutchins, K. M. Radio static forecasts thunderstorms. *BAMS*, v. 16, Mar. 1935, p. 74-5.
- Jensen, J. C. Further studies on the electrical fields of thunderclouds. *BAMS*, v. 11, Apr. 1930, p. 94-5.

- Jensen, J. C. The branching of lightning and the polarity of thunderclouds. *Jour. Franklin Inst.*, v. 216, Dec. 1933, p. 707-48.
- Jensen, J. C. The relation of branching of lightning discharges to changes in the electrical field of thunderstorms. *Phys. Rev.*, ser. 2, v. 40, no. 6, June 15, 1932, p. 1013-14.
- Kähler, K. Die Elektrizität der Gewitter. Sammlung Borntraeger, v. 3. Berlin, Borntraeger, 1924. 148 p.
- Lenard, P. "Über Wasserfallelektrizität und über die Oberflächenbeschaffenheit der Flüssigkeiten. *Annalen der Physik* (Leipzig, Barth), ser. 4, v. 47, no. 12, 1915, p. 463-524.
- Lenard, P. Zur Wasserfalltheorie der Gewitter. *Annalen der Physik* (Leipzig, Barth), ser. 4, v. 65, no. 5, 1921, p. 629-39.
- Loeb, L. B. Fundamental processes of electrical discharge in gases. New York, Wiley, 1939. 717 p.
- Lutkin, F. E. Directional recording of radio atmospherics. *Jour. Institution of Electrical Engineers* (London), v. 82, Mar. 1938, p. 289-302.
- Lutkin, F. E. Nature of atmospherics. *Proc. Roy. Soc. of London*, ser. A, v. 171, no. 946, p. 285-313. 1939.
- McAdie, A. Franklin's kite experiment and the energy of lightning. *MWR*, v. 56, June 1928, p. 216-19.
- McAdie, A. Phenomena preceding lightning. *MWR*, v. 56, June 1928, p. 219-20.
- McEachron, K. B., and W. A. McMorris. The lightning stroke: mechanism of discharge. *General Electric Rev.*, v. 39, Oct. 1936, p. 487-96.
- McEachron, K. B., and K. G. Patrick. Playing with lightning. New York, Random House, 1940. 231 p.
- Malan, D. J., B.F.J. Schonland, and H. Collens. Intensity variations in the channel of the return lightning stroke. *Nature* (London, Macmillan), v. 136, Nov. 23, 1935, p. 831.
- Marwick, T. C. The electric charge of rain. *QJRMS*, v. 56, Jan. 1930, p. 39-44.
- Matthias, A. Der gegenwärtige Stand der Blitzschutzfrage. *Elektrotechnische Zeitschrift* (Berlin), v. 50, no. 41, Oct. 1929, p. 1469-74.

- Maussier-Dandelot, J. La bruit du tonnerre. La Nature (Paris, Masson and Co.), v. 65, no. 3001, May 15, 1937, p. 436-8.
- Maxfield, F. A., and R. R. Benedict. Theory of gaseous conduction and electronics. New York, McGraw-Hill, 1941. 483 p.
- Minser, E. J. Meteorological conditions associated with aircraft lightning discharges and atmospherics. BAMS, v. 21, May 1940, p. 200-202.
- Norinder, H. Lightning currents and their variations. Jour. Franklin Inst., v. 220, Jul. 1935, p. 69-92.
- Nukiyama, D., and H. Noto. A contribution on the charges of thunderclouds. Japanese Jour. of Astronomy and Geophysics, v. 6, 1928-1929, no. 2, p. 71-81.
- Ollendorff, F. Der Einfluss des Erdwiderstandes auf den Blitz. Physikalische Zeitschrift (Leipzig, S. Hirzel), v. 33, no. 9, May 1, 1932, p. 368-76.
- Ollendorff, F. Versuch einer Theorie der Blitzsäule. Archiv für Elektrotechnik (Berlin, Springer), v. 27, no. 3, p. 169-84. Mar. 15, 1933.
- Peek, F. W., Jr. Lightning. Jour. Franklin Inst., v. 199, Feb. 1925, p. 141-82.
- Perry, F. R., G. H. Webster, and P. W. Baguley. The measurement of lightning voltages and currents in Nigeria, 1938-1939. Jour. Institution of Electrical Engineers (London), pt. 2, v. 89, no. 9, June 1942, p. 185-209.
- Peters, O. S. Protection of life and property against lightning. National Bureau of Standards (Washington, D. C.), Tech. Paper no. 56, 1915. 127 p.
- Pockels, F. Ein Versuch, die bei Blitzschlägen erreichte maximale Stromstärke zu schätzen. MZ, v. 15, Feb. 1898, p. 41-6.
- Pockels, F. Über die bei Blitzentladungen erreichte Stromstärke. Physikalische Zeitschrift (Leipzig, S. Hirzel), v. 2, no. 20, Feb. 16, 1901, p. 306-7.
- Pockels, F. Weitere Beobachtungen über die magnetisierende Wirkung von Blitzentladungen. Physikalische Zeitschrift (Leipzig, S. Hirzel), v. 3, no. 2, Oct. 15, 1901, p. 22-3.
- Pockels, F. Zur Bestimmung der Maximalstärke von Blitzen. MZ, v. 18, Jan. 1901, p. 40-41.

- Reynolds, O. On the electrical properties of clouds and the phenomena of thunderstorms. Papers on Mechanical and Physical Subjects (in 3 volumes), ed. by O. Reynolds, Paper no. 5, v. I, p. 30-34. Cambridge Univ. Press, 1900.
- Robinson, G. D. The distribution of electricity in thunderclouds. QJRM, v. 67, Oct. 1941, p. 332-40.
- Rüdenberg, R. Die Kopfgeschwindigkeit elektrischer Funken und Blitze. Wissenschaftliche Veröffentlichungen aus dem Siemens-Konzern (Berlin, Julius Springer), v. 9, no. 1, p. 1-6. 1930.
- Schonland, B.F.J. Atmospheric electricity. Methuen Monographs on Physical Subjects. London, Methuen and Co., 1932.
- Schonland, B.F.J. Thunder-clouds, shower-clouds, and their electrical effects. In Physics of the earth, v. VIII, Terrestrial magnetism and electricity, ed. by J. A. Fleming. New York, McGraw-Hill, 1939.
- Schonland, B.F.J., and J. S. Elder. Anticipatory triggering devices for lightning and static investigations. Jour. Franklin Inst., v. 231, Jan. 1941, p. 39-47.
- Schonland, B.F.J., and D. B. Hodges. Direction-finding of sources of atmospherics and South African meteorology. QJRM, v. 66, Jan. 1940, p. 23-46.
- Schonland, B.F.J., and others. The wave form of atmospherics at night. Proc. Roy. Soc. of London, ser. A, v. 176, no. 965, p. 180-202. Oct. 1940.
- Scrase, F. J. Electricity on rain. GBMO, Geoph. Mem., v. 9, no. 75. 1938.
- Sheppard, P. A. Atmospheric electricity. Met. Mag., v. 74, June 1939, p. 129-36.
- Shipley, J. F. The air currents in a lightning storm. QJRM, v. 67, Oct. 1941, p. 340-45; Discussion, p. 350-61.
- Simpson, G. C. On the Wilson-Gerdien theory of thunderstorm electricity. Phil. Mag., ser. 6, v. 17, Apr. 1909, p. 619-34.
- Simpson, G. C. The electricity of cloud and rain. QJRM, v. 68, Jan. 1942, p. 1-34.
- Simpson, G. C. The mechanism of a thunderstorm. Proc. Roy. Soc. of London, ser. A, v. 114, no. 768, p. 376-401. Apr. 1, 1927. (Abstr. by C. E. Britton, QJRM, v. 54, Apr. 1928, p. 155-6; also, MWR, v. 56, Aug. 1928, p. 311-12.)

- Simpson, G. C., and G. D. Robinson. The distribution of electricity in thunderclouds, pt. II. Proc. Roy. Soc. of London, ser. A, v. 177, no. 970, p. 281-329. Feb. 24, 1941.
- Simpson, G. C., and F. J. Scrase. The distribution of electricity in thunderclouds. Proc. Roy. Soc. of London, ser. A, v. 161, no. 906, p. 309-52. Aug. 3, 1937.
- Slipher, V. M. The spectrum of lightning. Harvard Univ. Lowell Observatory (Flagstaff, Ariz.) Publications, v. III, no. 4, Bull. 79. Sept. 1917.
- Swann, W.F.G. Atmospheric electricity and allied phenomena. Science, v. 96, no. 2479, Jul. 3, 1942, p. 4-6.
- Wait, G. R., and A. G. McNish. Atmospheric ionization near the ground during thunderstorms. MNR, v. 62, Jan. 1934, p. 1-4.
- Watson-Watt, R. A., J. F. Herd, and F. E. Lutkin. On the nature of atmospherics. Proc. Roy. Soc. of London, ser. A, v. 162, no. 909, p. 267-91. Sept. 15, 1937.
- Whipple, F.J.W. Modern views on atmospheric electricity. QJMS, v. 64, Apr. 1938, p. 199-214.
- Whipple, F.J.W. On the association of the diurnal variation of electric potential gradient in fine weather with the distribution of thunderstorms over the globe. QJMS, v. 55, Jan. 1929, p. 1-17.
- Wichmann, Heinz. Über die Bedeutung des Blitzes im elektrischen Mechanismus des Gewitters. Archiv der Deutschen Seewarte (Hamburg), v. 58, no. 10. 1938.
- Wilson, C.T.R. Investigation on lightning discharges and on the electric field of thunderstorms. Phil. Trans. Roy. Soc. of London, ser. A, v. 221, no. 584, p. 73-115. May 6, 1920.
- Wilson, C.T.R. On thunderstorm electricity. Phil. Mag., ser. 6, v. 17, Apr. 1909, p. 634-41.
- Wilson, C.T.R. Some thundercloud problems. Jour. Franklin Inst., v. 208, Jul. 1929, p. 1-12.
- Wilson, C.T.R. The acceleration of β -particles in strong electric fields such as those of thunderclouds. Proc. Cambridge (England) Phil. Soc., v. 22, pt. 4, p. 534-8. Mar. 12, 1925.
- Workman, E. J., J. W. Beams, and L. B. Snoddy. Photographic study of lightning. Physics, v. 7, Oct. 1936, p. 375-9.

- Workman, E. J., and R. E. Holzer. A preliminary investigation of the electrical structure of thunderstorms. NACA, Tech. Note no. 850. Washington, July 1942. 39 p.
- Workman, E. J., and R. E. Holzer. A recording generating voltmeter for the study of atmospheric electricity. Rev. of Scientific Instruments, v. 10, May 1939, p. 160-63.
- Wormell, T. W. Currents carried by point-discharges beneath thunderclouds and showers. Proc. Roy. Soc. of London, ser. A., v. 115, no. 771, p. 443-55. Jul. 1, 1927.
- Wormell, T. W. The effects of thunderstorms and lightning discharges on the earth's electric field. Phil. Trans. Roy. Soc. of London, ser. A, v. 238, p. 249-303. 1939.
- Wormell, T. W. Vertical electric currents below thunderstorms and showers. Proc. Roy. Soc. of London, ser. A, v. 127, no. 806, p. 567-90. June 2, 1930.

Recommended Meteorology Texts

Introductory

- Brunt, D. Weather study. New York, Ronald Press, 1942.
- GBMO. Admiralty weather manual. London, 1938.
- Harrison, L. P. Meteorology. New York, National Aeronautics Council, Inc., 1942.
- Haynes, B. C. Meteorology for pilots. CAA Bull. no. 25. Washington, D. C., GPO, 1943.
- Namias, J. Introduction to air mass and isentropic analysis. 5th ed., rev. and enl. Milton, Mass., AMS, 1940.
- Petterssen, S. Introduction to meteorology. New York, McGraw-Hill, 1941.
- Sutcliffe, R. C. Meteorology for aviators. New York, Chem. Pub. Co., 1940.
- Willet, H. C. Descriptive meteorology. New York, Academic Press, 1944.

Intermediate

- Byers, H. R. General meteorology. New York, McGraw-Hill, 1944.

Hewson, E. W., and R. W. Longley. Meteorology theoretical and applied. New York, John Wiley, 1944.

Humphreys, W. J. Physics of the air. New York, McGraw-Hill, 1940.

Petterssen, S. Weather forecasting and analysis. New York, McGraw-Hill, 1940.

Shaw, W. N. Manual of meteorology. New York, Macmillan, 1926-31. (4 vols.)

Taylor, G. F. Aeronautical meteorology. New York, Pitman, 1941.

Advanced

Brunt, D. Physical and dynamical meteorology. New York, Macmillan, 1939.

Haurwitz, B. Dynamic meteorology. New York, McGraw-Hill, 1941.

Holmboe, J., G. Forsythe, and W. Gustin. Dynamic meteorology. New York, John Wiley, 1945.

Abbreviations and Publication Information

Abhandl.	- Abhandlungen	ff.	- following
acad.	- academy	geog.	- geographical
adv.	- advisory	geoph.	- geophysical
agric.	- agriculture	govt.	- government
Amer.	- American		
Brit.	- British	hyd.	- hydrology, hydrologic
bull.	- bulletin(s)	hydromet.	- hydrometeorological
chap.	- chapter(s)	inc.	- incorporated
chem.	- chemical	inst.	- institute
coll.	- collection	int.	- international
comm.	- committee		
conf.	- conference	jour.	- journal
coop.	- cooperation	"	
		kon.	- königlich
dept.	- department		
dir.	- director	lib.	- library
dist.	- district		
div.	- division	mag.	- magazine
		mem.	- memoir(s)
ed	- edition, edited, editor	met.	- meteorology, meteorological
eng.	- engineer(s), engineering	misc.	- miscellaneous
enl.	- enlarged	ms.	- manuscript

no(s).	- number(s)	sci.	- science
off.	- office	ser.	- series
p.	- page(s)	soc.	- society
Pacif.	- Pacific	supp.	- supplement
phil.	- philosophical	tech.	- technology, technical
phys.	- physical	tr.	- translation, translated, translator
proc.	- proceedings	trans.	- transaction(s)
prof.	- professional	Univ.	- University
pt(s).	- part(s)	unpubl.	- unpublished
pub.	- publication, publishing	v.	- volume(s)
publ.	- published, publisher	vol(s).	- volume(s)
rec.	- record	Veroff.	- Veröffentlichungen
ref.	- reference		
repr.	- reprint(ed)		
rev.	- revised, review		
roy.	- royal		
rpt(s)	- report(s)		

AAF - U. S. Army Air Forces.

AH - Annalen der Hydrographie und Maritimen Meteorologie, Hydrographisches Amt und Deutsche Seewarte, Berlin.

Amer. Met. Jour. - American Meteorological Journal, Ann Arbor, Mich., Register Pub. House.

AMS - American Meteorological Society, Milton, Mass.

ASCE - American Society of Civil Engineers, 33 W. 39th St., New York City.

BAMS - Bulletin of the American Meteorological Society, Milton, Mass.

BG - Beiträge zur Geophysik, Leipzig, beginning with v. 54, no. 1, 1939; formerly, Gerlands Beiträge zur Geophysik, Akademische Verlagsgesellschaft, Leipzig.

BPFA - Beiträge zur Physik der Freien Atmosphäre, Leipzig.

CAA - Civil Aeronautics Administration, U. S. Department of Commerce, Washington, D. C.

CE - Civil Engineering, published monthly by the American Society of Civil Engineers.

CIT - California Institute of Technology, Pasadena.

Das Wetter - see ZAM

Elettrotecnica - Associazione Elettrotecnica Italiana, Milan.

GBMO - Great Britain Meteorological Office, Air Ministry, London.

General Electric Rev. - Schenectady, N. Y., General Electric Co., publ.

Geofys. Pub. - Geofysiske Publikasjoner, Norske Videnskaps Akademi, Oslo.

GPO - U. S. Government Printing Office, Washington, D. C.

HMS - Hydrometeorological Section, U. S. Weather Bureau, Washington, D. C.

Int. Assoc. of Hyd. - Association Internationale d'Hydrologie, Paris.

Japanese Jour. of Astronomy and Geophysics - National Research Council of Japan, Tokyo.

Jour. Franklin Inst. - published by the Franklin Institute of the State of Pennsylvania, Philadelphia.

Kon. Adad. Wetensch. - Koninklijke Akademie van Wetenschappen te Amsterdam.

Marine Observer - published quarterly, Meteorological Committee, Air Ministry, London.

Met. Mag. - Meteorological Magazine, published monthly, Meteorological Committee, Air Ministry, London.

MI - Memoirs of the India Meteorological Department, Delhi.

MIT Papers - Massachusetts Institute of Technology (Cambridge) and Woods Hole Oceanographic Institute, Papers in Meteorology and Physical Oceanography.

MWR - Monthly Weather Review, U. S. Weather Bureau, Washington, D. C.

MZ - Meteorologische Zeitschrift, Österreichische Gesellschaft für Meteorologie und Deutsche Meteorologische Gesellschaft, Braunschweig.

NACA - National Advisory Committee for Aeronautics, Washington, D. C.

PCA - Pennsylvania Central Airlines, Washington Natl. Airport, Washington 25, D. C.

Phil. Mag. - London, Edinburgh and Dublin Philosophical Magazine and Journal of Science. London, Taylor and Francis.

Physics - Journal of Applied Physics, published by the American Physical Society, American Institute of Physics, New York City. Before 1937, Physics, A Journal of General and Applied Physics.

Phys. Rev. - Physical Review, American Institute of Physics, New York City.

PMI - Preussisches Meteorologisches Institut, Berlin. Before 1918, Königliches Preussisches Meteorologisches Institut.

QJRMS - Quarterly Journal of the Royal Meteorological Society, London.

Rev. of Scientific Instruments, American Institute of Physics, New York City.

RMS - Royal Meteorological Society, London.

SBAW - Sitzungsberichte der Bayerischen Akademie der Wissenschaften, München. Before World War I, Sitzungsberichte der Königlichen Bayerischen Akademie der Wissenschaften, München.

Science - American Association for the Advancement of Science, Cambridge, Mass.

SCS - Soil Conservation Service, U. S. Department of Agriculture.

Sitzungsb. Akad. München - Sitzungsberichte, Akademie, München.
SPAW - Sitzungsberichte der Preussischen Akademie der Wissenschaften,
Berlin.

TAGU - Transactions of the American Geophysical Union, National Research
Council, Washington, D. C.

TWA - Transcontinental and Western Air, Inc., Kansas City, Mo.

UATC - United Airlines Transport Corporation, Chicago, Ill.

USDA - U. S. Department of Agriculture, Washington, D. C.

USNA - U. S. Naval Academy, Annapolis, Md.

USWB - U. S. Weather Bureau, Department of Commerce, Washington, D. C.

WACM - War Advisory Council on Meteorology, U. S. Weather Bureau.

WB - Weather Bureau.

WBO - Weather Bureau Office.

ZAM - Zeitschrift für Angewandte Meteorologie, Berlin. Before 1928,
the title was Das Wetter.

ROSTER OF HYDROMETEOROLOGICAL SECTION

January 1, 1945

Office of Hydrologic Director

Merrill Bernard

Hydrometeorological Section

A. K. Showalter

G. N. Brancato

Meteorological Unit

A. L. Shands
H. K. Gold
R. A. McCormick
H. C. Hamilton
E. H. Townsend

Hydrologic Unit

W. T. Wilson
E. S. Thompson
G. D. Abrams
I. B. Braman
J. T. Lindgren

Storm Review Unit

D. J. Stevlingson
A. H. Jennings
W. E. Remmele
W. W. Swayne
E. Sherrill
B. B. Hull
P. A. Carr
M. E. Linehan
F. N. Everard
L. F. Ewing
J. M. Kenyon

Office Administration

H. S. Marshall
M. G. Ezekiel

Drafting and Reproduction

W. E. Kinnear
C. S. Gladden

Names Not Included in Roster Because of Personnel Changes

P. Light
M. A. Garstens
J. P. Winner
M. E. Dorney
D. Ammerman
A. E. Hirsch
C. S. Gilman

P. G. Anderson
F. E. Caldwell
R. F. Buening
D. Haber
M. L. McCary
H. W. Detrich, Jr.
J. L. Callahan